Award Number: DAMD17-99-1-9559

TITLE: Toxic Neuronal Death by Glyeraldehyde-3-Phosphate Dehydrogenase and Mitochondria

PRINCIPAL INVESTIGATOR: William Tatton, Ph.D.

CONTRACTING ORGANIZATION: Mount Sinai School of Medicine
New York, New York 10029

REPORT DATE: August 2003

TYPE OF REPORT: Final

PREPARED FOR: U.S. Army Medical Research and Materiel Command
Fort Detrick, Maryland 21702-5012

REPORT DOCUMENTATION PAGE

Form Approved
OMB No. 0704-0188

1. REPORT DATE *(DD-MM-YYYY)*	2. REPORT TYPE	3. DATES COVERED *(From - To)*
August 2003	Final	1 July 1999 – 1 Jul 2003

4. TITLE AND SUBTITLE
Toxic Neuronal Death by Glyeraldehyde-3-Phosphate Dehydrogenase and Mitochondria

5a. CONTRACT NUMBER

5b. GRANT NUMBER
DAMD17-99-1-9559

5c. PROGRAM ELEMENT NUMBER

6. AUTHOR(S)
Principal Investigator: William Tatton, Ph.D.

5d. PROJECT NUMBER

5e. TASK NUMBER

5f. WORK UNIT NUMBER

7. PERFORMING ORGANIZATION NAME(S) AND ADDRESS(ES)
Mount Sinai School of Medicine
New York, New York 10029

8. PERFORMING ORGANIZATION REPORT NUMBER

9. SPONSORING / MONITORING AGENCY NAME(S) AND ADDRESS(ES)
U.S. Army Medical Research and Materiel Command Fort Detrick, Maryland 21702-5012

10. SPONSOR/MONITOR'S ACRONYM(S)

11. SPONSOR/MONITOR'S REPORT NUMBER(S)

12. DISTRIBUTION / AVAILABILITY STATEMENT
Approved for public release; distribution unlimited

13. SUPPLEMENTARY NOTES

14. ABSTRACT
Our project aimed at determining pathways and proteins that mediate or resist apoptosis in PD. Protein and mRNA chemistry coupled with confocal laser scanning microscopic investigation of post mortem PD brain tissue was used to identify the cell's subcellular organelles and signaling proteins that mediate or resist PD apoptosis. The subcellular translocation of specific proteins between different organelles is integral to apoptosis signaling. We emphasized four proteins, p53, GAPDH, BAX, and NFkB that undergo subcellular translocation, induce apoptosis and may contribute to PD apoptosis. We found a decrease in mitochondrial membrane potential in fibroblast from PD patients which appear similar to a defect previously found in PD substantia nigra neurons and may render the cells vulnerable to apoptosis. The experiments were designed to define the elements responsible for mitochondrial defects and to determine the mechanisms underlying those defects.

15. SUBJECT TERMS
Neurotoxin

16. SECURITY CLASSIFICATION OF:			17. LIMITATION OF ABSTRACT	18. NUMBER OF PAGES	19a. NAME OF RESPONSIBLE PERSON
a. REPORT	b. ABSTRACT	c. THIS PAGE			USAMRMC
U	U	U	UU	98	19b. TELEPHONE NUMBER *(include area code)*

Table of Contents

Page

Introduction to Final Report (October 2012):

Due to his illness and death, after this work was completed, Principal Investigator Dr. William Tatton was unable to assemble and submit a Final Report for the project entitled 'Toxic Neuronal Death by Glyeraldehyde-3-Phosphate Dehydrogenase and Mitochondria.' We were able to reconstruct a Final Report for this project by gathering a draft copy of the project's three progress reports and referencing Dr. Tatton's publications that cite additional progress.

Dr. Tatton's Introduction (2002):

This proposal was designed to examine the role of glyceraldehyde-3-phosphate deydrogenase (GAPDH), mitochondrial permeability and mitochondrial membrane potential in some forms of toxic neuronal death. Mitochondria have been shown to play a critical decisional role in some forms of cell death, namely apoptotic cell death. Determining the mechanism of the toxin induced apoptosis night reveal potential therapeutic targets which could slow or alleviate the apoptosis. To address these issues, we proposed a series of experiments which include and in vitro study of neurons and neuron-like cells in culture that would be immunostained to determine which toxic insults involved changes in GAPDH levels or distribution, changes mitochondrial membrane potential and permeability transition pore opening. We proposed to examine mutated cell lines of PC12 and 3T3 cells with inducible GAPDH expression. The direct actions of GAPDH and NAD+ will be examined using a cell free system of nuclear mitochondria; and cystolic subfractions. Finally, we proposed to examine whether GAPDH alters the transcription or translation of specific subsets of genes and/or their RNA targets using a lysate system. At this point, we addressed many of the objectives and are on schedule for the completion of the study by the end of the funding period.

Toxic Neuronal Death by GAPDH and Mitochondria
Report of Progress

Background

We have developed a hypothetical step by step model for GAPDH induction of apoptosis: 1) NAD^+ levels modulate the participation of GAPDH in glycolysis, since NAD^+ causes GAPDH to be freed from AU-rich RNA; 2) the higher the energy demands of the cell, as signaled by NAD^+ levels, the greater the amounts of GAPDH available for glycolysis; 3) the majority of NAD^+ is found in the matrix of mitochondria, which is released upon PTP opening and frees GAPDH from AU-RNA for nuclear translocation. We propose that NAD^+ is one of the unidentified heat labile mitochondrial factors that facilitates apoptosis, 4) similarly, high levels of superoxide radicals, nitric oxide or peroxynitrite can free GAPDH from AU-RNA to facilitate apoptosis; 5) excess freed GAPDH enters the nucleus and binds to DNA-associated proteins; 6) the nuclear GAPDH serves to blocks the transcriptional event necessary for intrinsic neuroprotection but not apoptosis itself which depends on constitutive proteins; 7) the transcriptional blockade requires GAPDH to be in a tetrameric form; and 8) agents like DES or CGP3466, which tend to maintain GAPDH as a dimer, reduce the blockade of intrinsic neuroprotection by GAPDH.

Review of Hypotheses

a1. A decrease in $\Delta\Psi_M$ and opening of the PTP is a critical event in a number of forms of toxic neuronal apoptosis and neuronal death in PD.
a2. GAPDH upregulation and nuclear translocation is a major factor in the progression of toxic neuronal apoptosis and neuronal apoptosis in PD.
a3. GAPDH facilitates toxic neuronal apoptosis by blocking transcriptional events necessary for the induction of a damage activated intrinsic neuroprotective program of new protein synthesis that includes a maintenance of BCL-2 levels and a decrease in BAX with a resultant maintenance of $\Delta\Psi_M$ and PTP closure.
a4. PTP opening during the effector phase of toxic neuronal apoptosis results in the release of NAD+ from mitochondria which in turn frees RNA bound GAPDH to translocate to the nucleus and block the transcriptional events necessary for the damage activated intrinsic neuroprotective program which accounts for the facilitation of toxic neuronal apoptosis by GAPDH.

c. Progress in Technical Objectives

b1. Determine which forms of toxic apoptosis involve GAPDH and do they also involve a decrease in $\Delta\Psi_M$ and PTP opening?
b2. Determine whether GAPDH overexpression induces apoptosis in neuronally differentiated PC12 cells and 3T3 fibroblasts, whether (-)-desmethyldeprenyl and related compounds block or reduce any apoptosis facilitation by GAPDH overexpression and whether the tetrameric form of GAPDH is essential for toxic apoptosis induction.
b3. Determine whether increased GAPDH is sufficient by itself to facilitate toxic apoptosis and whether NAD^+ released by opening of the PTP frees GAPDH from cytosolic RNA binding sites for nuclear translocation and apoptosis facilitation . - We have shown that the controlled increase in expression of GAPDH through a tetracycline responsive expression system leads to the immediate death approximately 40% of otherwise uncompromised neuronally differentiated PC12 cells. Further to this observation is that the surviving GAPDH expressing cells become increasingly vulnerable to toxic insult by rotenone, trophic withdrawal or H_2O_2 treatment.
b4. Determine whether GAPDH induces changes in transcription and /or translation that are appropriate for blockade of an intrinsic neuroprotection program of new protein synthesis activated by cell damage.

Methods

Specific Methods

Determine which forms of toxic apoptosis involve GAPDH and do they involve a decrease in $\Delta\Psi_M$ and PTP opening?

Rationale - We have show that early GAPDH upregulation and dense nuclear translocation is a feature of apoptosis induced in neuronally differentiated PC12 cells by trophic withdrawal and have preliminary evidence for GAPDH involvement in apoptosis caused by H_2O_2 (a pro-oxidant) and MPP^+ (a mitochondrial complex I/α-ketoglutarate toxin) exposure and idiopathic PD. We have developed a number of other toxic

apoptosis models in neuronally differentiated PC12 cells including staurosporine-, calcimycin-, glutamate-, kainic acid-, dopamine-, manganese chloride- and TNFα-induced apoptosis. Those toxins involve a number of different initiation signaling pathways. We also have models that involve direct mitochondrial toxins that act on different mitochondrial elements such as atractyloside that induces PTP opening; FCCP, antimycin A, and dinitrophenol that cause permeability of mitochondrial membranes; rotenone, 3-nitroproprionic acid and cyanide that inhibit complexes I, II and III respectively. We propose to determine which, if any, of the above models involve GAPDH upregulation/translocation and whether GAPDH association only occurs in apoptosis that involves a decrease in $\Delta\Psi_M$ and PTP opening. We also propose to examine GAPDH association of apoptosis induced by the above toxins in primary cultures of mesencephalic embryonic dopaminergic neurons and cerebellar granule cells.

Research Plan - We have determined the optimal concentration of all of the above toxins for induction of apoptosis in the neuronally-differentiated PC12 cells (for example calcimycin 50 μM, atractyloside 5 mM, $MnCl_2$ 300 mM, staurosporine 1.0 μM).

Nuclear Translocation of GAPDH-GFP Fusion Protein. We have examined PC12 cells that have been stabley transfected with the gene construct for GAPDH-GFP fusion protein (see above) to determine the identity of some toxins which induce GAPDH dense nuclear translocation and determined the time course of the nuclear translocation. The cells were grown on 50 mm coverslips, maintained in our environmentally controlled chamber and imaged as live cells on the CLSM. We followed the time course of changes in $\Delta\Psi_M$ using JC-1 (resulting publication is in preparation for submission). Calcimycin, atractyloside and $MnCl_2$ treatment of these neuronally differentiated PC12 cells resulted in a decrease in $\Delta\Psi_M$ prior to nuclear signs of apoptosis however, apoptosis induced with staurosporine does not show a similar involvement.

Nuclear Translocation of GAPDH Immunoreactivity. Parallel experiments will examine neuronally differentiated PC12 cells for nuclear translocation of GAPDH immunoreactivity at time points of 0.5, 1.0, 2.0, 3.0, 6.0, 12 and 24 hours after the initiation of toxic exposure. Western blots will be prepared for whole cell protein and for the nuclear, mitochondrial and cytosolic protein fractions at the same time points. The cells for immunocytochemistry will be exposed to CMTMR for 10 minutes for each of the time points in order to determine the temporal relationships between any GAPDH nuclear translocation and changes in $\Delta\Psi_M$. We have extensive experience in examining cells simultaneously reacted for NCC with YOYO-1, immunostained for GAPDH and incubated with CMTMR for $\Delta\Psi_M$ and determining the relative time courses for each of the apoptosis associated events.

We have also utilized a CLSM method for directly visualizing PTP opening in living cells. The method depends on the fact that calcein AM fluoresces in the cytosol but does not enter mitochondria if the PTP is closed. In contrast, rhodamine derivatives such as TMRE concentrate in mitochondrial. Accordingly, green fluorescing calcein is seen in the cytosol but not in mitochondria which appear as holes. TMRE fluoresces red in mitochondria and is entirely separate from calcein AM fluorescence, if the PTPs of a given mitochondrion are closed. PTP opening results in mitochondrial co-localization of calcein AM and TMRE fluorescence, since calcein enters the mitochondrial matrix through an open PTP. We will examine the temporal relationships between PTP opening, decreases in $\Delta\Psi_M$, intramitochondrial Ca^{2+} levels and cytosolic peroxyl levels in living cells for the above toxins.

In order to determine whether the toxic agents mediate any GAPDH and $\Delta\Psi_M$ related changes in cells other than neuronally differentiated PC12 cells, we will carry out similar experiments to those above in primary cultures of rat mesencephalic embryonic dopaminergic neurons and cerebellar granule cells. R. Chalmers-Redman has extensive experience with mesencephalic embryonic dopaminergic neurons. She has also perfected culture methods for cerebellar granule cells taken from 5 day postnatal rats based on the methods described.

Finally, similar experiments will be carried out on cutaneous fibroblasts cultured from PD patients and age-matched controls (see above). We have acquired and passaged fibroblasts for more than 20 PD and age-matched control patients. The experiments are designed to determine whether GAPDH plays a role in toxic apoptosis in the PD fibroblasts with or without the constitutive decrease in $\Delta\Psi_M$ that we have found for the cells. We will determine whether the relationship between toxin concentration and the induction of apoptosis is the same or different for the PD fibroblasts and age-matched fibroblasts. It has been suggested that PD neurons are abnormally sensitive to toxic exposure.

We will determine whether DES and related compounds reduce the different forms of toxic apoptosis examined. We will determine whether any anti-apoptotic action of DES and related compounds correlates

with a maintenance of $\Delta\Psi_M$, PTP closure, and a reduction of GAPDH upregulation and nuclear translocation.

Determine whether GAPDH overexpression induces apoptosis in neuronally differentiated PC12 cells and 3T3 fibroblasts , whether (-)-desmethyldeprenyl and related compounds block or reduce any apoptosis facilitation by GAPDH overexpression and whether the terameric form of GAPDH is essential for apoptosis induction.

Rationale –GAPDH levels have been shown to increase in nerve cells entering apoptosis and it has been shown that antisense oligonucleotides against GAPDH reduce neuronal apoptosis but the effect of increased GAPDH expression on apoptosis has not been determined. GAPDH induction of apoptosis seems to be dependent on nuclear translocation but it may also result in part from increased new synthesis of the protein. DES and CGP3466 reduce apoptosis and convert GAPDH from a tertramer to dimer in the test tube. We will mutate GAPDH so that it cannot form a tertramer and determine if overexpression of the wild form and mutant forms induce apoptosis.

Research Plan.

Variable GAPDH Overexpression - We over-expressed the gene for GAPDH using a system that allows variable expression of the gene and therefore variably increased levels of the protein. We determined that the newly synthesized GAPDH induces apoptosis in the cells in the absence of other stressors and that the GAPDH overexpression alters the cells' vulnerability to other damage that induces apoptosis. The expression system also allowed us to determine the time course of any apoptosis-related changes that are induced by GAPDH over-expression and to evaluate that time course with regard to other apoptotic events like decreased $\Delta\Psi_M$ or nuclear DNA cleavage and the results are published in NeuroReport.

PC12 cells have been transfected with the rat brain GAPDH cDNA that was cloned by this group using the Tet-Off system. Similar transfection will be produced in 3T3 fibroblasts. PC12 cells that have been maintained in serum without NGF or PC12 cells that have been neuronally differentiated by NGF and serum have been examined. 3T3 fibroblasts will be similarly examined. The extent and time course of apoptosis induced by varying levels of GAPDH over-expression has been determined. Immunocytochemistry will be employed at various times after the onset of GAPDH over-expression to determine if any apoptosis is associated with GAPDH nuclear translocation, changes in $\Delta\Psi_M$, alterations in the levels or subcellular localization of other apoptosis-related proteins (particularly BCL-2 and the superoxide dismutases which have been shown to participate in an intrinsic neuroprotective program that may be opposed in GAPDH - induced apoptosis). RT-PCR and in situ hybridization will be utilized to determine whether nay changes in apoptosis-related or intrinsic neuroprotective proteins are mediated through corresponding changes in gene expression.

Mutational Studies Of GAPDH In Apoptosis Facilitation -The three dimensional structures of GAPDH from several organisms have been determined and are in the Brookhaven data base (PDB). The three dimensional structures are highly conserved. We have taken the GAPDH from the l. mexicana as the crystal structure. The sequence for the rat GAPDH was built onto this structure of GAPDH using family sequence alignments from CLUSTAL and the molecular modeling software INSIGHT (Biosymm). We are using this model of GAPDH to design mutations for transfection studies into PC12 cells.

We wish to design mutants that will disrupt the tetramer without unfolding the monomer. Mutant GAPDH will be overexpressed in E. coli using the GST fusion protein system. The GAPDH-GST fusion protein will be purified using glutathione affinity chromatography and the GAPDH will be freed from the GST by thrombin cleavage. Protein overproduction and purification will be carried out using standard protocols. Biophysical characterization will be carried out to show that the monomer is unaffected. Such studies include circular dichroism to measure both secondary and tertiary structure to ensure that mutations did not affect folding of the monomers. Also, fluorescence studies will indicate if there are significant alterations in the hydrophobic core of GAPDH. It is unlikely that there is substantial change in the conformation of each monomer upon tetramerization so CD and fluorescence would be valid indicators of ability for monomers to correctly fold in the absence of subsequent quartenary structure formation. Any changes due to tetramerization will be determined by carrying out CD and fluorescence studies with wild type protein in conditions known to favor the monomer or the tetramer.

In order to avoid disruption of the monomer structure, mutations will focus on the surface of the monomer, leaving internal residues, which may be important to the stability of the monomer untouched. The surface residues involved in making contacts with other subunits in the tetramer will be targeted for mutation. Where possible, at inter-monomer contact points within the tetramer large bulky residues will be

placed for the most effective disruption of contracts needed to form the tetramer. It is expected that multiple mutations will be required to disrupt the tetramer. We have used molecular modeling techniques to determine the best candidate residues for mutation. Initially all of the below listed mutations will be constructed resulting in a GAPDH protein with six point mutations. However, mutations will be made in a serial fashion, where after each step the ability of the mutant protein to properly fold will be assessed. PCR stitch will be used to generate mutations as one of us (K. Borden) has done previously. Mutants will be sequenced to confirm the mutation and to determine that no spurious mutations arose during PCR. To assess if mutations were effective at disrupting the tetramer, size exclusion chromatography will be carried out as we described above.

Mutation	Strategy
Val 279 to Arg	Val279 is near to an Arg from the neighboring subunit so this mutation should cause electrostatic repulsion
Met 43 to Lys	M43 is close packed to a glycine residue from the neighboring subunit so the hydrophobic surface from the subunit should repel the charge of the Lys and the long chain of the lysine should interfere with the close packing
Ala 200 to Lys	Ala 200 interacts with Ala200 on the adjacent subunit. Mutating to a charged residue should act similarly as above. The long side-chain of the lys should cause steric interaction as well.
Ile 203 to Asp	Mutation to a charged residue should disrupt hydrophobic contacts between subunits
Phe 230 to Asp	same as above
Ile 304 to Arg	Mutation to the positive Arg residue should repel a nearby Arg from the adjacent residue

The mutated dimeric only GAPDH will then be transfected into PC12 cells as above and the findings compared to those for the wild type overexpression. This portion of the project is in progress.

Use Of A Neuronal Rather than Xenopus Cell Free System To Examine The Role Of NAD^+ And GAPDH In Apoptosis

Rationale – In order to create a more reflective cell free system model of neuronal apoptosis, we have instead of examining a cell free system derived from Xenopus, we have developed a system derived from PC12 and liver origin. Nuclear and cytoplasmic components of the cell free system are obtained from neuronally differentiated PC12 cultures while the mitochondrial component is obtained from differential centrifugation of fresh rat liver.

Experimental Plan

We will be able to add varying amounts of GAPDH, with or without GAPDH antibodies, to the PC12 cell free system. This system is maintained in low melting point agar on glass slides or on 25mm coverslips in our environmentally controlled chamber placed on the CLSM. The oocyte nuclei will assayed for nuclear chromatin condensation (NCC) using YOYO-1 as an indicator of apoptotic nuclear degradation. $\Delta\Psi_M$, intramitochondrial Ca^{2+} and peroxyl radical levels will be measures using JC-1, Rhod-2AM and DCF as above. At the conclusion of the measurements, the coverslips will be fixed in paraformaldehyde for GAPDH immunocytochemistry.

A series of experiments will be carried out to determine if added GAPDH facilitates apoptosis induced in the oocyte system by the toxins presented above. Similar experiments will be carried out with the addition of variable amounts of NAD^+ or NADH. We will determine whether NAD^+ frees GAPDH from RNA binding sites and causes the protein to translocate to the PC12 nucleus. Graded NAD^+ addition will allow us to determine whether the concentrations of NAD+ are within the range possible after PTP opening. The calcein AM/TMRE techniques described above will used to follow PTP opening after GAPDH or NAD^+ addition.

Determine Whether GAPDH Alters The Transcription And/Or Translation Of Specific Subsets of Genes And/Or Their mRNAs

Rationale We will use commercially available TNT Coupled Reticulocyte Lysate Systems to determine the effect of GAPDH on the transcription and translation of specific pro-apoptotic (e.g. c-JUN, BAX) and anti-apoptotic (e.g. BCL-2, BCL-X_L, SOD1) proteins. The systems offer the advantage of studying transcriptional and translational events in a single tube or in the above cell free system as a one step

process. Antibodies and other large molecules can interact freely with the system components without having to cross lipid membranes present with intact cells. The lysate system includes all of the protein and RNA components necessary for translation including hammerhead ribozymes, a co-enzyme for the translational activity of GAPDH.

Research Plan DNA constructs of apoptosis-related genes with attached T3 or T7 promoter sequences are incubated with the lysate system for 1-2 hours and the resultant protein product analyzed by SDS gel electrophoresis and autoradiography. We have the advantage of having recently acquired a phospho imager in a cooperative purchase with the Department of Neurobiology at the Sinai School of Medicine. The imager is located on the same floor as the investigators involved in this proposal and will greatly accelerate the progress of these studies.

In these experiments, we will use antibodies against GAPDH to render any intrinsic GAPDH in the lysate inactive. Varying amounts of GAPDH will then be added to the lysate in a controlled manner. In the test tube experiments, DNA constructs coding for specific pro-apoptotic and anti-apoptotic proteins will be used to determine if GAPDH influences the synthesis of each of the proteins. Varying levels of pro-oxidants, nitric oxide or NAD^+ will be added to determine how the freeing of GAPDH from AU rich RNA influences the synthesis. Other experiments will vary the concentration of AU rich RNA in the GAPDH-lysate mixture. Controls for changes in transcriptional activity will be assayed with the RipoProbe Transcription system (Promega).

GAPDH may to some degree bind DNA or to DNA associated proteins as our preliminary results from histological co-localization and chromatography studies indicate. Thus, GAPDH may play a role in transcriptional events *in vivo* or *in vitro* if the protein can translocate to the nucleus. So, the experiments outlined above will be repeated with this transcriptional system.

In subsequent experiments, anti-apoptotic agents like DES will be added to the system with varying amounts of GAPDH to determine whether DES alters the transcriptional or translational events modified by GAPDH. If no GAPDH is required for DES to induce transcriptional and/or translational changes, it will invalidate GAPDH as a mediator of the changes in protein synthesis induced by DES or other agents. Alternately, use of the systems should allow complete identification of elements involved in GAPDH induced apoptosis or that induced by other proteins. Size exclusion chromatography will be used to determine the proportion of GAPDH that is in a dimer form versus that in a tetrameric form after the different treatments (see details above).

The lysate systems will also be used with the cell free systems described above. Nuclei with and without mitochondria will be added to the GAPDH-lysate mixtures to determine if mitochondrial factors influence any transcriptional or translational actions of GAPDH. The systems will be exposed to mitochondria treated with 5 mM atractyloside to open the PTP and allow putative AIFs to influence transcription and translation. Control mitochondria will be treated with cyclosporin A to insure PTP closure. NAD^+ levels will be measured in the systems after the addition of atractyloside (which opens the PTP) treated and control mitochondria. As described above, anti-GAPDH antibodies will be used to determine if mitochondrially-released factors and/or NAD^+ require GAPDH to mediate apoptosis.

To date, the experiments proposed in the original grant proposal are approximately 40% completed. Minor technical revisions to the original protocol have been described although there are no changes to the overall experiaments.

BODY OF WORK

Background To Statement of Work

Similarities And Differences Between PD And MPTP Parkinsonism. Sporadic PD is characterized by CAergic neuronal loss, including melanin-containing, dopaminergic neurons (DAns) in the substantia nigra (SNc) and noradrenergic neurons in the locus coeruleus (LC). The pathobiology of the initiation and progression of PD remains uncertain (see [1] for a review). Stereological counting has shown that SNc melanin-containing DAns are decreased by 60% or more before PD becomes clinically evident PD [2, 3].

MPTP kills SNc DAns in non-human primates [4-6] as well as other CAergic neurons [7-10] with a similar, but not identical, regional distribution to human PD [11]. MPTP does not induce neuronal cell body protein aggregations similar to the Lewy bodies found in PD. Lewy bodies are a key-identifying feature of PD and contain a variety of proteins including ubiquitin, α-synuclein and GAPDH [12-14].

Decreased mtRCxI Activity In PD And MPTP Parkinsonism. Examination of homogenates from PD postmortem SNc revealed decreases of 20 to 40% in mtRCx I activity without similar activity decreases for complex II, III or IV [15-19]. Western blots and immunocytochemistry using a mtRCx I antibody revealed decreased immunoreaction for PD SNc [15, 18, 20, 21], possibly suggesting a deficiency of mtRCx I protein(s).

MPTP is converted to MPP^+ in astroglia by MAO-B [22, 23]. MPP^+ selectively accumulates in CAergic neurons by the plasma membrane dopamine transporter (DAT) [24, 25]. Inside CAergic neurons, MPP^+ undergoes high affinity uptake by the vesicular monoamine transporter (VMAT2) [26-28]. It binds less avidly to mtRCxI, where it inhibits NADH dehydrogenase [29-31]. The majority of MPP^+ appears to reside in CAergic vesicles rather than mitochondria [32]. Imaging studies have shown that ROS production caused by MPP^+ treatment of cultured DAns can results from vesicular release of dopamine rather than mtRCx I inhibition [33, 34]. Studies in nigral slices [35] and those in marmosets have similarly suggested that mtRCx I inhibition does not contribute to the pathology induced by MPTP [36]. In further support of the predominant role for vesicular dopamine release, VMAT2 overexpressing cells maintain dopamine in vesicles and resist MPP^+ [37, 38], while VMAT2 knockout mice are susceptible to MPP^+ [39, 40]. Accordingly, the selective involvement of CAergic neurons in MPTP parkinonism may result primarily from MPP^+ uptake by the DAT and not from MPP^+ inhibition of mtRCx I [34].

Neuronal Loss By Apoptosis In PD. Neuronal death can be broadly divided into two processes, necrosis and apoptosis. Morphologically, necrosis involves rapidly progressive cellular disruption marked by cell swelling, organelle disintegration, plasma membrane fracture, and cytoplasmic extrusion. In contrast, apoptosis proceeds more slowly and involves cellular degradation rather than disruption. Apoptotic degradation features cell shrinkage, plasma membrane blebbing, nuclear chromatin condensation, nuclear DNA fragmentation, maintenance of plasma membrane integrity but a loss of phospholipid asymmetry, cytoskeletal digestion, and the formation of membrane wrapped cytoplasmic and nuclear bodies. The degradation avoids the spilling of cytoplasmic contents into the extracellular space and primes cells for macrophage ingestion, thus preventing immune responses that injure neighbouring cells.

Concepts of apoptotic degradation have changed relatively little since the original descriptions thirty years ago [41, 42]. The degradation shows some variation in morphology from one form of apoptosis to another but is largely independent of cell type and the insult that initiates the process [43]. Although the degradation can be used to recognize apoptosis, it does not define the numerous signaling pathways, which set the stage for degradation and can differ markedly from one form of apoptosis from another. Over the last several years a myriad of molecules have been shown to operate within specific subcellular decisional networks that can be either pro- or anti-apoptotic (see [44] for a detailed and exciting review of organelle based signaling molecules in apoptosis). A variety of cysteine proteases (caspases) and molecules that induce or prevent increases in mitochondrial

membrane permeability function as the critical arbiters or integrators in apoptosis - they signal whether to degrade or not to degrade.

Is apoptosis involved in the neuronal loss found in PD? The use of *in situ* end labeling (ISEL), also termed as TdT dUTP nick end labeling (TUNEL), provided the initial means to recognize apoptotic nuclear DNA cleavage in neurons in PD postmortem brain but its use also engendered five years of controversy. Evidence for neuronal apoptosis in PD postmortem brain initially depended on nuclear DNA cleavage shown with ISEL [45], which appeared consistent with the subsequent finding of nuclear ultrastructural changes typical of apoptosis with electron microscopy [46]. But ISEL also seemed to rule against neuronal apoptosis in PD by the findings of : 1) similar numbers of ISEL positive nuclei in PD brain relative to controls [47]; 2) ISEL positive nuclei in glia rather than neurons [48]; and 3) large numbers of ISEL positive nuclei in control brains [49].

The conflicting evidence likely resulted from technical problems with the terminal transferase (TdT) used in ISEL (see [50] for details). TdT can label both single strand and double strand DNA breaks and can label nuclei in necrotic cells as well as apoptotic cells [51]. Depending on tissue preparation and ion concentrations, it can provide either false negatives or false positives and therefore cannot be used reliably to identify apoptotic cells.

Part of the interpretive difficulties were overcome by the application of dual labeling techniques that allowed for the simultaneous demonstration of DNA cleavage and chromatin condensation in the same nucleus. Nuclear DNA cleavage and chromatin condensation are mediated by different signaling events [52, 53]. Chromatin condensation can be readily visualized with fluorescent DNA binding dyes (see [54, 55] for our use of the dyes). The joint use of fluorescence ISEL and fluorescent DNA binding dyes allows for the demonstration of nuclear DNA fragmentation and chromatin condensation in the same nucleus [14, 50, 56]. If both are present in the same nucleus, it is virtually certain that the nucleus is undergoing apoptotic degradation. The joint labeling did not reveal high levels of apoptotic degradation in control brains or in glia in PD brains found with ISEL alone. It did show apoptotic degradation in a proportion of nigral neuromelanin containing neurons that seemed consistent with rates of loss of the neurons found in PD [14]. The number of neuromelanin-containing neurons in the PD SNc containing nuclei, which were both ISEL positive and chromatin condensation positive were about 300 times as frequent as those in the age-matched controls [14, 56].

Further conclusive evidence for apoptosis in PD was provided by two independent groups at about the same time. They demonstrated increased neuronal levels of activated caspase 3, the so called executioner caspase, in PD postmortem nigra [14, 57]. Caspase 3 is a key apoptosis signaling protein and is only found in apoptotic cells [43]. Other key pro-apoptotic signaling proteins have also been demonstrated in PD nigral neurons including Bax [58,14], caspase 8 [59], p53 [60], Fas and FasL [61, 62] and the dense nuclear accumulation of GAPDH [14]. Together these findings strongly support the view that apoptosis contributes to neuronal loss in PD and open the door to studies that fully define the apoptosis signaling pathways in PD. A complete understanding of the signaling pathways may provide insights into the cellular insults or defects that initiate the disease. Defining the signaling pathways may also offer new therapeutic approaches in PD since apoptosis-based therapies for a variety of diseases, including CGP3466 in PD (see below), are now in clinical trial (see [63] for a recent review).

Rotenone As A Potential Model Of Decreased mtRCx I Activity In PD. Rotenone, a pesticide, which occurs naturally in plants like thistles, specifically and potently reduces mtRCx I activity by inhibiting NADH dehydrogenase [64]. Animals that ingest plants containing rotenone can develop a nigropallidal, PD-like neurodegenerative condition [65] and epidemiological studies have implicated pesticides like rotenone in the increasing incidence of PD [66-68]. Rotenone is highly lipophilic so that it might be expected to cause a generalized decrease in mtRCx I activity that would not selectively damage or kill CAergic neurons and thereby mimic PD.

Injections of rotenone into the rat medial forebrain bundle, which carries the axons of SNc DAns projecting to the striatum, resulted in a depletion of striatal dopamine and dopamine metabolites, possibly as a result of selective dopaminergic axonal damage by rotenone [69]. Acute or subacute intravenous delivery of high rotenone dosages (14 - 24 mg/kg/day) to rats caused loss of neurons in the striatum and the globus pallidus, but not in the SNc [70]. The striatal damage involved focal regions of astrogliosis shown by increased glial fibrillary acidic protein (GFAP) immunoreaction with preservation

of GABA-ergic neurons, which form the majority of striatal neurons. Acute or subacute intravenous delivery of rotenone (5-15 mg/kg) to mice produced transient increases in striatal dopamine metabolites without altering dopamine levels [71], which suggested increased dopamine turnover without DAergic terminal loss. The subchronic intravenous administration of low rotenone doses (1.5 mg/kg, 3 times over 1 week) to the mice did not alter any dopamine indices.

Rotenone was also intravenously delivered to rats using Alzet osmotic minipumps at concentrations of 2 to 3 mg/kg/day over 7 to 35 days. Approximately 50% of surviving rats developed PD-like movement deficits together with pathological changes that included loss of SNc DAns and SNc neuronal protein aggregations with similarity to Lewy bodies [72]. The DAn loss was accompanied by focal areas of decreased striatal TH immunoreactivity, a marker of DAergic terminals. There was preservation of GAD and acetyl cholinesterase immunoreaction indicating that GABA-ergic and cholinergic neuronal populations were unaffected by rotenone. The prolonged low dose intravenous rotenone induced ubiquinated cell body protein accumulations in a proportion of surviving SNc DAns. The accumulations were α-synuclein immunopositive and shared features with PD Lewy bodies. Together with the SNc DAn loss, the Lewy body-like accumulations suggest that chronic rotenone treatment can mimic PD pathology.

Rotenone Induces or Reduces Apoptosis. *In vitro*, acute rotenone treatment has been shown to induce apoptosis in a variety of different cells in culture, including tumor cells [73], PC12 cells [74, 75], myeloid cells [76], lymphoblasts [77], SK-N-MC dopaminergic cell lines [75], HL-60 cells [64, 78], AK-5 tumor cells [79], PAJU human neuroblastoma cells [80], liver cells [81], human dopaminergic neuron-like cells [82], and cerebellar granule neurons [83]. In contrast, rotenone has been found to reduce apoptosis in models like 1-O-octadecyl-2-methyl- rac-glycero-3-phosphocholine in p53-defective hepatocytes [84], glutamate in rat hippocampal neurons [85], hypoxia in cardiac myocytes [86] and protein kinase C overexpressing keratinocytes [87]. In short, rotenone can either increase or decrease apoptosis, depending on cell type and the insult that initiates the apoptosis.

Rotenone Reduces, Rather Than Increases, ROS Generation *In Vitro.* Imaging studies of cultured neurons, including DAns [33, 34] or neuron-like cells [88] utilized dyes whose fluorescence increases in proportion to the concentrations of superoxide or peroxyl radicals. Those studies showed that decreased mtRCx I activity caused by rotenone is accompanied by a decrease, rather than an increase, in ROS levels [33, 88, 89]. Like those studies, we have also found that acute rotenone treatment of cultured CAergic neuron-like cells decreases peroxyl levels and does not alter superoxide levels in the somata of the cells (see below). Therefore, decreased mtRCxI activity may not induce neuronal loss through ROS peroxidation of macromolecules which was previously supposed to form the basis for neuronal death caused by decreased mtRCx I activity [90, 91].

Rotenone, Mitochondrial Membrane Permeability, Mitochondrial Membrane Potential ($\Delta\Psi_M$) And The Mitochondrial Permeability Transition Pore Complex (PTPC). Mitochondria can play a role in either apoptotic or necrotic cell death [92]. Cytochrome c, AIF and smac/diablo are constituents of the mitochondrial intermembrane space. Once released into the cytosol, cytochrome c binds to Apaf-1 and leads to the activation of caspases, particularly caspase 3. Smac/diablo counteracts inhibitor of apoptosis proteins (IAP) capacity to prevent caspase activation [93-95], while AIF activates nuclear endonucleases [96, 97]. The mechanisms which increase permeability of the outer mitochondrial membrane and allow the release of the three proteins are incompletely understood. Two processes have been implicated: 1) the formation of channels in the outer membrane and 2) mitochondrial swelling due to opening of the PTPC causing outer membrane rupture [98, 99] .

A number of studies have used cyclosporin A (CSA), N-methyl-4-valine cyclosporin (N-Val-CSA) or bongkrekic acid (BA), each of which facilitates PTPC closure, to determine whether the PTPC opening contributes to cell death caused by rotenone. Studies using CSA in rotenone treated cells suggested that apoptosis due to mtRCx I inhibition depended on PTPC opening [75, 81, 100]. The PTPC closing agents decrease apoptosis and prevent decreases in $\Delta\Psi_M$ that are thought to result from dissipation of the transmembrane proton gradient caused by PTPC opening (see [92, 101, 102] for

reviews). Similar to studies in other cell types [103-106], we have used CSA and BA in CAergic neuron-like cells to reduce apoptosis and prevent $\Delta\Psi_M$ dissipation caused by rotenone (see below). BA was particularly effective at concentrations as low as 10^{-9} M.

GAPDH In Neurodegeneration And Apoptosis – GAPDH was found to co-immunoprecipitate with the mutant proteins in Huntington's disease (HD) and related degenerative conditions [107]. It was hypothesized that GAPDH binding to the mutant proteins might impair glycolysis [108] but that possibility has not been supported by glycolytic measurements in postmortem brain tissue and cultured cells [54, 109, 110].

Studies with antisense oligonucleotides showed that GAPDH is essential to the progression of apoptosis involving a variety of neuronal cells [111, 112]. GAPDH mRNA and protein levels increase in neurons early in apoptosis caused by reduction of media K^+ [113, 114], cytosine arabinoside exposure [112] and aging [111]. We found that GAPDH levels begin to increase at 1.5-2.0 hours after serum and NGF withdrawal, which is 4 hours before nuclear DNA cleavage and chromatin condensation began to appear in the same cells [54]. Studies with antisense oligonucleotides have shown that p53 is upstream to GAPDH increases in apoptosis [115].

In non-apoptotic cells, GAPDH is primarily in the extra-nuclear cytoplasm with sparse localization to small punctate areas in the nucleus [116]. In apoptosis involving GAPDH upregulation, GAPDH accumulates densely in the nucleus [54, 117-119], which serves as a marker of GAPDH associated apoptosis.

We cloned a GAPDH cDNA from rat brain and used the cDNA to produce a GAPDH-green fluorescent protein (GFP) construct [120], which was transiently transfected transiently into COS1 cells and stably transfected into HEK 293 cells. The living cells had little or no GAPDH-GFP protein in their nuclei and showed a distribution for the fusion protein that was largely cytosolic. The GAPDH-GFP fusion protein progressively accumulated in the nucleus of a proportion of the cells in the first two hours after exposure to apoptosis initiating agents, which established that GAPDH movement from the cytosol to nucleus occurs dynamically during the early stages of apoptosis. Our western blots for the nuclear subcellular fraction have shown progressive increases in nuclear GAPDH immunoreaction over the first 3-6 hours of some forms of apoptosis [54]. Ischitani et al. have used antibodies that are specific for GAPDH tetramer or for GAPDH dimer/monomer to show that the dimer/monomer form rather than the tetramer form translates to the nucleus in apoptosis (personal communication).

We recently showed that GAPDH co-localizes and co-immunoprecipitates with promyelocytic leukemia (PML) protein [116]. The co-localization and co-immunoprecipitation depended on an association of the proteins with RNA. PML protein is pro-apoptotic and is involved with nuclear proteins that control translation [121-125]. Our finding is in keeping with previous work suggesting that GAPDH modulates transcription or translation [126].

Deprenyl-Related Propargylamines Target GAPDH To Reduce Apoptosis. (-)-Deprenyl, an MAO-B inhibitor, was first used in PD together with levodopa to reduce dopamine metabolism and increase striatal dopamine availability [127, 128]. Studies of MPTP toxicity in the monkey [129] were interpreted to show that (-)-deprenyl reduced dopaminergic neuronal necrosis caused by ROS generated by dopamine metabolism. The finding fostered clinical trials examining the effect of (-)-deprenyl on the clinical progression of PD (see [130-134] for examples). The trials provided clear evidence that (-)-deprenyl slows the clinical progression of PD. There has not been agreement on the mechanisms responsible for the slowing (see [132, 135-137]), particularly whether the results indicate slowing of neuronal death in the disease.

Although it is uncertain whether (-)-deprenyl slows the progressive neuronal death in PD, it does reduce neuronal death in a wide variety of *in vivo* and *in vitro* experimental models. The models have included neuronal death induced by 6-hydroxydopamine [138], MPP^+ [139-146]; MPTP [129, 144, 147], nitric oxide or peroxynitrite [148], DSP-4 [149-151]; glutathione depletion [152], peripheral nerve crush or axotomy [153-157]; optic nerve crush [158]; hypoxia and/or ischemia [159] [160-163]; cytosine arabinoside [164]; excitotoxins [165] [163, 166, 167], trophic insufficiency [54, 55, 168, 169]; thiamine deficiency [170] and aging [171-174].

A number of investigations have established that (-)-deprenyl can reduce neuronal death independently of MAO-B or MAO-A inhibition [141-144, 149, 153, 165, 175, 176]. Studies in a number of models have shown that (-)-deprenyl can reduce apoptosis [55, 80, 141, 148, 159, 164, 165, 168, 169, 177-189]. The reduction of apoptosis by (-)-deprenyl has been found to involve prevention of decreases in mitochondrial membrane potential [55, 164], which may indicate maintenance of mitochondrial membrane impermeability.

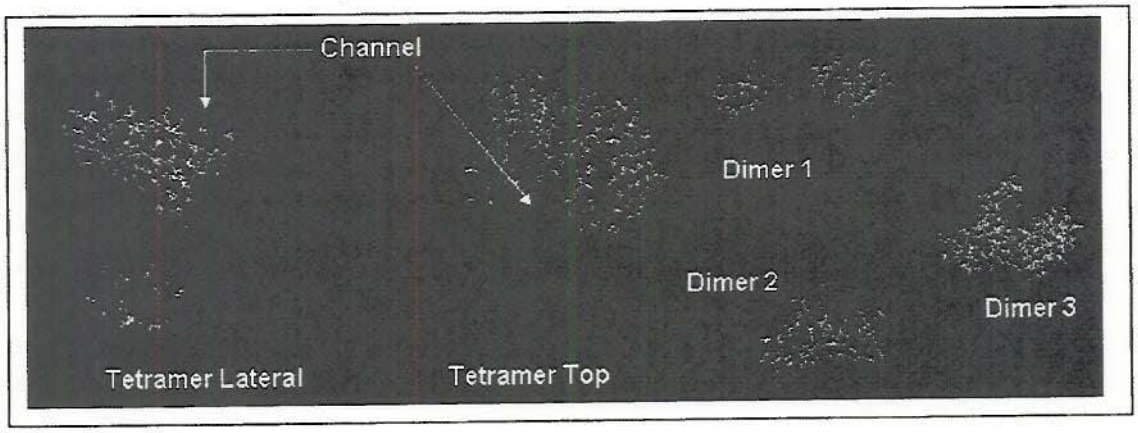

Figure 1 – Conversion of GAPDH Tetramer To A Dimer By CGP3466 In Solution. Our use of Size exclusion chromatography showed that the tricyclic deprenyl analog, CGP3466 and other propargylamines convert GAPDH tetramer to a dimer in solution [54]. The figure shows a computer generated model of GAPDH three dimensional structure based on yeast crystal structure with substitution of human amino acid differences (see higher resolution images and the details of our image generation in [54]). Our studies indicated that CGP3466 binds into the channel of GAPDH in order to convert the tetramer to dimer, likely dimer 3 shown in the figure and stabilizes the protein in that form. Studies by Ishitani and coworkers (Ishitani, personal communication) have shown that GAPDH translocates to the nucleus in apoptosis as a monomer or as dimer 1 or dimer 2. Antibodies against dimers 1 or 2 or against GAPDH monomer but not GAPDH tetramer block MPP+ induced apoptosis in cultured dopaminergic neurons [190].

Together with workers at Novartis, we developed a tri-cyclic deprenyl analog, CGP3466 [191], which reduces a number of forms of apoptosis in a variety of models, but does not inhibit MAO-B [192]. Photoaffinity labeled CGP3466 [193] established that CGP3466 binds to GAPDH in rat hippocampus [80] and cultured catecholaminergic cells [54]. (-)-Deprenyl and CGP3466 reduce apoptosis over similar concentration ranges (10^{-5} to 10^{-11} M) [54, 80]. CGP3466 prevented the GAPDH upregulation and the dense GAPDH nuclear accumulation typical of GAPDH-associated apoptosis [54]. We used size exclusion chromatography to show that the CGP3466 converted GAPDH from a tetramer to a specific dimer in solution ([54] and figure 1). Our findings suggest that CGP3466 binding to GAPDH prevents apoptosis signaling by the protein, while allowing it to retain glycolytic capacity.

We initially showed anti-apoptosis by (-)-deprenyl requires new protein synthesis [168]. It was not known how changes in new protein synthesis might cause the reduced apoptosis induced by propargylamines like CGP3466. We have now used metabolic labeling and western blotting to show that the propargylamines induce marked changes in new protein synthesis, particularly in the nuclear and mitochondrial protein fractions, and that those changes affect apoptosis related proteins (see below). It remains to be determined how propargylamine binding to GAPDH might induce anti-apoptotic new protein synthesis.

Report Of Progress

Progress In Ascertaining Whether GAPDH Contributes To Apoptosis In A Decreased mtRCx I Activity Model Of PD - In our previous progress report, we presented our findings from work aimed at investigating mechanisms of GAPDH and mitochondria in apoptosis signaling. Although MPTP has provided the standard model of PD over the last 20 years, a number of recent findings indicate that the capacity of MPTP to model decreased mtRCx I activity PD is limited. In contrast, rotenone may offer a superior PD model from the aspect of decreased mtRCx I activity. Studies of postmortem brain suggest that GAPDH signaling may be implicated in PD neuronal apoptosis. Accordingly, we sought to determine whether rotenone models the GAPDH-related aspects of PD.

Rotenone Induced Apoptosis Requires New Protein Synthesis, Including A Pathway Involving Increased GAPDH Levels And Dense GAPDH Nuclear Translocation. Some forms of apoptosis require the new synthesis of proteins, while other forms do not (see discussion in [194], appended). We used actinomycin D at 2 μg/ml and cycloheximide at 8 μg/ml to inhibit transcription and translation respectively in NGF differentiated PC12 cells, a CAergic neuron-like cell line. The cells were exposed to varying rotenone concentrations. In other studies, we had showed that those concentrations of actinomycin D and cycloheximide did not decrease survival of the serum and NGF supported CAergic cells but did decrease levels newly metabolically labeled proteins in the cells by 94% or greater ([194], appended). The protein synthesis inhibition revealed that about two-thirds or more of the decreased survival induced by rotenone required new protein synthesis (figure 2) and established that new protein synthesis is required for rotenone induced apoptosis in the cells

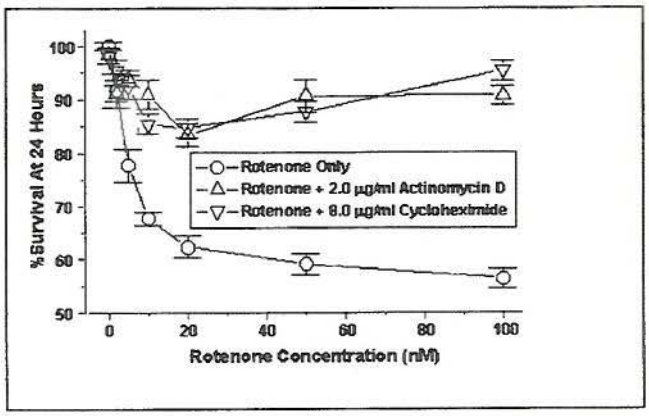

Figure 2 –Transcriptional Inhibition And Translational Inhibition Reduce The Loss Of Catecholaminergic Neuron-Like Cells Induced By Rotenone. Actinomycin D and cycloheximide were utilized to determine whether apoptosis induced by rotenone depends on new protein synthesis . Both inhibitors increased cell survival indicating that a major proportion of the decreased survival induced by rotenone depends on new protein synthesis in the cultured cells. The proteins that are newly synthesized in rotenone induced apoptosis are not known. It is also not known whether or how decreased mtRCxI activity induces the new protein synthesis.

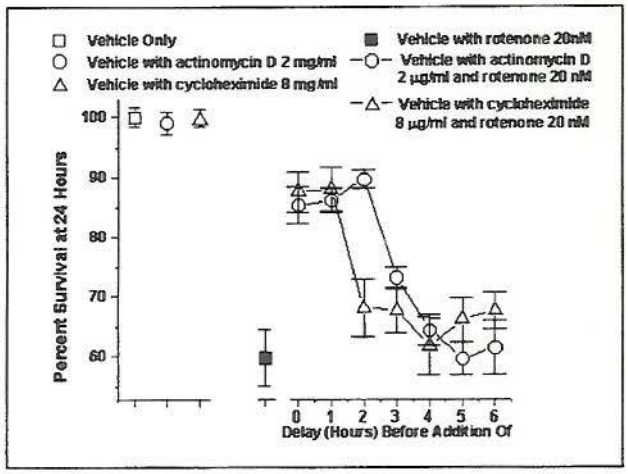

Figure 3 – Delayed Application Of Transcriptional And Translational Inhibitors Reveals the Timing Of Expression Of Essential Apoptotic Proteins. Experiments in which the application of the transcriptional and the translational inhibitor were delayed relative to the addition of rotenone to the cultured catecholaminergic cells showed that the genes for proteins that are essential to decreasing survival were translated between 0 and 3 hours after rotenone addition. Our western blots have shown that GAPDH levels begin to increase between 2.5 and 3.0 hours after rotenone addition to the cultured cells

Experiments in which the application of new protein synthesis inhibitors was delayed relative to the addition of rotenone indicated that pro-apoptotic new protein synthesis induced by rotenone was largely transcribed and translated

between 1 and 4 hours after rotenone addition (figure 3, also see [194] appended for details of the methods and interpretation of the delay experiments). GAPDH has been shown to upregulate in a number of forms of neuronal apoptosis and antisense oligonucleotide application or intracellular antibody injection has shown that increased synthesis of GAPDH is essential to the neuronal apoptosis [54, 111, 113, 114], including apoptosis induced by MPP^+ in primary cultures of dopaminergic mesencephalic neurons [190]. Accordingly, GAPDH synthesis is critical to some forms of apoptosis. We previously found that GAPDH levels increased at 1.5 to 2 hours after serum and NGF withdrawal from the CAergic cells [54]. In the present experiments, We found that GAPDH levels increase in the CAergic cells after exposure to rotenone. GAPDH levels were found to be increased by 3 hours after rotenone application and the GAPDH immunodensity varied with rotenone concentration for concentrations of 2 - 20 nM according to a U shaped relationship with the maximum increase for 10 nM (figure 4).

An identifying feature of apoptosis involving GAPDH signaling is the dense nuclear accumulation of GAPDH immunoreaction [54, 117-119], due to GAPDH translocation from the cytosol to the nucleus [120]. GAPDH is normally sparsely distributed in the nucleus in association with promyelocytic leukemia (PML) protein [116]. Since dense accumulation GAPDH nuclear immunoreaction has been found in neuromelanin containing neurons of the PD SNc [14], we examined the CAergic neuron-like cells acute rotenone exposure for GAPDH dense nuclear accumulation.

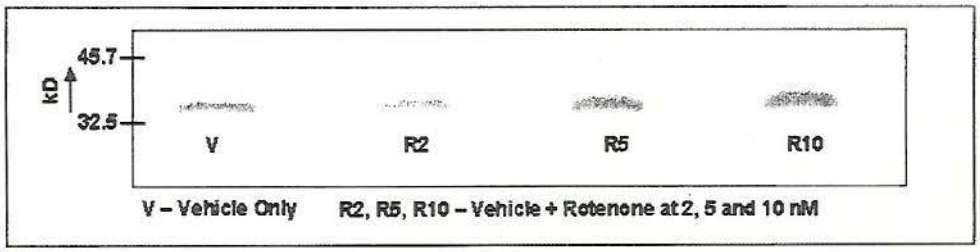

Figure 4 - Rotenone Increases GAPDH Levels In A Concentration Dependent Manner. Western blots showed that rotenone concentrations which induced decreases in mtRCxI activity of 15-45%, also increased GAPDH levels in a concentration related fashion beginning at 2-3 hours after the rotenone addition (this blot is for 6 hours after rotenone addition).

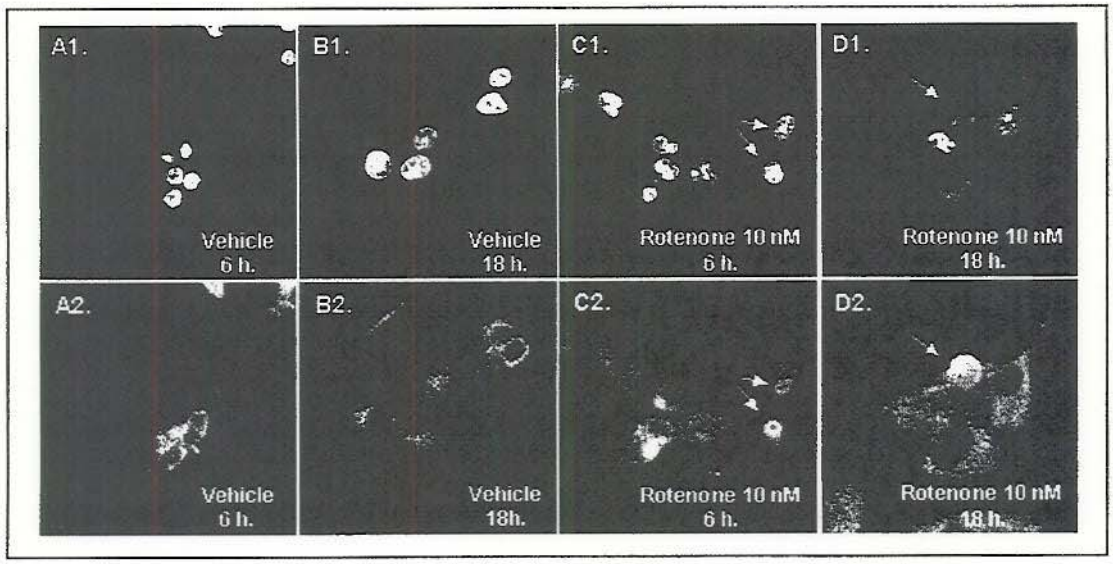

Figure 5 - Rotenone Induces Accumulation Of Dense Nuclear GAPDH Immunoreaction - Rotenone induced GAPDH dense nuclear immunoreaction typical of GAPDH signaling in apoptosis. Vertical pairs of LCSM images are for identical image fields. Upper images are for YOYO-1 staining of DNA and lower images for GAPDH immunofluorescence. A1,A2 and B1,B2 are for vehicle treated cells and C1,C2 and D1,D2 for rotenone treated cells. The arrows denote nuclei with dense nuclear GAPDH immunoreaction.

fragmented DNA typical of apoptotic degradation (figure 7C).

Rotenone concentrations of 5 to 20 nM induced 32 and 38% decreases in survival respectively (figure 8A) and mean decreases in mtRCxI activity of 16 to 60 % (figure 8B). Concentrations of 10 and 20 nM induced the maximum percentages of cells with nuclear chromatin condensation (figure 8E, typical chromatin condensation associated with cell/nuclear shrinkage is illustrated in 8C1/C2 and 8D1/D2). These data suggest that 10 nM is the most effective concentration for inducing apoptosis in

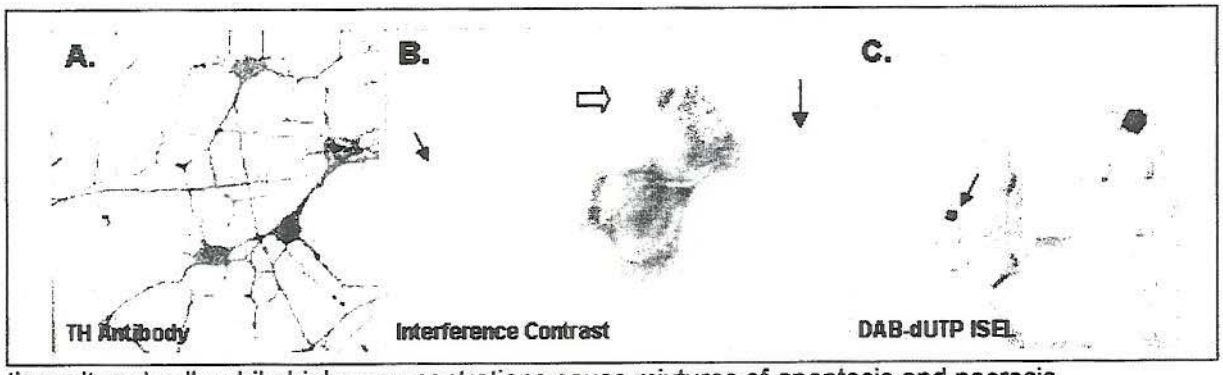

the cultured cells while higher concentrations cause mixtures of apoptosis and necrosis..

Figure 7 – Rotenone Induced Process Damage And Apoptosis In CAergic PC12 Cells - A. shows immunoreaction for an antibody against TH in NGF differentiated PC12 cells. **B.** Higher power interference contrast LCSM image of rotenone treated NGF differentiated PC12 cells showing a shrunken cell with a condensed nucleus (marked by open arrow) and two other cells with normal cell bodies and nuclear morphology but truncation of their processes (shown by small arrows). **C.** dUTP in situ DNA end labeling demonstrating nuclear DNA fragmentation typical of apoptotic nuclear degradation in a shrunken NGF differentiated PC12 cell (marked by an arrow and shown at higher magnification in the inset image).

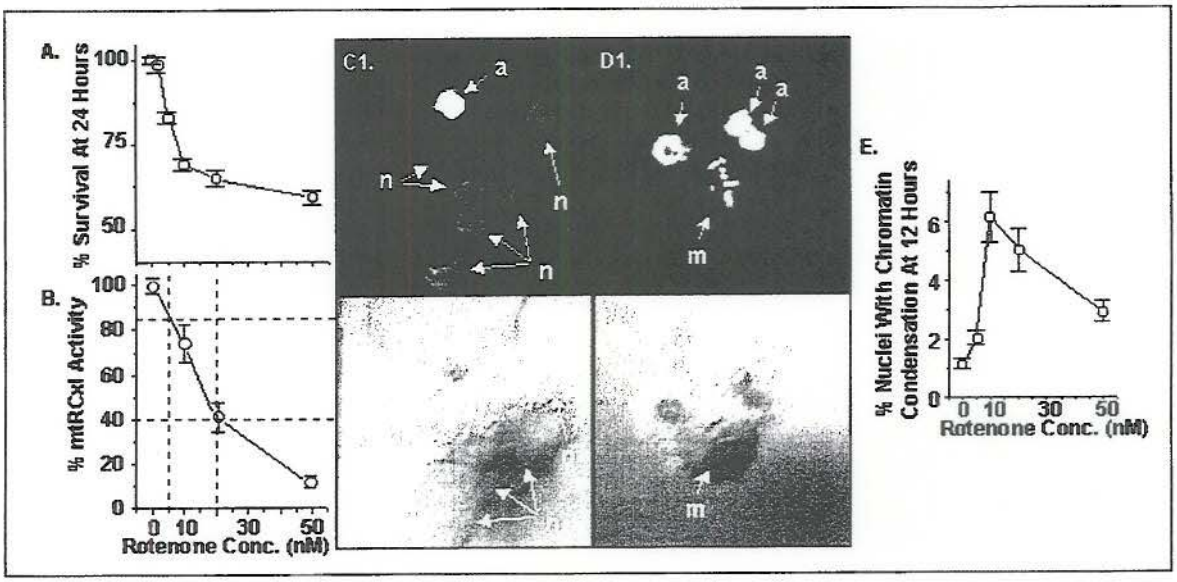

Figure 8 – Rotenone Reduces Survival, Induces Apoptosis And Decreases mtRCxI Activity In NGF Differentiated, Catecholaminergic PC12 Cells In Culture. A. shows the % survival of the cells at 24 hours after the application of different rotenone concentrations while B. shows the % mtRCxI activity versus rotenone concentration for the mitochondrial fraction of cell lysates at 3 hours after rotenone addition. The C1/C2 and D1/D2 pairs are for identical laser confocal image fields. The upper images of each pair are for the fluorescence of the nucleic acid binding dye YOYO-1 and the lower images are interference contrast images. The images show typical nuclei with chromatin condensation (labeled a),

As shown in figure 5, rotenone exposure of the CAergic cells induced dense nuclear GAPDH immunofluorescence in a proportion of the cells and the dense nuclear accumulation was not present in vehicle treated cells (compare figure 5 A1/A2 and B1/B2 to C1/C2 and D1/D2). Accordingly, decreased mtRCx I activity caused by rotenone exposure induces GAPDH upregulation and dense nuclear GAPDH accumulation similar to that found in SNc neuromelanin containing neurons in PD postmortem brain.

Chronic Rotenone Exposure Induces Ubiquitin Immunopositive Aggregations In The Cell Bodies Of Cultured Catecholaminergic Cells. DAergic neurons in the rat SNc have shown protein aggregations with similarity to Lewy bodies found in PD after chronic intravenous rotenone exposure [72]. This contrasts to MPTP or MPP+ treated cells which do not show PD-like protein accumulations. We treated NGF differentiated CAergic neuron-like cells for 8 to 21 days with 1 to 2 nM of rotenone. The rotenone containing media was replaced daily. About 17% of cells surviving for 14 to 21 days showed patchy regions of intense ubiquitin immunofluorescence (see figure 6). Although ubiquitin is a marker of Lewy bodies [12], α-synuclein has become to be considered as the major component of Lewy bodies [13, 195] and it has been shown that α-synuclein aggregations and even fully formed Lewy bodies are prominent constituents of axons and terminals of CAergic neurons in PD and several related conditions [196]. Our preliminary findings showed that α-synuclein immunofluorescence co-localized with the patchy ubiquitin immunofluorescence in cell bodies. While ubiquitin and α-synuclein were localized to the peripheral portion of the patches, GAPDH immunofluorescence localized to the central portion . In PD Lewy bodies, the three proteins are found with a similar distribution - ubiquitin and α-synuclein in the peripheral or radial portion of the bodies and GAPDH in the central portion [14].

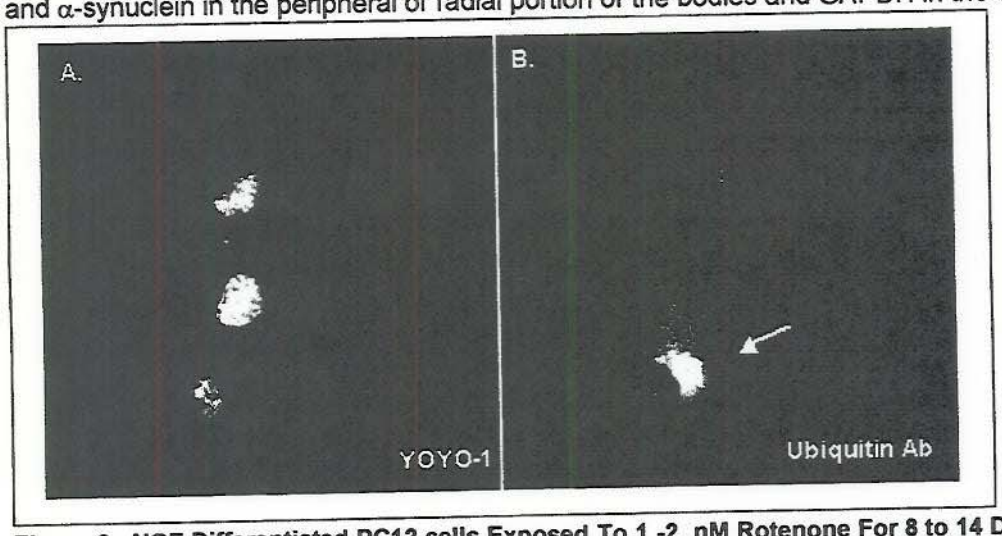

Figure 6. NGF Differentiated PC12 cells Exposed To 1 -2 nM Rotenone For 8 to 14 Days Show Cell Body Ubiquitin Immunopositive Accumulations With LCSM A. and B. are for identical image fields. A. shows YOYO-1 fluorescence for nuclear DNA while shows ubiquitin immunofluorescence. Approximately 17% of the surviving CAergic neuron-like cells showed ubiquitin immunopositive cell body accumulations similar to that in B.

Progress In Determining The Mechanisms Of Neuronal Loss Caused By Decreased mtRCx I Activity.

Decreased mtRCxI Activity Caused By Rotenone Is Associated With Process Withdrawal And Apoptosis Of Cultured Catecholaminergic Cells. We examined the effects of acute rotenone treatment on NGF differentiated PC12 cells. As illustrated in figure 7A, the cells are catecholaminergic as shown by their tyrosine hydroxylase (TH) immunoreactivity. Single applications of rotenone (5 to 20 nM) induced process truncation (solid arrows in figure 7B) with cytosolic and nuclear shrinkage of a proportion of the cells (open arrow in figure 7B). ISEL showed that the shrunken nuclei contained

normal nuclei (labeled n) and one nucleus in mitosis (labeled m), each at 12 hours after treatment with 10 nM rotenone. E. shows the relationship between the % nuclei with chromatin condensation versus rotenone concentration at 12 hours after treatment with 10 nM rotenone. Rotenone concentrations of 5 to 20 nM induced 32 and 38% decreases in survival respectively (figure 3A) and mean decreases in mtRCxI activity of about 16 to 60 % (figure 3B). Concentrations of 10 and 20 nM induced the maximum percentages of cells with nuclear chromatin condensation (figure 3E, typical chromatin condensation associated with cell/nuclear shrinkage is illustrated in 3C1, C2 and 3D1, D2). These data suggest that 10 nM is the most effective concentration for inducing apoptosis in the cultured cells while higher concentrations increasingly induce necrosis.

Loss Of CAergic Cells Induced By Rotenone In Culture Is Caspase Dependent But Is Energy Independent And Can Be Modulated By The Availability Of Glycolytic ATP

Previous research has shown that apoptosis induced by rotenone in AK-5 cells is caspase dependent [79]. We found that rotenone increased levels of activated caspase 3 in cells with evidence of nuclear chromatin condensation after rotenone exposure (figure 9 A1 and A2). The irreversible general caspase inhibitor ZVAD-FMK at concentrations of 10 μM induced maximum reversal of the decreased survival induced by rotenone (figure 9B). An average of approximately two-thirds of the decreased survival were reversed at different rotenone concentrations, suggesting that a major portion of the cellular loss induced by rotenone was caspase dependent. Accordingly, GAPDH associated apoptosis induced by rotenone is caspase dependent, particularly caspase 3 dependent, which is similar to the apoptosis found in neuromelanin containing neurons in the SNc of PD postmortem brain (see references above).

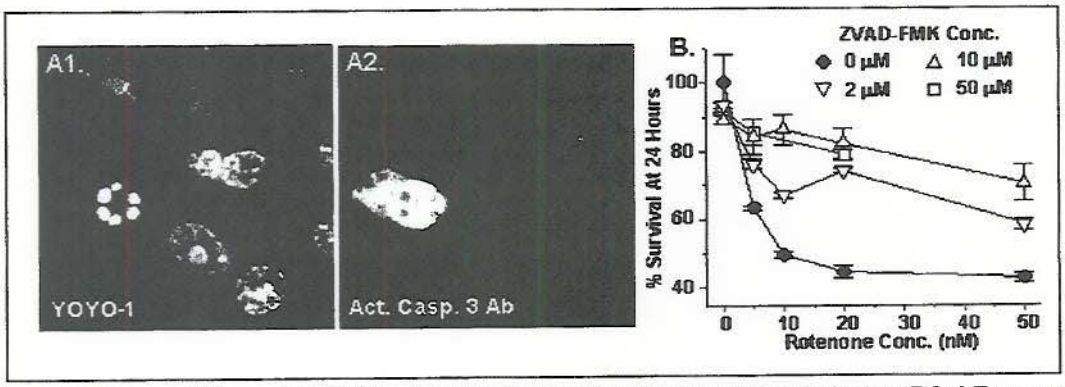

Figure 9 – General Caspase Inhibitor Increases Survival After Rotenone And mtRCxI Energy Or Glucose Dependence Of Rotenone Induced Neuronal Death. A1. and A2. show identical LCSM image fields. YOYO-1 staining shows one nucleus with chromatin condensation in a number of nuclear bodies. Other nuclei show normal staining. The cell with nuclear chromatin condensation shows high levels of activated caspase 3 immunofluorescence. **B.** ZVAD-FMK at varying concentrations was delivered to the cells 30 minutes prior to rotenone addition. ZVAD-FMK is an irreversible, cell permeant caspase inhibitor.

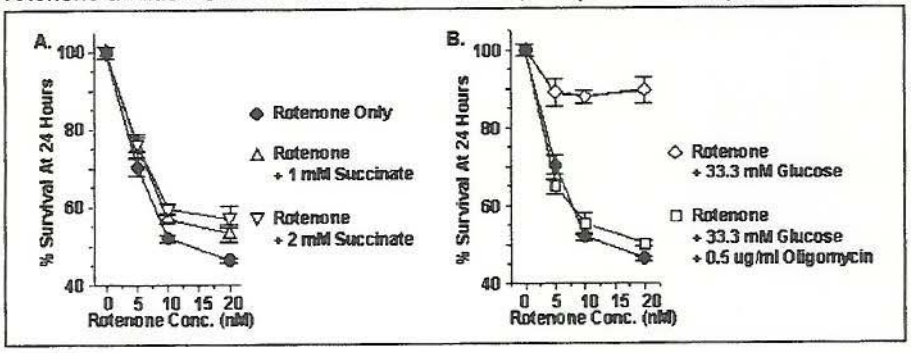

Figure 10 –Mitochondrial Energy Independence And Glycolytic Energy Dependence Of Rotenone Induced Neuronal Death. A. High concentrations of succinate provide energy to mitochondrial complex II, bypassing energy decreases induced by rotenone by inhibiting mtRCxI. The plots show that less than 10% of the death is mtRCxI energy dependent for rotenone concentrations of 10 nm or less, concentrations, which largely induce apoptosis (see above). About 15% of the death caused by 20 nM rotenone is mtRCxI energy dependent.

B. Increased glycolytic ATP produced by high glucose concentrations is used by ATP synthase to reverse pump protons outward across the inner mitochondrial membrane and can reduce decreases in $\Delta\Psi_M$ caused by mtRCxI inhibition (see below and [198]). We found that high glucose concentrations in the supporting media reverses 75% or more of the cell loss induced by rotenone and that oligomycin, an ATP synthase inhibitor, blocks the compensation offered by high glucose concentrations.

We used varying concentrations of succinate, the substrate for mitochondrial respiratory complex II [197], in order to assess the role that decreased provision of energy by mtRCxI played in the reduced survival induced by rotenone (figure 10A). The experiments revealed that increasing energy provision to complexes II - IV induced relatively small increases in survival and therefore showed that a reduction in energy provision by mtRCx I played little role in rotenone induced apoptosis in the differentiated PC12 cells. Deficient energy availability has been a central tenet of the hypothesized mechanisms of PD neuronal loss caused by decreased mtRCx I activity and now must be re-evaluated.

A second series of experiments provided high glucose concentrations to the cells as a means of increasing the availability of glycolytic ATP (see [198] for our similar experiments with MPP^+). The experiments showed that high glucose largely reversed the decreased survival caused by rotenone (figure 10B) and that oligomycin, a selective inhibitor of mitochondrial ATP synthase, almost completely eliminated the prevention of cell loss provided by high glucose. A number of studies have shown that ATP synthase can use glycolytic ATP to pump protons outward across the inner mitochondrial membrane and thereby maintain $\Delta\Psi_M$ (see [198] for details). mtRCx I as well as complexes III and IV normally use energy extracted from NADH, reduced ubiquinone and cytochrome C to pump protons outward across the inner mitochondrial membrane and the resulting transmembrane proton gradient contributes to the generation of $\Delta\Psi_M$. Accordingly, it appears that reverse proton pumping by ATP synthase can compensate for neuronal death caused by mtRCx I inhibition

Rotenone Does Not Increase ROS Levels In Cell Bodies Of CAergic Neuron-Like Cells. We used the dyes 2'-7'-dichlorofluorescein ($DCFH_2$-DA) [199-201] and dihydroethidium (HEth) [202-204] to estimate peroxyl radical and superoxide radical levels in the cell bodies of the CAergic cells after rotenone treatment (see figure 11 for typical LCSM images for the two dyes).

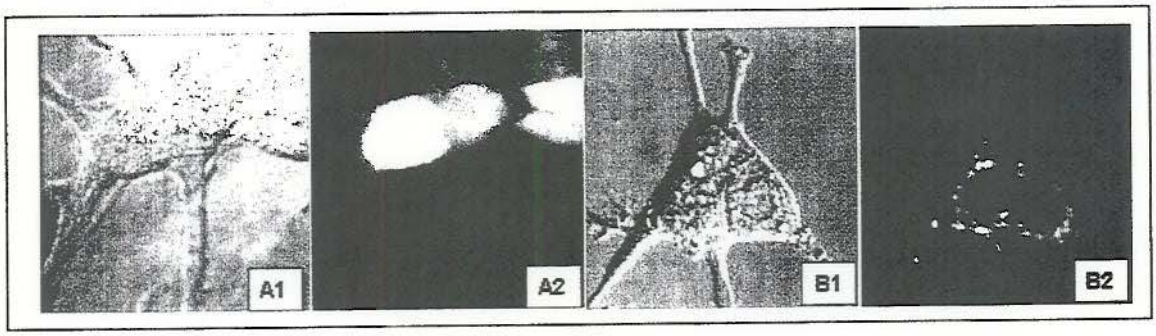

Figure11 - $DCFH_2$-DA and Dihydroethidium LCSM Images. A1 and B1 are LCSM interference contrast images while **A2 and B2** present 2', 7'-dichlorofluorescein and ethidium ion fluorescence in the cell bodies of living NGF differentiated PC12 cells. The images were taken at maximum gain to display the localization of the ROS fluorescence. Note the cell to cell variation in peroxyl radical induced fluorescence shown by DCF in A2 and the punctate nature of superoxide radical induced fluorescence in B2. The cells were treated with 10 nM rotenone 3 hours prior to the imaging.

Loss of mitochondrial energy due to decreased mtRCx I activity, which in turn fosters increased ROS levels leading to neuronal death, has been a central hypothesis for the basis of neuronal loss in PD. Our findings suggest that decreased mtRCx I activity is not necessarily accompanied by either of those defects. Accordingly, decreased mtRCx I activity may induce neuronal apoptosis in PD through other means.

Rotenone Decreases $\Delta\Psi_M$ In Cell Body Mitochondria Of Catecholaminergic Cells And Opening Of The Mitochondrial Permeability Transition Pore Contributes To Rotenone Induced Apoptosis. Decreases in $\Delta\Psi_M$ accompany a number of forms of apoptosis and likely result from increases in the permeability of the inner mitochondrial membrane with dissipation of the transmembrane protein gradient. As shown in figure 13, we found that rotenone induced a concentration dependent decrease in $\Delta\Psi_M$ and oligomycin caused a further decrease in $\Delta\Psi_M$. This data (also see above) suggest that ATP synthase partially compensates for caused by rotenone, likely by pumping protons out across the inner membrane using energy provided by glycolytic ATP. In other experiments, succinate was added as in the survival experiments shown above (data not shown) and revealed that provision of substrate to complex II did not significantly alter the rotenone-$\Delta\Psi_M$ relationships. This suggested that a reduction in proton pumping by mtRCxI is unlikely to be a major factor in the generation of the decreased $\Delta\Psi_M$ caused by rotenone induced decreases in mtRCx I activity.

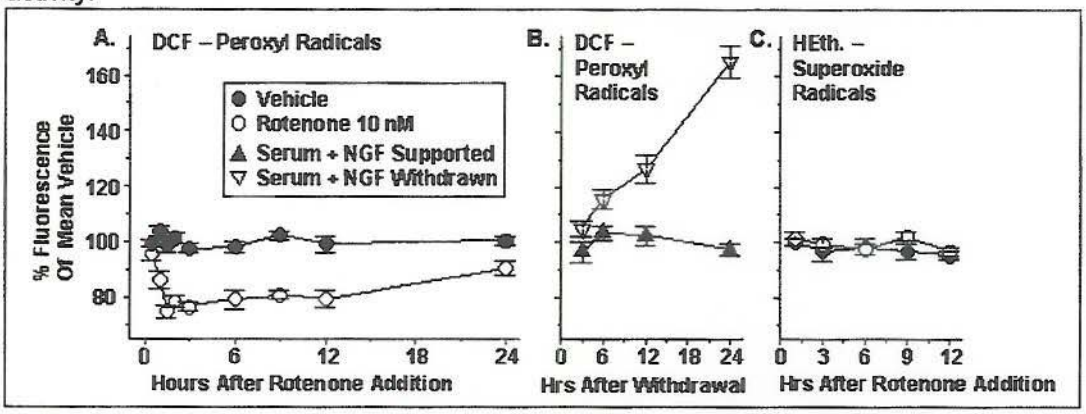

Figure 12 - Rotenone Decreases Peroxyl Radicals And Does Not Alter Superoxide Radical Levels In The Cell Bodies Of Living Catecholaminergic Neuron-Like Cells - A. Peroxyl radical levels estimated from LCSM images of living cells that compared vehicle treated to 10 nM rotenone treated cells at time points varying from 30 minutes to 24 hours after treatment. B. Peroxyl radical levels estimated by $DCFH_2$-DA induced florescence compared in serum and NGF supported versus serum and NGF withdrawn cells at multiple time points (see [55] for more details). C. Superoxide radical levels shown by HEth. florescence comparing cells treated with 10 nM rotenone or vehicle. All points are for 200 to 400 cell body measurements in living cells.

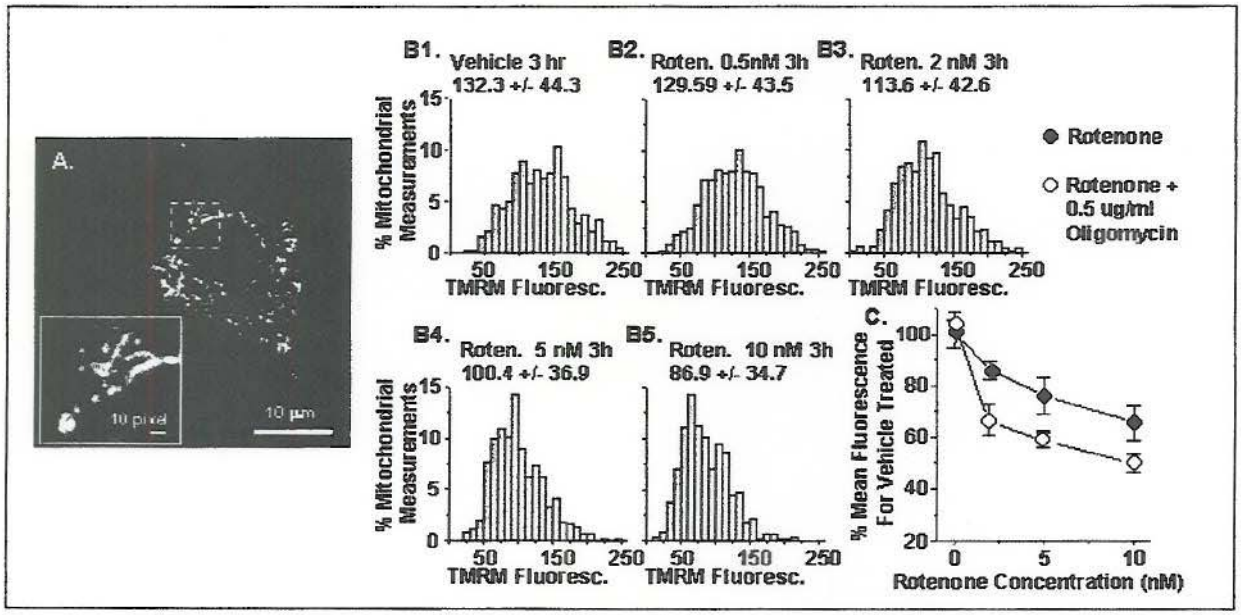

Figure 13 - Measurement Of $\Delta\Psi_M$ In Live Cells Exposed To Varying Concentrations Of Rotenone. We used three different mitochondrial potentiometric dyes to measure $\Delta\Psi_M$ by imaging dye fluorescence with LCSM (see [55] appended for details). A. Typical image for Tetramethylrhodamine methyl ester (TMRM) fluorescence is shown for single NGF differentiated PC12 cells. The inset is included to demonstrate the capacity to resolve single mitochondrial profiles. **B1. - B5.** TMRM, used in living cells, revealed a rotenone concentration dependent shift of the distributions found for mitochondrial fluorescence toward lower values (each distribution represents 600 - 900 measurements) that was evident as early as 30 minutes after rotenone addition. The decreases remained unchanged after 3 hours. **C.** Addition of oligomycin with rotenone increased the shifts toward lower values. Oligomycin is an inhibitor of ATP synthase and blocks glycolytic ATP proton pumping by ATP synthase that partially compensates for $\Delta\Psi_M$ dissipation.

Several studies have shown that agents, which facilitate closure of the PTPC, can reduce cell death caused by rotenone [75, 81, 100]. We found that BA, which binds to the adenine nucleotide translocator (ANT), a major component of the PTPC, and cyclosporine A, which prevents cyclophilin D binding to ANT , both increased the survival of rotenone treated cells (figure15A). BA was most effective at 10^{-9} M and was able to increase survival to a significantly greater extent than CSA (data not shown). We also used LCSM imaging of 5,5',6, 6'-tetrachloro-1,1',3,3'-tetraethybenzimidazol carbocyanine iodide (JC-1) fluorescence to estimate $\Delta\Psi_M$ in living cells (see [55] for details and figure 14 for an example). The studies showed that 10^{-9} M BA markedly attenuated the decreased $\Delta\Psi_M$ induced by rotenone (figures 7B1-7B3 and 7C1 -7C3). We interpret these findings to show that both the decrease in survival and the decrease in $\Delta\Psi_M$ caused by rotenone in the cultured Catecholaminergic cells were in large part due to opening of the PTPC.

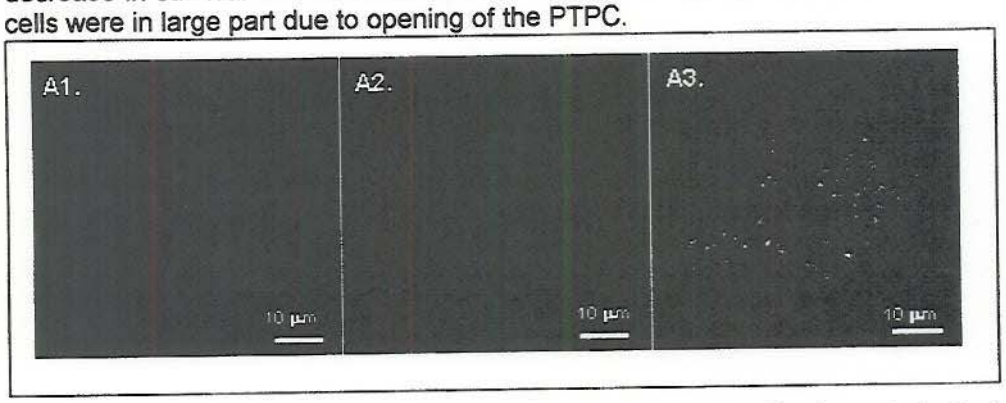

Figure 14 - Typical images for 5,5',6, 6'-tetrachloro-1,1',3,3'tetra-ethybenzimidazol carbocyanine iodide (JC-1) fluorescence to estimate $\Delta\Psi_M$ in living cells living NGF differentiated PC12 cells. The red-green added figure in C3 illustrates the range of $\Delta\Psi_M$ in different mitochondrial profiles (green indicates low $\Delta\Psi_M$, yellow indicates intermediate $\Delta\Psi_M$ and orange-red indicates high $\Delta\Psi_M$).

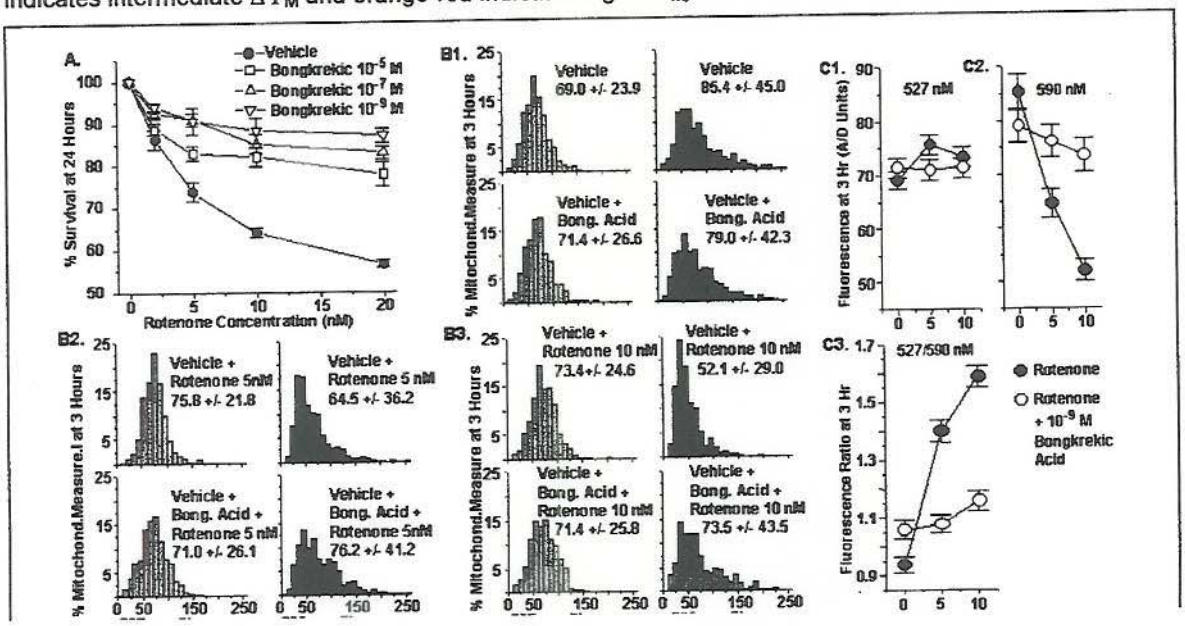

Figure 15. Bongkrekic Acid Attenuates The Decreased Survival And Cell Body $\Delta\Psi_M$ Dissipation Caused By Rotenone In Cultured Catecholaminergic Neuron-Like Cells. A. BA concentrations of 10^{-9} M were most effective in reducing the cellular loss caused by rotenone (78% or more at all concentrations of rotenone). **B1-B3.** BA shifted the distributions for the 590 nm emission of JC-1 to higher values compared to those for rotenone alone. It either decreased or maintained the values of distributions for the 527 nm JC-1 emission. **C1-C3** summarize the changes in dual emission and present the values for the 527 nm/590 nm ratio (all of the distributions are for 600 or more LCSM measurements and the plots present mean +/- SEM).These findings indicate that the majority of cell loss and the decrease in cell body $\Delta\Psi_M$ caused by rotenone depend on opening of the PTPC.

Rotenone Induces Greater Dissipation Of $\Delta\Psi_M$ In Axon Terminal Mitochondria Than In Cell Body Mitochondria. Examination of LCSM images of primary cultures of ventral mesencephalon suggested that rotenone induces relatively greater decreases in $\Delta\Psi_M$ for TH immunopositive terminals than TH immunopositive cell bodies, GABA-ergic cell bodies and terminals, and glia cells in the same cultures (figure 16, see [55] for details of our use of CMTMR to measure $\Delta\Psi_M$). Similarly , mitochondria in the terminals of CAergic neuron-like cells exposed to serum and NGF cells for 17 days to maximize axon growth and terminal development showed a similar apparent disparity in terminal and cell body $\Delta\Psi_M$ after rotenone exposure (figure 16A). We used TMRM with LCSM imaging to compare $\Delta\Psi_M$ measurements for two rotenone concentrations (2 nM and 10 nM) in the cell bodies and terminals of the 17 day differentiated cells . Those preliminary measurements revealed a considerably greater dissipation of $\Delta\Psi_M$ in the terminals compared to the cell body mitochondria. (figure 16B).

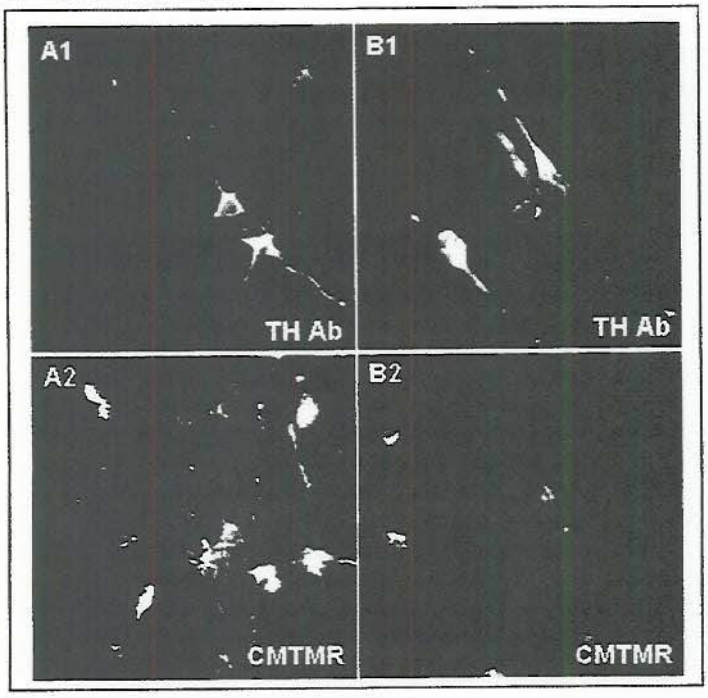

Figure 16. DAns In Primary Mesencephalic Cultures. A1 and A2 and B1 and B2 are for identical LCSM image fields. **A1 and B1** show DAn cell bodies and processes identified by TH immunofluorescence. **A2 and B2** show images of $\Delta\Psi_M$ by the potentiometric dye CMTMR. The intensity of CMTMR fluorescence estimates $\Delta\Psi_M$ if the potentiometric dye is incubated with the cells only briefly before fixation (i.e. 10 minutes, see [205] appended). Immunofluorescence for the TH antibodies showed little difference for vehicle treated (A1) and those treated with 10 nM rotenone (B1). In contrast, overall CMTMR fluorescence was greatly reduced for 10 nM rotenone treatment (B2) compared to vehicle treatment (A2). TH immunopositive cell bodies as well as neuron like non TH immunopositive cell bodies (putative GABAergic neurons) and the larger glial cells also showed decreased CMTMR fluorescence. CMTMR fluorescence can still be detected in cell bodies but is no longer detectable in TH immunopositive processes. Accordingly, the greatest decrease in CMTMR fluorescence and likely $\Delta\Psi_M$ was evident in the processes of the TH immunopositive cells.

A number of factors might account for greater $\Delta\Psi_M$ dissipation in the terminals: 1) rotenone binding to NADH dehydrogenase might be increased in the terminals; 2) rotenone might cause a greater decrease in NADH dehydrogenase activity in the terminals (decreased conversion of NADH to NAD^+); 3) a greater reduction in transmembrane proton pumping might result for a given decrease in NADH dehydrogenase activity; 4) decreased mtRCxI activity might have an increased capacity to open the PTPC in terminal mitochondria and 5) decreased mtRCxI activity might induce greater increases the levels of intramitochondrial Ca^{2+} in terminals, since a recent study has shown that chronic rotenone

treatment of a SH-SY5Y neuroblastoma cells increased Ca^{2+} in the cells and reduced $\Delta\Psi_M$ [206], or 6) increased ROS levels in terminals, but not cell bodies, might reduce $\Delta\Psi_M$. One or more of those factors could result in greater vulnerability of terminals to rotenone compared to cell bodies. For example, a decreased NADH dehydrogenase-ANT interaction would result in increased $\Delta\Psi_M$ dissipation due to greater PTPC opening (see above).

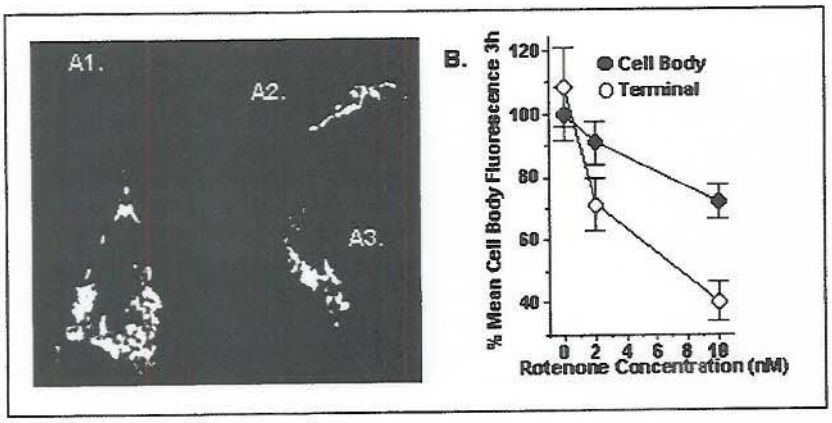

Figure 17. A1. Typical TMRM stained mitochondria in the **A1.** cell body of a CAergic neuron-like cell in culture treated with NGF for 17 days to maximize axon growth and terminal development. **A2.** and **A3.** Terminal processes of the same cell. **B.** Plots of Mean+/- SEM TMRM fluorescence of cell body mitochondria and terminal mitochondria treated with vehicle, rotenone 2 nM or 10 nM. The plots indicate that rotenone dissipates $\Delta\Psi_M$ in terminal mitochondria to a considerably greater extent compared to mitochondria in cell bodies.

Progress In Determining How Propargylamines That Bind To GAPDH Reduce Apoptosis.

Anti-Apoptotic Propargylamines Reduce Apoptosis Induced By Rotenone. The tricylic propargylamine CGP3466 does not inhibit MAO-B but binds to GAPDH and converts tetrameric GAPDH to a dimer [54, 80]. CGP3466 has been found to be extremely effective in reducing some forms of neuronal apoptosis (see [192], for a review), including that involving SNc DAergic neurons in monkeys treated with intra-carotid injections of MPTP [207]. CGP3466 is now in clinical trial as an anti-apoptotic therapy for PD (see [63] for a review of new anti-apoptotic therapies and considerations of the utility of CGP3466 in treating neurodegeneration). We are particularly pleased with the therapeutic possibilities offered by CGP3466, since it was discovered in our laboratory in 1995 [191, 192].

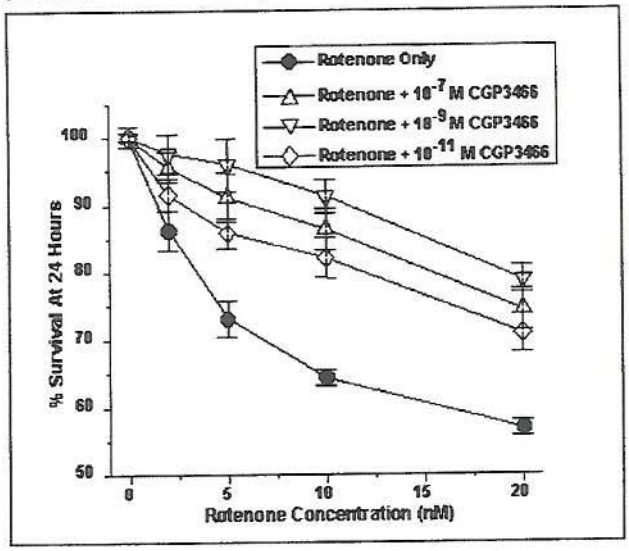

Figure 18 – The propargylamineCGP3466 Increases The Survival Of CAergic Neuron-Like Cells Exposed To The mtRCx I Inhibitor Rotenone.

We first carried out studies to determine whether CGP3466 can reduce neuronal loss induced by rotenone. As shown in figure 18, CGP3466 was most effective at nanomolar concentrations and was particularly effective in increasing the survival of the CAergic cells for rotenone concentrations in the range that induced apoptosis and caused mtRCxI activity decreases in the range reported for the PD SNc (see background material above).

Anti-Apoptotic Propargylamines Induce A Program Of Altered New Protein Synthesis That Increases Anti-Apoptotic Proteins And Decreases or Subcellularly Relocates Pro-Apoptotic Proteins. It remains to be determined how the binding of anti-apoptotic propargylamines like CGP3466 to GAPDH and the conversion of GAPDH to a dimer reduces

apoptosis, particularly apoptosis induced by decreased mtRCx I activity similar to that found in PD. In our previous progress report and our published work, we showed that the propargylamines cause down regulation of GAPDH and the prevention of dense GAPDH nuclear translocation [54]. Furthermore, our previous publications [127, 168, 208] and the rotenone research shown above suggests that the propargylamines reduce apoptosis by inducing new protein synthesis, which serves, at least in part, to maintain mitochondrial membrane impermeability [55, 164, 209] and thereby to prevent release of mitochondrial apoptosis signaling factors.

We carried out experiments in PC12 cells at various stages of NGF differentiation that were induced into apoptosis by trophic withdrawal. We used metabolic labeling with radioactive methionine combined with subcellular fractionation to show that the propargylamines alter new protein synthesis largely in the nuclear and mitochondrial subfractions. The altered new protein synthesis involved prevention of a number signaling events that promote apoptosis: 1) transient c-JUN upregulation; 2) BAX translocation to mitochondria; and 3) decreases in BCL-2, Cu/Zn superoxide dismutase (SOD1), Mn superoxide dismutase (SOD2), and glutathione peroxidase. The levels of a number of other proteins, for example cytoskeletal proteins, were unaffected by propargylamine treatment. The protein synthesis changes are appropriate to maintain impermeability of the inner mitochondrial membrane as indicated by prevention of $\Delta\Psi_M$ dissipation. They also suggest that signaling by early activating pro-apoptotic transcriptional activators like Jun-n-terminal kinase (JNK) are down regulated by propargylamine treatment. Finally, they suggest that the propargylamines maintain the ROS scavenging capacity of cells by preventing decreases in scavengers like SOD1, SOD2 and glutathione peroxidase. A number of studies have suggested that ROS play essential roles in some forms of apoptosis [210-213]. The finding are in press in the May 2002 issue of the Journal of Pharmacology and Experimental Therapeutics [194] and fully credit our Army grant for support of the research. The manuscript is appended to this progress report.

A further series of our experiments showed that exposure of the NGF differentiated CAergic cells to low, non-lethal levels of pro-oxidants induces a program of new protein synthesis that is anti-apoptotic and is very similar, if not identical, to the program induced by the anti-apoptotic propargylamines. The program maintains $\Delta\Psi_M$ like the propargylamines and alters the levels of the same spectrum of proteins as the propargylamines. is Pharmacological inhibitors of PI3-K block anti-apoptosis by low level pro-oxidant exposure and by the propargylamines. The PI3-K pathway has been shown to mediate anti-apoptosis by phosphorylating protein kinase B (Akt), which acts through a number of transcriptionally -dependent and post translational linkages to reduce apoptosis [214-216]. Accordingly, the data suggests that propargylamines activate an intrinsic pathway that protects cells from low-level damage. The finding are in press in Neuroscience [205] and fully credit our Army grant for support of the research. The manuscript is appended to this progress report.

The exposure of nerve cells to a variety of toxins can induce cell death by apoptosis and may contribute to neuronal loss in some neurodegenerative conditions and after exposure to a variety of toxins.

It is not known what role GAPDH upregulation or nuclear accumulation plays in apoptosis or whether another unrecognized event involving GAPDH is responsible. Data from our laboratory and others suggests that GAPDH is involved in the early stages of apoptosis signaling, well before decreases in mitochondrial membrane potential ($\Delta\Psi_M$), opening of the mitochondrial permeability transition pore (PTP), the release of apoptosis-inducing mitochondrial factors, caspase 3 activation or nuclear degradation. Yet the specific aspects of GAPDH activity and interactions that contribute to apoptosis remain unknown, particularly those events which may link GAPDH to the final degradative events typical of apoptosis.

Cell death by necrosis is characterized by cell swelling, plasma membrane fracture, nuclear and mitochondrial disruption, rapid ATP depletion, cytoplasmic extrusion and the induction of inflammation. In contrast, the process of apoptosis involves cell shrinkage, membrane blebbing, nuclear chromatin condensation, nuclear DNA cleavage by endonucleases, partial maintenance of ATP levels, maintenance of organelle and plasma membrane integrity, loss of plasma membrane phospholipid asymmetry, formation of membrane wrapped cytoplasmic and nuclear bodies, and the activation of cysteine proteases (caspases). Apoptosis consists of series of signaling events, often divided into three phases; an initiation phase, an effector phase and a degradation phase [Kroemer, 1995 #34]. A wide variety of insults, including a number that may be relevant to human neurodegeneration, can initiate apoptosis in neurons (see [Tatton, 1997 #52; Tatton, 1999 #45]). A number of different signaling events, comprising what might be termed different forms of apoptosis, can lead to a similar constellation of final degradative events typical of apoptosis. Furthermore, identical insults can activate different signaling pathways in different cell types (see [Yin, 1999 #58]).

GAPDH catalyzes the conversion of glyceraldehyde-3-phosphate to 1,3-bisphosphoglycerate in the glycolytic pathway. As part of the conversion, GAPDH converts NAD^+ to the high-energy electron carrier NADH. A number of other functions have been attributed to GAPDH including roles in endocytosis, microtubule bundling, viral pathogenesis, mRNA regulation, tRNA export, DNA replication, and DNA repair (see [Sirover, 1999 #59] for a review).

GAPDH was initially linked to neurodegeneration by the finding that it binds to the polyglutamine repeats in the abnormal gene products in Huntington's disease and other inherited CGA repeat disorders [Burke, 1996 #2]. It has been found in amyloid plaques in AD brains [Sunaga, 1995 #3]. The protein-protein interactions between GAPDH and huntingtin do not appear to alter GAPDH-mediated glycolysis measured in postmortem HD brain tissue [Kish, 1998 #61; Browne, 1997 #60], so that any role that GAPDH played in HD seems unrelated to glycolysis.

GAPDH mRNA and protein levels were found to increase during apoptosis caused by reduction of media K^+ [Sunaga, 1995 #3], exposure to cytosine arabinoside [Ishitani, 1997 #4] and aging of cultured cerebellar granule neurons and cerebrocortical neurons [Ishitani, 1996 #5]. We found similar upregulation of GAPDH levels in neuronally differentiated PC12 cells entering apoptosis caused by serum and NGF withdrawal. GAPDH upregulation has also been found in apoptotic thymocytes, undifferentiated PC12 cells, and HEK293 cells [Sawa, 1997 #6]. Antisense oligonucleotides against GAPDH mRNA have been shown to block forms of apoptosis involving GAPDH upregulation [Sawa, 1997 #6; Chen, 1999 #7; Ishitani, 1996 #8].

Western blots and immunocytochemistry have shown the accumulation GAPDH in the nuclear fraction or in nuclei respectively in apoptosis involving GAPDH upregulation [Saunders, 1997 #9; Sawa, 1997 #6; Saunders, 1999 #10; Carlile, 2000 #35]. In normal cells, GAPDH is concentrated in the extranuclear cytosol and only a small amount is localized in the nucleus. We found that the nuclear GAPDH is bound to a translational control protein, promyelocytic leukemia protein (PML) [Carlile, 1998 #12], in so-called PML nuclear bodies [Matera, 1999 #62; Bloch, 1999 #13]. PML overexpression has been shown to induce a form of apoptosis, which involves BAX, but is independent of caspase activation [Quignon, 1998 #14].

Relevant Aspects Of GAPDH Biochemistry- GAPDH has been shown to bind to tubulin in vitro [Huitorel, 1985 #15; Volker, 1997 #16], but only when GAPDH is in its tetrameric form [Carlile, 2000 #35]. More importantly, tetrameric GAPDH binds to the 5'-UTR and 3'-UTR regions of mRNA (i.e. to the AU rich portions of RNA) [Nagy, 1995 #17]. The AUUA RNA binds to the Rossman fold region of GAPDH, the site of its glycolytic activity. The binding to the cis-acting RNA elements important in the stability and translation of mRNA have led to the hypothesis that GAPDH plays a role in translational regulation, which is strengthened by our finding that GAPDH binds nuclear PML [Carlile, 1998 #12]. Other works have suggested that nuclear GAPDH acts directly

on transcription [Zang, 1998 #63].

Both nitric oxide (NO) and superoxide radical have been shown to release GAPDH from AU-rich RNA binding [Itoga, 1997 #18; Beckman, 1996 #19; Brune, 1995 #20; Brune, 1996 #22; Mohr, 1996 #23]. Similarly, NAD+ can release GAPDH from AU-rich RNA binding [McDonald, 1994 #24; Nagy, 1995 #17; Gabellieri, 1996 #26]. Since AU-rich RNA bound GAPDH cannot contribute to glycolysis, increased NAD^+ may free GAPDH and then be converted to NADH. Similarly NO and superoxide radical may increase the proportion of GAPDH available for glycolysis. Therefore, we questioned whether high levels of NO, superoxide radical or NAD+ can free GAPDH from AU-rich RNA binding and thereby make GAPDH available to contribute to apoptosis.

Although mitochondria are central to oxidative phosphorylation, they also contribute to generation of reactive oxygen species (ROS), control of intracellular Ca^{2+} levels, and apoptosis signaling (see (16, 24)). The mitochondrion is a double membraned organelle. Four multi-protein respiratory complexes (MtCxs I to IV), ATP synthase and the adenine nucleotide transporter (ANT) are located within the inner membrane and are involved in oxidative phosphorylation. Other components involved in the transfer of the electrons necessary for oxidative phosphorylation are ubiquinone and holocytochrome C (cytC). Sequential extraction of electron energy provides for outward proton pumping at MtCxs I, III, and IV. The resulting proton concentration gradient causes an electrochemical potential across the inner mitochondrial membrane, reflected by a pH gradient and a potential difference, termed the mitochondrial membrane potential ($\Delta\Psi_M$) (24). $\Delta\Psi_M$ drives the phosphorylation of ADP to ATP by ATP synthase (25) and decreases in $\Delta\Psi_M$ can be an early marker for some forms of mitochondrially dependent (MtDep) apoptosis signaling (see (14) for a review).

The mitochondrial permeability transition pore complex (PTPC) involves proteins and factors in the mitochondrial matrix, the inner membranous space, and the outer membrane (see (26, 27) for more details). Proteins known to participate in the PTPC include: a) the ANT, which exchanges ADP and ATP between the mitochondrial matrix and the extra-mitochondrial space; b) a putative chaperone, cyclophilin D (cyD); c) a porin molecule localized to the outer mitochondrial membrane, a possible voltage dependent anion channel (VDAC); d) hexokinase-2, a glycolytic enzyme; e) creatine kinase, which reversibly converts ATP plus creatine to phosphocreatine + ADP; f) a peripheral benzodiazepine binding protein; g) BAX and related pro-apoptotic proteins like BAD; and h) BCL-2 or BCL-X_L, which are anti-apoptotic proteins.

The protein-protein interactions between the components of the PTPC are controversial. It can be defined as a voltage-dependent, cyclosporin A (CSA) sensitive, high conductance membrane channel (28) and appears to open in two states: a transient, low conductance, ion selective state and a sustained, high conductance, non selective state, which allows passage of solutes up to 1.5 kD (see (29) for details). Sustained opening results in $\Delta\Psi_M$ dissipation due to proton influx, and the efflux of Ca^{2+}, metabolites, and other small molecules from the matrix. Mitochondrial respiration is decreased due to loss of pyridine nucleotide linked substrates from the matrix (30). Osmotic swelling of mitochondria can produce membrane fracture. PTPC conformation is influenced by $\Delta\Psi_M$ - high $\Delta\Psi_M$ favors closure, while a decreased $\Delta\Psi_M$ increases probability of PTPC opening (31). Ca^{2+} binding to the matrix side of the PTPC is a required for opening.

PTPC closure results from the binding of CSA to cyD, which prevents cyD from interacting with the ANT (32-35). Bongkrekic acid binding to the ANT directly facilities PTPC closure. We and others have used PTPC-closing agents like CSA to serve as indicators for PTPC participation in different forms of apoptosis (see (36) and (23), appended).

Members of the BCL-2 family of proteins mediate part of their pro- or anti-apoptotic actions by localizing to mitochondrial membranes, in part through the PTPC (see (37, 38)). The association of BCL-2 or BCL-X_L with the PTPC facilitates PTPC closure and maintenance of $\Delta\Psi_M$ (39-41). A BCL-2 family member, BAD forms heterodimers with BCL-2 or BCL-X_L and inactivates the anti-apoptotic actions of BCL-X_L and possibly BCL-2 (42-45). Binding of BAX dimer to the ANT increases mitochondrial permeability, possibly by PTPC opening (37, 46).

We have shown that early-apoptotic decreases in $\Delta\Psi_M$ are a feature of apoptosis caused by NGF and serum withdrawal in cultured neural cells (17) and similar early decreases in $\Delta\Psi_M$ have been reported for apoptosis initiated by a wide variety of insults (see (14) for a detailed review). Not all forms of apoptosis involve decreases in $\Delta\Psi_M$. For example, apoptosis induced by staurosporine in cultured hippocampal cells (47) did not involve $\Delta\Psi_M$ decreases (5), while staurosporine induced apoptosis in P6 cells did involve early apoptosis decreases in $\Delta\Psi_M$ (48).

At least two factors, released from mitochondria, signal for apoptotic degradation, cytC, and apoptosis initiation factor (AIF), a 50 kD flavoprotein. CytC interacts with Apaf-1 (49-51), dATP/ATP and procaspase 9 to

form a complex known as the apoptosome, in which procaspase 9 is converted to caspase 9 (schematized in figure 1). Caspase 9 converts procaspase 3 to active caspase 3. The apoptosome seems to function as a multi-caspase activating complex (see (51)). Activated caspase 3 in turn activates DNA fragmentation factor (52), an endonuclease activator that enables DNA cleavage and also cleaves other proteins such as lamin, and fodrin (49). AIF induces DNA loss, peripheral chromatin condensation and digestion of chromatin into 50 kbp-fragments (53). The caspase-3 inhibitor ZVAD-Fmk inhibits chromatin condensation induced by AIF. Pro-caspase 2 and 9, have been found in the intermembranous space of mitochondria (54) and their microinjection of can induce apoptotic nuclear degradation. The release of cytC was initially proposed to be independent of PTPC opening and decreased $\Delta\Psi_M$ (55-57). The interpretations of those studies have been found to be complicated by technical considerations related to the measurement of $\Delta\Psi_M$ (see (30) for details). Furthermore, similar to earlier findings in isolated mitochondria (41, 58), several studies of mitochondria in situ have shown that PTPC opening and decreased $\Delta\Psi_M$ can be associated with the induction of apoptotic degradation in models (59,60), including apoptosis induced by the PD-like toxin MPP^+ (22). Examination of individual mitochondria in situ using laser confocal scanning microscopy (LCSM) has shown that decreased $\Delta\Psi_M$ can accompany cytC release into the cytosol (48).

Mitochondrial BCL-2 can block the release of the mitochondrial factors that signal for apoptotic degradation, possibly due to its capacity to facilitate PTPC closure and maintain $\Delta\Psi_M$ (see (27) for a detailed and recent review of the role of the PTPC in cell death). BCL-X_L has a similar capacity (61). Mitochondrial BAX is necessary for cytC release in some systems (62-64). Caspase-activated BID also facilities cytC release (61). Accordingly, the demonstration of increases in mitochondrial BAX levels, increased extra-mitochondrial cytC levels, decreased mitochondrial BCL-2 or BCL-X_L levels, decreased $\Delta\Psi_M$ and caspase 3 activation can together serve as markers of MtDep apoptosis signaling.

REPORT OF PROGRESS

We have produced seven clones that overexpress GAPDH according to a Tet-Low system (see for details of our previous use of the system to express p53 in bladder cancer cells [Sugrue, 1997 #64; Sugrue, 1999 #28]). The rat brain cDNA that we cloned for the construction of the green fluorescent protein-GAPDH was used with the Tet-low system (see [Shashidharan, 1999 #40] for details of the cDNA). We have produced 7 stable PC12 clones that overexpress GAPDH in response to a sudden decrease in media tetracycline (tet) concentration. (see figure 1).

In at least one of the clones, increased GAPDH levels seem to induce spontaneous apoptosis in the cells and increase the cells' vulnerability to several insults that induce apoptosis (see figure 1). We have obtained similar estimates of increased GAPDH protein using LCSM fluorescence measurements of GAPDH immunoreactivity (see [Carlile, 2000 #35] for details of the cell preparation). With a complete withdrawal of tet there is a 225% increase in average GAPDH immunofluorescence in the cytoplasm and a 178% increase in average GAPDH immunofluorescence levels in the nuclei at 6 hours after the tet withdrawal (see immunofluorescence distributions in figure 2). The levels of increase in GAPDH appear similar to that found in the PC12 cells at 6 hours and 24 hours after serum and NGF withdrawal (see figure 9 below taken from [Carlile, 2000 #35] appended).

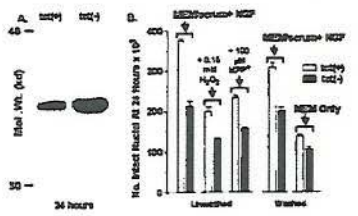

Figure 1 –PC12 cells were differentiated in minimum essential media (MEM) with serum and NGF plus high tet (tet(+)) for 5 days in order to neuronally-differentiate the cells (see [Tatton, 1994 #57; Wadia, 1998 #49] for details). On the sixth day (24 hours in low tet (tet(-)), three groups of cells in MEM with serum and NGF were exposed to: added MEM as a control, 0.15 mM H_2O_2 (concentrations of 0.10-0.25 μM H_2O_2 induce apoptosis in the cells, see below) or 100 μM MPP^+ (see [Chalmers-Redman, 1999 #43] for details of our initiation of apoptosis in the neuronally-differentiated PC12 cells with this concentrations of MPP^+). The three groups of cells were matched with three groups that were maintained in tet(+). Two further groups in either tet (+) or tet(-) were washed repeatedly to remove the trophic support offered by serum factors and NGF (see[Wadia, 1998 #49] for details of the apoptosis initiated by this procedure). One group was returned to MEM with serum and NGF as a control and the other was placed in MEM only. The 24 hours in tet(-) markedly increased GAPDH levels compared to tet(+) cells as shown in the western blot in A. The tet (-) cell maintained in MEM with serum and NGF without washing

showed a decrease of about 45% compared to the tet(+) cells. Furthermore, the tet (-) cells showed greater net losses to H_2O_2, MPP^+ and serum+NGF withdrawal than the tet(+) cells. This data appears to show that the increased GAPDH expression in the tet (-) cells induces spontaneous apoptosis and increases the cells' vulnerability to apoptosis induced by to H_2O_2, MPP^+ and serum+NGF withdrawal.

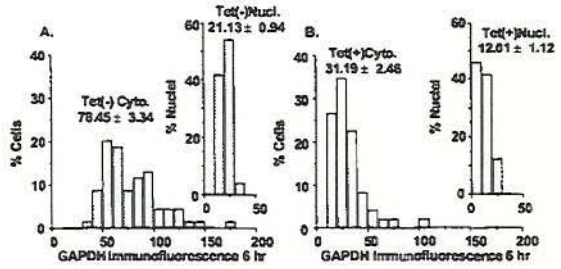

Figure 2 – GAPDH overexpression using the Tet(-)-system in neuronally-differentiated PC12 cell. Abscissae show levels of GAPDH immunofluorescence in LCSM detector units while ordinates show percentages of cells.

An increased proportion of the tet(-) cells (approximately 11% compared to less than 1% for tet(+) cells) showed dense nuclear GAPDH immunoreaction, which is reflected in the average nuclear GAPDH immunofluorescence in figure 2.

We and others, have reported that a decrease in $\Delta\Psi_M$ is a very early event in some forms of apoptosis and precedes the onset of apoptotic nuclear degradation. Others measured whole cell mitochondrial potentiometric dye fluorescence using fluorescence flow cytometry (FFC) (see [Susin, 1998 #65] for a review), while we have imaged individual mitochondria *in situ* using LCSM (see [Grant, 1999 #66; Chalmers-Redman, 1999 #43; Sugrue, 1999 #28; Jing, 1999 #37; Wadia, 1998 #49]).

The validity of the use of some potentiometric dyes to measure $\Delta\Psi_M$ has recently been questioned, particularly rhodamine-1,2,3 (R123) [Metivier, 1998 #67] and dyes which bind to mitochondrial thiols like chloromethyl-X-rosamine (CMXRos or mitotracker red) and chloromethyltetramethyl rosamine (CMTMR or mitotracker orange) [Gilmore, 1999 #68; Scorrano, 1999 #69].

Kroemer and colleagues [Metivier, 1998 #67] examined the utility of a variety of possible mitochondrial potentiometric dyes using m-chlorophenylhydrazone (CCCP), a protonophore, to deplete the mitochondrial proton gradient and therefore the $\Delta\Psi'_M$. They examined DiOC6, R123, CMXRos, tetramethylrhodamine methylester (TMRM), mitotracker green (MG) and nonyl-acridine orange (NOA). CMXRos contains a chloromethyl moiety that binds to matrix thiols and is structurally very similar to CMTMR, which we have used in some of our studies. MG differs markedly in structure from CMXRos and CMTMR (Molecular Probes Handbook of Fluorescent Porbes and Research Chemicals, 6th ed.1996).

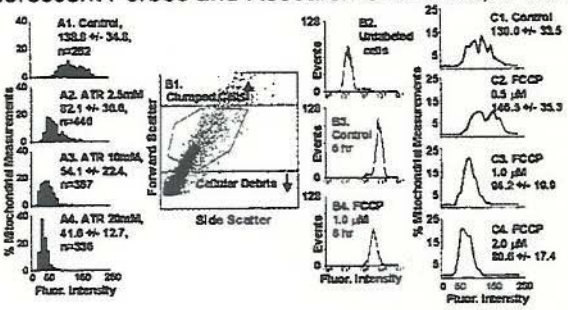

Figure 3 – Distributions of *in situ* laser confocal scanning microscopy (LCSM) measurements of mitochondrial membrane potential ($\Delta\Psi_M$) in neuronally-differentiated PC12 cells with CMTMR for varying concentrations of atractyloside (ATR) and comparison of estimation between FFC and *in situ* LCSM measurement. A1 shows a typical distribution of CMTMR fluorescence in cells supported by serum and NGF. The addition of increasing concentrations of ATR from 2.5 (A2), 10 (A3) and 20 (A4) mM causes a progressive shift of the CMTMR fluorescence distributions to lower values and a progressive narrowing of the distributions. These data are consistent with an increasing proportion of mitochondria having dissipated their proton gradients and therefore $\Delta\Psi_M$ due to PTP opening and demonstrates the $\Delta\Psi_M$ sensitivity of the *in situ* LCSM measurement of CMTMR fluorescence. For B1-C4, cerebellar granule neuron cultures were exposed to varying concentrations of the protonophore FCCP in order to induce the leakage of protons from mitochondria and thereby reduce $\Delta\Psi_M$. B1–B4 show typical examples for FFC analysis while C1-C4 show values obtained using LCSM measurement of mitochondrial profiles. Both methods revealed graded decreases in fluorescence with increasing FCCP concentrations. The *in situ* LCSM distributions revealed a greater dynamic range than FFC for a given increase in FCCP concentration.

They exposed cells to Fas ligand to induce apoptosis and CCCP. By comparing the fluorescence changes

induced by Fas ligand exposure and proton dissipation by CCCP, they were able to assess the relative sensitivity of the different dyes to changes in $\Delta\Psi_M$. They found that NAO and MG were completely insensitive to $\Delta\Psi_M$, while CMXRos and TMRM were very sensitive. DiOC6 showed a lower degree of sensitivity while R123 showed an inappropriate increase in fluorescence in response to decreases in $\Delta\Psi_M$. Accordingly, it is most important to choose an optimal dye for $\Delta\Psi_M$ measurements.

Recently, $\Delta\Psi_M$ measurement using CMXRos were examined [Gilmore, 1999 #68]. It was found that the dye leaked out of mitochondria, if it was left in place for an extended period of time. The leakage was considered to result from opening of the PTP by CMXRos. Since a chloromethyl moiety on the dye fixes it to protein in the mitochondrial matrix, the authors found that early fixation of the dye provided for accurate $\Delta\Psi_M$ values. CMTMR has been found to have a similar action on PTP opening and to inhibit mitochondrial complex I at high concentrations [Scorrano, 1999 #69].

In order to evaluate CMTMR, we have now employed similar comparisons to those of Kroemer et al. using atractyloside, which opens the PTP and dissipates $\Delta\Psi_M$, and FCCP, which also dissipates $\Delta\Psi_M$, similar to CCCP. We evaluated CMTMR, both with LCSM measurements of $\Delta\Psi_M$ and those provided by FFC. Figures 3A1-3A4 demonstrate the sensitivity of LCSM *in situ* measurements of CMTMR fluorescence to progressive reductions in the proton gradient induced by increasing concentrations of atractyloside. We have also compared the sensitivity of the dyes to changes in $\Delta\Psi_M$ induced by FCCP examined by LCSM *in situ* measurements and to those obtained by FFC analysis (figure 3B1-3C4). Both methods showed graded decreases in fluorescence in response to increasing concentrations of agents that dissipate $\Delta\Psi_M$. The LCSM measurements offered a greater dynamic range over which to evaluate $\Delta\Psi_M$ than FFC.

We have found that the key aspect of using CMTMR relates to the time the cells are incubated with the dye and the concentration of the dye that is used. We carried out experiments in which cells were treated with varying concentrations of atractyloside or FCCP as above, followed by incubation with varying concentrations of CMTMR for varying lengths of time before fixation (10 minutes to 3 hours). We found that CMTMR incubation for periods exceeding 30 minutes resulted in a progressive decrease in $\Delta\Psi_M$. By 3 hours virtually all LCSM measurements showed distributions that were similar to those for the highest concentrations of atractyloside or FCCP (i.e. when the proton gradients have been maximally compromised by PTP opening). We found that ***100 nM CMTMR concentrations and CMTMR incubation times before fixation at 15 minutes offered the greatest sensitivity of the dye to changing atractyloside or FCCP concentrations.***

We then compared the sensitivity of CMTMR using the above fixation procedures to TMRM and the 527 nm wavelength of JC-1 in living cells. We used both LCSM and FFC measurements. Both dyes are widely used to measure $\Delta\Psi_M$ in living cells (see [Wadia, 1998 #49] for our use of JC-1). We found that TMRM and JC-1 offered similar sensitivity to changing atractyloside or FCCP concentrations but that both agents offered less sensitivity than CMTMR measurements.

Use of dyes possessing a chloromethyl moiety, like CMXRos and CMTMR, might also be criticized in models using agents like MPP^+ or glutamate that could alter the oxidative state of mitochondrial matrix thiols. Increased oxidation of matrix thiols might alter the binding of the dyes and invalidate fluorescence measurements. We examined the effect of pre-exposure of cells to MPP^+ on LCSM CMTMR fluorescence reductions caused by atractyloside [Chalmers-Redman, 1999 #43]. We did not find changes in CMTMR fluorescence for pre-exposure to a range of MPP^+ concentrations, which seemed to indicate that short incubation times and low CMTMR concentrations preserve the graded nature of CMTMR $\Delta\Psi_M$ measurements, even with agents that induce increased concentrations of mitochondrial matrix oxidative radicals.

We have carried out experiments in which the changes in CMTMR fluorescence were compared to those for JC-1 in identically prepared cells (see [Wadia, 1998 #49] for an example). JC-1 is a dual emission dye reported to offer high sensitivity to changes in $\Delta\Psi_M$ [Reers, 1995 #70; Salvioli, 1997 #71; Smiley, 1991 #72]. In those experiments, values obtained with the two dyes followed the same trends. Given the controversy surrounding the use of various dyes for $\Delta\Psi_M$ measurement, we now routinely use both CMTMR and JC-1 in all experiments and plan to do so in the proposed studies.

We have previously shown that margination of nuclear histone immunoreactivity occurs in association with nuclear DNA cleavage and nuclear chromatin condensation (see [Wadia, 1998 #49]). We have now examined the temporal relationships between histone margination, nuclear chromatin condensation and nuclear DNA

cleavage in cerebellar granule neuron (CGn) apoptosis caused by exposure to glutamatergic agonists or to reduced K^+. We have found that DNA condensation occurs in four stages: stage 1) condensation of DNA around the outer border of the nucleus (examples labeled 1 in figure 4B1); stage 2) DNA condensation involves the whole nucleus (examples labeled 2 in figure 4B1and B2); stage 3) shrinkage of the condensed DNA with the appearance of cracks or breaks in the nuclei (examples labeled 3 in 4B1 and B2); and stage 4) the formation of multiple spherical nuclear bodies of condensed DNA (not shown). Histone margination surrounds the areas of condensed DNA in stages 1 and 2. DNA fragmentation appears during stage 2. The histone margination may correspond to changes of the structure of H1 histones that have been reported to occur in association with DNA fragmentation in apoptosis.

In order to determine whether cells have entered the phase of nuclear apoptotic degradation in the proposed studies, we have employed three separate measures as shown in figure 4: 1) the demonstration of DNA chromatin condensation using YOYO-1 staining, 2) demonstration of DNA fragmentation using in situ end labeling (ISEL) of DNA with BODIPY-dUTP, and 3) demonstration of histone margination using immunoreaction with anti-histone antibodies. Use of ISEL alone can produce false positives, while the combination of multiple markers of apoptosis in the same nuclei greatly increases confidence in the findings [Tatton, 1998 #47; Tatton, 1997 #51].

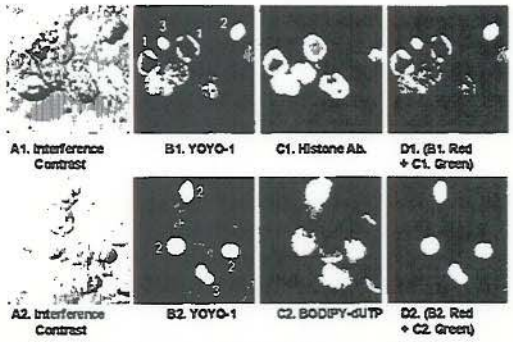

gure 4 – LCSM images of CGns 12 hours after exposure to 5 x 10^{-5} M NMDA. Each horizontal row of images was taken for an entical field. DNA chromatin condensation revealed with OYO-1 (B1 and B2), and DNA fragmentation revealed with EL using BODIPY-dUTP (C2), is accompanied by the nuclear margination of histone immunoreaction (C1). Nuclei without evidence of DNA condensation or fragmentation show a pattern of histone immunoreaction that extends across the whole nucleus. In apoptotic nuclei, the histone immunoreaction surrounds the fragmented and condensed DNA but does not co-localize with either (D1). Examination of a large number of cells has shown that DNA condensation proceeds according to 4 stages (examples of stages 1, 2 and 3 are shown in B1 and B2). In the right hand panels of rows, D1 and D2, the images in B1 or B2 and C1 or C2 have been colored red and green respectively and then added. Regions in the added images that are red or green indicate no spatial overlap while yellow -green, yellow or orange coloration indicate varying levels of spatial overlap. The added figures show that histone margination surrounds condensed DNA areas in stage 1 and stage2 but not in stage 3. DNA fragmentation is not evident until stage 2 and is co-extensive with condensed DNA.

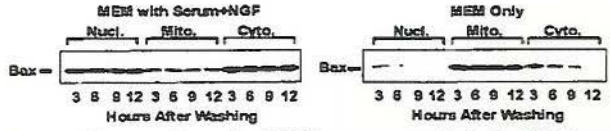

Figure 5 –Western blots for BAX immunoreactivity in PC12 cell nuclear, mitochondrial and cytosolic subcellular protein fractions at 3, 6, 9 and 12 hours after NGF and serum withdrawal (right hand blot labeled MEM Only) versus control cells that were washed and replaced in serum and NGF (left hand blot labeled MEM with Serum and NGF)). Note that BAX immunoreactivity is concentrated in the nuclear and cytosolic subfractions with relatively lower levels of mitochondrial subcellular fraction in control cells. In contrast, BAX immunoreactivity is decreased in the nuclear and cytosolic subfractions but markedly increased in the mitochondrial subfraction after NGF and serum withdrawal.

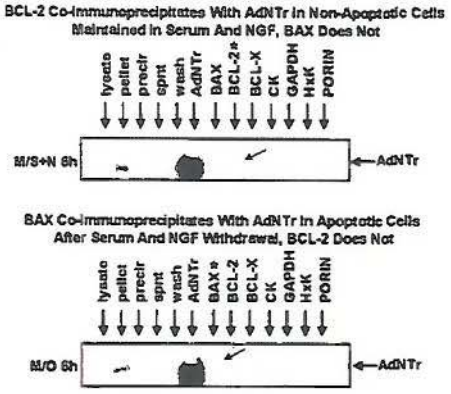

Figure 6 – Co-Immunoprecipitaion studies show that the AdNtr co-immunoprecipitates with BCL-2 but not BAX in control cells maintained in serum and NGF for 6 hours after washing (upper blot). In contrast, in cells entering apoptosis at 6 hours after serum and NGF withdrawal, the AdNtr co-immunoprecipitates with BAX but not BCL-2. These findings are in keeping with reports that BAX binds to the AdNtr in apoptosis. It is the first demonstration of a BAX-BCL-2 exchange at the AdNtr. The changing co-immunoprecipitation does not mean that BAX and BCl-2 bind at the same site on the AdNtr but rather that they do not bind to the protein at the same time.

We have used western blots for subcellular protein fractions, co-immunoprecipitation and LCSM immunocytochemistry to show: 1) that BAX accumulates in mitochondria, and co-localizes and binds with AdNtr protein in early apoptosis (see figures 4, 5, 6 and 7) in association with a marked decrease in $\Delta\Psi_M$ (see figure 8). The movement to mitochondria is not associated with a general cellular increase in the level of BAX (see figures 4); 2) that BCL-2, normally bound to the AdNtr, shows decreased binding in early apoptosis in association with a decrease in $\Delta\Psi_M$ (see figure 5). The decrease in BCL-2 binding to the AdNtr is associated with a decrease in BCL-2 immunoreactivity that co-localizes with mitochondria; 3) that Hx normally binds to porin and leaves porin early in apoptosis in association with a decrease in $\Delta\Psi_M$ (not illustrated); and 4) an increase in mitochondrial CK occurs early in apoptosis, in association with a decrease in $\Delta\Psi_M$ (not illustrated). The CK, which accumulates in mitochondria during apoptosis, co-localizes with BAX. We propose that these dynamics in protein interactions and subcellular localization may be fundamental to the control of PTP opening and closing.

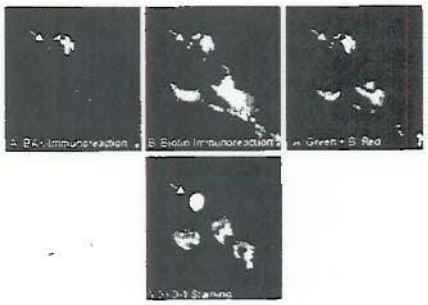

Figure 7 – Biotin immunoreaction marks mitochondrial carboxylases independently of $\Delta\Psi_M$ and co-localizes with increased BAX in cerebellar granule neurons (CGns) that have been maintained in culture for 7 days and are entering apoptosis caused by reducing media potassium. The arrow shows a CGn with chromatin condensation and high levels of mitochondrially-localized BAX immunoreactivity. Other CGns without apoptotic nuclear degradation show lower levels of mitochondrial BAX immunoreactivity. The colored image was generated by coloring image A green and image B red and then adding the images. Red or green indicate loci where BAX and biotin do not co-localize while orange and yellow indicate loci of increasing relative co-localization (see [Sugrue, 1999 #28] for details).

A variety of evidence has shown that BCL-2 (or BCL-X_L) binds at or near to the PTP and that the binding facilitates PTP closure and therefore reduces the release of mitochondrial factors causing apoptotic degradation [Zamzami, 1998 #87]. In contrast, BAX forms dimers and its binding to the PTP at the AdNtr appears to facilitate PTP opening and therefore apoptosis [Marzo, 1998 #73; Marzo, 1998 #74].

All of the changes in protein subcellular localization and PTP protein-protein interactions shown here were determined for apoptosis induced by NGF and serum withdrawal in neuronally differentiated PC12 cells and after reduced K^+ in CGns. ***It is not known whether GAPDH upregulation or nuclear accumulations play any role in those changes in levels, subcellular localization and protein-protein interactions.***

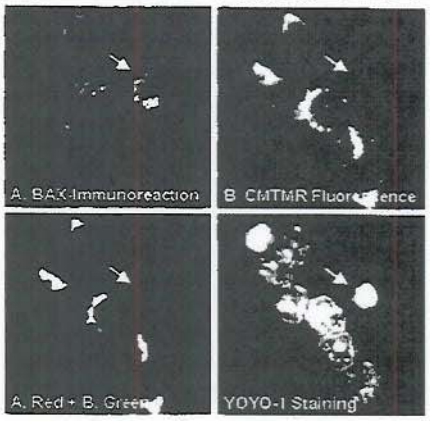

Figure 8- CMTMR fluorescence and BAX immunoreaction do not co-localize in CGns that have been maintained in culture for 7 days and are entering apoptosis or are undergoing apoptotic nuclear degradation caused by reducing media potassium. The arrows show a CGn with chromatin condensation that expresses high levels of punctate BAX immunoreactivity and an apparent loss of $\Delta\Psi_M$ as indicated by CMTMR fluorescence. Other CGns without apoptotic nuclear degradation do not show BAX immunoreactivity that co-localizes with CMTMR fluorescence. The colored image was generated as described above. Red or green indicate loci where BAX and $\Delta\Psi_M$ do not co-localize. The absence of orange and yellow coloration suggests that mitochondrial BAX immunoreactivity varies inversely with $\Delta\Psi_M$.

Deprenyl Related Propargylamines and Neuronally Differentiated PC12 Cells. We and others have shown that (-)-deprenyl related propargylamines can reduce apoptosis in a variety of models [Suuronen, 2000 #75; Boulton, 1999 #76; Maruyama, 1999 #77; Magyar, 1999 #78; Gelowitz, 1999 #79; Kragten, 1998 #80; Maruyama, 1998 #81; Wadia, 1998 #49; Paterson, 1997 #83] and that it prevents the decrease in $\Delta\Psi_M$ that is an early feature of some forms of apoptosis [Wadia, 1998 #49; Paterson, 1998 #50]. (-)-Desmethyldeprenyl (DES), the major metabolite of (-)-deprenyl, has been found to mediate the anti-apoptotic action [Tatton, 1996 #54; Mytilineou, 1997 #85; Mytilineou, 1998 #84] and the maintenance of $\Delta\Psi_M$ (Chalmers-Redman and Tatton, unpublished observations).

A tricyclic analog of (-)-deprenyl, CGP3466 (N-methyl-N-propargyl-10-aminomethyl-dibenzo{b,f}oxepin) has been shown to reduce apoptosis in PADJU cells and to bind to GAPDH in homogenates of rat hippocampus Kragten, 1998 #372. We examined the capacity of DES and CGP3466 to reduce apoptosis in partially neuronally differentiated PC12 cells as a prerequisite to determining whether GAPDH played a role in apoptosis in the cells (see [Carlile, 2000 #35] appended).

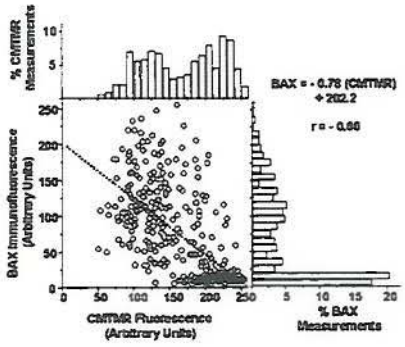

Figure 9 – BAX immunofluorescence and CMTMR fluorescence were measured for individual mitochondria in CGns that had been exposed to 10^{-4} M NMDA 6 hours earlier. The plot shows intra-mitochondrial BAX levels have a high probability of being at background fluorescence for CMTMR fluorescence levels exceeding 170 arbritray units. In contrast BAX levels increase proportionally for CMTMR fluorescence levels of less than 170 arbritary units.

We determined the relative concentration-survival relationships for (-)-deprenyl, DES and CGP3466 treated neuronally differentiated PC12 cells induced into apoptosis by serum and NGF (figures 2A1 to 2A5). (-)-Deprenyl, DES and CGP3466 increase the numbers of intact nuclei and to decrease the numbers of nuclei with apoptotic degradation (see figure 1 in [Carlile, 2000 #35]). The cells were treated with a ^{125}I labeled photoaffinity analog of CGP3466 and autoradiograms revealed a number of bands, including those at 30, 38, 50 and 70 kd (see figure 2 in [Carlile, 2000 #35]). The same membranes used for the autoradiograms were probed with a monoclonal antibody against GAPDH and revealed that the location of the 38 kd autoradiography band corresponded to that of GAPDH immunoreactivity (see figure 2 in [Carlile, 2000 #35] appended).. Accordingly, we concluded that CGP3466 bound to GAPDH in the NGF and serum withdrawn PC12 cells in a similar manner to that found for rat hippocampus.

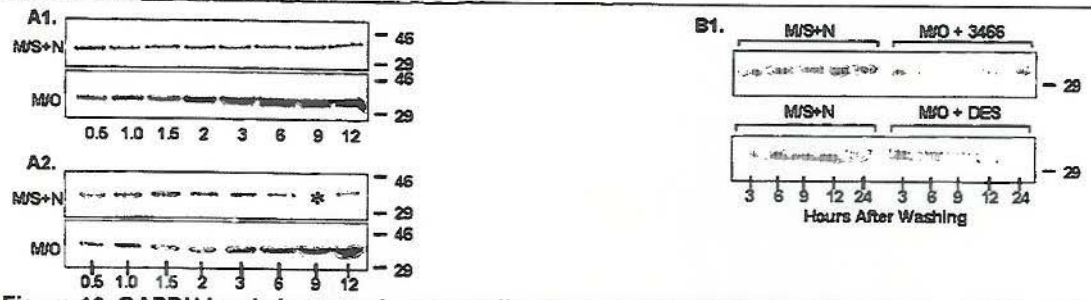

Figure 10. GAPDH levels increase in neuronally differentiated PC12 cells after serum and NGF withdrawal. DES and CGP3466 prevent the increase in GAPDH levels. A1 and A2. Western blots for two identical experiments - M/S+N, cells were washed and then replaced in MEM with serum and NGF as a control; M/O, cells were washed and placed in MEM only to induce apoptosis by serum and NGF withdrawal. B1. Similar experiments but CGP3466 or DES were added to the MEM only. Note that additions blocked the increase in GAPDH levels Taken from figure 4, [Carlile, 2000 #35] appended

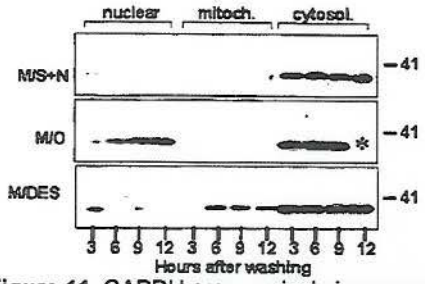

Figure 11. GAPDH progressively increases in the nuclear protein fraction at 3, 6, 9 and 12 hours in partially neuronally differentiated PC12 cells after serum and NGF withdrawal. Each panel shows western blots for protein taken from nuclear (Nuclear.), mitochondrial (Mitoch.) and cytosolic (Cytosol.) subcellular fractions at 3, 6, 9,and12 hours after washing and then replacement into MEM with serum and NGF as a control (upper panel) or placement into MEM only to induce apoptosis by serum and NGF withdrawal (lower panel). Note the progressive increase in nuclear GAPDH immunoreactivity beginning between 3 and 6 hours after washing and serum and NGF withdrawal together with the maintained increase in cytosolic GAPDH that was present at 3 hours Taken from figure 4, [Carlile, 2000 #35] appended.

Increased Levels of GAPDH and GAPDH Nuclear Translocation Reduced by Propargylamines.

Western blots for protein extracts from the same cells showed that GAPDH levels begin to increase markedly and progressively at 2-3 hours after washing and withdrawal of serum and NGF (figure 10A). By 12 hours after washing, immunodensity had increased to more than 600% of that found for cells that were washed and replaced in serum and NGF. Treatment with 10^{-9} M CGP3466 or DES prevented any increase in the GAPDH immunodensity (figure 10B).

More striking than the increase in GAPDH levels in the cytosol is the translocation of GAPDH to nucleus that occurs in early apoptosis in the neuronally differentiated PC12 cells after serum and NGF withdrawal (figure 11). The translocation is similar to that previously reported for HEK293 cells, S49 cells, primary thymocytes, PC12 cells entering apoptosis after a variety of insults, and primary cerebral cortical neuronal cultures and cultured cerebellar granule neurons after cytosine arabinoside treatment (see references above). ***The bases for the increase in GAPDH levels or the nuclear translocation are not known.***

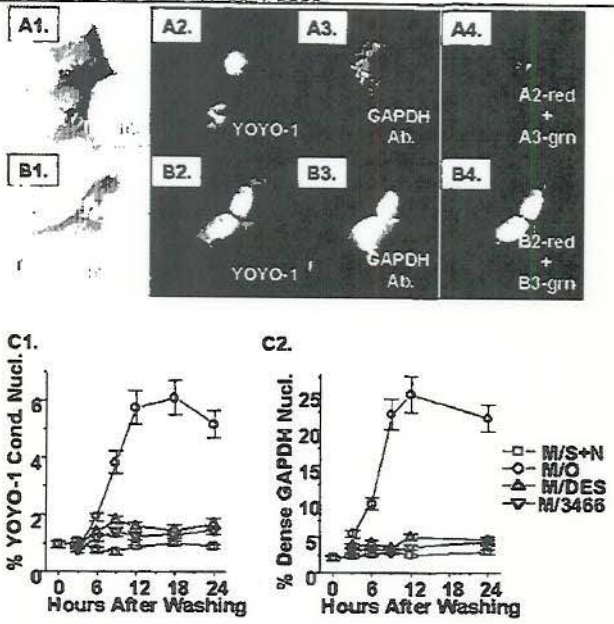

Figure 12. - GAPDH immunoreactivity in pnd-PC12 cells after serum and NGF withdrawal visualized with LCSM. A1, A2, A3 and A4. present LCSM micrographs from identical image fields and consist of an interference contrast micrograph, fluorescence micrograph for YOYO-1 DNA binding, immunocytochemistry for GAPDH and a combined image in which A2. (re-colored red) and A3.(re-colored green) were digitally added. The cells were washed and then replaced in MS+N as a control (example at 6 hours after washing). The maintained separation of the red and green color in A4 shows that GAPDH is largely extranuclear in location . **B1, B2, B3 and B4.** An identical series of LCSM micrographs for cells which were washed and placed in MO to induce apoptosis by serum and NGF withdrawal showed dense GAPDH immunoreaction in the nucleus that spared the nucleolus (example at 6 hours after washing). The orange-yellow color in B4 shows the co-localization of DNA YOYO-1 binding and GAPDH immunoreaction and illustrates typical dense nuclear GAPDH accumulation. **C1 and C2.** Counts of cells with nuclei showing YOYO-1 stained chromatin condensation and those with dense GAPDH nuclear immunoreaction, respectively, show that the percentages of nuclei with GAPDH nuclear accumulation was significantly increased by 3 hours after washing while the percentages with apoptotic chromatin condensation did not begin to increase until 6 hours after washing and placement in MEM only. DES (plots labeled M/DES) and CGP3466 (plots labeled M/3466) at 10^{-9} M markedly decreased the percentage of nuclei with chromatin condensation and those with dense GAPDH nuclear immunoreaction. Taken from figure 5, [Carlile, 2000 #35] appended.

Counts of nuclei with dense GAPDH accumulation and those with chromatin condensation from LCSM images (figures 12A1 to A4) showed that the translocation led apoptotic nuclear degradation and had a similar time course to the decrease of $\Delta\Psi_M$ previously found in the same cells after serum and NGF withdrawal (see [Wadia, 1998 #49]). Therefore dense GAPDH nuclear translocation is an early event in this form of apoptosis and occurs before or at the same time as a loss of $\Delta\Psi_M$, which is believed to represent opening of the PTP. Similar to the finding with the increase in GAPDH levels on western blots shown above, treatment with DES and CGP3466 markedly attenuated the accumulation of GAPDH to nuclei and induce an apparently commensurate decrease in nuclei with chromatin condensation. The data suggest that the prevention of the increase in GAPDH levels and/or nuclear accumulation by the two compounds may account for their capacity to reduce apoptosis in the cells The dense character of the GAPDH nuclear accumulation is important to emphasize. We have recently reported that GAPDH is normally found in the nucleus in low concentration as part of punctate bodies ([Carlile, 1998 #12], appended). The punctate bodies contain promyelocytic leukemia protein (PML protein) that we found co-immunoprecipitates with GAPDH. PML protein has been implicated in apoptosis, but we do not know whether the dense nuclear accumulation of GAPDH found in early apoptosis involves a relationship between GAPDH and PML protein.

Green Fluorescent Protein Fusion Protein for GAPDH.

With the participation of S. Shashidharan and S. Sealfon, we have cloned a GAPDH cDNA from rat brain The cDNA was used to produce a GAPDH-green fluorescent protein (GFP) construct and has been transiently transfected into COS1 cells and stably transfected into HEK 293 and PC12 cells. We used several methods to induce apoptosis in the transfected cells maintained in a physiological chamber on a confocal laser microscope (see [Wadia, 1998 #49], appended for details of the chamber). Living cells were shown to have little or no GAPDH-GFP protein in their nuclei and showed a cytosolic distribution for the fusion protein that seemed identical to that shown with immunocytochemistry for GAPDH. The GAPDH-GFP fusion protein was shown to concentrate in the nucleus of a proportion of the cells in the first two hours after exposure to apoptosis initiating agents like Rose Bengal (see below). Published details of the cytoplasmic-nuclear translocation found using the fusion protein are presented in [Shashidharan, 1999 #40] appended. These data established that at least part of

the GAPDH that accumulates in the nucleus during some forms of apoptosis translocates from the cytoplasm.

GAPDH-RNA And NAD^+, NO and Peroxide.

GAPDH in the cellular cytosol is bound in large part to AU-rich RNA and tRNA. It unwinds RNA and can straighten RNA stem loops during translation [Sioud, 1996 #88]. We postulate that GAPDH might be freed from the AU-rich RNA in early apoptosis, which would allow it to migrate to the nucleus and associate with nuclear DNA. DNase-free RNase treatments of permeablized, paraformaldehyde fixed PC12cells on coverslips to digest RNA caused GAPDH to relocate to the nucleus in a manner similar to that found in early apoptosis (unpublished data, not shown).

At least three molecules associated with toxin-induced neuronal apoptosis – nitric oxide (NO), superoxide radical and peroxynitrite – have the capacity to free GAPDH from AU-rich RNA (see references above). In accord with that idea, our treatment of partially differentiated PC12 cells or fibroblasts with H_2O_2 (see figure 13A) or the nitric oxide (NO) donor, SNAP (see figure 13B) induced a dense nuclear translocation of GAPDH, which appeared similar to that found after serum and NGF withdrawal.

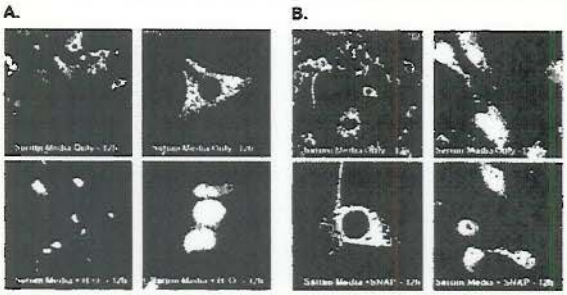

Figure 13 - 3T3 Fibroblasts Showing GAPDH Nuclear Translocation After Exposure To An NO Donor or To H_2O_2. Figures show laser confocal microscope images of 3T3 fibroblast immunoreacted with a GAPDH antibody. Exposure to 0.25 mM H_2O_2 (**A**) or to SNAP, an NO donor (**B**), induced GAPDH nuclear translocation in the cells

NAD^+ Levels Determine the Proportion of GAPDH Bound to AU-Rich RNA versus That Involved in Glycolysis.

We carried out measurements of the capacity of GAPDH to convert NAD^+ to NADH in the glycolytic pathway depending upon the presence or absence of AU-rich RNA (data not shown). Increasing concentrations of AU-rich RNA reduced NADH production in a graded manner indicating that GAPDH cannot function as a glycolytic enzyme when it is bound to RNA. (-)-Desmethyldeprenyl or CGP3466 did not alter the glycolytic capacity of GAPDH in the absence of RNA but reversed the reduced glycolytic capacity of GAPDH induced by the presence of RNA (see figure 6 in [Carlile, 2000 #35], appended).

In parallel experiments, we found that NAD^+ releases GAPDH from AU-rich RNA as previously reported (not shown) and thereby, increases the enzyme's glycolytic activity. Importantly, NAD^+ that had been exposed to temperatures of 55-70°C was found to no longer release GAPDH from AU-rich RNA (not shown), probably because NAD^+ is heat labile and folds when exposed to those temperatures.

Deprenyl Related Propargylamines Decrease GAPDH Tetramer And Increase GAPDH Dimer In Vitro.

GAPDH, a 37 kDa protein, forms tetramers in which four GAPDH proteins join to each other forming a complex of 148 kDa (a computer generated model of the structure is shown in figure 7 of [Carlile, 2000 #35], appended). Modeling of the three dimensional crystal structure taken from the Brookhaven data base shows that a channel will form at the side-to-side joining of dimeric pairs with each other and suggested that CGP3466 might bind in that channel. We used size exclusion chromatography to show that GAPDH is largely in a tetrameric form when bound to poly-U RNA in solution (figure 6 in [Carlile, 2000 #35]. 10^{-9} M CGP3466 or (-)-desmethyldeprenyl freed a significant portion of GAPDH from RNA and shifted it to a dimeric form. Previous studies had shown that the dimer is a more efficient glycolytic enzyme than the tetramer. Accordingly, the ***deprenyl-related compounds may induce GAPDH to a dimer, a form in which it may not be able to participate in apoptosis but can be fully effective in its glycolytic role***.

Deprenyl-Related Propargylamines Reduce Neuronal Apoptosis By Inducing Changes In New Protein Synthesis.

(-)-Deprenyl was initially thought to only reduce nerve cell death by inhibiting monoamine oxidase B and thereby preventing the conversion of MPTP to the toxin, MPP^+. More than thirty five studies have found that (-)-deprenyl can reduce cell death in a variety of models other than MPTP, including trophic withdrawal, pro-oxidant

exposure, hypoxia-ischemia, mitochondrial toxin exposure, metabolic toxins, aluminum toxicity, DNA damaging agents, axonal transection, aging (see [Tatton, 1996 #55]). We were the first to establish that (-)-deprenyl could reduce nerve cell death, specifically apoptotic nerve cell death, independently of monoamine oxidase B (MAO-B) inhibition, which has subsequently been confirmed in a number of laboratories (see references above). The anti-apoptotic action of (-)-deprenyl is mediated by its major metabolite, (-)-desmethyldeprenyl (DES) in neurons *in vitro* and *in vivo* , since: 1) DES has the same capacity as (-)-deprenyl to reduce apoptosis and to maintain $\Delta\Psi_M$ in early apoptosis, 2) transcriptional and translational inhibitors block the capacity of both (-)-deprenyl and DES to reduce apoptosis and maintain $\Delta\Psi_M$ and 3) P450 inhibitors, which block drug metabolism, prevent (-)-deprenyl, but not DES, from reducing apoptosis and maintaining $\Delta\Psi_M$.

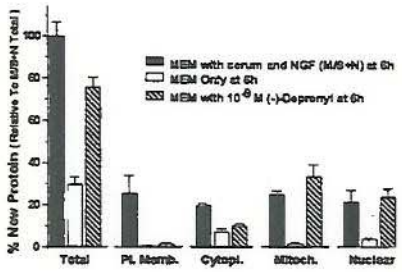

Figure 14 - Metabolic labeling of newly synthesized proteins with 35 S methionine shows a marked decrease in total protein and protein in specific sub-fractions in the first six hours of apoptosis. (-)-Deprenyl (and DES and CGP3466) markedly reduce the decrease in total newly synthesized protein but show significant increases only in the mitochondrial and nuclear fractions and not the plasma membrane and cytosolic fractions.

(-)-Deprenyl requires new protein synthesis to reduce apoptosis [Tatton, 1994 #57]. We have now studied the changes in new protein synthesis induced by (-)-deprenyl, DES and CGP3466. Metabolic studies using 35S-methionine showed that new protein synthesis decreased to about 30% at 6 hrs after NGF and serum withdrawal and was maintained at 70% by each of the three compounds (see figure 11). The major subcellular protein fractions whose levels of newly synthesized protein were the mitochondrial and nuclear fractions and there was little, if any, effect on the plasma membrane or cytosolic fractions. Metabolically-labeled two dimensional protein auto-radiograms for protein sub-fractions showed that these compounds induced the synthesis of a number of proteins in the pre-apoptotic cells that were not normally synthesized in cells supported by serum and NGF.

In brief, the pre-apoptotic cells showed a maintenance of BAX levels and a transient increase in c-JUN together with a decrease in BCL-2, BCL-X_L, SOD1, SOD2, glutathione peroxidase, tyrosine hydroxylase, and the cytoskeletal proteins, tubulin and MAP-2. The deprenyl-related compounds prevented the decreases in BCL-2, BCL-X_L, SOD1, SOD2, glutathione peroxidase and tyrosine hydroxylase, but did not alter the decreases in tubulin or MAP-2. They also induced a gradual decrease in BAX and prevented the increase in c-JUN. Immunocytochemistry for the different proteins and *in situ* hybridization for their messages showed complementary changes. Since the deprenyl-related compounds bind to GAPDH and appear to convert GAPDH to a dimer while preventing the upregulation of GAPDH and reducing the nuclear accumulation of GAPDH, it could be argued that the changes in new protein synthesis induced by the propargylamines are the result of preventing GAPDH from influencing transcription and or translation.

Since proteins like BCL-2 and SOD1 have been shown to contribute to the maintenance of $\Delta\Psi_M$ by facilitating PTP losure in early apoptosis, we used LCSM imaging of partially neuronally-differentiated PC12 cells entering apoptosis after serum nd NGF withdrawal to show that (-)-deprenyl [Wadia, 1998 #49] prevents the decrease in $\Delta\Psi_M$ in early apoptosis, even when tramitochondrial Ca^{2+} was markedly increased ([Wadia, 1998 #49]). Subsequently, we have shown similar findings for DES and GP3466. The maintenance of $\Delta\Psi_M$ despite increased intramitochondrial Ca^{2+} levels seem to indicate that (-)-deprenyl and DES can hange the relationship between the level of intramitochondrial Ca^{2+} and $\Delta\Psi_M$. We concluded that the observation depended upon e capacity of (-)-deprenyl to maintain the synthesis of BCL-2 in pre-apoptotic neurons (see below) and thereby maintain itochondrial BCL-2 levels. ***Most importantly, mitochondrial actions of (-)-deprenyl related propargylamines may be taken to suggest that e mitochondrial PTP is downstream from GAPDH in some forms of apoptosis signaling.***

GAPDH May Induce A Decrease In New Protein Synthesis

We have carried out preliminary experiments with rabbit reticulocyte lysate systems and in vitro transcription systems. he synthesis of two proteins and their mRNAs have been examined: the pGEM protein supplied with the kits and luciferase (see gure 15). The addition of *amounts of GAPDH* varying from 5 μg to 500 μg resulted in a *marked decrease in protein synthesis* as an dicator of decreased transcription and/or translation and a decrease in the mRNAs as a indicator of decreased transcription. Hence e preliminary experiments suggest that GAPDH has the capacity to *inhibit the transcriptional machinery*. At present, it is not known

hether GAPDH effects on transcription are selective or generalized. **That is, does GAPDH increase the synthesis of some proteins while ecreasing that of others? Are any changes in protein synthesis appropriate for the induction of apoptosis and are they appropriate oppose the changes induced by low level damage and or the deprenyl-related compounds?**

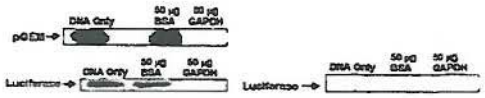

Figure 15 – GAPDH Addition To An In Vitro Transcriptional System GAPDH addition prevents the synthesis of control luciferase RNA species in an *in vitro* transcriptional system as detected by ethidium bromide staining and B. GAPDH prevents the synthesis of control luciferase RNA species in an *in vitro* transcriptional system as detected by ethidium bromide staining.

Protein-Protein Interactions Involving GAPDH With Possible Significance To Apoptosis or Neurodegeneration. As described above we have shown that GAPDH binds to the pro-apoptotic, translational control protein, PML[Carlile, 1998 #12].

Recently, we have begun to carry out co-immunoprecipitation and LCSM studies in our laboratory in collaboration with M. Polymeropoulos and A. Dehejia from the Novartis laboratories at Gaithersburg using cells co-transfected with constructs coding for multiple proteins that have been implicated in human neurodegeneration or apoptosis. Preliminary results indicate that GAPDH, huntingtin (implicated in HD) and α-synuclein (a mutant form is found in dominantly inherited PD), all co-immunoprecipitate with phospholipase D2 (PLD2) (figure 16 shows example of co-immunoprecipitation of GAPDH and PLD2 and GAPDH and huntingtin). Also, as previously reported [Burke, 1996 #2], the studies show co-immunoprecipitation of GAPDH and huntingtin.

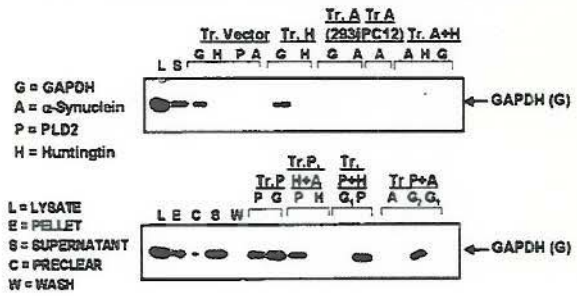

Figure 16 - Co-immunoprecipitation of protein extracted from cells that were multiply transfected with combinations of GAPDH, αsyn, htn and PLD2. The blot shows that GAPDH and PLD2 co-immunoprecipitate (lower blot) and GAPDH and htn co-immunoprecipitate. Other blots showed that PLD2 could also co-immunoprecipitate with αsyn or htn in absence of GAPDH transfection. In the presence of GAPDH-PLD immunoprecipitation, neither htn nor αsyn co-immunoprecipitated with PLD2. Similarly, htn-GAPDH co-immunoprecipitation was not seen in the presence of PLD2-GAPDH co-immunoprecipitation.

These protein-protein interactions seem to be competitive, since in the presence of high levels of PLD2, PLD2 co-immunoprecipitation with α-synuclein or that with huntingtin were found to be absent. The hypothesized competitive interactions are summarized in figure 17. At present, we do not understand the implications of the interactions. PLD2 might serves to "control" GAPDH subcellular movements and protein-protein signaling. If GAPDH levels are high, as in early apoptosis, PLD2 might lose its normal signaling functions and/or its capacity to interact with huntingtin and α-synuclein. Accordingly, mutant a-synuclein and mutant huntingtin protein might not participate in the PLD2 interactions normally and could possibly "free" GAPDH to participate in apoptosis. Similarly, GAPDH has been found to bind to huntingtin in HD brain tissue. These finding may reflect abnormal interactions amongst those disease-related proteins and GAPDH and PLD2.

As shown in figure 18, we have run co-immunoprecipitation gels for GAPDH in neuronally differentiated PC12 cells under a variety of conditions [Wadia, 1998 #49]. We have used sensitive silver staining to determine the maximum number of proteins that bind to GAPDH (see figure 18). This and other gels suggest that less than a dozen proteins bind to GAPDH under various conditions: four of those proteins are known – α-tubulin, PLD2, huntingtin and PML protein.

Co-Transfection And Co-Immunprecipitation Reveal Competitive Interactions Amongst Phospholipase D2, Glyceraldehyde-3-Phosphate Dehydrogenase, a-Synuclein And Huntingtin

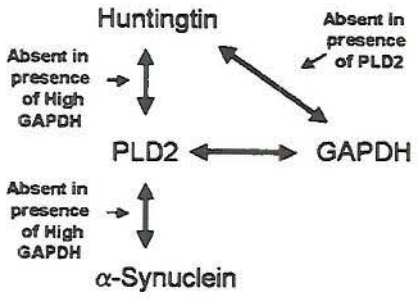

Figure 17 -Summary of hypothesized protein-protein interactions amongst GAPDH, PLD2, αsyn and htn in multiply transfected cells.

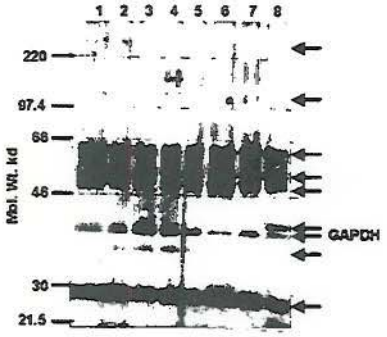

Figure 18 – Staining of co-immunoprecipitation gels shows that GAPDH can be involved in a relatively small number of protein-protein interactions in neuronally differentiated PC12 cells. Each lane is for lysate taken for PC12 cells after a different experimental treatment. The gel was stained with silver to provide a sensitive assay of all the protein-protein interactions of GAPDH. The silver staining shows that GAPDH binds to a relatively small number of proteins and that some of the binding is in different experimental conditions while others vary under different conditions.

Key Research Accomplishments:

1. The role of diverse signal mediators, including p53, GAPDH, BAX and NFKB in mediating apoptosis in PD brain were characterized.

2. The temporal stages of apoptosis in dopamine neurons determined by YOYO-1 and BODIPY-labeled TUNEL staining were refined.

3. The mechanism of propargylamines such as deprenyl in opposing apoptosis in dopamine neurons and in improving the course of Parkinsons was found to be suppression of the synthesis of pro-apoptotic proteins.

Reportable Outcomes:

Five peer reviewed publications that resulted from this research program:

1. Carlile, G., Chalmers-Redman, R., Tatton n., Pong, A., Borden, K., Tatton, W. Reduced Apoptosis after nerve growth factor and serum withdrawal: Conversion of tetrameric Glyceraldehyde-3-Phosphate Dehydrogenase to a dimer. Molecular Pharmacology 2000, 57:2-12.

2. Tatton, W. G., Chalmers-Redman, R. M., Elstner, M., Leesch, W., Jagodzinski, F. B., Stupak, D. P., et al. (2000). Glyceraldehyde-3-phosphate dehydrogenase in neurodegeneration and apoptosis signaling. J Neural Transm Suppl(60), 77-100.

3. Tatton WG, Chalmers-Redman RM, Ju WJ, Mammen M, Carlile GW, Pong AW, Tatton NA. Propargylamines induce antiapoptotic new protein synthesis in serum- and nerve growth factor (NGF)-withdrawn, NGF-differentiated PC-12 cells. J Pharmacol Exp Ther. 2002; 301 (2): 753-64.

4. Tatton WG, Chalmers-Redman R, Brown D, Tatton N. Apoptosis in Parkinson's disease: signals for neuronal degradation. Ann Neurol. 2003; 53 Suppl 3: S61-70; discussion S70-2.

5. Tatton, W., Chalmers-Redman, R., & Tatton, N. (2003). Neuroprotection by deprenyl and other propargylamines: glyceraldehyde-3-phosphate dehydrogenase rather than monoamine oxidase B. J Neural Transm, 110(5), 509-515.

Conclusions:

This research program refined the understanding of the timing of apoptosis and the stages involved and provided insight into the mechanisms of propargylamines in preventing apoptosis. This work advanced insight into the mechanisms of neuronal loss in PD and into new pharmacological approaches that could be used to delay the progression of this neurodegenerative disease.

References:

Olanow, C.W. and W.G. Tatton, Etiology and pathogenesis of Parkinson's disease. Annu Rev Neurosci, 1999. 22: p. 123-44.

Pakkenberg, B., A. Möller, H.J. Gundersen, A. Mouritzen Dam, and H. Pakkenberg, The absolute number of nerve cells in substantia nigra in normal subjects and in patients with Parkinson's disease estimated with an unbiased stereological method. J Neurol Neurosurg Psychiatry, 1991. 54(1): p. 30-3.

Ma, S.Y., J.O. Rinne, Y. Collan, M. Roytta, and U.K. Rinne, A quantitative morphometrical study of neuron degeneration in the substantia nigra in Parkinson's disease. J Neurol Sei, 1996. 140(1-2): p. 40-5.

Langston, J.W., P. Ballard, J.W. Tetrud, and I. Irwin, Chronic Parkinsonism in humans due to a product of mependine-analog synthesis. Science, 1983. 219(4587): p. 979-80.

Langston, J.W., E.B. Langston, and I. Irwin, MPTP-induced parkinsonism in human and nonhuman primates-clinical and experimental aspects. Acta Neurol Scand Suppl, 1984.100: p. 49-54.

Burns, R.S., S.P. Markey, J.M. Phillips, and C.C. Chiueh, The neurotoxicity of 1-methyl-4-phenyl-1,2,3,6-tetrahydropyridine in the monkey and man. Can J Neurol Sei, 1984.11(1 Suppl): p. 166-8.

Forno, L.S., J.W. Langston, L.E. DeLanney, I. Irwin, and G.A. Ricaurte, Locus ceruleus lesions and eosinophilic inclusions in MPTP-treated monkeys. Ann Neurol, 1986. 20(4): p. 449-55.

Crossman, A.R., C.E. Clarke, S. Boyce, R.G. Robertson, and M.A. Sambrook, MPTP-induced parkinsonism in the monkey: neurochemical pathology, complications of treatment and pathophysiological mechanisms. Can J Neurol Sei, 1987.14(3 Suppl): p. 428-35.

Miyoshi, R., S. Kito, H. Ishida, and S. Katayama, Alterations of the central noradrenergic system in MPTP-induced monkey parkinsonism. Res Commun Chem Pathol Pharmacol, 1988. 62(1): p. 93-102.

Seniuk, N.A., W.G. Tatton, and C.E. Greenwood, Dose-dependent destruction of the coeruleuscortical and nigral-striatal projections by MPTP. Brain Res., 1990. 527: p. 7-20.

Pifl, C, G. Schingnitz, and O. Hornykiewicz, The neurotoxin MPTP does not reproduce in the rhesus monkey the interregional pattern ofstriatal dopamine loss typical of human idiopathic Parkinson's disease. Neurosci Lett, 1988. 92(2): p. 228-33.

Kuzuhara, S., H. Mori, N. Izumiyama, M. Yoshimura, and Y. Ihara, Lewy bodies are ubiquitinated. A light and electron microscopic immunocytochemical study. Acta Neuropathol, 1988. 75(4): p. 345-53.

Bayer, T.A., P. Jakala, T. Hartmann, L. Havas, C. McLean, J.G. Culvenor, Q.X. Li, C.L. Masters, P. Falkai, and K. Beyreuther, Alpha-synuclein accumulates in Lewy bodies in Parkinson's disease and dementia with Lewy bodies but not in Alzheimer's disease beta-amyloid plaque cores. Neurosci Lett, 1999. 266(3): p. 213-6.

Tatton, N.A., Increased caspase 3 and Bax immunoreactivity accompany nuclear GAPDH translocation and neuronal apoptosis in Parkinson's disease. Exp Neurol, 2000. 166(1): p. 29-43.

Mizuno, Y., S. Ohta, M. Tanaka, S. Takamiya, K. Suzuki, T. sato, H. Oya, T. Ozawa, and Y. Kagawa, Deficiencies in complex I subunits of the respiratory chain in Parkinson's disease. Biochem. Biophys. Res. Comm., 1989. 163: p. 1450-1455.

Parker, W.D., Jr., S.J. Boyson, and J.K. Parks, Abnormalities of the electron transport chain in idiopathic Parkinson's disease. Ann Neurol, 1989. 26(6): p. 719-23.

Schapira, A.H., J.M. Cooper, D. Dexter, J.B. Clark, P. Jenner, and CD. Marsden, Mitochondria! complex I deficiency in Parkinson's disease. J Neurochem, 1990. 54(3): p. 823-7.

Schapira, A.H., V.M. Mann, J.M. Cooper, D. Dexter, S.E. Daniel, P. Jenner, J.B. Clark, and CD. Marsden, Anatomic and disease specificity ofNADH CoQ1 reductase (complex I) deficiency in Parkinson's disease. J Neurochem, 1990. 55(6): p. 2142-5.
Yoshino, H., Y. Nakagawa Hattori, T. Kondo, and Y. Mizuno, Mitochondria! complex I and II activities of lymphocytes and platelets in Parkinson's disease. J Neural Transm Park DisDement Sect, 1992. 4(1): p. 27-34.
Mizuno, Y., S. Matuda, H. Yoshino, H. Mori, N. Hattori, and S. Ikebe, An immunohistochemical study on alpha-ketoglutarate dehydrogenase complex in Parkinson's disease. Ann Neurol, 1994. 35(2): p. 204-10.
Hattori, N., M. Tanaka, T. Ozawa, and Y. Mizuno, Immunohistochemical studies on complexes I, II, III, and IV of mitochondria in Parkinson's disease. Ann Neurol, 1991. 30(4): p. 563-71.
Chiba, K., A. Trevor, and N. Castagnoli, Jr., Metabolism of the neurotoxic tertiary amine, MPTP, by brain monoamine oxidase. Biochem Biophys Res Commun, 1984.120(2): p. 574-8.
Di Monte, D.A., E.Y. Wu, I. Irwin, L.E. Delanney, and J.W. Langston, Biotransformation of 1- methyl-4-phenyl-1,2,3,6-tetrahydropyridine in primary cultures of mouse astrocytes. J Pharmacol ExpTher, 1991. 258(2): p. 594-600.
Chiba, K., A.J. Trevor, and N. Castagnoli, Jr., Active uptake ofMPP+, a metabolite of MPTP, by brain synaptosomes. Biochem Biophys Res Commun, 1985.128(3): p. 1228-32.
Pifl, C, B. Giros, and M.G. Caron, Dopamine transporter expression confers cytotoxicity to low doses of the parkinsonism-inducing neurotoxin 1-methyl-4-phenylpyridinium. J Neurosci, 1993. 13(10): p. 4246-53.
Peter, D., J. Jimenez, Y. Liu, J. Kim, and R.H. Edwards, The chromaffin granule and synaptic vesicle amine transporters differ in substrate recognition and sensitivity to inhibitors. J BiolChem, 1994. 269(10): p. 7231-7.
Del Zompo, M., M.P. Piccardi, S. Ruiu, G.U. Corsini, and A. Vaccari, Characterization of a putatively vesicular binding site for[3H]MPP+ in mouse striatal membranes. Brain Res, 1992. 571(2): p. 354-7.
Del Zompo, M., M.P. Piccardi, S. Ruiu, G.U. Corsini, and A. Vaccari, High-affinity binding of [3H]1-methyl-4-phenyl-2,3-dihydropyridinium ion to mouse striatal membranes: putative vesicular location. Eur J Pharmacol, 1991. 202(2): p. 293-4.
Mizuno, Y., N. Sone, and T. Saitoh, Dopaminergic neurotoxins mptp and mpp-+ inhibit activity of mitochondrial nadh-ubiquinone oxidoreductase. Proc Jpn Acad Ser B Phys Biol Sei, 1986. 62(7): p. 261-263.
Mizuno, Y., K. Suzuki, N. Sone, and T. Saitoh, Inhibition ofATP synthesis by 1-methyl-4-phenylpyridinium (MPP+) in isolated mitochondria from mouse brains. Neurosci. Lett., 1987. 81: p. 204-208.
Nicklas, W.J., I. Vyas, and R.E. Heikkila, Inhibition of NADH-linked oxidation in brain mitochondria by 1-methyl-4- phenyl-pyridine, a metabolite of the neurotoxin, 1-methyl-4-phenyl-1,2,5,6-tetrahydropyridine. Life Sei, 1985. 36(26): p. 2503-8.
Reinhard, J.F., Jr., E.J. Diliberto, Jr., O.H. Viveros, and A.J. Daniels, Subcellular compartmentalization of 1-methyl-4-phenylpyridinium with catecholamines in adrenal medullary chromaffin vesicles may explain the lack oftoxicity to adrenal chromaffin cells. Proc Natl Acad Sei USA, 1987. 84(22): p. 8160-4.
Lotharius, J. and K.L. O'Malley, The parkinsonism-inducing drug 1-methyl-4-phenylpyridinium triggers intracellular dopamine oxidation. A novel mechanism oftoxicity. J Biol Chem, 2000. 275(49): p. 38581-8.
Nakamura, K., V.P. Bindokas, J.D. Marks, D.A. Wright, D.M. Frim, R.J. Miller, and U.J. Kang, The selective toxicity of 1-methyl-4-phenylpyridinium to dopaminergic neurons: the role of mitochondrial complex I and reactive oxygen species revisited. Mol Pharmacol, 2000. 58(2): p. 271-8.

Sriram, K., K.S. Pai, M.R. Boyd, and V. Ravindranath, Evidence for generation ofoxidative stress in brain by MPTP: In vitro and in vivo studies in mice. Brain Research, 1997. 749(1): p. 44-52.
Gerlach, M., M. Götz, A. Dirr, A. Kupsch, B. Janetzky, W. Oertel, J. Sautter, J. Schwarz, H. Reichmann, and P. Riederer, Acute MPTP treatment produces no changes in mitochondrial complex activities and indices ofoxidative damage in the common marmoset ex vivo one week after exposure to the toxin. Neurochem Int, 1996. 28(1): p. 41-9.
Liu, Y., D. Peter, A. Roghani, S. Schuldiner, G.G. Prive, D. Eisenberg, N. Brecha, and R.H. Edwards, A cDNA that suppresses MPP+ toxicity encodes a vesicular amine transporter. Cell, 1992. 70(4): p. 539-51.
Liu, Y., A. Roghani, and R.H. Edwards, Gene transfer of a reserpine-sensitive mechanism of resistance to N- methyl-4-phenylpyridinium. Proc Natl Acad Sei USA, 1992. 89(19): p. 9074-8.
Takahashi, N., L.L. Miner, I. Sora, H. Ujike, R.S. Revay, V. Kostic, V. Jackson-Lewis, S. Przedborski, and G.R. Uhl, VMAT2 knockout mice: heterozygotes display reduced amphetamine- conditioned reward, enhanced amphetamine locomotion, and enhanced MPTP toxicity. Proc Natl Acad Sei USA, 1997. 94(18): p. 9938-43.
Gainetdinov, R.R., F. Fumagalli, Y.M. Wang, S.R. Jones, A.I. Levey, G.W. Miller, and M.G. Caron, Increased MPTP neurotoxicity in vesicular monoamine transporter 2 heterozygote knockout mice. J Neurochem, 1998. 70(5): p. 1973-8.
Kerr, J.F.R., Shrinkage necrosis: a distinct form of cell death. J. Pathol., 1971.105: p. 13-20.
Kerr, J.F.R., A.H. Wyllie, and A.R. Currie, Apoptosis: A basic biological phenomenon with wide ranging implications in tissue kinetics. Br. J. Cancer, 1972. 26: p. 239-257.
Leist, M. and M. Jaattela, Four deaths and a funeral: from caspases to alternative mechanisms. Nat Rev Mol Cell Biol, 2001. 2(8): p. 589-98.
Ferri, K.F. and G. Kroemer, Organelle-specific initiation of cell death pathways. Nat Cell Biol, 2001. 3(11): p. E255-63. .
Mochizuki, H., K. Goto, H. Mori, and Y. Mizuno, Histochemical detection of apoptosis in Parkinson's disease. Journal of the Neurological Sciences, 1996.137(2): p. 120-123.
Anglade P., S. Vyas, F. Javoy-Agid, M.T. Herrero, P.P. Michel, J. Marquez, A. Mouatt-Prigent, M. Ruberg, EC. Hirsch, and Y. Agid, Apoptosis and autophagy in nigral neurons of patients with Parkinson's disease. Histol Histopathol, 1997.12(1): p. 25-31.
Kosel, S., R. Egensperger, U. vonEitzen, P. Mehraein, and M.B. Graeber, On the question of apoptosis in the parkinsonian substantia nigra. Acta Neuropathologica, 1997. 93(2): p. 105-108.
Banati, R.B., S.E. Daniel, and S.B. Blunt, Glial pathology but absence ofapoptotic mgral neurons in long- standing Parkinson's disease. Mov Disord, 1998.13(2): p. 221-7.
Kingsbury, A.E., CD. Mardsen, and O.J. Foster, DNA fragmentation in human substantia nigra: apoptosis orperimortem effect? Mov Disord, 1998. 13(6): p. 877-84.
Tatton, N.A. and H.J. Rideout, Confocal microscopy as a tool to examine DNA fragmentation, chrom'atin condensation and otherapoptotic changes in Parkinson's disease. Parkinsonism and Rel. Disord., 1999. 5: p. 179-186. .
Grosse, F. and A. Manns, Terminal deoxyribonucleotidyl transferase (EC 2.7.7.31), in Methods in Molecular Biology, Burrell, Editor. 1993, Humana Press, Inc.: Totowa. p. 95-105.
Kass, G.E.N., J.E. Eriksson, M. Weiss, S. Orrenius, and S.C. Chow, Chromatin condensation during apoptosis requires ATP. Biochem. J., 1996. 318: p. 749-752.
Susin, S.A., et al., Two distinct pathways leading to nuclear apoptosis. J Exp Med, 2000.192(4): p. 571-80.
Carlile, G.W., R.M. Chalmers-Redman, N.A. Tatton, A. Pong, K.E. Borden, and W.G. Tatton,

Reduced apoptosis after nerve growth factor and serum withdrawal: conversion of tetrameric glyceraldehyde-3-phosphate dehydrogenase to a dimerfln Process Citation]. Mol Pharmacol, 2000. 57(1): p. 2-12.
Wadia, J.S., R.M.E. Chalmers-Redman, W.J.H. Ju, G.W. Carlile, J.L. Phillips, A.D. Fräser, and W.G. Tatton, Mitochondria! membrane potential and nuclear changes in apoptosis caused by serum and nerve growth factor withdrawal: time course and modification by (-)-deprenyl. J Neurosci, 1998. 18(3): p. 932-47.
Tatton, N.A., A. Maclean-Fraser, W.G. Tatton, D.P. Perl, and C.W. Olanow, A fluorescent double-labeling method to detect and confirm apoptotic nuclei in Parkinson's disease. Ann Neurol, 1998. 44(3 Suppl 1): p. S142-8.
Hartmann, A., et al., Caspase-3: A vulnerability factor and final effector in apoptotic death of dopaminergic neurons in Parkinson's disease. Proc Natl Acad Sei USA, 2000. 97(6): p. 2875-80.
Hartmann, A., P.P. Michel, J.D. Troadec, A. Mouatt-Prigent, B.A. Faucheux, M. Ruberg, Y. Agid, and E.C. Hirsch, Is Bax a mitochondria! mediator in apoptotic death of dopaminergic neurons in Parkinson's disease? J Neurochem, 2001. 76(6): p. 1785-93.
Hartmann, A., J.D. Troadec, S. Hunot, K. Kikly, B.A. Faucheux, A. Mouatt-Prigent, M. Ruberg, Y. Agid, and E.C. Hirsch, Caspase-8 is an effector in apoptotic death of dopaminergic neurons in Parkinson's disease, but pathway inhibition results in neuronal necrosis. J Neurosci, 2001. 21(7): p. 2247-55.
de la Monte, S.M., Y.K. Sohn, N. Ganju, and J.R. Wands, P53- and CD95-associatedapoptosis in neurodegenerative diseases. Lab Invest, 1998. 78(4): p. 401-11.
Ferrer, I., R. Blanco, B. Cutillas, and S. Ambrosio, Fas and Fas-L expression in Huntingtons disease and Parkinson's disease. Neuropathol Appl Neurobiol, 2000. 26(5): p. 424-33.
Mogi, M., M. Harada, T. Kondo, Y. Mizuno, H. Narabayashi, P. Riederer, and T. Nagatsu, The soluble form of Fas molecule is elevated in parkinsonian brain tissues. Neurosci Lett, 1996. 220(3): p. 195-8.
Reed, J.C., Apoptosis-Based Therapies. Nature Reviews - Drug Discovery, 2002.1: p. 111-121.
Matsunaga, T., J. Kudo, K. Takahashi, K. Dohmen, K. Hayashida, S. Okamura, H. Ishibashi, and Y. Niho, Rotenone, a mitochondria! NADH dehydrogenase inhibitor, induces cell surface expression ofCD13 and CD38 and apoptosis in HL-60 cells. Leukemia & Lymphoma, 1996. 20(5-6): p. 487-494.
Sanders, S.G., R.L. Tucker, R.S. Bagley, and P.R. Gavin, Magnetic resonance imaging features of equine nigropallidal encephalomalacia. Vet Radiol Ultrasound, 2001. 42(4): p. 291-6.
Lockwood, A.H., Pesticides andparkinsonism: is there an etiological link? Curr Opin Neurol, 2000. 13(6): p. 687-90.
Priyadarshi, A., S.A. Khuder, E.A. Schaub, and S.S. Priyadarshi, Environmental risk factors and Parkinson's disease: a metaanalysis. Environ Res, 2001. 86(2): p. 122-7.
Engel, L.S., H. Checkoway, M.C. Keifer, N.S. Seixas, W.T. Longstreth, Jr., K.C. Scott, K. Hudnell, W.K. Anger, and R. Camicioli, Parkinsonism and occupational exposure to pesticides. Occup Environ Med, 2001. 58(9): p. 582-9.
Heikkila, R.E., W.J. Nicklas, I. Vyas, and R.C. Duvoisin, Dopaminergic toxicity of rotenone and the 1-methyl-4-phenylpyridinium ion after their stereotaxic administration to rats: implication for the mechanism of 1-methyl-4-phenyl-1,2,3,6-tetrahydropyridine toxicity. Neurosci Lett, 1985. 62(3): p. 389-94.
Ferrante, R.J., J.B. Schulz, N.W. Kowall, and M.F. Beal, Systemic administration of rotenone produces selective damage in the striatum and globus pallidus, but not in the substantia nigra. Brain Research, 1997. 753(1): p. 157-162.
Thiffault, C, J.W. Langston, and D.A. Di Monte, Increased striatal dopamine turnover

following acute administration of rotenone to mice. Brain Res, 2000. 885(2): p. 283-8.
Betarbet, R., T.B. Sherer, G. MacKenzie, M. Garcia-Osuna, A.V. Panov, and J.T. Greenamyre, Chronic systemic pesticide exposure reproduces features of Parkinson's disease. Nat Neurosci, 2000. 3(12): p. 1301-6.
Barrientos, A. and C.T. Moraes, Titrating the effects of mitochondrial complex I impairment in the cell physiology. J Biol Chem, 1999. 274(23): p. 16188-97.
Hartley, A., J.M. Stone, C. Heron, J.M. Cooper, and A.H. Schapira, Complex I inhibitors induce dose-dependent apoptosis in PC12 cells: relevance to Parkinson's disease. J Neurochem, 1994. 63(5): p. 1987-90.
Seaton, T.A., J.M. Cooper, and A.H. Schapira, Cyclospohn inhibition of apoptosis induced by mitochondrial complex I toxins. Brain Res, 1998. 809(1): p. 12-7.
Higuchi, M., R.J. Proske, and E.T. Yeh, Inhibition of mitochondrial respiratory chain complex I by TNF results in cytochrome c release, membrane permeability transition, and apoptosis. Oncogene, 1998. 17(19): p. 2515-24.
Wolvetang, E.J., K.L. Johnson, K. Krauer, S.J. Ralph, and A.W. Linnane, Mitochondrial respiratory chain inhibitors induce apoptosis. FEBS Lett, 1994. 339(1-2): p. 40-4.
Mills, K.I., LJ. Woodgate, A.F. Gilkes, V. Walsh, M.C. Sweeney, G. Brown, and A.K. Burnett, Inhibition of mitochondrial function in HL60 cells is associated with an increased apoptosis and expression of CDU. Biochem Biophys Res Commun, 1999. 263(2): p. 294-300.
Khar, A., A.M. Ali, Z. Begum, B.V. Pardhasaradhi, and C. Varalakshmi, Induction of apoptosis in AK-5 cells by rotenone involves participation ofcaspases. Indian J Biochem Biophys, 1999. 36(2): p. 77-81.
Kragten, E., I. Lalande, K Zimmermann, S. Roggo, P. Schindler, D. Mü ller, J. van Oostrum, P. Waldmeier, and P. Fü rst, Glyceraldehyde-3-phosphate dehydrogenase, the putative target of the antiapoptotic compounds CGP 3466 and R-(-)-deprenyl. J Biol Chem, 1998. 273(10): p. 5821-8.
Isenberg, J.S. and J.E. Klaunig, Role of the mitochondrial membrane permeability transition (MPT) in rotenone-induced apoptosis in liver cells. Toxicol Sei, 2000. 53(2): p. 340-51.
Duan, W., Z. Zhang, D.M. Gash, and M.P. Mattson, Participation of prostate apoptosis response-4 in degeneration of dopaminergic neurons in models of Parkinson's disease. AnnNeurol, 1999. 46(4): p. 587-97.
Leist, M., C. Volbracht, E. Fava, and P. Nicotera, 1-Methyl-4-phenylpyridinium induces autocrine excitotoxicity, protease activation, and neuronal apoptosis. Mol Pharmacol, 1998. 54(5): p. 789- 801.
Vrablic, A.S., CD. Albright, C.N. Craciunescu, R.I. Salganik, and S.H. Zeisel, Altered mitochondrial function and overgeneration of reactive oxygen species precede the induction of apoptosis by 1-0-octadecyl-2-methyl- rac-glycero-3-phosphocholine in p53-defective hepatocytes. Faseb J, 2001.15(10): p. 1739-44.
Luetjens, CM., N.T. Bui, B. Sengpiel, G. Munstermann, M. Poppe, A.J. Krohn, E. Bauerbach, J. Krieglstein, and J.H. Prehn, Delayed mitochondrial dysfunction in excitotoxic neuron death: cytochrom'e c release and a secondary increase in Superoxide production. J Neurosci, 2000. 20(15): p. 5715-23.
Lin, Z., J.M. Weinberg, R. Malhotra, S.E. Merritt, L.B. Holzman, and F.C Brosius, 3rd, GLUT-1 reduces hypoxia-induced apoptosis and JNK pathway activation. Am J Physiol Endocrinol Metab, 2000. 278(5): p. E958-66.
Li, L, P.S. Lorenzo, K. Bogi, P.M. Blumberg, and S.H. Yuspa, Protein kinase Cdelta targets mitochondria, alters mitochondrial membrane potential, and induces apoptosis in normal and neoplastic keratinocytes when overexpressed by an adenoviral vector. Mol Cell Biol, 1999. 19(12): p. 8547-58.
Seyfried, J., F. Söldner, W.S. Kunz, J.B. Schulz, T. Klockgether, K.A. Kovar, and U.

Wullner, Effect of 1-methyl-4-phenylpyridinium on glutathione in rat pheochromocytoma PC 12 cells. Neurochem Int, 2000. 36(6): p. 489-97.
Esposti, M.D., I. Hatzinisiriou, H. McLennan, and S. Ralph, Bcl-2 and mitochondnal oxygen radicals. New approaches with reactive oxygen species-sensitive probes. J Biol Chem, 1999. 274(42): p. 29831-7.
Schapira, A.H., M. Gu, J.W. Taanman, S.J. Tabrizi, T. Seaton, M. Cleeter, and J.M. Cooper, Mitochondria in the etiology and pathogenesis of Parkinson's disease. Ann Neurol, 1998. 44(3Suppl 1): p. S89-98.
Seaton, T.A., J.M. Cooper, and A.H. Schapira, Free radical scavengers protect dopammergic cell lines from apoptosis induced by complex I inhibitors. Brain Res, 1997. 777(1-2): p. 110-8.
Crompton, M., The mitochondrial permeability transition pore and its role in cell death. Biochemical Journal, 1999. 341: p. 233-249.
Du, C, M. Fang, Y. Li, L. Li, and X. Wang, Smac, a mitochondrial protein that promotes cyiochrome c-dependent caspase activation by eliminating IAP inhibition. Cell, 2000.102(1): p.33-42.
Chai J , C. Du, J.W. Wu, S. Kyin, X. Wang, and Y. Shi, Structural and biochemical basis of apoptotic activation by Smac/DIABLO. Nature, 2000. 406(6798): p. 855-62.
Verhagen, A.M., P.G. Ekert, M. Pakusch, J. Silke, LM. Connolly, G.E. Reid, R.L Moritz, R.J. Simpson, and D.L. Vaux, Identification of DIABLO, a mammalian protein that promotes apoptosis by binding to and antagonizing IAP proteins. Cell, 2000.102(1): p. 43-53.
Susin, S.A., et al., Molecular characterization of mitochondrial apoptosis-inducing factor [see comments]'. Nature, 1999. 397(6718): p. 441-6.
Daugas, E., S.A. Susin, N. Zamzami, K.F. Ferri, T. Irinopoulou, N. Larochette, M.C. Prevost, B. Leber, D. Andrews, J. Penninger, and G. Kroemer, Mitochondrio-nucleartranslocation ofAIP in apoptosis and necrosis. Faseb J, 2000.14(5): p. 729-39.
Reed, J.C. and G. Kroemer, Mechanisms of mitochondrial membrane permeabilization. Cell Death Differ, 2000. 7(12): p. 1145.
Feldmann, G., D. Haouzi, A. Moreau, A.M. Durand-Schneider, A. Bnnguier, A. Berson, A. Mansouri, D. Fau, and D. Pessayre, Opening of the mitochondrial permeability transition pore causes matrix expansion and outer membrane rupture in Fas-mediated hepatic apoptosis in mice. Hepatology, 2000. 31(3): p. 674-83.
Ichas, F. and J.P. Mazat, From calcium signaling to cell death: two conformations for the mitochondrial permeability transition pore. Switching from low- to high- conductance state. Biochim Biophys Acta, 1998.1366(1-2): p. 33-50.
Lemasters, J.J., T. Qian, S.P. Elmore, L.C. Trost, Y Nishimura, B. Herman, CA. Bradham, D.A. Brenner, and A.L Nieminen, Confocal microscopy of the mitochondrial permeability transition in necrotic cell killing, apoptosis and autophagy Biofactors, 1998. 8(3-4): p. 283-5.
Kroemer, G. and J.C. Reed, Mitochondrial control of cell death. Nat Med, 2000. 6(5): p. 513-9.
Pastorino, J.G., M. Tafani, R.J. Rothman, A. Marcineviciute, J.B. Hoek, and J.L. Färber, Functional consequences of the sustained or transient activation by Bax of the mitochondria! permeability transition pore. J Biol Chem, 1999. 274(44): p. 31734-9.
Marchetti, P., M. Castedo, S.A. Susin, N. Zamzami, T. Hirsch, A. Macho, A. Haeffner, F. Hirsch, M. Geuskens, and G. Kroemer, Mitochondria! permeability transition is a central coordinating event of apoptosis. Journal of Experimental Medicine, 1996. 184(3): p. 1155-1160.
Hehner, S.P., M. Heinrich, P.M. Bork, M. Vogt, F. Ratter, V. Lehmann, K. Schulze-Osthoff, W. Droge, and M.L. Schmitz, Sesquiterpene lactones specifically inhibit activation ofNF-kappa B by preventing the degradation of I kappa B-alpha and I kappa B-beta. J Biol Chem, 1998. 273(3): p. 1288-97.

Gastman, B.R., D.E. Johnson, T.L. Whiteside, and H. Rabinowich, Tumor-induced apoptosis of T lymphocytes: elucidation of intracellular apoptotic events. Blood, 2000. 95(6): p. 2015-23.
Burke, J.R., J.J. Enghild, M.E. Martin, Y. Jou, R.M. Myers, A.D. Roses, J.M. Vance, and W.J. Strittmatter, Huntingtin and DRPLA proteins selectively interact with the enzyme GAPDH. Nature Medicine, 1996. 2(3): p. 347-350.
Browne, S.E., A.C. Bowling, U. MacGarvey, M.J. Baik, S.C. Berger, M.M. Muqit, E.D. Bird, and M.F. Beal, Oxidative damage and metabolic dysfunction in Huntington's disease: selective vulnerability of the basal ganglia. Ann Neural, 1997. 41(5): p. 646-53.
Kish, S.J., I. Lopes-Cendes, M. Guttman, Y. Furukawa, M. Pandolfo, G.A. Rouleau, B.M. Ross, M. Nance', L. Schut, L. Ang, and L. DiStefano, Brain glyceraldehyde-3-phosphate dehydrogenase activity in human trinucleotide repeat disorders. Arch Neural, 1998. 55(10): p. 1299-304.
Tabrizi, S.J., M.W. Cleeter, J. Xuereb, J.W. Taanman, J.M. Cooper, and A.H. Schapira, Biochemical abnormalities and excitotoxicity in Huntington's disease brain. Ann Neural, 1999. 45(1): p. 25-32.
Ishitani, R., M. Kimura, K. Sunaga, N. Katsube, M. Tanaka, and D.M. Chuang, An antisense oligodeoxynucleotide to glyceraldehyde-3-phosphate dehydrogenase blocks age-induced apoptosis of mature cerebrocortical neurons in culture. Journal of Pharmacology and Experimental Therapeutics, 1996. 278(1): p. 447-454.
Ishitani, R. and D.M. Chuang, Glyceraldehyde-3-phosphate dehydrogenase antisense oligodeoxynucleotides protect against cytosine arabinonucleoside-induced apoptosis in cultured cerebellar neurons. Proceedings of the National Academy of Sciences of the United States of America, 1996. 93(18): p. 9937-9941.
Sunaga, K., H. Takahashi, D.M. Chuang, and R. Ishitani, Glyceraldehyde-3-phosphate dehydrogenase is over-expressed during apoptotic death of neuronal cultures and is recognized by a monoclonal antibody against amyloid plaques from Alzheimer's brain. Neuroscience Letters, 1995. 200(2): p. 133-136.
Ishitani, R., K. Sunaga, M. Tanaka, H. Aishita, and D.M. Chuang, Overexpression of glyceraldehyde-3-phosphate dehydrogenase is involved in low K+-induced apoptosis but not necrosis of cultured cerebellar granule cells. Molecular Pharmacology, 1997. 51(4): p. 542-550.
Chen, R.W., P.A. Saunders, H. Wei, Z. Li, P. Seth, and D.M. Chuang, Involvement of glyceraldehyde-3-phosphate dehydrogenase (GAPDH) andp53in neuronal apoptosis: evidence that GAPDH is upregulated by p53. J Neurosci, 1999.19(21): p. 9654-62.
Carlile, G.W., W.G. Tatton, and K.L. Borden, Demonstration of a RNA-dependent nuclear interaction between the promyelocytic leukaemia protein and glyceraldehyde-3-phosphate dehydrogenase. Biochem J, 1998. 335(Pt 3): p. 691-6.
Ishitani, R., M. Tanaka, K. Sunaga, N. Katsube, and D.M. Chuang, Nuclear localization of overexpressed glyceraldehyde-3-phosphate dehydrogenase in cultured cerebellar neurons undergoing apoptosis. Mol Pharmacol, 1998. 53(4): p. 701-7.
Saunders, P.A., E. ChaleckaFranaszek, and D.M. Chuang, Subcellulardistribution of glyceraldehyde-3-phosphate dehydrogenase in cerebellar granule cells undergoing cytosine arabinoside-induced apoptosis. J. Neurochem., 1997. 69(5): p. 1820-1828.
Sawa, A., A.A. Khan, L.D. Hester, and S.H. Snyder, Glyceraldehyde-3-phosphate dehydrogenase: Nuclear translocation participates in neuronal and nonneuronal cell death. Proceedings of the National Academy of Sciences of the United States of America, 1997. 94(21): p. 11669-11674.
Shashidharan, P., R.M. Chalmers-Redman, G.W. Carlile, V. Rodic, N. Gurvich, T. Yuen, W.G. Tatton, and S.C. Sealfon, Nuclear translocation of GAPDH-GFP fusion protein during apoptosis. Neuroreport, 1999.10(5): p. 1149-53.

Borden, K.L.B., E.J. Campbell-Dwyer, and M.S. Salvato, An arenavirus RING (zinc-binding) protein binds the oncoprotein PML and relocates PML nuclear bodies to the cytoplasm. J. Virol., 1988. 72: p. 758-766.

Borden, K.L.B., E.J. CampbellDwyer, and M.S. Salvato, The promyelocytic leukemia protein PML has a pro-apoptotic acitvity mediated through its RING. Febs. Lett., 1997. 418(30-34).

Melnick, A. and J.D. Licht, Reconstructing a disease:RARa, its fusion protein oartners and their roles in the pathogenesis of acute promyelocytic leukemia. Blood, 1999. In press.

Shaknovich, R., P.L. Yeyati, S. Ivins, A. Melnick, C. Lempert, S. Waxman, A. Zelent, and J.D. Licht, The promyelocytic leukemia zinc finger protein affects myeloid cell growth, differentiation, and apoptosis. Mol Cell Biol, 1998. 18(9): p. 5533-45.

Licht, J.D., R. Shaknovich, M.A. English, A. Melnick, J.Y. Li, J.C. Reddy, S. Dong, S.J. Chen, A. Zelent, and S. Waxman, Reduced and altered DNA-binding and transcriptional properties of the PLZF-retinoic acid receptor-alpha chimera generated in t(11; 17)-associated acute promyelocytic leukemia. Oncogene, 1996.12(2): p. 323-36.

Ronai, Z., Glycolytic enzymes as DNA binding proteins. Int J Biochem, 1993. 25(7): p. 1073-6.

Tatton, W.G. and R.M.E. ChalmersRedman, Modulation of gene expression rather than monoamine oxidase inhibition: (-)-deprenyl-related compounds in controlling neurodegeneration. Neurol, 1996. 47(6): p. S171-S183.

Tatton, W.G., K. Ansari, W. Ju, P.T. Salo, and P.H. Yu, Selegiline induces "trophic-like"rescue of dying neurons without MAO inhibition. Adv Exp Med Biol, 1995. 363: p. 15-6.

Cohen, G., P. Pasik, B. Cohen, A. Leist, C. Mytilineau, and M.D. Yahr, Pargyline and deprenyl prevent the neurotoxicity of 1-methyl-4-phenyl -1,2,3,6- tetrahydropyridine (MPTP) in monkeys. Eur.J.Pharmacol., 1984. 106(209-210).

Larsen, J. P. and J. Boas, The effects of early selegiline therapy on long-term levodopa treatment and parkinsonian disability: an interim analysis of a Norwegian- Danish 5-year study. Norwegian-Danish Study Group. Mov Disord, 1997.12(2): p. 175- 82.

Myllyla, V.V., K.A. Sotaniemi, J.A. Vuorinen, and E.H. Heinonen, Selegiline in de novo parkinsonian patients: the Finnish study. Mov Disord, 1993. 8(Suppl 1): p. S41-4.

Olanow, C.W., R.A. Häuser, L. Gauger, T. Malapira, W. Koller, J. Hubble, K. Bushenbark, D. Lilienfeld, and J. Esterlitz, The effect of deprenyl and levodopa on the progression of Parkinson's Disease. Ann. Neurol., 1995. 38: p. 771-777.

Tetrud, J.W. and J.W. Langston, The effect of deprenyl (selegiline) on the natural history of Parkinson's disease. Science, 1989. 245: p. 519-522.

Group, T.P.S., Effects of tocopherol and deprenyl on the progression of disability in early Parkinson's disease. N Engl J Med, 1993. 328(3): p. 176-83.

Fahn, S., Controversies in the therapy of Parkinson's disease. Adv Neurol, 1996. 69: p. 477-86.

LeWitt, P.A., Deprenyl's effect at slowing progression ofparkinsonian disability: the DATA TOP study. The Parkinson Study Group. Acta Neurol Scand Suppl, 1991.136: p. 79-86.

Schulzer, M., E. Mak, and D.B. Calne, The anitparkinsonism efficacy of deprenyl derives from transient improvement which is likely to be symptomatic. Ann. Neurol., 1992. 32: p. 795-798.

Salonen, T., A. Haapalinna, E. Heinonen, J. Suhonen, and A. Hervonen, Monoamine oxidase B inhibitor selegiline protects young and aged rat peripheral sympathetic neurons against 6- hydroxydopamine-induced neurotoxicity. Acta Neuropathologica, 1996. 91(5): p. 466-474.

Koutsilieri, E., O.C. JF, T.S. Chen, P. Riederer, and W.D. Rausch, Selegiline enhances survival and neurite outgrowth of MPP(+)-treated dopaminergic neurons. EurJ

Pharmacol, 1994. 269(3).
Koutsilieri, E., T.S. Chen, W.D. Rausch, and P. Riederer, Selegiline is neuroprotective in primary brain cultures treated with 1-methyl-4-phenylpyridinium. European Journal of Pharmacology, 1996. 306(1-3): p. 181-186.
Le W J Jankovic, W. Xie, R. Kong, and S.H. Appel, (-)-Deprenyl protection of 1-methyl-4 phenylpyridium ion (MPP+)-induced apoptosis independent ofMAO-B inhibition [published erratum appears in Neurosci Lett 1997 May 30;228(1):67J. Neurosci Lett, 1997. 224(3): p. 197-
Mytilineou, C. and G. Cohen, Deprenyl protects dopamine neurons from neurotoxic effect of 1- methyl-4-phenylpyridinium ion. J. Neurochem., 1985. 45(6): p. 1951-1953.
Schmidt, D.E., M.H. Ebert, J.C. Lynn, and W.O. Whetsell, Attenuation of 1-methyl-4-phenylpyhdinium (MPP+) neurotoxicity by deprenyl in organotypic canine Substantia nigra cultures. Journal of Neural Transmission, 1997.104(8-9): p. 875-885.
Tatton, W.G. and C.E. Greenwood, Rescue of Dying Neurons: A New Action For Deprenyl In MPTPParkinsonism. J. Neurose. Res., 1991. 30: p. 666-627.
Vizuete, M.L., V. Steffen, A. Ayala, J. Cano, and A. Machado, Protective effect of deprenyl against 1-methyl-4-phenylpyridinium neurotoxicity in rat sthatum. Neurosci Lett, 1993.152(1-2).
Wu R M , D.L. Murphy, and C.C. Chiueh, Neuronal protective and rescue effects of deprenyl against MPP+ dopaminergic toxicity. Journal of Neural Transmission General Section, 1995. 100(1): p. 53-61.
Fuller, R.W., S.K. Hemrick-Luecke, and K.W. Perry, Deprenyl antagonizes acute lethality of 1- methyl-4-ph'enyl-1,2,3,6- tetrahydropyridine in mice. J Pharmacol Exp Ther, 1988. 247(2): p. 531-5
Maruyama, W., T. Takahashi, and M. Naoi, (-)-Deprenyl protects human dopaminergic neuroblastoma SH-SY5Y cells from apoptosis induced by peroxynitrite and nitnc oxide. J Neurochem, 1998. 70(6): p. 2510-5.
Finnegan K T , J.J. Skratt, I. Irwin, L.E. DeLanney, and J.W. Längsten, Protection against DSP-4-induced neurotoxicity by deprenyl is not related to its inhibition of MAO B. Eur J Pharmacol, 1990. 184(1): p. 119-26.
Yu P H B A. Davis, J. Fang, and A.A. Boulton, Neuroprotective effects of some monoamme oxidase-B inhibitors against DSP-4-induced noradrenaline depletion in the mouse hippocampus. J Neurochem, 1994. 63(5): p. 1820-8.
Zhang, X. and P.H. Yu, Depletion of NOS activity in the rat dentate gyms neurons by DSP-4 and protection by deprenyl. Brain Research Bulletin, 1995. 38(4): p. 307-311.
Mytilineou C, E.K. Leonard!, P. Radcliffe, E.H. Heinonen, S.K. Han, P. Werner, G. Cohen, and C.W. Olanow, Deprenyl and desmethylselegiline protect mesencephalic neurons from toxicity induced by glutathione depletion. J Pharmacol Exp Ther, 1998. 284(2): p. 700-6.
Ansari, K.S., P.H. Yu, T.P. Kruck, and W.G. Tatton, Rescue ofaxotomized immature rat facial motoneurons by R(-)'-deprenyl: stereospecificity and independence from monoamine oxidase inhibition. J Neurosci, 1993. 13(9): p. 4042-53.
Iwasaki, Y., K. Ikeda, T. Shiojima, T. Kobayashi, N. Tagaya, and M. Kinoshita, Deprenyl and pergolide rescue spinal motor neurons from axotomy-induced neuronal death in the neonatal rat. Neurological Research, 1996.18(2): p. 168-170.
Ju W Y, D.P. Holland, and W.G. Tatton, (-)-Deprenyl alters the time course of death of axotomized facial motoneurons and the hypertrophy of neighboring astrocytes in immature rats. Exp Neural, 1994.126(2): p. 233-46.
Oh, O, B. Murray, N. Bhattacharya, D. Holland, and W.G. Tatton, (-)-Deprenyl alters the survival of adult murine facial motoneurons after axotomy: increases in vulnerable C57BL strain but decreases in motor neuron degeneration mutants. J Neurosci Res,

1994. 38(1): p. 64-74.
Salo, P.T. and W.G. Tatton, Deprenyl reduces the death of motoneurons caused by axotomy. J Neurosci Res, 1992. 31(2): p. 394-400. .,..-,
Buys, Y.M., G.E. Trope, and W.G. Tatton, (-)-Deprenyl increases the survival of rat retinal ganglion cells after optic nerve crush. Curr Eye Res, 1995.14(2): p. 119-126.
Paterson, I.A., A.J. Barber, D.L. Gelowitz, and C. Voll, (-)Deprenyl reduces delayed neuronal death of hippocampal pyramidal cells. Neurosci Biobehav Rev, 1997. 21 (2): p. 181-6.
Knollema, S., W. Aukema, H. Horn, J. Korf, and G.J. TerHorst, L-deprenyl reduces brain damage in rats exposed to transient hypoxia-ischemia. Stroke, 1995. 26(10): p. 1883-1887.
Lahtinen, H., J. Koistinaho, R. Kauppinen, A. Haapalinna, R. Keinanen, and J. Sivenius Selegiline treatment after transient global ischemia in gerbils enhances the survival of CA1 pyramidal cells in the hippocampus. Brain Research, 1997. 757(2): p. 260-267.
Ravikumar, R., M.K. Lakshmana, B.S. Rao, B.L. Meti, P.N. Bindu, and T.R. Raju, (-)-Deprenyl attenuates spinal motor neuron degeneration and associated locomotordeficits in rats subjected to spinal cord ischemia. Exp Neurol, 1998. 149(1): p. 123-9.
Semkova, I., P. Wolz, M. Schilling, and J. Krieglstein, Selegiline enhances NGF synthesis and protects central nervous system neurons from excitotoxic and ischemic damage. European Journal of Pharmacology, 1996. 315(1): p. 19-30.
Paterson I.A., D. Zhang, R.C. Warrington, and A.A. Boulton, R-Deprenyl and R-2-Heptyl-Nmethylpmpargylamine prevent apoptosis in cerebellar granule neurons induced by cytosme arabinoside but not low extracellular potassium. Journal of Neurochemistry, 1998. 70(2): p. 515- 523.
Gelowitz, D.L. and I.A. Paterson, Neuronal sparing and behavioral effects of the antiapoptotic drug, (- jdeprenyl, following kainic acid administration. Pharmacol Biochem Behav, 1999. 62(2): p 255-62.
Mytilineou, C, P.M. Radcliffe, and C.W. Olanow, L-(-)-desmethylselegiline, a metabolite of selegiline [L-(-)-deprenyl], protects mesencephalic dopamine neurons from excitotoxicity in vitro. Journal of Neurochemistry, 1997. 68(1): p. 434-436.
Pereira, CM. and C.R. Oliveira, Glutamate toxicity on a PC12 cell line involves glutathione (GSH) depletion and oxidative stress. Free Radic Biol Med, 1997. 23(4): p. 637-47.
Tatton, W.G., W.Y. Ju, D.P. Holland, C. Tai, and M. Kwan, (-)-Deprenyl reduces PC12 cell apoptosis by inducing new protein synthesis. J Neurochem, 1994. 63(4): p. 1572-5.
Ragaiey, T., J.X. Ma, W.J. Jiang, W. Greene, G.M. Seigel, and W.C. Stewart, L-deprenyl protects injured retinal precursor cells in vitro. J Ocul Pharmacol Ther, 1997.13(5): p. 479-88.
Todd, K.G. and R. F. Butterworth, Increased neuronal cell survival after L-deprenyl treatment in experimental thiamine deficiency. J Neurosci Res, 1998. 52(2): p. 240-6.
Amenta F., S. Bongrani, S. Cadel, F. Ferrante, B. Valsecchi, and Y.C. Zeng, Influence of treatment with L-deprenyl on the structure of the cerebellar cortex of aged rats. Mech Ageing Dev, 1994. 75(2): p. 157-67.
Amenta F S Bograni, S. Cadel, F. Ferrante, B. Valsecchi, and J.A. Vega, Microanatomical change's in the frontal cortex of aged rats: effect of L-deprenyl treatment. Brain Res Bull, 1994. 34(2): p. 125-31.
Amenta F S Bongrani, S. Cadel, A. Ricci, B. Valsecchi, and Y.C. Zeng, Neuroanatomy of aging brain Influence of treatment with L-deprenyl. Ann N Y Acad Sei, 1994. 717: p. 33-44.
Zeng YC..S. Bongrani, E. Bronzetti, S. Cadel, A. Ricci, B. Valsecchi, and F. Amenta, Effect of long-term treatment with L-deprenyl on the age-dependent microanatomical changes in the rat hippocampus. Mechanisms of Ageing and Development, 1995. 79(2-3): p. 169-

185.
Tatton, W.G., J.S. Wadia, W.Y.H. Ju, R.M.E. ChalmersRedman, and N.A. Tatton, (-)-Deprenyl reduces neuronal apoptosis and facilitates neuronal outgrowth by altering protein synthesis without inhibiting monoamine oxidase. J Neural Trans, 1996(48): p. 45-59.
Klegeris, A. and P.L. McGeer, R-(-)-Deprenyl inhibits monocytic THP-1 cell neurotoxicity independently of monoamine oxidase inhibition. Exp Neurol, 2000.166(2): p. 458-64.
Unal I Y. Gursoy-Ozdemir, H. Bolay, F. Soylemezoglu, O. Saribas, and T. Dalkara, Chronic daily administration of selegiline and EGb 761 increases brain's resistance to ischemia in mice. Brain Res, 2001. 917(2): p. 174-81.
Szende, B., G. Bokonyi, J. Bocsi, G. Keri, F. Timar, and K. Magyar, Anti-apoptotic andapoptotic action of (-j-deprenyl and its metabolites. J Neural Transm, 2001.108(1): p. 25-33.
Szende, B., K. Magyar, and Z. Szegedi, Apoptotic and antiapoptotic effect of (-)deprenyl and (-)- desmet'hyl-deprenyl on human cell lines. Neurobiology, 2000. 8(3-4): p. 249-55.
Naoi, M., W. Maruyama, T. Takahashi, Y. Akao, and Y. Nakagawa, Involvement of endogenous N-methyl(R)salsolinol in Parkinson's disease: induction of apoptosis and protection by (-)deprenyl. J Neural Transm Suppl, 2000. 58: p. 111-21.
Naoi, M., W. Maruyama, K. Yagi, and M. Youdim, Anti-apoptotic function of L-(-)deprenyl (Selegiline) and related compounds. Neurobiology, 2000. 8(1): p. 69-80.
Mothersill, C, T.D. Stamato, M.L Perez, R. Cummins, R. Mooney, and C.B. Seymour, Involvement of energy metabolism in the production of 'bystander effects' by radiation. Br J Cancer, 2000. 82(10): p. 1740-6.
Kitazawa M V. Anantharam, and A.G. Kanthasamy, Dieldrin-induced oxidative stress and neurochemical changes contribute to apoptopic cell death in dopaminergic cells. Free Radic Biol Med, 2001. 31(11): p. 1473-85.
Toronyi, E., J. Hamar, K. Magyar, and B. Szende, Antiapoptotic effect of (-)-deprenyl in rat kidney after ischemia- reperfusion. Med Sei Monit, 2002. 8(2): p. BR19-22.
Guo, M., S. Chen, Z. Liu, and H. Chen, Eldeprylprevents 1-methyl-4-phenyl-1,2,3,6-tetrahydropyridine-induced nigral neuronal apoptosis in mice. Chin Med J (Engl), 2001.114(3): p. 240-3.
Suuronen, T., P. Kolehmainen, and A. Salminen, Protective effect of L-Deprenyl against apoptosis induced by okadaic acid in cultured neuronal cells. Biochem Pharmacol, 2000. 59(12): p. 1589-1595.
Huebscher, K.J., J. Lee, G. Rovelli, B. Ludin, A. Matus, D. Stauffer, and P. Fü rst, Protein isoaspartyl methyltransferase protects from Bax-induced apoptosis. Gene, 1999. 240(2): p. 333- 41.
Xu, L, J. Ma, G.M. Seigel, and J.X. Ma, l-Deprenyl, blocking apoptosis and regulating gene expression in cultured retinal neurons. Biochem Pharmacol, 1999. 58(7): p. 1183-90.
Magyar, K., B. Szende, J. Lengyel, J. Tarczali, and I. Szatmary, The neuroprotective and neuronal rescue effects of (-)-deprenyl. J Neural Transm Suppl, 1998. 52: p. 109-23.
Fukuhara, Y., T. Takeshima, Y. Kashiwaya, K. Shimoda, R. Ishitani, and K. Nakashima, GAPDH knockdown rescues mesencephalic dopaminergic neurons from MPP+ -induced apoptosis. Neuroreport, 2001. 12(9): p. 2049-52.
Zimmerman, K., P.C. Waldmeier, and W.G. Tatton, Dibenzoxepines As Treatments For Neurodegenerative Diseases. Pure Appl. Chem., 1999. 71: p. 2039-2046.
Waldmeier P C, A.A. Boulton, A.R. Cools, A.C. Kato, and W.G. Tatton, Neurorescumg effects of the GAPDH ligand CGP 3466B. J Neural Transm Suppl, 2000. 60: p. 197-214.
Zimmermann, K., S. Roggo, E. Kragten, P. Fü rst, and P. Waldmeier, Synthesis of tools for target identification of the anti-apoptotic compound CGP 3466; Part I. Bioorg Med Chem Lett, 1998. 8(10): p. 1195-200.

Tatton, W.G., R.M.E. Chalmers-Redman, W.J.H. Ju, G.W. Carlile, M. Mammen, and N.A. Tatton', Propargylamines Induce Anti-Apoptotic New Protein Synthesis In Serum And NGF Withdrawn NGF-Differentiated PC12 Cells. J. Pharmacol. Exper.Therapeut., 2002. In Press.

Mezey, E, A.M. Dehejia, G. Harta, N. Tresser, S.F. Suchy, R.L. Nussbaum, M.J. Brownstem, and M.H. Polymeropoulos, Alpha synuclein is present in Lewy bodies in sporadic Parkinson's disease. Mol Psychiatry, 1998. 3(6): p. 493-9.

Braak, H., D. Sandmann-Keil, W. Gai, and E. Braak, Extensive axonal Lewy neuntes in Parkinson's disease: a novel pathological feature revealed by alpha-synuclein immunocytochemistry. Neurosci Lett, 1999. 265(1): p. 67-9.

Krueger, M.J., A.K. Tan, B.A. Ackrell, and T.P. Singer, Is complex II involved in the inhibition of mitochondria! respiration by N-methyl-4-phenylpyridinium cation (MMP+) and N-methyl-betacarbolines? Biochem J, 1993. 291 (Pt 3): p. 673-6.

Chalmers-Redman, R.M., A.D. Fräser, G.W. Carlile, A. Pong, and W.G. Tatton, Glucose protection from MPP+-induced apoptosis depends on mitochondrial membrane potential and ATPsynthase. Biochem Biophys Res Commun, 1999. 257(2): p. 440-7.

Cathcart, R., E. Schwiers, and B.N. Ames, Detection ofpicomole levels of hydroperoxides using a fluorescent dichlorofluorescein assay. Anal Biochem, 1983. 134(1): p. 111-6.

Zhu, H., G.L. Bannenberg, P. Moldeus, and H.G. Shertzer, Oxidation pathways for the intracel'lularprobe 2',7'-dichlorofluorescein. Arch Toxicol, 1994. 68(9): p. 582-7.

LeBel, C.P., H. Ischiropoulos, and S.C. Bondy, Evaluation of the probe 2',7'-dichlorofluorescin as an indicator of reactive oxygen species formation and oxidative stress. Chem Res Toxicol, 1992. 5(2): p. 227-31.

Budd, S.L., R.F. Castilho, and D.G. Nicholls, Mitochondrial membrane potential and hydroethidine-monitored Superoxide generation in cultured cerebellar granule cells. FEBS Letters, 1997. 415(1): p. 21-24.

Sanchez, A., A.M. Alvarez, M. Benito, and I. Fabregat, Cycloheximide prevents apoptosis, reactive oxygen species production, and glutathione depletion induced by transforming growth factor beta in fetal rat hepatocytes in primary culture. Hepatology, 1997. 26(4): p. 935-943.

Zamzami, N., P. Marchetti, M. Castedo, D. Decaudin, A. Macho, T. Hirsch, S.A. Susin, P.X. Petit, B. Mignotte, and G. Kroemer, Sequential reduction of mitochondrial transmembrane potential and generation of reactive oxygen species in early programmed cell death. J Exp Med, 1995. 182(2): p. 367-77.

Chalmers-Redman, R.M.E. and W.G. Tatton, Low Level Pro-oxidant Exposure Induces An Anti-Apoptotic Program OfNew Protein Synthesis Similar To Propargylamines. Neuroscience, 2002. In Press.

Sherer, T.B., P.A. Trimmer, K. Borland, J.K. Parks, J.P. Bennett, Jr., and J.B. Tuttle, Chronic reduction in complex I function alters calcium signaling in SH- SY5Y neuroblastoma cells. Brain Res, 2001. 891(1-2): p. 94-105.

Andringa, G. and A.R. Cools, The neuroprotective effects of CGP 3466B in the best in vivo model of Parkinson's disease, the bilaterally MPTP-treated rhesus monkey. J Neural Transm Suppl, 2000. 60: p. 215-25.

Seniuk, N.A., J.T. Henderson, W.G. Tatton, and J.C. Roder, Increased CNTFgene expression in process-bearing astrocytes following injury is augmented by R(-)-deprenyl. J Neurosci Res, 1994. 37(2): p. 278-86.

Zhang, D., M.D. Berry, I.A. Paterson, and A.A. Boulton, Loss of mitochondrial membrane potential is dependent on the apoptotic program activated: Prevention by R-2HMP. Journal of Neuroscience Research, 1999. 58(2): p. 284-292.

Mates, J.M. and F.M. Sanchez-Jimenez, Role of reactive oxygen species in apoptosis: implications for cancer therapy. Int J Biochem Cell Biol, 2000. 32(2): p. 157-70.

Kim, P.K., R. Zamora, P. Petrosko, and T.R. Billiar, The regulatory role of nitric oxide in apoptosis. Int Immunopharmacol, 2001.1(8): p. 1421-41.
Carmody, R.J. and T.G. Cotter, Signalling apoptosis: a radical approach. Redox Rep, 2001. 6(2): p. 77-90.
Simon, H.U., A. Haj-Yehia, and F. Levi-Schaffer, Role of reactive oxygen species (ROS) in apoptosis induction. Apoptosis, 2000. 5(5): p. 415-8.
Datta, S.R., A. Brunet, and M.E. Greenberg, Cellular survival: a play in three Akts. Genes Dev, 1999. 13(22): p. 2905-27.
Brazil, D.P. and B.A. Hemmings, Ten years of protein kinase B signalling: a hard Akt to follow. Trends Biochem Sei, 2001. 26(11): p. 657-64.
O'Connor, R., Survival factors and apoptosis. Adv Biochem Eng Biotechnol, 1998. 62: p. 137-66.
Beckman, D. A., Brent, R. L., & Lloyd, J. B. (1996). Sources of amino acids for protein synthesis during early organogenesis in the rat. 4. Mechanisms before envelopment of the embryo by the yolk sac. Placenta, 17(8), 635-641.
Bloch, K. D. (1999). Regulation of endothelial NO synthase mRNA stability: RNA-binding proteins crowd on the 3'-untranslated region. Circ Res, 85(7), 653-655.
Boulton, A. A. (1999). Symptomatic and neuroprotective properties of the aliphatic propargylamines. Mech Ageing Dev, 111(2-3), 201-209.
Browne, S. E., Bowling, A. C., MacGarvey, U., Baik, M. J., Berger, S. C., Muqit, M. M., et al. (1997). Oxidative damage and metabolic dysfunction in Huntington's disease: selective vulnerability of the basal ganglia. Ann Neurol, 41(5), 646-653.
Brune, B., Messmer, U. K., & Sandau, K. (1995). The role of nitric oxide in cell injury. Toxicol Lett, 82-83, 233-237.
Brune, B., Mohr, S., & Messmer, U. K. (1996). Protein thiol modification and apoptotic cell death as cGMP-independent nitric oxide (NO) signaling pathways. Rev Physiol Biochem Pharmacol, 127, 1-30.
Burke, J. R., Enghild, J. J., Martin, M. E., Jou, Y. S., Myers, R. M., Roses, A. D., et al. (1996). Huntingtin and DRPLA proteins selectively interact with the enzyme GAPDH. Nat Med, 2(3), 347-350.
Carlile, G. W., Chalmers-Redman, R. M., Tatton, N. A., Pong, A., Borden, K. E., & Tatton, W. G. (2000). Reduced apoptosis after nerve growth factor and serum withdrawal: conversion of tetrameric glyceraldehyde-3-phosphate dehydrogenase to a dimer. Mol Pharmacol, 57(1), 2-12.
Carlile, G. W., Tatton, W. G., & Borden, K. L. (1998). Demonstration of a RNA-dependent nuclear interaction between the promyelocytic leukaemia protein and glyceraldehyde-3-phosphate dehydrogenase. Biochem J, 335 (Pt 3), 691-696.
Chalmers-Redman, R. M., Fraser, A. D., Carlile, G. W., Pong, A., & Tatton, W. G. (1999). Glucose protection from MPP+-induced apoptosis depends on mitochondrial membrane potential and ATP synthase. Biochemical and biophysical research communications, 257(2), 440-447.
Chen, C., Wei, T., Gao, Z., Zhao, B., Hou, J., Xu, H., et al. (1999). Different effects of the constituents of EGb761 on apoptosis in rat cerebellar granule cells induced by hydroxyl radicals. Biochem Mol Biol Int, 47(3), 397-405.
Gabellieri, E., Rahuel-Clermont, S., Branlant, G., & Strambini, G. B. (1996). Effects of NAD+ binding on the luminescence of tryptophans 84 and 310 of glyceraldehyde-3-phosphate dehydrogenase from Bacillus stearothermophilus. Biochemistry, 35(38), 12549-12559.
Gelowitz, D. L., & Paterson, I. A. (1999). Neuronal sparing and behavioral effects of the antiapoptotic drug, (-)deprenyl, following kainic acid administration. Pharmacol Biochem Behav, 62(2), 255-262.

Gilmore, K., & Wilson, M. (1999). The use of chloromethyl-X-rosamine (Mitotracker red) to measure loss of mitochondrial membrane potential in apoptotic cells is incompatible with cell fixation. Cytometry, 36(4), 355-358.
Grant, S. M., Shankar, S. L., Chalmers-Redman, R. M., Tatton, W. G., Szyf, M., & Cuello, A. C. (1999). Mitochondrial abnormalities in neuroectodermal cells stably expressing human amyloid precursor protein (hAPP751). Neuroreport, 10(1), 41-46.
Huitorel, P., & Pantaloni, D. (1985). Bundling of microtubules by glyceraldehyde-3-phosphate dehydrogenase and its modulation by ATP. Eur J Biochem, 150(2), 265-269.
Ishitani, R. (1997). [A role for GAPDH in neuronal apoptosis]. Seikagaku, 69(9), 1107-1111.
Ishitani, R., Sunaga, K., Hirano, A., Saunders, P., Katsube, N., & Chuang, D. M. (1996). Evidence that glyceraldehyde-3-phosphate dehydrogenase is involved in age-induced apoptosis in mature cerebellar neurons in culture. J Neurochem, 66(3), 928-935.
Itoga, M., Tsuchiya, M., Ishino, H., & Shimoyama, M. (1997). Nitric oxide-induced modification of glyceraldehyde-3-phosphate dehydrogenase with NAD+ is not ADP-ribosylation. J Biochem, 121(6), 1041-1046.
Jing, Y., Dai, J., Chalmers-Redman, R. M., Tatton, W. G., & Waxman, S. (1999). Arsenic trioxide selectively induces acute promyelocytic leukemia cell apoptosis via a hydrogen peroxide-dependent pathway. Blood, 94(6), 2102-2111.
Kish, S. J., Lopes-Cendes, I., Guttman, M., Furukawa, Y., Pandolfo, M., Rouleau, G. A., et al. (1998). Brain glyceraldehyde-3-phosphate dehydrogenase activity in human trinucleotide repeat disorders. Archives of neurology, 55(10), 1299-1304.
Kragten, E., Lalande, I., Zimmermann, K., Roggo, S., Schindler, P., Muller, D., et al. (1998). Glyceraldehyde-3-phosphate dehydrogenase, the putative target of the antiapoptotic compounds CGP 3466 and R-(-)-deprenyl. J Biol Chem, 273(10), 5821-5828.
Kroemer, G. (1995). The pharmacology of T cell apoptosis. Adv Immunol, 58, 211-296.
Maruyama, W., & Naoi, M. (1999). Neuroprotection by (-)-deprenyl and related compounds. Mech Ageing Dev, 111(2-3), 189-200.
Maruyama, W., Takahashi, T., & Naoi, M. (1998). (-)-Deprenyl protects human dopaminergic neuroblastoma SH-SY5Y cells from apoptosis induced by peroxynitrite and nitric oxide. J Neurochem, 70(6), 2510-2515.
Marzo, I., Brenner, C., Zamzami, N., Jurgensmeier, J. M., Susin, S. A., Vieira, H. L., et al. (1998). Bax and adenine nucleotide translocator cooperate in the mitochondrial control of apoptosis. Science, 281(5385), 2027-2031.
Matera, A. G. (1999). Nuclear bodies: multifaceted subdomains of the interchromatin space. Trends Cell Biol, 9(8), 302-309.
McDonald, F. J., & Heath, J. K. (1994). Developmentally regulated expression of fibroblast growth factor receptor genes and splice variants by murine embryonic stem and embryonal carcinoma cells. Dev Genet, 15(2), 148-154.
Metivier, D., Dallaporta, B., Zamzami, N., Larochette, N., Susin, S. A., Marzo, I., et al. (1998). Cytofluorometric detection of mitochondrial alterations in early CD95/Fas/APO-1-triggered apoptosis of Jurkat T lymphoma cells. Comparison of seven mitochondrion-specific fluorochromes. Immunol Lett, 61(2-3), 157-163.
Mohr, S., Stamler, J. S., & Brune, B. (1996). Posttranslational modification of glyceraldehyde-3-phosphate dehydrogenase by S-nitrosylation and subsequent NADH attachment. J Biol Chem, 271(8), 4209-4214.
Mytilineou, C., Leonardi, E. K., Radcliffe, P., Heinonen, E. H., Han, S. K., Werner, P., et al. (1998). Deprenyl and desmethylselegiline protect mesencephalic neurons from toxicity induced by glutathione depletion. J Pharmacol Exp Ther, 284(2), 700-706.
Mytilineou, C., Radcliffe, P., Leonardi, E. K., Werner, P., & Olanow, C. W. (1997). L-deprenyl protects mesencephalic dopamine neurons from glutamate receptor-mediated toxicity in vitro. J Neurochem, 68(1), 33-39.

Nagy, E., & Rigby, W. F. (1995). Glyceraldehyde-3-phosphate dehydrogenase selectively binds AU-rich RNA in the NAD(+)-binding region (Rossmann fold). J Biol Chem, 270(6), 2755-2763.
Paterson, I. A., Barber, A. J., Gelowitz, D. L., & Voll, C. (1997). (-)Deprenyl reduces delayed neuronal death of hippocampal pyramidal cells. Neurosci Biobehav Rev, 21(2), 181-186.
Paterson, I. A., & Tatton, W. G. (1998). Antiapoptotic actions of monoamine oxidase B inhibitors. Advances in pharmacology, 42, 312-315.
Quignon, F., De Bels, F., Koken, M., Feunteun, J., Ameisen, J. C., & de The, H. (1998). PML induces a novel caspase-independent death process. Nat Genet, 20(3), 259-265.
Reers, M., Smiley, S. T., Mottola-Hartshorn, C., Chen, A., Lin, M., & Chen, L. B. (1995). Mitochondrial membrane potential monitored by JC-1 dye. Methods Enzymol, 260, 406-417.
Salvioli, S., Ardizzoni, A., Franceschi, C., & Cossarizza, A. (1997). JC-1, but not DiOC6(3) or rhodamine 123, is a reliable fluorescent probe to assess delta psi changes in intact cells: implications for studies on mitochondrial functionality during apoptosis. FEBS Lett, 411(1), 77-82.
Saunders, P. A., Chalecka-Franaszek, E., & Chuang, D. M. (1997). Subcellular distribution of glyceraldehyde-3-phosphate dehydrogenase in cerebellar granule cells undergoing cytosine arabinoside-induced apoptosis. J Neurochem, 69(5), 1820-1828.
Saunders, P. A., Chen, R. W., & Chuang, D. M. (1999). Nuclear translocation of glyceraldehyde-3-phosphate dehydrogenase isoforms during neuronal apoptosis. J Neurochem, 72(3), 925-932.
Sawa, A., Khan, A. A., Hester, L. D., & Snyder, S. H. (1997). Glyceraldehyde-3-phosphate dehydrogenase: nuclear translocation participates in neuronal and nonneuronal cell death. Proc Natl Acad Sci U S A, 94(21), 11669-11674.
Scorrano, L., Petronilli, V., Colonna, R., Di Lisa, F., & Bernardi, P. (1999). Chloromethyltetramethylrosamine (Mitotracker Orange) induces the mitochondrial permeability transition and inhibits respiratory complex I. Implications for the mechanism of cytochrome c release. J Biol Chem, 274(35), 24657-24663.
Shashidharan, P., Chalmers-Redman, R. M., Carlile, G. W., Rodic, V., Gurvich, N., Yuen, T., et al. (1999). Nuclear translocation of GAPDH-GFP fusion protein during apoptosis. Neuroreport, 10(5), 1149-1153.
Sioud, M., & Jespersen, L. (1996). Enhancement of hammerhead ribozyme catalysis by glyceraldehyde-3-phosphate dehydrogenase. J Mol Biol, 257(4), 775-789.
Sirover, M. A. (1999). New insights into an old protein: the functional diversity of mammalian glyceraldehyde-3-phosphate dehydrogenase. Biochim Biophys Acta, 1432(2), 159-184.
Smiley, S. T., Reers, M., Mottola-Hartshorn, C., Lin, M., Chen, A., Smith, T. W., et al. (1991). Intracellular heterogeneity in mitochondrial membrane potentials revealed by a J-aggregate-forming lipophilic cation JC-1. Proc Natl Acad Sci U S A, 88(9), 3671-3675.
Sugrue, M. M., Shin, D. Y., Lee, S. W., & Aaronson, S. A. (1997). Wild-type p53 triggers a rapid senescence program in human tumor cells lacking functional p53. Proc Natl Acad Sci U S A, 94(18), 9648-9653.
Sugrue, M. M., Wang, Y., Rideout, H. J., Chalmers-Redman, R. M., & Tatton, W. G. (1999). Reduced mitochondrial membrane potential and altered responsiveness of a mitochondrial membrane megachannel in p53-induced senescence. Biochemical and biophysical research communications, 261(1), 123-130.
Sunaga, K., Takahashi, H., Chuang, D. M., & Ishitani, R. (1995). Glyceraldehyde-3-phosphate dehydrogenase is over-expressed during apoptotic death of neuronal cultures and is recognized by a monoclonal antibody against amyloid plaques from Alzheimer's brain. Neurosci Lett, 200(2), 133-136.

Susin, S. A., Zamzami, N., & Kroemer, G. (1998). Mitochondria as regulators of apoptosis: doubt no more. Biochim Biophys Acta, 1366(1-2), 151-165.
Suuronen, T., Kolehmainen, P., & Salminen, A. (2000). Protective effect of L-deprenyl against apoptosis induced by okadaic acid in cultured neuronal cells. Biochem Pharmacol, 59(12), 1589-1595.
Tatton, W. G. (1999). Apoptotic mechanisms in neurodegeneration: possible relevance to glaucoma. European journal of ophthalmology, 9 Suppl 1, S22-29.
Tatton, W. G., Chalmers-Redman, R. M., Ju, W. Y., Wadia, J., & Tatton, N. A. (1997). Apoptosis in neurodegenerative disorders: potential for therapy by modifying gene transcription. Journal of neural transmission. Supplementum, 49, 245-268.
Tatton, W. G., Ju, W. Y., Holland, D. P., Tai, C., & Kwan, M. (1994). (-)-Deprenyl reduces PC12 cell apoptosis by inducing new protein synthesis. Journal of neurochemistry, 63(4), 1572-1575.
Tatton, W. G., Wadia, J. S., Ju, W. Y., Chalmers-Redman, R. M., & Tatton, N. A. (1996). (-)-Deprenyl reduces neuronal apoptosis and facilitates neuronal outgrowth by altering protein synthesis without inhibiting monoamine oxidase. Journal of neural transmission. Supplementum, 48, 45-59.
Volker, K. W., & Knull, H. (1997). A glycolytic enzyme binding domain on tubulin. Arch Biochem Biophys, 338(2), 237-243.
Wadia, J. S., Chalmers-Redman, R. M., Ju, W. J., Carlile, G. W., Phillips, J. L., Fraser, A. D., et al. (1998). Mitochondrial membrane potential and nuclear changes in apoptosis caused by serum and nerve growth factor withdrawal: time course and modification by (-)-deprenyl. The Journal of neuroscience : the official journal of the Society for Neuroscience, 18(3), 932-947.
Yin, L., Lynch, D., & Sell, S. (1999). Participation of different cell types in the restitutive response of the rat liver to periportal injury induced by allyl alcohol. J Hepatol, 31(3), 497-507.
Zamzami, N., Brenner, C., Marzo, I., Susin, S. A., & Kroemer, G. (1998). Subcellular and submitochondrial mode of action of Bcl-2-like oncoproteins. Oncogene, 16(17), 2265-2282.
Zang, W. Q., Fieno, A. M., Grant, R. A., & Yen, T. S. (1998). Identification of glyceraldehyde-3-phosphate dehydrogenase as a cellular protein that binds to the hepatitis B virus posttranscriptional regulatory element. Virology, 248(1), 46-52.

Apoptosis in Parkinson's Disease: Signals for Neuronal Degradation

William G. Tatton, MD, PhD,[1,2] Ruth Chalmers-Redman, PhD,[1] David Brown, MD,[1] and Nadine Tatton, PhD[1]

Controversy has surrounded a role for apoptosis in the loss of neurons in Parkinson's disease (PD). Although a variety of evidence has supported an apoptotic contribution to PD neuronal loss particularly in the nigra, two factors have weighed against general acceptance: (1) limitations in the use of in situ 3′-end labeling techniques to demonstrate nuclear DNA cleavage; and (2) the insistence that a specific set of nuclear morphological features be present before apoptotic death could be declared. We first review the molecular events that underlie apoptotic nuclear degradation and the literature regarding the unreliability of 3′ DNA end labeling as a marker of apoptotic nuclear degradation. Recent findings regarding the multiple caspase-dependent or caspase-independent signaling pathways that mediate apoptotic nuclear degradation and determine the morphological features of apoptotic nuclear degradation are presented. The evidence shows that a single nuclear morphology is not sufficient to identify apoptosis and that a cytochrome c, pro–caspase 9, and caspase 3 pathways is operative in PD nigral apoptosis. BAX-dependent increases in mitochondrial membrane permeability are responsible for the release of mitochondrial factors that signal for apoptotic degradation, and increased BAX levels have been found in a subset of PD nigral neurons. Studies using immunocytochemistry in PD postmortem nigra have begun to define the premitochondrial apoptosis signaling pathways in the disease. Two, possibly interdependent, pathways have been uncovered: (1) a p53–glyceraldehyde-3-phosphate dehydrogenase (GAPDH)–BAX pathway; and (2) FAS receptor–FADD–caspase 8–BAX pathway. Based on the above, it seems unlikely that apoptosis does not contribute to PD neuronal loss, and the definition of the premitochondrial signaling pathways may allow for the development and testing of an apoptosis-based PD therapy.

Ann Neurol 2003;53 (suppl 3):S61–S72

Several different insults that can induce necrosis may be responsible for neuronal loss in Parkinson's disease (PD)[1] and PD models.[2] The classic features of necrosis can be induced by the exposure of cells to high concentrations of glutamate or other glutamate receptor agonists. This necrosis results from massive transmembrane ion fluxes that rapidly cause swelling of organelles (including the nucleus) and cellular disruption with rupture of the outer membrane.[3] Membrane rupture allows extrusion of cytoplasmic contents into the extracellular space, which can cause local inflammation and subsequent necrosis of nearby cells in a wave-like fashion. ATP depletion or lipid and protein peroxidation induced by reactive oxygen species, often implicated in PD,[4] can kill neurons by similar necrotic processes.[5]

A second death process called apoptosis can also mediate neuronal loss after exposure of cells to glutamate receptor agonists[6,7] or to increased reactive oxygen species levels[8] and has been proposed to contribute to PD neuronal loss.[9] Apoptosis is fundamental to the physiology of living organisms because it normally serves to balance cell replication, to optimize cellular organization, or to shape organ development by degrading unsuitable cells so that they can be selectively phagocytosed without risk of damage to nearby cells. It has been estimated that tens of billions of cells die by apoptosis in the human body each day, largely the replicating cells of the gastrointestinal, hematopoetic, cutaneous, immunological, and reproductive systems.

Pathological apoptosis contributes to a wide variety of diseases including cardiomyopathy, inflammation, osteoarthritis, diabetes, acquired immunodeficiency syndrome, and graft rejection. Despite the well-documented role of apoptosis in many diseases, debate has raged as to whether apoptosis contributes to neuronal loss in PD. In retrospect, the debate has been fueled by two factors: methodological limitations and the inappropriate imposition of narrow criteria for the recognition of apoptosis. The methodological problems relate to the use of terminal deoxynucleotidyl transferase–mediated deoxyuridine triphosphate nick-end labeling (TUNEL) to detect cells with apoptotic nuclear DNA fragmentation, whereas the problem with inclusion cri-

From the Departments of [1]Neurology and [2]Ophthalmology, Mount Sinai School of Medicine, New York, NY.

Published online Mar 24, 2003, in Wiley InterScience (www.interscience.wiley.com). DOI: 10.1002/ana.10489.

Address correspondence to Dr Tatton, Department of Neurology, Annenberg 14-70, Mount Sinai Medical Center, One Gustave Levy Place, New York, NY10029. E-mail: william.tatton@mssm.edu

teria results from the view that apoptotic nuclear degradation must specifically conform to the morphological features originally described by Kerr in his original studies of liver cells.

Recognition of Apoptotic Nuclear Degradation

In contrast with the swelling and cellular disruption found in necrosis, apoptosis involves marked nuclear and cellular shrinkage combined with lytic degradation of nucleic acids and cytoskeletal proteins, but maintenance of membrane integrity. Apoptotic cellular shrinkage and intranuclear or chromatin condensation were first shown by Kerr in liver cells using electron microscopy.[10] Kerr's original findings often have been taken to provide a morphological stereotype for apoptotic degradation.

Each chromosome consists of a long double strand of DNA. DNA gel electrophoresis or pulse-field electrophoresis can be used to demonstrate DNA cleavage by nucleases activated in the final stages of apoptosis. The utility of electrophoresis is limited to models in which many cells undergo apoptotic degradation synchronously. In neurodegenerative disorders such as PD, only a few neurons would be expected to undergo nuclear degradation over the course of any day (see Kanazawa[11] for a recent consideration of the time course of nigral dopaminergic neuronal loss in PD). Because the use of DNA gel electrophoresis or pulse-field electrophoresis requires that the DNA of 10^5 or more cells be in the stage of apoptotic DNA degradation, electrophoresis cannot detect apoptotic nuclear DNA fragmentation in PD postmortem brain. The labeling of cut 3□DNA ends with d-UTP attached to a fluorochrome offers the opportunity to show nuclear DNA cleavage in situ and has been widely used in both tissue sections and cultured cells.

Apoptotic nuclear degradation can include several different components including (1) the separation of histones and lamins from nuclear DNA; (2) the cleavage of the DNA into shorter fragments by endonucleases; (3) the condensation or compaction of the fragmented DNA; and (4) the formation of membrane wrapped subnuclear bodies containing fragmented and condensed DNA. The sequence, relative extent and pattern of the different components have been shown to differ for different cellular phenotypes and different types of insults.[12,13] Figure 1 illustrates one example of the different components of apoptotic nuclear degradation and their relative subnuclear distributions. The figure shows the pattern of nuclear degradation in cultured cerebellar granule neurons (CGNs) at 9 hours after exposure to 10^{-5} M glutamate (R. Chalmers-Redman and W. Tatton, unpublished observations and see Wadia and colleagues[14] for details of the histological and imaging techniques). CGNs have large nuclei relative to their cell body diameters with little variation in nuclear and cell body size among the different neurons. This uniformity allows for easy examination of apoptotic degradation in the neurons, especially with high-resolution laser confocal scanning microscopy as shown in Figure 1. In Figure 1, the leftmost three laser confocal scanning microscopy images in each horizontal row (see Fig 1A1–A3 and B1–B3) were taken for an identical image field but with different fluorescence or interference contrast detectors. Figures 1A1 to A4 illustrate the relationship between nuclear chromatin condensation shown by the fluorescent nucleic acid binding dye YOYO-1 (see Fig 1A2) and nuclear DNA fragmentation shown by TUNEL using BODIPY fluorescence (see Fig 1A3). In the interference contrast image of Figure 1A1, 4 of the 10 CGN nuclei have shrunken, smooth-appearing nuclei that have lost the granularity present in the other six nuclei. The four shrunken nuclei have markedly intensified YOYO-1 fluorescence (each labeled 2 in Fig 1A2), which contrasts with the duller, reticulated fluorescent pattern of YOYO-1 fluorescence seen in the larger nuclei. TUNEL-BODIPY fluorescence (see Fig 1A3) shows that each of the four nuclei has undergone DNA fragmentation, whereas the other six nuclei only fluoresce at background levels. Figures 1A2 and 1A3 have been recolored red and green, respectively, and then digitally added to produce Figure 1A4. The four shrunken nuclei have a yellow-orange color, which indicates that chromatin condensation and DNA fragmentation are exactly coextensive in the nuclei. The nuclei without yellow-orange coloration show a reticulated pattern of red coloration resulting from YOYO-1 binding to DNA that has not undergone fragmentation. All of the 10 cells show areas of bright green coloration in cytoplasm outside of the nuclei due to TUNEL labeling of RNA. The four apoptotic nuclei are labeled 2 to indicate that they have entered stage 2 of apoptotic degradation. In stage 2, the DNA of the entire nucleus has become both fragmented and condensed, whereas in stage 1 only a portion of the nucleus is affected as shown in Figures 1B1 to B4.

In stage 1, DNA around the outer margins of the CGN nuclei is fragmented and then condensed (see distribution of YOYO-1 fluorescence in CGNs labeled 1 in Fig 1B2). Histone immunofluorescence (Fig 1B3) is distributed in a reticulated pattern that largely colocalizes with YOYO-1 DNA binding in normal nuclei (see yellow-green coloration in the lower three nuclei in Fig 1B4), but moves to the outside margin of areas of DNA fragmentation or chromatin condensation (see Fig 1B2 and B4) in stage 1 nuclei. In stage 2 nuclei, only a small outer rim of histone immunofluorescence surrounding the DNA fragmentation and chromatin condensation is retained (illustrated by the stage 2 nucleus in Fig 1B3 and orange coloration limited to the outer portion of same nucleus in Fig 1B4). The

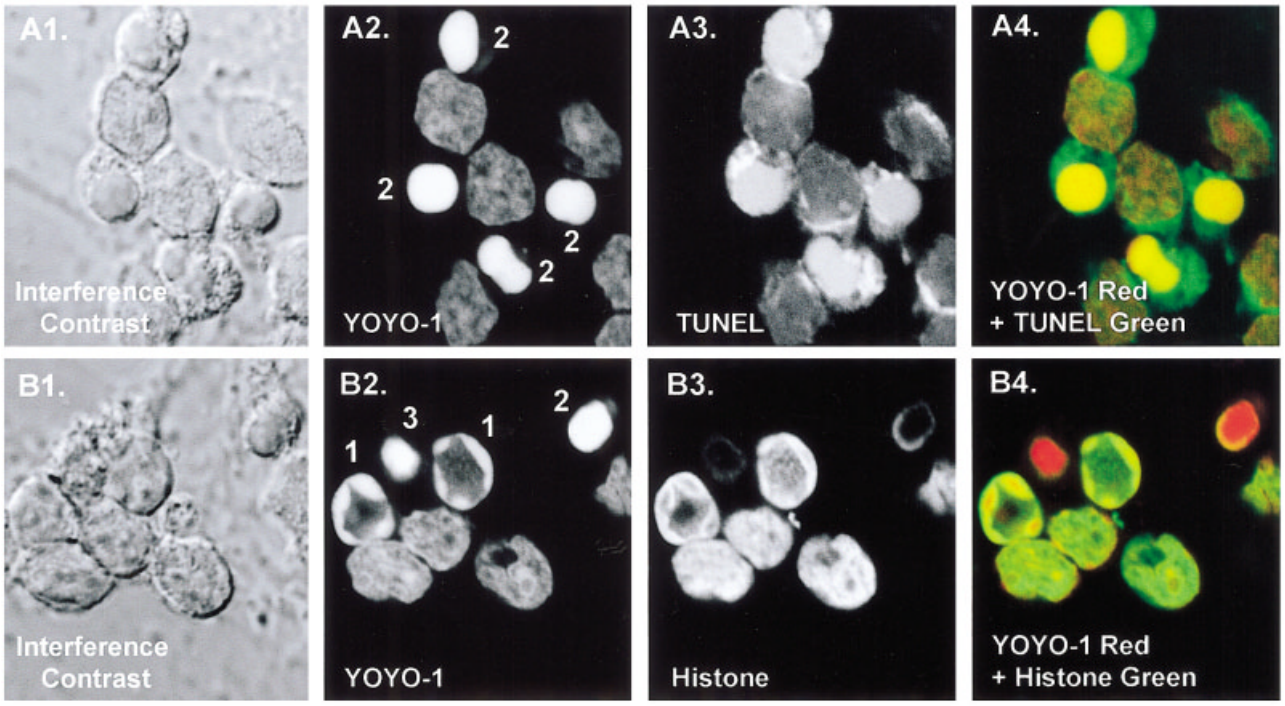

Fig 1. Stages and components of apoptotic nuclear degradation in cerebellar granule neurons exposed to low glutamate concentrations. Each horizontal row of laser confocal scanning microscope images are for identical image fields. (A1, B1) Interference contrast images showing typical cellular and nuclear shrinkage of a subset of neurons undergoing apoptotic degradation. (A2, B2) YOYO-1 nucleic acid staining used to demonstrate chromatin condensation in the numbered nuclei. The numbers indicate the stage of degradation for each nucleus. (A3) DNA cleavage using BODIPY-labeled TUNEL. (B3) Typical reorganization of histone immunoreaction as a component of apoptotic degradation. (A4, B4) Red-green recolored and digitally added images show the colocalization of DNA fragmentation and chromatin condensation and the margination of histone immunoreaction to the outer portions of nuclear subregions undergoing chromatin condensation. Stage 2 nuclei show distributions of DNA fragmentation and chromatin condensation typical of those induced by AIF signaling, whereas the distributions in stage 2 nuclei would require cytochrome c signaling.

marked shrinkage and condensation of stage 3 nuclei (see Fig 1B1 and B2) is accompanied by the disappearance of nuclear histone immunofluorescence (see Fig 1B3 and B4) in association with DNA fragmentation and chromatin condensation as shown in Figures 1A1 to A4.

The component pattern of nuclear degradation in Figure 1 is typical of CGNs exposed to excitotoxins but differs from that found after exposure of the same cultured neurons to low K^{+} media, mitochondrial complex inhibitors, cytosine arabinoside, or kinase inhibitors (data not shown, but also see Wadia and colleagues[14] for our laser confocal scanning microscopy examination of cultured neuron-like cells after trophic withdrawal). Similarly, we have found marked variation in the patterns of nuclear degradation shown using multiple markers for MPTP-exposed murine nigral neurons,[15] hypoxic neurons in the porcine hippocampus,[16] retinal ganglion cells in postmortem glaucomatous eyes,[17] and nigral neuromelanin-containing neurons in PD postmortem brain.[18–20] Apoptotic nuclear degradation can be hard to detect on neuropathological examination because of the rapid shrinkage, degradation, and phagocytosis of affected neurons. Apoptotic nuclear degradation has an apparent life of less than 12 hours in culture[14] and apparently less than several days in intact neuropil.[16] Accordingly, only a small percentage of neurons show evidence of apoptotic degradation at any single time point, even when the cells are initiated into apoptosis almost simultaneously.[21]

Variation in Patterns of Apoptotic Nuclear Degradation Reflect Postmitochondrial Multiple Signaling Pathways

Apoptotic cellular degradation depends on several interacting signaling pathways as schematized in Figure 2. Different insults and/or cellular phenotypes activate different signaling events, which can be reflected in differences in the morphology of nuclear degradation, particularly those for chromatin condensation and/or DNA fragmentation. The caspase family of proteases comprise fundamental components of many apoptotic signaling pathways.[22,23] To date, approximately 14 caspases have been characterized in mammals. They are normally expressed as inactive proenzymes and are activated by proteolysis and can act on cytoskeletal pro-

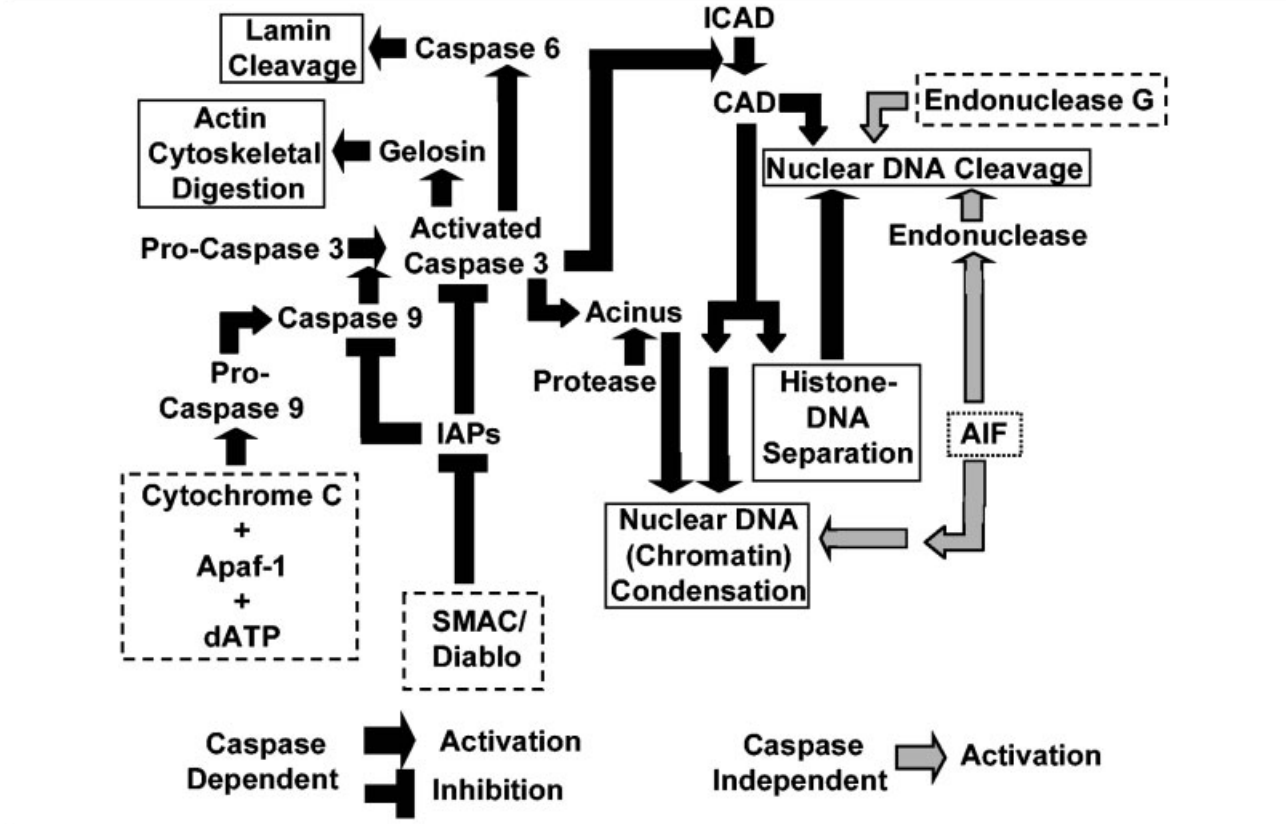

Fig 2. Schematic for postmitochondrial signaling for apoptotic degradation. The boxes with hatched borders enclose the four different signaling systems for apoptotic degradation. The arrows and T-bars linking the different signaling elements are black for caspase-dependent signaling and gray for caspase-independent signaling. Cytochrome c, SMAC/Diablo, AIF, and endonuclease G all are released from mitochondria because of increased mitochondrial membrane permeability. All of the abbreviations are defined in the text.

teins, nuclear proteins, or antiapoptotic signaling proteins. At least four different signaling systems can contribute to nuclear chromatin condensation and DNA fragmentation as shown in Figure 2 by the boxes with hatched borders. Two of the signaling systems depend on caspases: (1) the cytochrome c, apoptotic protease-activating factor 1 (Apaf-1), and pro–caspase 9 system; and (2) the second mitochondrial derived activator of caspases (SMAC)/direct IAP binding protein (Diablo) system. The caspase-dependent pathways are shown in Figure 2 by the black connectors. The other two systems are caspase independent: (1) the apoptosis initiation factor (AIF) system and (2) the endonuclease G system (both shown in Fig 2 by the gray connectors).

Initially, it was found that cytochrome c released from mitochondria interacts with Apaf-1 and dATP to provide a platform that provides for the conversion of pro–caspase 9 (also released from mitochondria) to activated caspase 9. Activated caspase 9 then converts pro–caspase 3 to activated caspase 3. Activated caspase 3 cleaves the inhibitor of caspase-activated DNase (ICAD) to generate caspase-activated DNase (CAD), which fragments nuclear DNA.[24] Activated caspase 3 also can signal for other aspects of apoptotic cellular degradation including nuclear chromatin condensation through protease-activated acinus, actin cytoskeletal digestion by the protease gelosin, and nuclear lamin cleavage through caspase 6.

Caspases, like caspase 3, can be inhibited by one or more members of a family of constitutively active proteins, the inhibitors of apoptosis (IAPs). IAPs bind to and inactivate the caspases and thereby can prevent or reduce nuclear degradation by the cytochrome c/Apaf-1 system. In turn, SMAC/Diablo, released from mitochondria, can bind and inactivate the IAPs, thereby allowing caspases 9, 3, and 6 to signal for apoptotic degradation as illustrated in Figure 2. One might expect that the joint release of cytochrome c, pro–caspase 9, and SMAC/Diablo from mitochondria would be particularly effective in mediating apoptotic degradation.

As shown in Figure 2, activated caspase 3 can play a pivotal role in the signaling for apoptotic degradation. It now appears that activated caspase 3 contributes to neuronal apoptosis in the PD nigra. Our group[19] and others[25] have independently shown immunoreaction

for activated caspase 3 in a small proportion (□2%) of neuromelanin-containing neurons in the nigra of PD postmortem brains. The activated caspase 3 immunoreaction was not present in nigral neuromelanin-containing cell bodies in postmortem brain tissue from age-matched controls. Accordingly, caspase 3 activation may be responsible for the joint presence of chromatin condensation and DNA fragmentation (similar to Fig 1A1–A4 above) in the nuclei of some nigral neuromelanin-containing neurons in PD postmortem brain.[18–20] The relative roles played by the cytochrome c/Apaf-1 and the SMAC/Diablo systems in the caspase 3 activation found in the PD nigra are not known. In normal cells, both cytochrome c and SMAC/Diablo are strictly localized to mitochondria, but in apoptosis they are concentrated in the cytosol. It remains to be determined whether one or both of the signaling proteins is present in the cytosol of PD neuromelanin-containing nigral neurons.

Examination of degradation signaling in several apoptosis models has established that a soluble flavoprotein, AIF,[26] can be released from the intermembrane space of mitochondria and then translocates to nuclei where it induces large-scale DNA fragmentation and also contributes to chromatin condensation (see Cande and colleagues[27] for a review). AIF has NADH oxidase activity and can be released from mitochondria independently of cytochrome c and pro–caspase 9.[28] The basis for selective AIF release is not known. Microinjection of cells with recombinant AIF causes only peripheral chromatin condensation (stage 1, see examples in Fig 1), whereas microinjection with activated caspase 3 or its downstream target CAD causes more pronounced, whole nuclear chromatin condensation (stage 2 as above in Fig 1).[29] In some forms of apoptosis, AIF induces cytochrome c release from mitochondria.[30] Accordingly, the stage 1 followed by stage 2 nuclear degradation shown in Figure 1 for glutamate-exposed CGNs may result from initial AIF release followed by subsequent cytochrome c/pro–caspase 9 release. AIF has been shown to induce nuclear degradation in approximately 50 different apoptosis models,[27] but, to date, we have not observed a stage 1 pattern of nuclear degradation in neuromelanin-containing neurons of the PD nigra (W. Tatton and N. Tatton, unpublished observations). Hence, AIF may not contribute to apoptotic nuclear degradation in the PD nigra.

Finally, a mitochondrial DNase, endonuclease G that normally acts on mitochondrial DNA can be released from mitochondria.[31,32] Nuclear DNA fragmentation caused by endonuclease G is independent of either caspase or CAD activity as shown in Figure 2. Endonuclease G can be released from mitochondria by BID (BCL-2 interacting domain) and is a feature of apoptosis induced by FAS ligand (see below). Although FAS ligand has been implicated in nigral apoptosis in PD,[33,34] it is not known whether endonuclease G contributes to apoptotic nuclear degradation in this disease.

The Confusion Regarding Parkinson's Disease Apoptosis Caused by TUNEL

There are several practical problems with the use of TUNEL to detect apoptosis in postmortem brain tissue (see Tatton and Rideout[18] Tatton and colleagues[20] for details): (1) direct damage to DNA by reactive oxygen species can be detected by TUNEL causing necrosis to be mistaken for apoptosis[35]; (2) prolonged postmortem delays before fixation, or prolonged fixation, increase nonspecific 3□ DNA end labeling resulting in false-positive evidence for apoptosis[36,37]; (3) dividing cells, for example, glia, can be labeled with d-UTP during mitosis and wrongly identified as apoptotic cells[38,39]; (4) protein cross-linking by overfixation can impede d-UTP access to cut 3□ DNA ends causing false-negatives[40]; (5) different endonucleases can cut DNA bluntly so that both strands are cut at the same level, or in an overhanging or in an underhanging manner, each of which differentially affects the affinity of TdT for d-UTP DNA end labeling[41] and can either promote false-positives or false-negatives; and (6) divalent cations, particularly Mg^{2+} or Ca^{2+}, increase d-UTP affinity for DNA 3□ends[42] so that small concentration changes can produce false results.

As might be expected based on the multiple deficiencies of TUNEL, different studies have reported markedly varying results for detecting apoptotic nuclei in the postmortem PD nigra. Some studies have reported that less than 1% of nigral neuromelanin-containing cells are TUNEL-positive in PD, which appears consistent with known rates of the loss of those cells in PD.[20,43–45] Yet, other studies failed to detect nigral cell TUNEL,[46] found high percentages of TUNEL in control nigra,[47] or reported that TUNEL was limited to glial cell nuclei.[48] Accordingly, the use of TUNEL fostered a confused picture, which has caused some to doubt a contribution of apoptosis to PD neuronal loss. Rather than decide for or against neuronal apoptosis in PD, the findings confirmed the view that TUNEL, used by itself, cannot reliably detect apoptosis in postmortem brain tissue.

The demonstration of nuclear DNA cleavage using TUNEL in PD nigra has been made reliable by the simultaneous application of fluorescent DNA binding dyes to jointly detect chromatin condensation and DNA cleavage in the same nuclei.[19,20,49] As shown in Figure 2, nuclear DNA cleavage and chromatin condensation are mediated by signaling steps that can be independent of each other, so that their joint demonstration in a single nucleus makes apoptotic nuclear degradation virtually certain. The conjugation of BODIPY to d-UTP for detecting DNA cuts coupled

with the use of fluorescent dyes such as YOYO-1 that detect chromatin condensation allows the two apoptosis markers to be fluorescently detected at different wavelengths in the same nucleus. The detection of apoptosis can be further enhanced by the use of a third fluorochrome that demonstrates a subnuclear distribution for lamin or histone immunofluorescence as illustrated in Figure 1.

Apoptosis Signaling Pathways in Parkinson's Disease Nigral Neurons

Increased levels of proteins that signal for apoptosis have been demonstrated in neurons in the PD postmortem nigra and provide a picture of the pathway(s) responsible for apoptotic degradation in the disease. Two groups have reported increases in BAX[19,50] in nigral neurons in PD. Changes in mitochondrial membrane permeability with the release of factors that signal for apoptotic degradation are now known to constitute the major decisional step in many apoptosis signaling pathways (schematized in Fig 3 and recently reviewed in Parone and colleagues[51]). Signaling factors for apoptotic degradation such as cytochrome c, pro–caspase 9, AIF, SMAC/Diablo, and endonuclease G are released from the intermembranous space that separates the inner and outer mitochondrial membranes. As shown in Figure 3, two mechanisms are thought to increase outer membrane permeability: (1) the formation of pores or the opening of existing pores in the outer mitochondrial membrane[52]; and (2) opening of a multiprotein megapore, the permeability transition pore complex (PTPC), which spans the inner and outer mitochondrial membranes.[53]

BAX, in association with its cousin BAK,[54] may play a role in either of those mechanisms, although the basis for the BAX-induced changes in outer mitochondrial membrane permeability are controversial.[55] BAX oligomers can insert into planar phospholipid bilayer membranes and promote dissolution of the membranes.[56] In some apoptosis models, BID can induce BAX oligomerization and the release of cytochrome c or SMAC/Diablo from liposomes[57] or mitochondria.[58,59] BID also can induce BAX insertion into the outer membrane[60] or cause BAX to bind to the PTPC.[61] In other forms of apoptosis, BID may not be required for BAX accumulation in mitochondria[62] (see Tatton and colleagues[21] for an example of BAX mitochondrial concentration in apoptosis).

Fig 3. Schematic for premitochondrial signaling for apoptosis in the PD nigra. The schematic illustrates the key role of the proapoptotic protein BAX in the induction of increased mitochondrial membrane permeability that allows the release of the different factors that signal for apoptotic degradation. Two possibly interdependent signaling pathways have been shown to activate BAX and/or its antagonists, BCL-2, and BCL-XL. The signaling elements that have been shown by immunocytochemistry of PD postmortem nigra are enclosed in boxes: (1) the p53–GAPDH–BAX pathway; and 2) the FAS receptor–FADD–caspase 8–BAX pathway. UPS □ ubiquitin-proteasomal system; SMase □ sphingomyelinase. The remaining abbreviations are defined in the text.

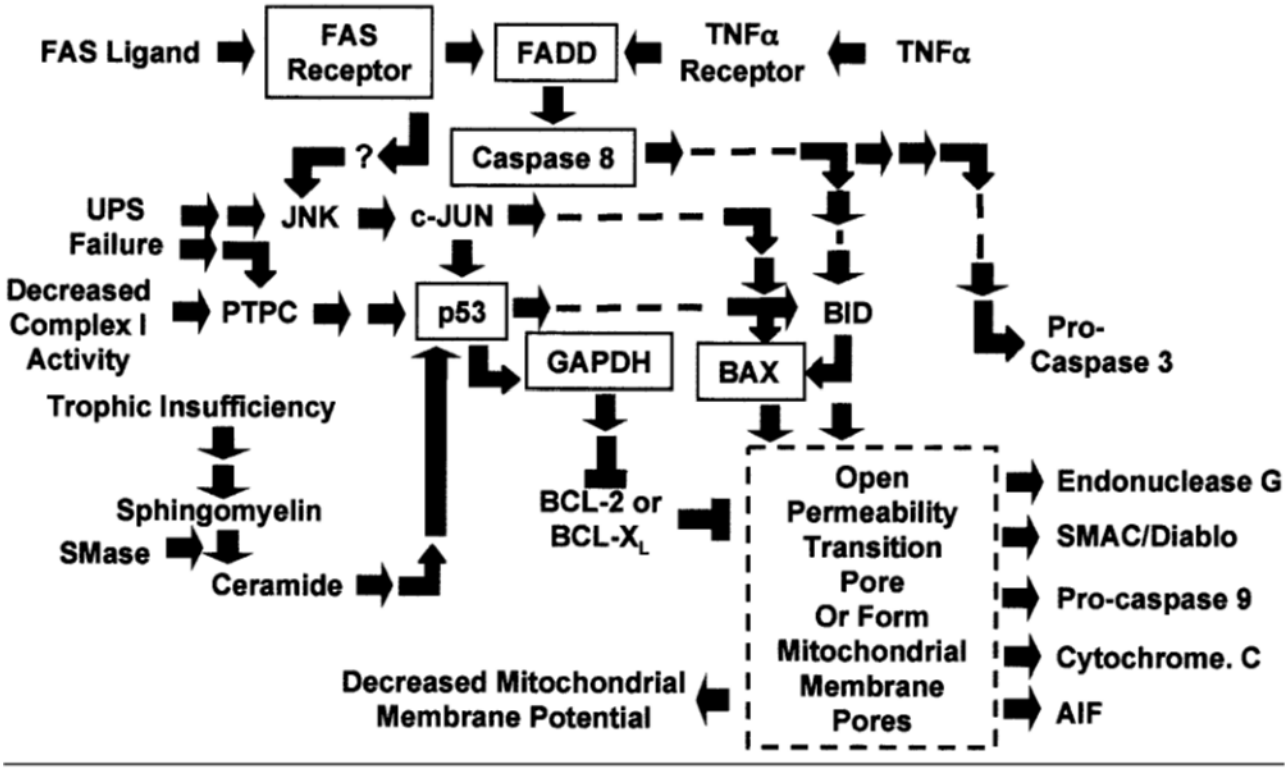

It has alternatively been proposed that opening of the PTPC causes osmotic shifts across the inner mitochondrial membrane with consequent mitochondrial swelling and rupture of the outer mitochondrial membrane, which may be responsible for the release of the apoptotic degradation factors from mitochondria (see Halestrap and colleagues[63] for a review of factors that influence the PTPC). That view is supported by studies showing that agents like cyclosporin A, which promote PTPC closure reduce cytochrome c release and apoptosis in some models.[64] Furthermore, BAX has been shown to bind to either the adenine nucleotide translocator (ANT) or the voltage dependent anion channel (VDAC) of the PTPC. BAX binding to ANT[65] or VDAC[66] markedly increases the conductance of isolated membranes. Accumulating data suggest that either ANT or VDAC[67] may increase inner mitochondrial permeability in different forms of apoptosis. A recent study suggests that two separate mechanisms are responsible for cytochrome c release from mitochondria in apoptosis.[68] First, it may be released via the formation of outer mitochondrial membrane pores; second, cytochrome c may be stored in mitochondrial cristae formed from the inner membrane that fuse with the outer membrane and allow the release cytochrome c through the PTPC. If confirmed, those findings may serve to defuse the controversy concerning the release of apoptotic degradation factors from mitochondria.

Although increased BAX levels have been shown in nigral neurons in PD postmortem brain,[19,50] it is not known whether BAX is concentrated in mitochondria or whether any such concentration involves the outer or inner mitochondrial membrane and/or the ANT or VDAC. EM immunocytochemistry will be required to determine the role of BAX relative to mitochondria in the postmortem nigra.

Two premitochondrial apoptosis signaling pathways have been implicated in nigral neuronal apoptosis by immunocytochemistry of PD postmortem brain: (1) a p53–GAPDH–BAX pathway; and (2) a FAS or tumor necrosis factor (TNF)–□ receptor–FADD–caspase 8–BAX pathway. The tumor suppressor protein, p53, has been implicated in numerous forms of apoptosis and can induce signaling for apoptosis by either transcriptional or posttranslational mechanisms.[69] In some forms of apoptosis, p53 induces transcriptionally mediated increases in GAPDH and BAX.[70,71] As shown in Figure 3, p53 also might contribute to apoptosis induced by decreased mitochondrial complex I activity,[72] dysfunction of the ubiquitin-proteasome system (UPS),[73–75] or trophic insufficiency,[76] all of which have been suggested to play a role in PD pathogenesis.[77–79]

GAPDH is a multifunction protein[80] that is best known as a glycolytic enzyme, but also functions as an apoptosis signaling protein.[81,82] Studies with antisense oligonucleotides show that GAPDH can be essential to the progression of apoptosis initiated by a variety of different insults to neuronal cells.[70,83–87] GAPDH mRNA and protein levels increase early in neuronal apoptosis caused by insults such as excitotoxins, reduction of media K□, cytosine arabinoside exposure, and aging (see Tatton and colleagues[88] for detailed references). Like others, we found that GAPDH levels begin to increase at least 4 hours before the appearance of nuclear DNA cleavage and chromatin condensation.[89] In apoptosis in model systems involving GAPDH upregulation, GAPDH accumulates densely in the nucleus.[85,87,89,90] For example, our studies with a GAPDH–green fluorescent protein (GFP) construct[91] show that the GAPDH–GFP fusion protein progressively accumulates in the nucleus of a proportion of the cells in the first 2 hours after exposure to apoptosis-initiating agents. GAPDH movement from the cytosol to the nucleus occurs progressively during the first 2 to 6 hours in some forms of apoptosis.[89] As shown in Figure 3, nuclear GAPDH appears to decrease the transcription of BCL-2 and BCL-X_L,[21] which oppose the increased mitochondrial membrane permeability and apoptotic degradation factor release induced by BAX[92] and thereby protect against the development of apoptosis. The dense nuclear accumulation of GAPDH immunoreaction is a marker of p53-GAPDH–dependent apoptosis signaling (see Tatton and colleagues[88] for references). GAPDH dense nuclear accumulation has been demonstrated in a small proportion of nigral neuromelanin-containing neurons in PD postmortem brain,[19] supporting the possibility that the p53–GAPDH–BAX signaling pathway is involved in apoptosis of PD nigral neurons.

Inflammation also has been proposed to contribute to PD pathogenesis,[93] in part through upregulation of inflammatory cytokines such as TNF-□.[79,94] The TNF receptor super family, that includes TNF-□[95] and FAS receptor,[96] causes apoptosis through caspase-dependent pathways that do not involve changes in transcription.[97] The receptors are linked to adapter proteins such as FADD that activate caspases, particularly caspase 8, which, as illustrated in Figure 3, can activate BAX-dependent increases in mitochondrial permeability or can bypass mitochondria and directly activate caspase 3. Studies of PD postmortem nigra have suggested that FAS,[33,34] FADD,[98] and caspase 8[99] may each contribute to PD neuronal loss. On the surface, these findings may suggest that two separate signaling pathways—a cytokine-activated pathway and a p53-dependent pathway may contribute to neuronal apoptosis in PD. Recent work in Down's syndrome suggests that FAS receptor and p53-GAPDH may contribute to cortical neuronal apoptosis in Down's syndrome,[100,101] whereas other studies suggest that

FAS-induced apoptosis may be linked to p53-induced apoptosis through jun N-terminal kinase (JNK) activation[102] (see Fig 3). It also has been shown that the FAS receptor can be upregulated by p53 after a lesion to the cell, particularly that induced by DNA-damaging agents.[103] This p53-induced upregulation of FAS receptor can induce apoptosis through a FAS/FAS ligand–dependent pathway. Accordingly, nigral apoptosis in PD might involve interdependent signaling by the FAS receptor and p53-dependent signaling pathways.

Does Apoptosis-Based Therapy Have a Place in Parkinson's Disease?

As described above, the presence of DNA fragmentation and chromatin clumping in the same nigral neurons coupled with upregulation of signals associated with apoptosis supports a role for apoptosis in PD neuronal loss, and work has begun to unravel the specific signaling pathways involved. As long as considerations of apoptosis in disease focused on the final degradative events and not on the upstream signaling pathways that link the initiating insults to early signals leading to apoptotic degradation, it appears unlikely that antiapoptosis-based therapies will succeed. The explosion in understanding of apoptosis-signaling networks has fostered clinical trials for apoptosis-based therapy in a variety of diseases, including PD (see Reed[104] for details). One of the apoptosis-based agents currently in PD clinical trial is the deprenyl-related propargylamine CGP3466 (TCH346), which does not inhibit monoamine oxidase B. CGP3466 binds to GAPDH[105] and alters its oligomeric form thereby reducing its capacity to translocate to the nucleus.[89] It has been shown to reduce apoptosis in a variety of models,[106,107] apparently by altering the new synthesis and subcellular movement of several apoptosis-related signaling proteins, including BCL-2 and BAX.[21] Further insights into the specific pathways that contribute to cell death in PD are likely to disclose further targets for putative neuroprotective therapy.

The research was supported by grants from the US Army (98222053, W.G.T.) and from Bachman-Strauss (W.G.T. and N.T.).

References

1. Jenner P, Olanow CW. Understanding cell death in Parkinson's disease. Ann Neurol 1998;44(suppl 1):S72–S84.
2. Jenner P. Parkinson's disease, pesticides and mitochondrial dysfunction. Trends Neurosci 2001;24:245–246.
3. Sapolsky RM. Cellular defenses against excitotoxic insults. J Neurochem 2001;76:1601–1611.
4. Olanow CW, Tatton WG. Etiology and pathogenesis of Parkinson's disease. Annu Rev Neurosci 1999;22:123–144.
5. Dawson VL, Dawson TM. Free radicals and neuronal cell death. Cell Death Differ 1996;3:71–78.
6. Gobbel GT, Chan PH. Neuronal death is an active, caspase-dependent process after moderate but not severe DNA damage. J Neurochem 2001;76:520–531.
7. Liu W, Liu R, Chun JT, et al. Kainate excitotoxicity in organotypic hippocampal slice cultures: evidence for multiple apoptotic pathways. Brain Res 2001;916:239–248.
8. Adams JD Jr, Chang ML, Klaidman L. Parkinson's disease—redox mechanisms. Curr Med Chem 2001;8:809–814.
9. Hirsch EC, Hunot S, Faucheux B, et al. Dopaminergic neurons degenerate by apoptosis in Parkinson's disease. Mov Disord 1999;14:383–385.
10. Kerr JFR, Wyllie AH, Currie AR. Apoptosis: a basic biological phenomenon with wide ranging implications in tissue kinetics. Br J Cancer 1972;26:239–257.
11. Kanazawa I. How do neurons die in neurodegenerative diseases? Trends Mol Med 2001;7:339–344.
12. Leist M, Jaattela M. Four deaths and a funeral: from caspases to alternative mechanisms. Nat Rev Mol Cell Biol 2001;2: 589–598.
13. Nicotera P. Apoptosis and age-related disorders: role of caspase-dependent and caspase-independent pathways. Toxicol Lett 2002;127:189–195.
14. Wadia JS, Chalmers-Redman RME, Ju WJH, et al. Mitochondrial membrane potential and nuclear changes in apoptosis caused by serum and nerve growth factor withdrawal: time course and modification by (-)-deprenyl. J Neurosci 1998;18: 932–947.
15. Tatton NA, Kish SJ. In situ detection of apoptotic nuclei in the substantia nigra compacta of 1-methyl-4-phenyl-1,2,3,6-tetrahydropyridine-treated mice using terminal deoxynucleotidyl transferase labelling and acridine orange staining. Neuroscience 1997;77:1037–1048.
16. Tatton NA, Hagl C, Nandor S, et al. Apoptotic cell death in the hippocampus due to prolonged hypothermic circulatory arrest: comparison of cyclosporine A and cycloheximide on neuron survival. Eur J Cardiothorac Surg 2001;19:746–755.
17. Tatton NA, Tezel G, Insolia SA, et al. In situ detection of apoptosis in normal pressure glaucoma: a preliminary examination. Surv Ophthalmol 2001;45(suppl 1):S268–S272.
18. Tatton NA, Rideout HJ. Confocal microscopy as a tool to examine DNA fragmentation, chromatin condensation and other apoptotic changes in Parkinson's disease. Parkinsonism Relat Disord 1999;5:179–186.
19. Tatton NA. Increased caspase 3 and Bax immunoreactivity accompany nuclear GAPDH translocation and neuronal apoptosis in Parkinson's disease. Exp Neurol 2000;166:29–43.
20. Tatton NA, Maclean-Fraser A, Tatton WG, et al. A fluorescent double-labeling method to detect and confirm apoptotic nuclei in Parkinson's disease. Ann Neurol 1998;44(suppl 1): S142–S148.
21. Tatton WG, Chalmers-Redman RME, Ju WJH, et al. Propargylamines induce anti-apoptotic new protein synthesis in serum and NGF withdrawn NGF-differentiated PC12 cells. J Pharmacol Exp Ther 2002;301:753–764.
22. Kohler C, Orrenius S, Zhivotovsky B. Evaluation of caspase activity in apoptotic cells. J Immunol Methods 2002;265: 97–110.
23. Troy CM, Salvesen GS. Caspases on the brain. J Neurosci Res 2002;69:145–150.
24. Nagata S. Apoptotic DNA fragmentation. Exp Cell Res 2000; 256:12–18.
25. Hartmann A, Hunot S, Michel PP, et al. Caspase-3: a vulnerability factor and final effector in apoptotic death of dopaminergic neurons in Parkinson's disease. Proc Natl Acad Sci USA 2000;97:28752880.

26. Susin SA, Lorenzo HK, Zamzami N, et al. Molecular characterization of mitochondrial apoptosis-inducing factor. Nature 1999;397:441–446.
27. Cande C, Cohen I, Daugas E, et al. Apoptosis-inducing factor (AIF): a novel caspase-independent death effector released from mitochondria. Biochimie 2002;84:215–222.
28. Loeffler M, Daugas E, Susin SA, et al. Dominant cell death induction by extramitochondrially targeted apoptosis-inducing factor. FASEB J 2001;15:758–767.
29. Susin SA, Daugas E, Ravagnan L, et al. Two distinct pathways leading to nuclear apoptosis. J Exp Med 2000;192:571–580.
30. Daugas E, Nochy D, Ravagnan L, et al. Apoptosis-inducing factor (AIF): a ubiquitous mitochondrial oxidoreductase involved in apoptosis. FEBS Lett 2000;476:118–123.
31. van Loo G, Schotte P, van Gurp M, et al. Endonuclease G: a mitochondrial protein released in apoptosis and involved in caspase-independent DNA degradation. Cell Death Differ 2001;8:1136–1142.
32. Li LY, Luo X, Wang X. Endonuclease G is an apoptotic DNase when released from mitochondria. Nature 2001;412: 95–99.
33. Mogi M, Harada M, Kondo T, et al. The soluble form of Fas molecule is elevated in parkinsonian brain tissues. Neurosci Lett 1996;220:195–198.
34. Ferrer I, Blanco R, Cutillas B, Ambrosio S. Fas and Fas-L expression in Huntington's disease and Parkinson's disease. Neuropathol Appl Neurobiol 2000;26:424–433.
35. Saraste A. Morphologic criteria and detection of apoptosis. Herz 1999;24:189–195.
36. Tamura T, Said S, Lu W, Neufeld D. Specificity of TUNEL method depends on duration of fixation. Biotech Histochem 2000;75:197–200.
37. Nishizaki K, Yoshino T, Orita Y, et al. TUNEL staining of inner ear structures may reflect autolysis, not apoptosis. Hear Res 1999;130:131–136.
38. Liu S, Edgerton SM, Moore DH II, Thor AD. Measures of cell turnover (proliferation and apoptosis) and their association with survival in breast cancer. Clin Cancer Res 2001;7: 1716–1723.
39. Lafarga M, Andres MA, Calle E, Berciano MT. Reactive gliosis of immature Bergmann glia and microglial cell activation in response to cell death of granule cell precursors induced by methylazoxymethanol treatment in developing rat cerebellum. Anat Embryol (Berl) 1998;198:111–122.
40. Negoescu A, Lorimier P, Labat-Moleur F, et al. In situ apoptotic cell labeling by the TUNEL method: improvement and evaluation on cell preparations. J Histochem Cytochem 1996; 44:959–968.
41. Deibel MR Jr, Coleman MS. Biochemical properties of purified human terminal deoxynucleotidyltransferase. J Biol Chem 1980;255:4206–4212.
42. Grosse F, Manns A. Terminal deoxyribonucleotidyl transferase (EC 2.7.7.31). In: Burrell F, ed. Methods in molecular biology. Totowa, NJ: Humana Press, 1993:95–105.
43. Agid Y. Aging, disease and nerve cell death. Bull Acad Natl Med 1995;179:1193–1203.
44. Mochizuki H, Goto K, Mori H, Mizuno Y. Histochemical detection of apoptosis in Parkinson's disease. J Neurol Sci 1996;137:120–123.
45. Anglade P, Vyas S, Javoy-Agid F, et al. Apoptosis and autophagy in nigral neurons of patients with Parkinson's disease. Histol Histopathol 1997;12:25–31.
46. Kosel S, Egensperger R, von Eitzen U, et al. On the question of apoptosis in the parkinsonian substantia nigra. Acta Neuropathol 1997;93:105–108.
47. Kingsbury AE, Mardsen CD, Foster OJ. DNA fragmentation in human substantia nigra: apoptosis or perimortem effect? Mov Disord 1998;13:877–884.
48. Banati RB, Daniel SE, Blunt SB. Glial pathology but absence of apoptotic nigral neurons in long-standing Parkinson's disease. Mov Disord 1998;13:221–227.
49. Whiteside G, Cougnon N, Hunt SP, Munglani R. An improved method for detection of apoptosis in tissue sections and cell culture, using the TUNEL technique combined with Hoechst stain. Brain Res Brain Res Protoc 1998;2:160–164.
50. Hartmann A, Michel PP, Troadec JD, et al. Is Bax a mitochondrial mediator in apoptotic death of dopaminergic neurons in Parkinson's disease? J Neurochem 2001;76: 1785–1793.
51. Parone PA, James D, Martinou JC. Mitochondria: regulating the inevitable. Biochimie 2002;84:105–111.
52. Martinou JC, Green DR. Breaking the mitochondrial barrier. Nat Rev Mol Cell Biol 2001;2:63–67.
53. Vieira HL, Haouzi D, El Hamel C, et al. Permeabilization of the mitochondrial inner membrane during apoptosis: impact of the adenine nucleotide translocator. Cell Death Differ 2000;7:1146–1154.
54. Wei MC, Zong WX, Cheng EH, et al. Proapoptotic BAX and BAK: a requisite gateway to mitochondrial dysfunction and death. Science 2001;292:727–730.
55. Reed JC, Kroemer G. Mechanisms of mitochondrial membrane permeabilization. Cell Death Differ 2000;7:1145.
56. Basanez G, Nechushtan A, Drozhinin O, et al. Bax, but not Bcl-x(L), decreases the lifetime of planar phospholipid bilayer membranes at subnanomolar concentrations. Proc Natl Acad Sci USA 1999;96:5492–5497.
57. Roucou X, Rostovtseva T, Montessuit S, et al. Bid induces cytochrome c-impermeable Bax channels in liposomes. Biochem J 2002;363:547–552.
58. Korsmeyer SJ, Wei MC, Saito M, et al. Pro-apoptotic cascade activates BID, which oligomerizes BAK or BAX into pores that result in the release of cytochrome c. Cell Death Differ 2000;7:1166–1173.
59. Deng Y, Lin Y, Wu X. TRAIL-induced apoptosis requires Bax-dependent mitochondrial release of Smac/DIABLO. Genes Dev 2002;16:33–45.
60. Eskes R, Desagher S, Antonsson B, Martinou JC. Bid induces the oligomerization and insertion of Bax into the outer mitochondrial membrane. Mol Cell Biol 2000;20:929–935.
61. Zamzami N, El Hamel C, Maisse C, et al. Bid acts on the permeability transition pore complex to induce apoptosis. Oncogene 2000;19:6342–6350.
62. Ruffolo SC, Breckenridge DG, Nguyen M, et al. BID-dependent and BID-independent pathways for BAX insertion into mitochondria. Cell Death Differ 2000;7:1101–1108.
63. Halestrap AP, McStay GP, Clarke SJ. The permeability transition pore complex: another view. Biochimie 2002;84: 153–166.
64. Narita M, Shimizu S, Ito T, et al. Bax interacts with the permeability transition pore to induce permeability transition and cytochrome c release in isolated mitochondria. Proc Natl Acad Sci USA 1998;95:14681–14686.
65. Brenner C, Cadiou H, Vieira HL, et al. Bcl-2 and Bax regulate the channel activity of the mitochondrial adenine nucleotide translocator. Oncogene 2000;19:329–336.
66. Shimizu S, Ide T, Yanagida T, Tsujimoto Y. Electrophysiological study of a novel large pore formed by Bax and the voltage-dependent anion channel that is permeable to cytochrome c. J Biol Chem 2000;275:12321–12325.
67. Shimizu S, Matsuoka Y, Shinohara Y, et al. Essential role of voltage-dependent anion channel in various forms of apoptosis in mammalian cells. J Cell Biol 2001;152:237–250.

68. Scorrano L, Ashiya M, Buttle K, et al. A distinct pathway remodels mitochondrial cristae and mobilizes cytochrome c during apoptosis. Dev Cell 2002;2:55–67.
69. Schuler M, Green DR. Mechanisms of p53-dependent apoptosis. Biochem Soc Trans 2001;29:684–688.
70. Chen RW, Saunders PA, Wei H, et al. Involvement of glyceraldehyde-3-phosphate dehydrogenase (GAPDH) and p53 in neuronal apoptosis: evidence that GAPDH is upregulated by p53. J Neurosci 1999;19:9654–9662.
71. Xiang H, Kinoshita Y, Knudson CM, et al. Bax involvement in p53-mediated neuronal cell death. J Neurosci 1998;18: 1363–1373.
72. Chang NS. A potential role of p53 and WOX1 in mitochondrial apoptosis. Int J Mol Med 2002;9:19–24.
73. Lopes UG, Erhardt P, Yao R, Cooper GM. p53-dependent induction of apoptosis by proteasome inhibitors. J Biol Chem 1997;272:12893–12896.
74. Chang YC, Lee YS, Tejima T, et al. mdm2 and bax, downstream mediators of the p53 response, are degraded by the ubiquitin-proteasome pathway. Cell Growth Differ 1998;9: 79–84.
75. Chen F, Chang D, Goh M, et al. Role of p53 in cell cycle regulation and apoptosis following exposure to proteasome inhibitors. Cell Growth Differ 2000;11:239–246.
76. Miller FD, Pozniak CD, Walsh GS. Neuronal life and death: an essential role for the p53 family. Cell Death Differ 2000; 7:880–888.
77. Schapira AH, Mann VM, Cooper JM, et al. Anatomic and disease specificity of NADH CoQ1 reductase (complex I) deficiency in Parkinson's disease. J Neurochem 1990;55: 2142–2145.
78. McNaught KS, Olanow CW, Halliwell B, et al. Failure of the ubiquitin-proteasome system in Parkinson's disease. Nat Rev Neurosci 2001;2:589–594.
79. Nagatsu T, Mogi M, Ichinose H, Togari A. Changes in cytokines and neurotrophins in Parkinson's disease. J Neural Transm 2000;60(suppl):277–290.
80. Sirover MA. New insights into an old protein: the functional diversity of mammalian glyceraldehyde-3-phosphate dehydrogenase. Biochim Biophys Acta 1999;1432:159–184.
81. Berry MD, Boulton AA. Glyceraldehyde-3-phosphate dehydrogenase and apoptosis. J Neurosci Res 2000;60:150–154.
82. Dastoor Z, Dreyer JL. Potential role of nuclear translocation of glyceraldehyde-3-phosphate dehydrogenase in apoptosis and oxidative stress. J Cell Sci 2001;114:1643–1653.
83. Ishitani R, Kimura M, Sunaga K, et al. An antisense oligodeoxynucleotide to glyceraldehyde-3-phosphate dehydrogenase blocks age-induced apoptosis of mature cerebrocortical neurons in culture. J Pharmacol Exp Ther 1996;278:447–454.
84. Ishitani R, Chuang DM. Glyceraldehyde-3-phosphate dehydrogenase antisense oligodeoxynucleotides protect against cytosine arabinonucleoside-induced apoptosis in cultured cerebellar neurons. Proc Natl Acad Sci USA 1996;93:9937–9941.
85. Sawa A, Khan AA, Hester LD, Snyder SH. Glyceraldehyde-3-phosphate dehydrogenase: nuclear translocation participates in neuronal and nonneuronal cell death. Proc Natl Acad Sci USA 1997;94:11669–11674.
86. Fukuhara Y, Takeshima T, Kashiwaya Y, et al. GAPDH knockdown rescues mesencephalic dopaminergic neurons from MPP□-induced apoptosis. Neuroreport 2001;12:2049–2052.
87. Saunders PA, Chalecka Franaszek E, Chuang DM. Subcellular distribution of glyceraldehyde-3-phosphate dehydrogenase in cerebellar granule cells undergoing cytosine arabinoside-induced apoptosis. J Neurochem 1997;69:1820–1828.
88. Tatton WG, Chalmers-Redman RM, Elstner M, et al. Glyceraldehyde-3-phosphate dehydrogenase in neurodegeneration and apoptosis signaling. J Neural Transm 2000; 60(suppl):77–100.
89. Carlile GW, Chalmers-Redman RM, Tatton NA, et al. Reduced apoptosis after nerve growth factor and serum withdrawal: conversion of tetrameric glyceraldehyde-3-phosphate dehydrogenase to a dimer. Mol Pharmacol 2000; 57:2–12.
90. Ishitani R, Tanaka M, Sunaga K, et al. Nuclear localization of overexpressed glyceraldehyde-3-phosphate dehydrogenase in cultured cerebellar neurons undergoing apoptosis. Mol Pharmacol 1998;53:701–707.
91. Shashidharan P, Chalmers-Redman RM, Carlile GW, et al. Nuclear translocation of GAPDH-GFP fusion protein during apoptosis. Neuroreport 1999;10:1149–1153.
92. Korsmeyer SJ. BCL-2 gene family and the regulation of programmed cell death. Cancer Res 1999;59(suppl):1693s–1700s.
93. McGeer PL, Yasojima K, McGeer EG. Inflammation in Parkinson's disease. Adv Neurol 2001;86:83–89.
94. Hirsch EC, Hunot S, Damier P, Faucheux B. Glial cells and inflammation in Parkinson's disease: a role in neurodegeneration? Ann Neurol 1998;44(suppl 1):S115–S120.
95. Chen G, Goeddel DV. TNF-R1 signaling: a beautiful pathway. Science 2002;296:1634–1635.
96. Wajant H. The Fas signaling pathway: more than a paradigm. Science 2002;296:1635–1636.
97. Schneider P, Tschopp J. Apoptosis induced by death receptors. Pharm Acta Helv 2000;74:281–286.
98. Hartmann A, Mouatt-Prigent A, Faucheux BA, et al. FADD: a link between TNF family receptors and caspases in Parkinson's disease. Neurology 2002;58:308–310.
99. Hartmann A, Troadec JD, Hunot S, et al. Caspase-8 is an effector in apoptotic death of dopaminergic neurons in Parkinson's disease, but pathway inhibition results in neuronal necrosis. J Neurosci 2001;21:2247–2255.
100. Sawa A. Neuronal cell death in Down's syndrome. J Neural Transm 1999;57(suppl):87–97.
101. Seidl R, Bidmon B, Bajo M, et al. Evidence for apoptosis in the fetal Down syndrome brain. J Child Neurol 2001;16: 438–442.
102. Mielke K, Herdegen T. JNK and p38 stresskinases—degenerative effectors of signal- transduction-cascades in the nervous system. Prog Neurobiol 2000;61:45–60.
103. Waring P, Mullbacher A. Cell death induced by the Fas/Fas ligand pathway and its role in pathology. Immunol Cell Biol 1999;77:312–317.
104. Reed JC. Apoptosis based therapies. Nat Rev Drug Discov 2002;1:111–121.
105. Kragten E, Lalande I, Zimmermann K, et al. Glyceraldehyde-3-phosphate dehydrogenase, the putative target of the antiapoptotic compounds CGP 3466 and R-(-)-deprenyl. J Biol Chem 1998;273:5821–5828.
106. Waldmeier PC, Spooren WP, Hengerer B. CGP 3466 protects dopaminergic neurons in lesion models of Parkinson's disease. Naunyn Schmiedebergs Arch Pharmacol 2000;362: 526–537.
107. Waldmeier PC, Boulton AA, Cools AR, et al. Neurorescuing effects of the GAPDH ligand CGP 3466B. J Neural Transm 2000;60(suppl):197–214.

Discussion

Schapira: Bill, you present a convincing case for apoptosis occurring in PD, but it is not clear what proportion of cells die by way of apoptosis as opposed to

necrosis. What proportion of nigral neurons do you believe die by apoptosis in PD.

Tatton: To my knowledge, no one has described necrotic cells in the PD nigra. However, necrotic cells may disappear very quickly and therefore they might exist, but be undetected. We reported that at any one time approximately 0.8 % of neuromelanin-containing neurons in the PD nigra are undergoing apoptotic degeneration based on both nuclear DNA fragmentation and nuclear chromatin condensation. Based on tissue culture studies, we had previously reported that the average life of a neuron in the stage of apoptotic degradation was approximately 12 hours. However, our more recent work in the intact hippocampus of pigs exposed to hypoxia/ischemia suggests that neurons may remain in the stage of apoptotic degradation for days or even weeks. Postmortem cell counts and serial PET studies in PD patients suggest that there is an annual rate of loss of nigral neurons of approximately 3 to 7%. If all cells are dying by apoptosis, this suggests that markers of apoptotic degradation can persist in the PD nigra for 1 to 3 months.

Another important factor to consider is that studies in tissue culture suggest that hypoxia can accelerate the premitochondrial signaling in several forms of apoptosis, including those induced by mitochondrial complex I or proteasome inhibition. Hence, hypoxia or other insults suffered during the late stages of life may increase the rates of nigral neurons entering apoptosis. Furthermore, agonal events at the time of death may cause vulnerable nerve cells to undergo apoptotic degeneration when otherwise this event might not occur for months or years. Thus, the number of neurons that show apoptotic changes at postmortem may be excessively represented.

In both the ischemic pig hippocampus and glaucomatous human retina, we have seen hippocampal neurons and retinal ganglion cells with swollen nuclei typical of necrosis similar to what has been shown by others using high concentrations of glutamate. We have not seen similar cells in the PD nigra, and, in fact, there is no direct evidence for necrosis of nigra neurons in PD. In both tissue culture and animal models, low-level chronic insults, like those proposed to underlie PD neuronal death, cause apoptosis rather than necrosis. Hence, viewed from the above perspectives, until proved otherwise, the findings to date indicate that most, if not all, of the loss of PD nigral neurons is apoptotic.

Hunot: Are you proposing a new definition for apoptosis? How do you define apoptosis?

Tatton: I think of apoptosis as a multistep, sometimes network-like, signaling process that connects an insult or a stimulus to the degradation and phagocytosis of cells. The signaling elements can vary for different insults or stimuli and/or for different cellular phenotypes. At its heart, apoptosis is a pleomorphic process that allows for the removal of cells without associated inflammation that might damage its neighbors. This significance of this definition is that it permits the introduction of agents that can interfere with these signals or stimuli and prevent cell death.

Olanow: There are many different signaling pathways that can lead to apoptosis, some of which are mitochondrially dependent and some of which are not. I support your position that apoptosis is occurring in the Parkinson's disease brain, but I wonder if you have any views as to which signaling pattern is the key one in Parkinson's disease. As different antiapoptotic agents interfere with different signaling pathways, this might be important for choosing which drugs to study in clinical trial.

Tatton: There is evidence that several different signals associated with apoptosis are upregulated or translocated in PD suggesting that they are involved in the neurodegenerative cascade. Upregulated expression of c-Jun, P53, GAPDH, bax, and activated caspase 3 have each been detected in neuromelanin-containing neurons in the Parkinson's disease nigra. Furthermore, there is evidence of nuclear translocation of GAPDH and NF□B in the nigra in PD. Another signal that may be involved is TNF-□ that can promote apoptosis either through mitochondria or directly by activating caspase 3 or caspase 1. There is also evidence indicating that opening of the mitochondrial permeability pore promotes a reduction in mitochondrial membrane potential with release of apoptosis initiating factors and cytochrome c. There is a question as to whether complex I, which is reduced in the PD nigra, is involved in the mitochondrial permeability pore and may be associated with a low resting mitochondrial membrane potential. Each of these provides an opportunity to use antiapoptotic agents that either interfere with proapoptotic signals or promote closure of the mitochondrial permeability pore.

Olanow: Let me ask you an extension of that question. What does it mean to block an apoptotic signal once the apoptotic sequence has begun? Is it too late at that point? Will the cell be protected for a short while only to die a little later perhaps by way of a different signaling pathway? Indeed, will it go on to necrosis because you blocked the suicide and create even more damage because this will be associated with an inflammatory response that might damage neighboring healthy neurons?

Tatton: You raise very good points. Once you get down into the cascade, for example, at the level where there is activation of caspase 3 or caspase 9 you are probably past the decisional point and there is nothing to gain. The trick is to find an agent that works early enough in the apoptotic signaling pathway such that the cell is still able to recover, perhaps at the level of

caspase 8. I particularly like the notion of using D2 or adrenergic agonists that appear to be able to turn on an intrinsic protective system. Alternatively, agents that promote closure of the mitochondrial permeability pore maintain the mitochondrial membrane potential and may prevent the release of signals that initiate the apoptotic process.

Isacson: What do you think is currently the best marker of apoptosis?

Tatton: I think caspase 3 is probably the best marker of apoptosis. When the antibody first came out it wasn't very good, but now it is excellent and a wonderful screening marker for apoptosis. We don't even use the ISEL or YOYO-1 markers any more.

Schapira: Let me get back to the point that Warren raised. How do we know that all you accomplish with antiapoptotic drugs is helping sick neurons survive a bit longer? What evidence is there that they function normally?

Tatton: Again, I think the issue is where in the cycle you are interfering with apoptosis. If you are early enough, I think you can protect a cell against cell death such that it retains its functional state. There are now numerous studies showing that antiapoptotic agents can protect dopamine neurons from a variety of toxins in both in vitro and in vivo models. Specifically, TCH346 has been shown to preserve functional effects in monkeys treated with MPTP.

Schapira: But logically your antiapoptotic drugs should not prevent or reverse those biochemical events that have caused the neuron to be sick in the first place.

Olanow: It is also possible that in PD, nigral neurons are vulnerable and may not be able to tolerate what would otherwise be normal stresses. For example, a defect in complex I might be associated with a decrease in resting mitochondrial membrane potential causing the cell to be vulnerable to undergo apoptosis when exposed to otherwise tolerable levels of oxidative stress. An antiapoptotic agent that promoted closure of the permeability transition pore and preserved the mitochondrial membrane potential thus might protect a cell that is capable of functioning normally.

Tatton: I agree. It is important not to think of antiapoptotic agents in terms of degenerative events that occur at the end of the cascade, but rather those that act early enough in the process that they might protect functionally normal cells. If you get far enough down the cascade you are in trouble, but apoptosis should be thought of as really just an extension of the pathogenesis of cell death.

Stocchi: You and others have suggested that agents that interrupt premitochondrial apoptosis signaling may slow the progression of PD. I am concerned that a reduction in physiological apoptosis by those same agents could induce uncontrolled proliferation and cancer.

Tatton: As we and others have shown, apoptosis in different diseases and in response to different toxins may depend on different signaling pathways. Those pathways may or may not intersect with those that induce physiological apoptosis that occurs as a balance to excess proliferation. Most neurons are postmitotic and do not contain the signaling machinery necessary to limit proliferation. Neurodegeneration-related alterations in apoptosis signaling in neurons therefore do not tend to involve proteins that can foster proliferation on their own. So, I think it is possible that we can identify an agent that will be antiapoptotic in PD but well tolerated with respect to cancer. Still, care must be taken to utilize antiapoptotic agents that interrupt a specific disease-related neuronal apoptosis signaling pathway and that does not affect apoptosis pathways that oppose proliferation. Of the several apoptosis-based therapies currently in clinical trial for neurodegenerative diseases, none have so far been found to increase the incidence of cancer to my knowledge.

DOI 10.1007/s00702-002-0827-z
J Neural Transm (2003) 110: 509–515

Journal of Neural Transmission

Neuroprotection by deprenyl and other propargylamines: glyceraldehyde-3-phosphate dehydrogenase rather than monoamine oxidase B

Review

W. Tatton, R. Chalmers-Redman, and N. Tatton

Departments of Neurology and Ophthalmology, Mount Sinai School of Medicine, New York, NY, USA

Received December 9, 2002; accepted December 12, 2002

Summary. Deprenyl and other propargylamines are clinically beneficial in Parkinson's disease (PD). The benefits were thought to depend on monoamine oxidase B (MAO-B) inhibition. A large body of research has now shown that the propargylamines increase neuronal survival independently of MAO-B inhibition by interfering with apoptosis signaling pathways. The propargylamines bind to glyceraldehyde-3-phosphate dehydrogenase (GAPDH). The GAPDH binding is associated with decreased synthesis of pro-apoptotic proteins like BAX, c-JUN and GAPDH but increased synthesis of anti-apoptotic proteins like BCL-2, Cu-Zn superoxide dismutase and heat shock protein 70. Anti-apoptotic propargylamines that do not inhibit MAO-B are now in PD clinical trial.

Keywords: Deprenyl, Parkinson's disease, GAPDH, anti-apoptosis.

Parkinson's disease (PD) is characterized by catccholaminergic neuronal loss, including the loss of melanin-containing, dopaminergic neurons in the substantia nigra compacta (SNc) and noradrenergic neurons in the locus coeruleus (LC). The pathobiology of the initiation and progression of PD remains uncertain (see (Olanow et al. 1999) for a review). Stereological counting has shown that SNc melanin-containing dopaminergic are decreased by 60% or more before PD becomes clinically evident (Ma et al., 1995). For more than a decade, pharmacological agents have been sought with the capacity to prevent or slow the loss of the 40% of dopaminergic SNc neurons that remain at the time of initial diagnosis of the disease.

The pro-toxin 1-methyl-4-phenyl-1,2,3,6-tetrahydropyridine (MPTP) kills SNc dopaminergic neurons (Langston et al., 1983) as well as other catecholaminergic neurons (Crossman et al., 1987) in non-human primates with a similar, but not identical, regional distribution of neuronal loss to that found in human PD (Pifl et al., 1988). MPTP is converted to the 1-methyl-4-phenylpyridinium ion (MPP$^+$) in astroglia by monoamine oxidase B (MAO-B) (Chiba et al., 1984; Dimonte et al., 1992). MPP$^+$ is released from astroglia and is selectively accumulated in catecholaminergic neurons by the plasma membrane dopamine transporter (DAT) (Pifl et al., 1993). Inside catcholaminergic neurons, MPP$^+$ undergoes high affinity uptake by the vesicular monoamine transporter (VMAT2) (Del Zompo et al., 1992; Peter et al., 1994). Imaging of cultured dopaminergic neurons have shown that MPP$^+$ binding to VMT2 causes the vesicular release of dopamine (Lotharius et al., 2000). Auto-oxidation of the released dopamine results in the production of reactive oxygen species (ROS) with consequent peroxidation of macromolecules leading to neuronal damage and death. MPP$^+$ also binds to mitochondrial respiratory complex I, where it inhibits NADH dehydrogenase (Nicklas et al., 1987). Complex I inhibition by MPP$^+$ is not the primary cause of neuronal death but likely augments the VMAT2 mediated cell damage caused by the toxin (Nakamura et al., 2000).

In 1984, Gerald Cohen and colleagues showed that selective inhibition of MAO-B by (−)-deprenyl prevented the depletion of striatal dopamine by MPTP in monkeys (Cohen et al., 1984). The finding was interpreted to show that (−)-deprenyl protected the nigrostriatal neurons by blocking the conversion of MPTP to MPP$^+$ by MAO-B in astroglia. Neurons in the SNc were hypothesized to be highly vulnerable to oxidative stress because of their dopamine metabolism and the presence of iron and neuromelanin in their cytosol, which together might favor ROS formation (Cohen et al., 1989; Olanow, 1993). Postmortem analysis had shown increased iron, decreased glutathione, and increased lipid peroxidation in substantia nigra lysates from patients with PD (Jenner et al., 1996). Selective inhibitors of MAO-B were considered as possible neuronal protectants in PD because of their capacity to interfere with the oxidative metabolism of dopamine resulting in a diminished likelihood of ROS formation. Accordingly, Cohen et al's finding provided a major impetus for clinical trials to investigate the capacity of MAO-B inhibition to alter the clinical progression of PD [see Group (1993) for an example]. Although the MAO-B inhibitors caused highly statistically significant clinical slowing in PD, it was uncertain whether the slowing resulted from reduced neuronal death or from a symptomatic action on dopaminergic neurotransmission. Despite the uncertainty regarding the interpretation of the clinical trials, it is certain that (−)-deprenyl and structurally related propargylamines (DRPs) can reduce neuronal death induced in vivo and in vitro by a wide variety of insults in a number of different neuronal models. Those insults have included 6-hydroxydopamine, MPP$^+$, MPTP, nitric oxide, peroxynitrite, DSP-4, glutathione depletion, peripheral nerve crush or axotomy, optic nerve crush, trophic insufficiency, hypoxia and/or ischemia, cytosine arabinoside, excitotoxins, thiamine deficiency, okadaic acid and

aging. Neurons or neuron-like cells whose survival has been increased by DRPs have included mesencephalic or nigral dopaminergic neurons, hippocampal neurons, dentate neurons, cerebellar granule and Purkinje neurons, cerebral cortical neurons, thalamic neurons, retinal ganglion neurons, spinal and facial motoneurons, neuroblastoma cells, and NGF differentiated PC12 cells [reviewed in Tatton et al. (2000)].

Just one year after the initial report, Cohen and coworkers reported a second MPTP-related finding (Mytilineou et al., 1985) that in retrospect led to a new understanding as to how (□)-deprenyl can increase neuronal survival. They showed that (□)-deprenyl could reduce the loss of cultured mesencephalic dopaminergic neurons caused by the direct application of MPP□. The finding was not easily accepted since it indicated that (□)-deprenyl reduced neuronal death by a mechanism other than blocking the conversion of MPTP to MPP□. The initial evidence for MAO-B independent neuroprotection by (□)-deprenyl was subsequently supported by nine different studies employing 8 different insults in 4 different tissue culture and 4 different animal models [reviewed in Tatton et al. (2000)]. Furthermore, DRPs that do not inhibit MAO-B or MAO-A have increased neuronal survival in a number of models (Waldmeier et al., 2000a,b; Zimmerman et al., 1999), including SNc dopaminergic neurons in monkeys receiving intra-carotid MPTP injections (Andringa et al., 2000). Furthermore, neurons in MAO-B knockout mice are not protected from damage caused by hypoxia or MPP□ (Holschneider et al., 2001). In short, there is no evidence to indicate that MAO-B inhibition by (□)-deprenyl or other DRPs can protect neurons from any insult other than MPTP exposure.

How then, do (□)-deprenyl and DRPs reduce neuronal death? More than 20 studies in a range of cell types exposed to a number of treatments, toxins or lesions have shown that (□)-deprenyl and DRPs can increase neuronal survival by reducing apoptosis [see Tatton et al. (2000) for detailed references]. In vitro, apoptosis has been reduced in NGF differentiated PC12 cells, neuroblastoma cells, human melanoma cells, rat cerebellar granule cells, rat retinal neurons, rat and mouse mesencephalic dopaminergic neurons, SHSY5 dopaminergic neurons, and hippocampal neurons while in vivo, it has been reduced in rat cortical neurons, SNc dopaminergic neurons, spinal neurons, motoneurons, hippocampal neurons and retinal ganglion cells. Causes of the apoptosis have included hypoxia, arterial occlusion, axon crush or division, dieldrin, MPTP, MPP□, peroxynitrite, kainic acid, 6-hydroxydopamine, n-methyl-l-salsolinol, okadaic acid, cytosine arabinoside and nitric oxide. The reduction in neuronal apoptosis depends on a capacity to alter new protein synthesis, particularly the new synthesis of proteins in the nuclear and mitochondrial fractions (Tatton et al., 2002, 1994). Importantly, the propargylamines do not alter new protein synthesis in undamaged nerve cells. Rather a period of one to two hours is required before damaged cells are responsive to DRP anti-apoptosis and the responsiveness continues to about 6 hours after cells are damaged. DRPs have been shown to prevent the dissipation of mitochondrial membrane potential ($D\Psi_M$) that accompanies some forms of apoptosis (Paterson et al., 1998; Wadia et al., 1998;

Zhang et al., 1999). Prevention of apoptotic decreases in BCL-2 or BCL-X_L and the translocation of BAX to mitochondria appear to be responsible for the capacity of DRPs to maintain $D\Psi_M$ (Tatton et al., 2002). DRPs also increase the levels of ROS scavengers like Cu/Zn superoxide dismutase, Mn superoxide dismutase and glutathione peroxide and thereby can prevent ROS induced apoptosis. DRPs also alter the levels of other proteins linked to apoptosis signaling like c-JUN, c-FOS, heat shock protein 70 and glyceraldehyde-3-phosphate dehydrogenase (GAPDH) (Tatton et al., 2002).

GAPDH may mediate (□)-deprenyl and DRP neuroprotection. A number of studies using antisense oligonucleotides showed that GAPDH is essential to the progression of some forms of neuronal apoptosis [see Tatton et al. (2000) for a review]. GAPDH mRNA and protein levels increase in neurons early in those apoptosis signaling processes and are associated with the dense nuclear accumulation of GAPDH, which can serve as a marker of those forms of apoptosis involving GAPDH. Studies with green fluorescent protein labelled GAPDH indicate the GAPDH translocates from the cytosol to the nucleus in some forms of apoptosis (Shashidharan et al., 1999).

Studies with photoaffinity labeled DRPs showed that DRPs bind to GAPDH in rat hippocampus (Kragten et al., 1998) and cultured catecholaminergic cells (Carlile et al., 2000). DRPs prevent the GAPDH upregulation and the dense GAPDH nuclear accumulation typical of GAPDH-associated apoptosis (Carlile et al., 2000). Size exclusion chromatography has shown that DRPs convert GAPDH from a tetramer to a specific dimeric form in solution (Carlile et al., 2000). DRP binding to GAPDH appears to prevent apoptosis signaling by the protein, while allowing the enzyme to retain glycolytic capacity. Recent studies in cultured dopaminergic mesencephalic neurons have shown that micro-injection of antibodies specific for GAPDH monomer or dimer can reduce MPP□ toxicity (Fukuhara et al., 2001).

Can the binding of DRPs to GAPDH alter the progression of PD? Is apoptosis involved in the neuronal loss found in PD? The use of in situ end labeling (ISEL, also termed as TdT dUTP nick end labeling or TUNEL) PD postmortem brain initially suggested that apoptosis contributed to SNc neuronal loss in PD but ISEL support for PD neuronal apoptosis has been inconsistent. The inconsistency has been overcome by the use of dual labeling for nuclear DNA cleavage and chromatin condensation (Tatton, 2000; Tatton et al., 1998, 1999). Furthermore, immunocytochemistry has shown apoptosis signaling proteins in neuromelanin containing neurons in the PD SNc. The signaling proteins have included BAX and activated caspase 3 (Hartmann et al., 2000, 2001; Tatton, 2000), which leaves little doubt that apoptosis contibutes to neuronal loss in PD. Dense GAPDH nuclear accumulation has also been found in neuromelanin containing neurons in the PD postmortem nigra, which seems to implicate GAPDH in PD neuronal apoptosis (Tatton, 2000). Accordingly, part of the benefits of (□)-deprenyl in PD may reflect the capacity of DRPs to reduce apoptosis. An anti-apoptotic DRP, which does

not inhibit MAO-B but binds to GAPDH, is currently in clinical trial as a neuroprotectant in PD (Reed, 2002).

References

Andringa G, Cools AR (2000) The neuroprotective effects of CGP 3466B in the best in vivo model of Parkinson's disease, the bilaterally MPTP-treated rhesus monkey. J Neural Transm [Suppl] 60: 215–225

Carlile GW, Chalmers-Redman RM, Tatton NA, Pong A, Borden KE, Tatton WG (2000) Reduced apoptosis after nerve growth factor and serum withdrawal: conversion of tetrameric glyceraldchyde-3-phosphate dehydrogenase to a dimer [in process citation]. Mol Pharmacol 57: 2–12

Chiba K, Trevor A, Castagnoli N Jr (1984) Metabolism of the neurotoxic tertiary amine, MPTP, by brain monoamine oxidase. Biochem Biophys Res Commun 120: 574–578

Cohen G, Spina MB (1989) Deprenyl suppresses the oxidant stress associated with increased dopamine turnover. Ann Neurol 26: 689–690

Cohen G, Pasik P, Cohen B, Leist A, Mytilineau C, Yahr MD (1984) Pargyline and deprenyl prevent the neurotoxicity of 1-methyl-4-phenyl-1,2,3,6-tetrahydropyridine (MPTP) in monkeys. Eur J Pharmacol 106: 209–210

Crossman AR, Clarke CE, Boyce S, Robertson RG, Sambrok MA (1987) MPTP-induced parkinsonism in the monkey: neurochemical pathology, complications of treatment and pathophysiological mechanisms. Can J Neurol Sci 14: 428–435

Del Zompo M, Piccardi MP, Ruiu S, Corsini GU, Vaccari A (1992) Characterization of a putatively vesicular binding site for [3H]MPP□ in mouse striatal membranes. Brain Res 571: 354–357

Dimonte DA, Wu EY, Delanney LE, Irwin I, Langston JW (1992) Toxicity of 1-methyl-4-phenyl-1,2,3,6-tetrahydropyridine in primary cultures of mouse astrocytes. J Pharmacol Exp Ther 261: 44-49

Fukuhara Y, Takeshima T, Kashiwaya Y, Shimoda K, Ishitani R, Nakashima K (2001) GAPDH knockdown rescues mesencephalic dopaminergic neurons from MPP□ –induced apoptosis. Neuroreport 12: 2049–2052

Hartmann A, Hunot S, Michel PP, Muriel MP, Vyas S, Faucheux BA, Mouatt-Prigent A, Turmel H, Srinivasan A, Ruberg M, Evan GI, Agid Y, Hirsch EC (2000) Caspase-3: a vulnerability factor and final effector in apoptotic death of dopaminergic neurons in Parkinson's disease. Proc Natl Acad Sci USA 97: 2875–2880

Hartmann A, Michel PP, Troadec JD, Mouatt-Prigent A, Faucheux BA, Ruberg M, Agid Y, Hirsch EC (2001) Is Bax a mitochondrial mediator in apoptotic death of dopaminergic neurons in Parkinson's disease? J Neurochem 76: 1785–1793

Holschneider DP, Chen K, Scif I, Shih JC (2001) Biochemical, behavioral, physiologic, and neurodevelopmental changes in mice deficient in monoamine oxidase A or B. Brain Res Bull 56: 453–462

Jenner P, Olanow CW (1996) Oxidative stress and the pathogenesis of Parkinson's disease. Neurology 47: S161–170

Kragten E, Lalande I, Zimmermann K, Roggo S, Schindler P, Muller D, van Oostrum J, Waldmeier P, Furst P (1998) Glyceraldehyde-3-phosphate dehydrogenase, the putative target of the antiapoptotic compounds CGP 3466 and R-(□)-deprenyl. J Biol Chem 273: 5821–5828

Langston JW, Ballard P, Tetrud JW, Irwin I (1983) Chronic Parkinsonism in humans due to a product of meperidine-analog synthesis. Science 219: 979–980

Lotharius J, O'Malley KL (2000) The parkinsonism-inducing drug 1-methyl-4-phenylpyridinium triggers intracellular dopamine oxidation. A novel mechanism of toxicity. J Biol Chem 275: 38581–38588

Ma SY, Collan Y, Roytta M, Rinne JO, Rinne UK (1995) Cell counts in the substantia nigra: a comparison of single section counts and disector counts in patients with Parkinson's disease and in controls. Neuropathol Appl Neurobiol 21: 10–17

Mytilineou C, Cohen G (1985) Deprenyl protects dopamine neurons from neurotoxic effect of 1-methyl-4-phenylpyridinium ion. J Neurochem 45: 1951–1953

Nakamura K, Bindokas VP, Marks JD, Wright DA, Frim DM, Miller RJ, Kang UJ (2000) The selective toxicity of 1-methyl-4-phenylpyridinium to dopaminergic neurons: the role of mitochondrial complex I and reactive oxygen species revisited. Mol Pharmacol 58: 271–278

Nicklas WJ, Yougster SK, Kindt MV, Heikkila RE (1987) MPTP, MPP□ and mitochondrial function. Life Sci 40: 721–729

Olanow CW (1993) A rationale for monoamine oxidase inhibition as neuroprotective therapy for Parkinson's disease. Mov Disord 8: S1–7

Olanow CW, Tatton WG (1999) Etiology and pathogenesis of Parkinson's disease. Annu Rev Neurosci 22: 123–144

The Parkinson Study Group (1993) Effects of tocopherol and deprenyl on the progression of disability in early Parkinson's disease. N Engl J Med 328: 176–183

Paterson IA, Zhang D, Warrington RC, Boulton AA (1998) R-Deprenyl and R-2-Heptyl-N-methylpropargylamine prevent apoptosis in cerebellar granule neurons induced by cytosine arabinoside but not low extracellular potassium. Neurochem 70: 515–523

Peter D, Jimenez J, Liu Y, Kim J, Edwards RH (1994) The chromaffin granule and synaptic vesicle amine transporters differ in substrate recognition and sensitivity to inhibitors. J Biol Chem 269: 7231–7237

Pifl C, Schingnitz G, Hornykicwicz O (1988) The neurotoxin MPTP does not reproduce in the rhesus monkey the interregional pattern of striatal dopamine loss typical of human idiopathic Parkinson's disease. Neurosci Lett 92: 228–233

Pifl C, Giros B, Caron MG (1993) Dopamine transporter expression confers cytotoxicity to low doses of the parkinsonism-inducing neurotoxin 1-methyl-4-phenylpyridinium. J Neurosci 13: 4246-4253

Reed JC (2002) Apoptosis-based therapies. Nature Rev – Drug Discovery 1: 111–121

Shashidharan P, Chalmers-Redman RM, Carlile GW, Rodic V, Gurvich N, Yuen T, Tatton WG, Sealfon SC (1999) Nuclear translocation of GAPDH-GFP fusion protein during apoptosis. Neuroreport 10: 1149–53

Tatton NA (2000) Increased caspase 3 and Bax immunoreactivity accompany nuclear GAPDH translocation and neuronal apoptosis in Parkinson's disease. Exp Neurol 166: 29–43

Tatton NA, Rideout HJ (1999) Confocal microscopy as a tool to examine DNA fragmentation, Chromatin condensation and other apoptotic changes in Parkinson's disease. Parkinsonism Rel Disord 5: 179–186

Tatton NA, Maclean-Fraser A, Tatton WG, Perl DP, Olanow CW (1998) A fluorescent double-labeling method to detect and confirm apoptotic nuclei in Parkinson's disease. Ann Neurol 44: S142–148

Tatton WG, Ju WY, Holland DP, Tai C, Kwan M (1994) (□)-Deprenyl reduces PC12 cell apoptosis by inducing new protein synthesis, J Neurochem 63: 1572–1575

Tatton WG, Chalmers-Redman RM, Elstner M, Leesch W, Jagodzinski FB, Stupak DP, Sugrue MM, Tatton NA (2000) Glyceraldehyde-3-phosphate dehydrogenase in neurodegeneration and apoptosis signaling. J Neural Transm [Suppl] 60: 77–100

Tatton WG, Chalmers-Redman RME, Ju WJH, Carlile GW, Mammen M, Tatton NA (2002) Propargylamines induce anti-apoptotic new protein synthesis in serum and NGF withdrawn NGF-differentiated PC12 cells. J Pharmacol Exp Ther 301: 753–764

Wadia JS, Chalmers-Redman RME, Ju WJH, Carlile GW, Phillips JL, Fraser AD, Tatton WG (1998) Mitochondrial membrane potential and nuclear changes in apoptosis caused by serum and nerve growth factor withdrawal: time course and modification by (□)-deprenyl. J Neurosci 18: 932–947

Waldmeier PC, Boulton AA, Cools AR, Kato AC, Tatton WG (2000a) Neurorescuing effects of the GAPDH ligand CGP 3466B. J Neural Transm [Suppl] 60: 197–214

Waldmeier PC, Spooren WP, Hengerer B (2000b) CGP 3466 protects dopaminergic neurons in lesion models of Parkinson's disease. Naunyn Schmiedebergs Arch Pharmacol 362: 526–537

Zhang D, Berry MD, Paterson IA, Boulton AA (1999) Loss of mitochondrial membrane potential is dependent on the apoptotic program activated: prevention by R-2HMP. J Neurosci Res 58: 248–292

Zimmerman K, Waldmeier PC. Tatton WG (1999) Dibenzoxepines as treatments for neurodegenerative diseases. Pure Appl Chem 71: 2039–2046

Authors' address: Dr. W. G. Tatton, Mount Sinai School of Medicine, Department of Neurology, One Gustave L. Levy Place, Annenburg 1470, Box 1137, New York, NY 10029-6574, U.S.A., e-mail: william.tatton@mssm.edu

0026-895X/00/010002-11$3.00/0

MOLECULAR PHARMACOLOGY, 57:2–12 (2000).

Reduced Apoptosis after Nerve Growth Factor and Serum Withdrawal: Conversion of Tetrameric Glyceraldehyde-3-Phosphate Dehydrogenase to a Dimer

GRAEME W. CARLILE, RUTH M. E. CHALMERS-REDMAN, NADINE A. TATTON, AMANDA PONG, KATHERINE E. BORDEN, and WILLIAM G. TATTON

Departments of Neurology (G.W.C., R.M.E.C.-R., N.A.T., A.P., K.L.B.B., W.G.T.) and Physiology and Biophysics (K.L.B.B.), Mount Sinai School of Medicine, New York, New York

Received August 5, 1999; accepted September 20, 1999

This paper is available online at http://www.molpharm.org

ABSTRACT

Antisense oligonucleotides against the glycolytic enzyme glyceraldehyde-3-phosphate dehydrogenase (GAPDH) are able to reduce some forms of apoptosis. In those forms, overall GAPDH levels increase and the enzyme accumulates in the nucleus. The monoamine oxidase B (MAO-B) inhibitor, (2)-deprenyl (DEP), its metabolite (2)-desmethyldeprenyl, and a tricyclic DEP analog, CGP3466, can reduce apoptosis independently of MAO-B inhibition and have been found to bind to GAPDH. We used neuronally differentiated PC12 cells to show that DEP, DES, and CGP3466 reduce apoptosis caused by serum and nerve growth factor withdrawal over the concentration range of 10^{2} to $10^{2\,13}$ M. We provide evidence that the DEP-like compounds bind to GAPDH in the PC12 cells and that they prevent both the apoptotic increases in GAPDH levels and nuclear accumulation of GAPDH. In vitro, the compounds enhanced the conversion of NAD^{1} to NADH by GAPDH in the presence of AUUUA-rich RNA and converted GAPDH from its usual tetrameric form to a dimeric form. Using cell lysates, we found a marked increase in rates of NAD^{1} to NADH conversion in early apoptosis, which was returned toward control values by the DEP-like compounds. Accordingly, the DEP-like compounds appear to decrease glycolysis by preventing the GAPDH increases in early apoptosis. GAPDH dimer may not have the capacity to contribute to apoptosis in a similar manner to the tetramer, which might account for the antiapoptotic capacity of the compounds. These actions on GAPDH, rather than MAO-B inhibition, may contribute to the improvements in Parkinson's and Huntington's diseases found with DEP treatment.

Studies with antisense oligonucleotides showed that glyceraldehyde-3-phosphate dehydrogenase (GAPDH) is necessary for apoptosis to proceed in cerebrocortical neurons and PC12 cells (Ishitani et al., 1996; Sawa et al., 1997). GAPDH levels increase during the early part of apoptosis (Sunaga et al., 1995; Ishitani et al., 1996, 1997, 1998; Saunders et al., 1997). In nonapoptotic cells, GAPDH is primarily found in the extra nuclear cytoplasm with only sparse localization to small punctate areas in the nucleus (Carlile et al., 1998). In apoptosis, GAPDH accumulates densely in the nucleus, and that accumulation has been proposed to underlie its role in apoptosis (Saunders et al., 1997; Sawa et al., 1997; Ishitani et al., 1998; Shashidharan et al., 1999).

GAPDH may participate in the pathogenesis of some neurodegenerative diseases. GAPDH binds to the mutant proteins with polyglutamine repeats in Huntington's disease (HD) and related degenerative conditions (Burke et al., 1996). GAPDH is found in amyloid plaques in Alzheimer's disease (AD) brains (Sunaga et al., 1995), and GAPDH nuclear accumulation is present in association with apoptosis in nigral neuronal nuclei in postmortem Parkinson's disease (PD) brain (N. Tatton, unpublished observations). Although there is evidence for metabolic abnormalities in HD tissues, GAPDH glycolytic activity does not appear to be altered in HD brain tissue (Kish et al., 1998).

Neuronal loss, likely by apoptosis, is central to AD, HD, and PD (Cotman, 1998; Tatton et al., 1998; Petersen et al., 1999). The monoamine oxidase B (MAO-B) inhibitor (2)-deprenyl (DEP) slows the progression of PD clinical deficits (Parkinson's Study Group, 1993; Olanow et al., 1995) and

The work was supported by a Lowenstein Foundation Grant and Medical Research Council of Canada Grants (to W.G.T. and K.L.B.B.).

ABBREVIATIONS: GAPDH, glyceraldehyde-3-phosphate dehydrogenase; DEP, (2)-deprenyl; DES, (2)-desmethyldeprenyl; PML, promyelocytic leukemia; BL, BODIPY-labeled; PND, partially neuronally differentiated; LCSM, laser confocal scanning microscopy; M/S1 N, minimum essential medium with serum and nerve growth factor; BCA, bicinchoninic acid; NGF, nerve growth factor; M/O, minimum essential medium only; CGP3466, N-methyl-N-propargyl-10^{2} aminomethyl-dibenzo[b,f]oxepin; HD, Huntington's disease; AD, Alzheimer's disease; PD, Parkinson's disease; MAO-B, monoamine oxidase B.

may also reduce clinical deficits in HD (Patel et al., 1996). The basis for clinical improvements with DEP are uncertain because the clinical trial data do not allow for the differentiation of a slowed rate of neuronal loss from a symptomatic effect like that caused by increased dopamine availability (see Fahn, 1996). DEP and its metabolite, (2)-desmethyldeprenyl (DES), reduce apoptosis in a variety of cells (Tatton et al., 1994; Le et al., 1997; Paterson et al., 1997, 1998; Kragten et al., 1998; Magyar et al., 1998; Maruyama et al., 1998; Wadia et al., 1998) via mechanisms that are independent of MAO-B inhibition (Tatton and Chalmers-Redman, 1996) and require new protein synthesis (Tatton et al., 1994). CGP3466, a tricyclic DEP analog (N-methyl-N-propargyl-10-aminomethyl-dibenzo[b,f]oxepin), which does not have the capacity to inhibit MAO-B, reduces apoptosis and binds specifically to GAPDH (Kragten et al., 1998). The GAPDH binding has been proposed to account for the antiapoptotic capacities of DEP-like compounds.

We have carried out experiments in vivo and in vitro to determine whether DES and CGP3466 reduce apoptosis caused by serum and NGF withdrawal in a similar manner to DEP (Tatton et al., 1994; Wadia et al., 1998) and whether any reduction in apoptosis by DES and CGP3466 can be linked to actions on GAPDH.

Materials and Methods

PC12 cells were propagated in minimum essential medium (MEM) containing 10% horse serum and 5% fetal bovine serum. The cells were transferred to 24-well plates and partially neuronally differentiated (PND) for 6 days in the same media supplemented with 100 ng/ml 7S nerve growth factor [NGF; MEM with serum and NGF (M/S1 N); see Wadia et al. (1998) for details of culture, treatment, preparation, staining, and counting]. On day 6, the cells were washed repeatedly to remove NGF and serum-borne trophic agents and replaced in M/S1 N as controls, in MEM only (M/O) for trophic withdrawal, or in MEM with DEP, DES, or CGP3466 at concentrations varying from $10^{2\,5}$ to $10^{2\,13}$ M. At 24 h after washing, cells were harvested and lysed, and intact nuclei were counted as an estimate of cell survival (Fig. 1A, filled circles).

The cells were also grown and treated as above on poly(L-lysine)-treated coverglass and were stained with YOYO-1 (Molecular Probes, Eugene, OR) at various times after washing to reveal chromatin condensation as a marker of apoptotic nuclear degradation (see Wadia et al., 1998, for references). Cells on coverglass were washed three times in PBS and then put in 100% methanol at 2 20°C

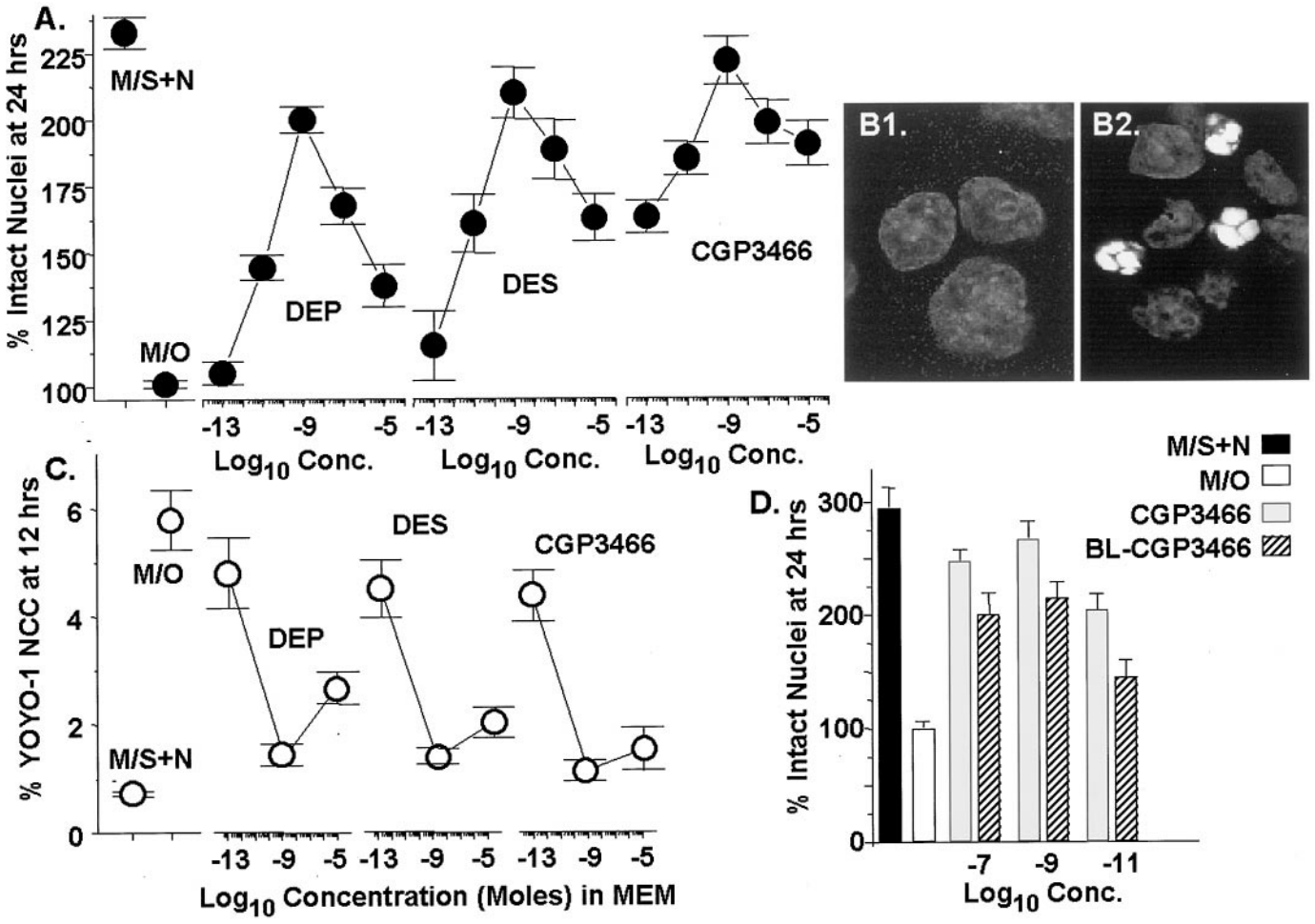

Fig. 1. DEP-related compounds reduce apoptosis. DEP, DES, and CGP3466 at concentrations ranging between $10^{2\,13}$ and $10^{2\,5}$ M increase the survival of PND-PC12 cells as estimated by numbers of intact nuclei (A) and decrease the number of nuclei with apoptotic nuclear degradation as shown by nuclear chromatin condensation revealed by YOYO-1 DNA staining at the same concentrations (C). M/S1 N indicates cells that were washed repeatedly to remove trophic support and then replaced in MEM with serum and NGF. M/O indicates cells that were washed and then placed in MEM only. B1 and B2, typical examples of YOYO-1 stained normal nuclei and nuclei with chromatin condensation, respectively. D, comparison of the numbers of intact nuclei for cells treated with CGP3466 and those treated with BL-CGP3466 showing that the BL compound retains most of the capacity of the unlabeled compound to reduce cell death.

for 30 s. The cells on coverglass were then incubated in 1.5 mM YOYO-1 in PBS at room temperature for 30 min. The cells were then washed three times in PBS and mounted in Aquamount (Gurr, England). The total number of YOYO-1 stained nuclei were counted on 25 fields for each coverslip, each field was chosen by the use of pairs of randomly generated x-y coordinates, and the number of nuclei with chromatin condensation were expressed as a percentage. The values were pooled for three coverslips for each treatment and time point.

Laser confocal scanning microscopic (LCSM) images were collected using a Leica TCS4D confocal microscope equipped with a tunable excitation filter. Images were collected with a 1003 1.4 NA objective at a pinhole setting of 20 to minimize focal depth. Images were collected in a 512 3 512 3 8 bit format and saved as TIFF files. Images of live cells exposed to BODIPY-labeled (BL)-CGP3466 or DES were similarly acquired using an environmentally controlled chamber (Medical Systems Corp.) that houses a 25-mm coverglass on which PC12 cells were plated and treated as above. YOYO-1 was imaged using excitation/emission values of 488 nm/515 to 545 nm, whereas BODIPY-FL images and GAPDH immunoreaction fluorescence were taken at 568/585 to 615 and 647/660 long pass, respectively.

To identify the proteins that bind CGP3466 in the PND PC12 cells, cells were incubated with ^{125}I photoaffinity-labeled CGP3466 at varying times after serum and NGF withdrawal. After exposure to ultraviolet light, total protein was extracted, run on gels, and transferred to a membrane. PC-12 cells were grown in MEM with serum and NGF for 6 days, and then serum and NGF were withdrawn. One hour before harvesting, 6 mCi of the photoaffinity-labeled CGP3466 was added. Thirty minutes later, the dishes were put in a UV transilluminator for 20 min to activate the azido group. After removal of the medium and one wash with balanced salt solution, the cells were harvested using trypsin-EDTA and then centrifuged at 1000g for 5 min. The supernatant was removed and the cells were washed twice in PBS. The cells were lysed in lysis buffer (25 mM Tris zHCl, pH 7.5, 150 mM NaCl, 1 mM EDTA, and 1% Triton X-100), and the samples were stored frozen at 2 20°C. Samples were run on an SDS-polyacrylamide gel and transferred to a nitrocellulose membrane. The membrane was dried and exposed on x-ray film. After completion of the autoradiographic exposure, the same membranes were probed for GAPDH immunoreactivity using a mouse monoclonal antibody (Chemicon International, Temecula, CA) at a dilution of 1:400.

For determinations of the time course of changes in GAPDH levels, cells were grown on 10-cm Petri dishes for 6 days and treated as above. At 0.5 to 12 h after washing, cells were harvested, and a lysate was produced. The medium was removed and placed in a separate tube on ice, and 2 ml of PBS was added to each dish. The cells were removed with a cell scraper and centrifuged for 5 min at 1500g at 4°C, followed by cold PBS washes. The cells were then centrifuged at 2000g and lysed in lysis buffer (25 mM Tris zHCl, pH 7.5, 150 mM NaCl, 1 mM EDTA, 1% Triton X-100, and 5 mg/ml leupeptin, chymostatin, pepstatin A, and aprotinin, plus 1 mM benzamidine). The lysate was stored at 2 30°C. Protein was assayed by the bicinchoninic acid (BCA) method.

To obtain protein from various subcellular fractions, the cells were treated as above and harvested by centrifugation at 1000g for 5 min at 4°C. The pellets were washed twice in cold PBS and resuspended buffer containing 25 mM HEPES-KOH, pH 7.5,10 mM KCl, 1.5 mM $MgCl_2$, 1 mM NaEDTA, 1 mM NaEGTA, 1 mM dithiothreitol, and 5 mg/ml leupeptin, chymostatin, pepstatin A, and aprotinin, plus 1 mM benzamidine and 250 mM sucrose. The cells were homogenized by 12 to 15 strokes of a glass Dounce homogenizer. The homogenates were then centrifuged at 700g for 10 min at 4°C. This pellet is the nuclear fraction, and the supernatants was further centrifuged at 10,000g for 15 min at 4°C. The resulting pellet represents the mitochondrially enriched fraction, and the supernatant represents the cytoplasmic fraction. Both nuclearly and mitochondrially enriched fractions were resuspended in 50 ml of the above buffer. Samples were then frozen at 2 30°C. Before use, the samples were protein assayed by the BCA method. Equal amounts of whole-cell or subcellular fraction lysates were run on a SDS-polyacrylamide gel, Western blotted, and probed for GAPDH as above.

To demonstrate the enrichment of cellular subfractions, equal amounts of protein from each fraction were Western blotted and probed with antibodies for nucleolin (1:500; Santa Cruz Biochemicals, Santa Cruz, CA), 14-3-3 b protein (1:400; Santa Cruz Biochemicals), and cytochrome oxidase (0.1 mg/ml; Molecular Probes, Eugene, OR), which are markers for the nuclear, cytoplasmic, and mitochondrial fractions, respectively.

For immunocytochemistry and the examination of the kinetics of cellular entry and accumulation of fluorescently labeled DES and CGP3466, PC-12 cells were grown on a coverglass and partially neuronally differentiated as described (for details, see Tatton et al., 1994; Wadia et al., 1998). Cells were fixed in 4% paraformaldehyde and then washed once in PBS and placed in 5% normal goat serum and 0.01% Tween-20 in PBS for 1 h at room temperature. The cell on coverglass were again washed with PBS; placed in a solution containing 0.5% normal serum, 0.01% Tween-20, and mouse monoclonal GAPDH antibody at a 1:300 dilution; and incubated overnight at 4°C. The cells on a coverglass were washed four times with PBS and exposed to a Cy5-labeled goat anti-mouse secondary antibody (Jackson Immunoresearch, West Grove, PA) at a dilution of 1:500 in PBS containing 0.5% normal serum and 0.01% Tween-20 for 1 h at room temperature. The cells on coverglass were washed five times in PBS and mounted in Aquamount.

Three-dimensional protein structural models of rat GAPDH were produced as in Borden (1998) and are described here briefly. The structure of rat GAPDH has not been reported. GAPDH structures were obtained from the Brookhaven protein database. GAPDH is highly conserved in terms of its amino acid sequence and three-dimensional structure (Kim et al., 1995). After inspection of structures of GAPDH from several species, we decided to use a GAPDH from Leishmania mexicana, in which the structure had been determined under physiological salt conditions, although this structure did not look significantly different from any other GAPDH structures in the database (Kim et al., 1995). Using the program Insight (Biosym, San Diego, CA), we modeled the rat GAPDH sequence onto the L. mexicana structure. The subsequent structure was subjected to molecular dynamics at 1000 K, followed by cooling to 300 K, and then underwent 1000 steps of conjugate gradient minimization using Discover (Biosym).

The glycolytic activity of GAPDH, measured by the increase in absorption at 340 nm, resulting from the reduction of NAD^+ to NADH according to the reaction glyceraldehyde-3-phosphate 1 NAD^+ 1 P_i 5 1,3-diphosphoglycerate 1 NADH. The enzyme assay was carried out in the presence of 0.015 M sodium pyrophosphate, pH 8.5, 7.5 mM NAD^+, 0.1 M dithiothreitol, and 0.015 M GAPDH. Immediately before its use, the enzyme was diluted in the pyrophosphate buffer to a concentration of 30 mg/ml. A synthetic RNA oligonucleotide of 15 residues consisting of three repeating AUUUA sequences (Genosys, Ltd., Cambridge, UK) was used in the glycolytic studies. The glycolytic activity of cell lysates produced from a 6-h exposure to MS1 N, M/O, and MO1 DES was similarly determined. Cells were collected in 0.015 M sodium pyrophosphate buffer, pH 8.5, and homogenized with a Dounce homogenizer; protein was assayed by the BCA method (Pierce Chemical, Rockford, IL) and stored at 2 20°C. Equal amounts of total protein were incubated in 0.015 M sodium pyrophosphate, pH 8.5, with NAD^+ and dithiothreitol, and the conversion of NAD1 to NADH was determined as above.

To examine the oligomeric states of GAPDH, Sephacryl H-300 was poured into a glass column to a height of 12 cm and diameter of 1 cm. The column was washed using a buffer containing 20 mM HEPES, pH 7.5, 25 mM KCl, and 10% glycerol. Samples were loaded onto the column in volumes of less than 100 ml. Samples including more than one component were coincubated briefly before addition to the column. GAPDH, CGP3466, and RNA were used in nanomolar concen-

trations in a strict ratio of 1 molecule of GAPDH to 2 of RNA and/or 2 of CGP3466. All samples were dissolved in this buffer. Where indicated, 0.1% of SDS was used. To calibrate the column, the fractions for the following proteins were determined: cytochrome c (12.4 kDa) fraction 23, lysozyme (14.4 kDa) fraction 23, carbonic anhydrase (20 kDa) fraction 20, BSA (67 kDa) fraction 18, *b*-galactosidase (116 kDa) fraction 16, aldolase (158 kDa) fraction 13, and macroglobulin (170 kDa) fraction 10 (see calibration bar below Fig. 7B3). Protein was detected by monitoring the absorbance of individual fractions at 280 nm and confirmed at 293 nm. Nucleic acid was detected similarly by monitoring absorbance at 260 nm.

Results

We previously showed that apoptosis initiated by serum and NGF withdrawal from PND-PC12 cells can be reduced by DEP (Tatton et al., 1994; Wadia et al., 1998). In this study, we used the same model to compare the antiapoptotic capacities of DEP, DES, and CGP3466. Reductions in apoptosis were estimated by two complementary measures: 1) counts of intact nuclei as an indicator of cell survival and 2) counts of cells with nuclear chromatin condensation using a fluorescent DNA binding dye, YOYO-1, as a measure of apoptotic nuclear degradation (examples in Fig. 1, B1 and B2). DES and CGP3466 showed similar or superior capacities to DEP to increase survival (Fig. 1A) and to reduce the proportion of nuclei with chromatin condensation (Fig. 1C) over concentration ranges of $10^{2\,5}$ to $10^{2\,13}$ M. At $10^{2\,9}$ M, all three agents at least doubled the proportion of cells that survived for 24 h after NGF and serum withdrawal. In a similar manner, the same concentration reduced the proportion of cells with nuclear chromatin condensation to less than 25% of that found at 12 h after NGF and serum withdrawal.

We also compared the capacity of a BL-CGP3466 (Zimmermann et al., 1998) for details of the fluorescently labeled DES and CGP3466) with that of CGP3466 in reducing apoptosis in the PND-PC12 model (Fig. 1D). Over the concentration range of $10^{2\,7}$ to $10^{2\,11}$ M, the BL-CGP3466 retained 75 to 80% of the capacity of CGP3466 to increase cell survival.

We then used the BL-CGP3466 with LCSM to follow the entry and localization of BL-CGP3466 in living PND-PC12 cells maintained in an environmentally controlled chamber. The BL-CGP3466 fluorescence revealed reproducible rates of entry and subcellular localization in the cells and displayed classic competition curves for preadded unlabeled CGP3466. Figure 2 provides an example of the competition in which the addition of $10^{2\,9}$ M BL-CGP3466 to the chamber resulted in a gradual accumulation of subcellular fluorescence over about 30 min (Fig. 2, top). The subcellular distribution of the BL-CGP3466

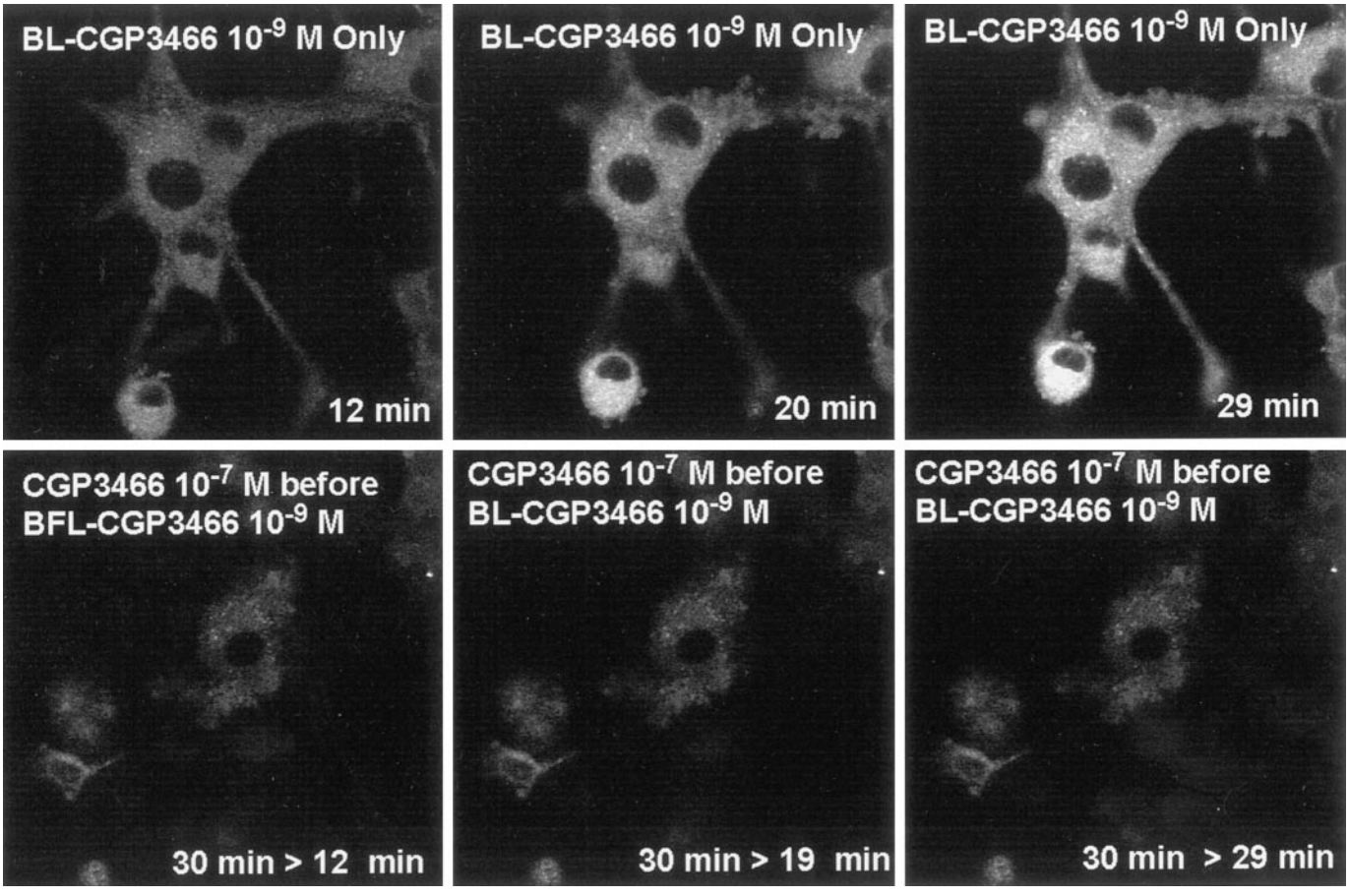

Fig. 2. BL-CGP3466 fluorescence seen with LCSM is gradually retained in the extranuclear cytosol, and preincubation with higher concentrations of unlabeled CGP3466 markedly reduces the retention. Top three panels, LCSM images of the retention of BL-CGP3466 fluorescence in living PND-PC12 cells maintained in an environmental chamber containing MEM with serum and NGF at 12, 20, and 29 min after the addition of $10^{2\,9}$ M BL-CGP3466. Note the gradual increase in extranuclear cytosolic fluorescence. Bottom three panels, LCSM images of another group of cells that were preincubated with $10^{2\,7}$ M of unlabeled CGP3466 for 30 min before the addition of $10^{2\,9}$ M BL-CGP3466 and then imaged at 12, 19, and 29 min. Note that the preincubation with the unlabeled CGP3466 reduced the appearance of the BL-CGP3466 fluorescence at all time points, showing that the BL-CGP3466 retention was specific for CGP3466 binding sites.

fluorescence was very similar to that found for antibodies against GAPDH in the cells (see examples in Fig. 5, A1–A4). That is, the BL-CGP3466 fluorescence gradually accumulated in the extra nuclear cytosol with relatively light and scattered accumulation in the nucleus. Thirty minutes of preincubation of the cells with 10^{27} M unlabeled CGP3466 followed by the addition of 10^{29} M BL-CGP3466 markedly reduced the accumulation of BL-CGP3466 fluorescence (Fig. 2, bottom). Similarly, incubation of BL-CGP3466 with paraformaldehyde-fixed PC12 cells on a coverglass showed subcellular distributions of BL-CGP3466 (Fig. 3A1) that were similar, if not identical, to those found in living cells using the environmentally controlled chamber (Fig. 2) and those found for a mouse monoclonal antibody against GAPDH (see Fig. 5A3). Similar results were obtained with BL-DES (not shown).

We used photoaffinity-labeled CGP3466 (Zimmermann et al., 1998) to determine whether the DEP analog binds to GAPDH in the serum and NGF-withdrawn PND-PC12 cells in a similar manner as that reported for rat hippocampal homogenates (Kragten et al., 1998). Autoradiographs revealed major bands at about 37, 43, 50, and possibly 200 kDa, which appeared similar to those found for rat hippocampal tissue. Figure 3B shows a typical autoradiograph for protein extracted from cells at 3, 6, and 9 h after washing and placement in M/O. Figure 3C1 shows a higher power example of the 37-kDa band. The same membranes used for autoradiography were immunoreacted with a monoclonal antibody against GAPDH, and an immunodense band corresponding in position to the 37-kDa autoradiographic band was found (Fig. 3C2 was immunoreacted for the same membrane examined autoradiographically in Fig. 3C1). The similarity of the subcellular distribution of BL-CGP3466 fluorescence and

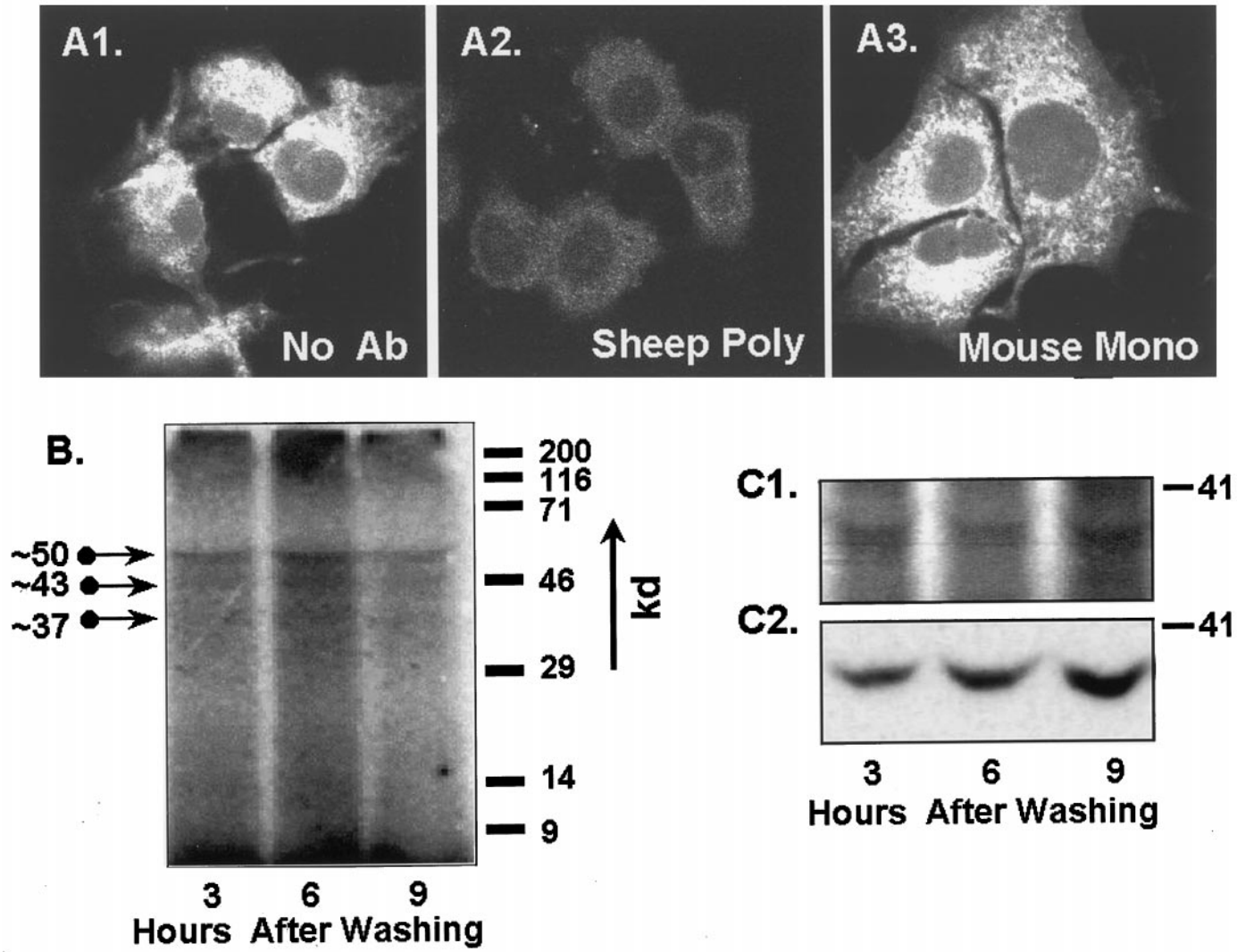

Fig. 3. CGP3466 photoaffinity labeling and BL-CGP3466 labeling of cells imaged with LCSM. A1–A3, paraformaldehyde-fixed cells on coverglass that were incubated with BL-CGP3466 for 30 min and then imaged using LCSM. A2 and A3, cells were preincubated with a sheep polyclonal (1:250) and a mouse monoclonal antibody (1:400) for 30 min before the addition of BL-CGP3466. Note that the BL-CGP3466 fluorescence is scattered throughout the extranuclear cytosol and that the sheep antibody, but not the mouse antibody, blocked the retention of the BL-3466 in the cells. B, autoradiogram for total protein extracted from PND-PC12 cells at 3, 6, and 9 h after serum and NGF withdrawal. Before withdrawal, the cells were incubated with a photoaffinity-labeled, ^{125}I-tagged CGP3466 and then exposed to ultraviolet light to activate the azido group of the photoaffinity label. The autoradiograms revealed at least three bands, as shown, at 37, 43, and 47 kDa. C1, section of a photoaffinity-labeled, ^{125}I-tagged CGP3466 autoradiogram for total protein extracted from PND-PC12 cells at 3, 6, and 9 h after serum and NGF withdrawal showing the distinct band at 37 kDa, which increased in intensity from 3 to 9 h. C2, probing the same membrane with an antibody against GAPDH showed an immunodense band that was located at the identical position to the 37-kDa autoradiography band and also increased in intensity from 3 to 9 h.

GAPDH immunofluorescence and the subcellular colocalization of a portion of photoaffinity-labeled CGP3466 autoradiographic activity with GAPDH immunoreaction seem in accord previous findings showing that one of the proteins binding CGP3466 is GAPDH (Kragten et al., 1998).

In solution, GAPDH can take a monomeric, dimeric, or tetrameric form but greatly favors the tetramer (Minton and Wilf, 1981). Molecular modeling of the GAPDH tetramer revealed a central channel at the interface between the four monomers (see Fig. 7, A1 and A2; also see Fig. 7 in Borden, 1998). Examination of the GAPDH tetramer model suggested that CGP3466 and DES were most likely to bind in this central channel. (See Figure 7B1 for a model of CGP3466 in the channel.) A sheep polyclonal antibody (Biogenesis, Poole, Dorset, UK), which was raised against residues located in a position that would likely block entry to the channel (see location of the residues in Fig. 7C), was applied to fixed cells on a coverglass that were subsequently treated with BL-CGP3466. Cells that were preincubated with the sheep antibody showed markedly reduced BL-CGP3466 cellular fluorescence, even after prolonged incubation with BL-CGP3466 (compare Fig. 3, A1 and A2). In contrast, preincubation with a mouse antibody against GAPDH (Chemicon), which reacted against residues near to the N terminus, placing the residues in or near to the Rossman fold region of the tetramer (see Fig. 7A1, RF), did not alter the BL-CGP3466 fluorescence (compare Fig. 3, A1 and A3).

To determine whether the PND-PC12 cell apoptosis was typical of GAPDH-associated apoptosis found in other cellular models, WESTERN blots were prepared for total protein extracted from cells at multiple time points after washing and placement in medium without serum and NGF. The blots showed that GAPDH levels began to increase at about 2 h after washing and placement in serum and NGF-free medium (Fig. 4A). GAPDH levels did not appear to increase in serum and NGF-withdrawn cells that were treated with 10^{29} M CGP3466 or 10^{29} M DES (Fig. 4B).

In parallel experiments, Western blots for protein extracted from the nuclear, mitochondrial, and cytosolic cellular subfractions at 3, 6, 9, and 12 h after serum and NGF withdrawal were examined for GAPDH protein levels. Control blots were prepared for the subfractions using antibodies against nucleolin, cytochrome oxidase, and 14-3-3 *b* protein that are known to react with proteins in the nuclear, mito-

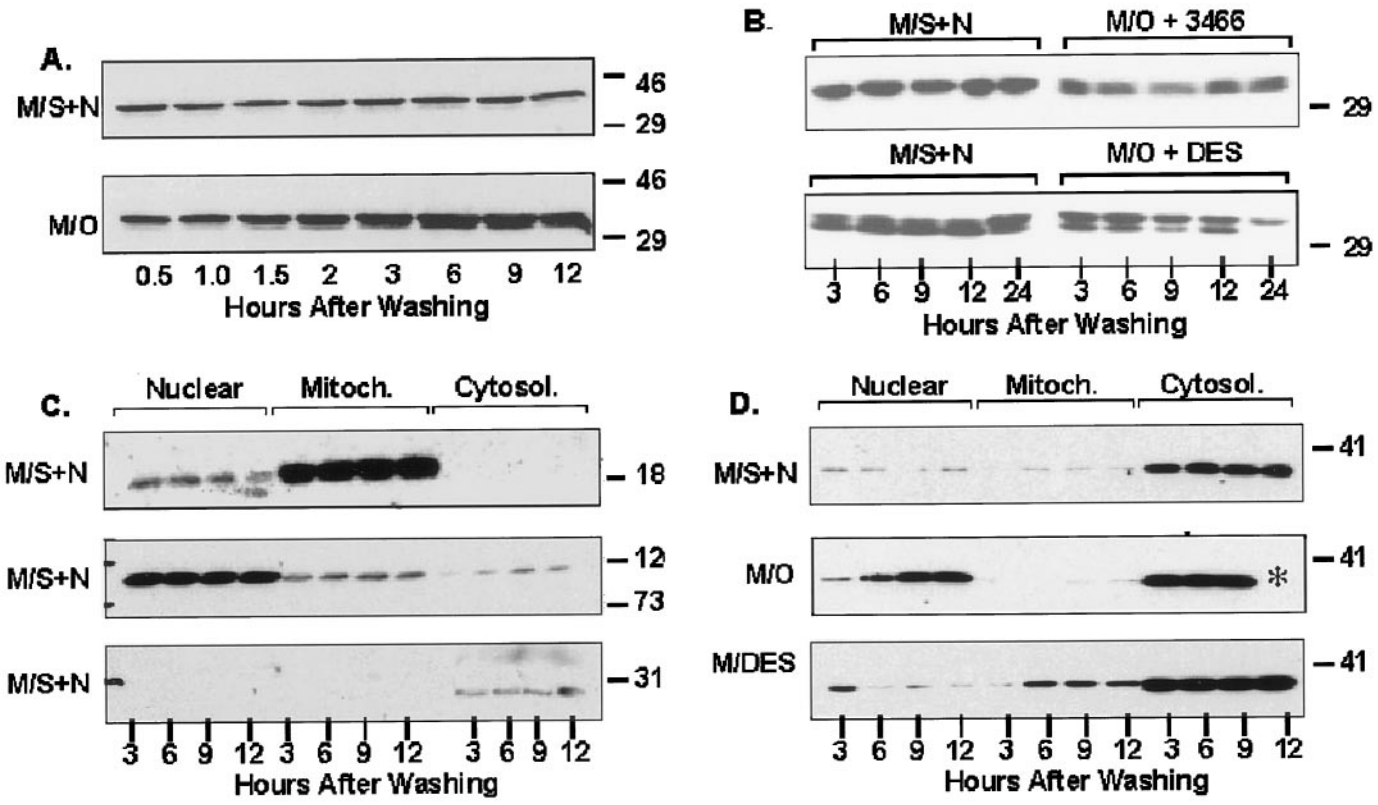

Fig. 4. GAPDH levels increase in PND-PC12 cells after serum and NGF withdrawal, and DES and CGP3466 prevent the increase. A, Western blot labeled M/S1 N for an experiment in which cells were washed and replaced in MEM with serum and NGF (top) as a control together with a blot for an experiment in which cells were washed and placed in MEM only (bottom) to induce apoptosis by trophic withdrawal. Note the relative increase in GAPDH immunodensity beginning at the 2-h band after washing for the trophically withdrawn cells but not the control cells. B, similar experiments to those in A but CGP3466 (top) or DES (bottom) at 10^{29} M was added to the MEM only. Note that the additions prevented increases in GAPDH levels. C, each panel from top to bottom shows immunodensity for the nuclear (Nuclear), mitochondrial (Mitoch.), and cytosolic (Cytosol.) subcellular fractions at 3, 6, 9, and 12 h after washing for nucleolin, cytochrome oxidase, and 14-3-3 *b*, respectively. Note that each of the protein immunoreactions is concentrated in a different subfraction. D, each panel shows Western blots for protein taken from the subcellular fractions at 3, 6, 9, and 12 h after washing and replacement into MEM with serum and NGF as a control (top) or placement into MEM only to induce apoptosis (middle). Note the progressive increase in nuclear GAPDH beginning between 3 and 6 h after washing and serum and NGF withdrawal together with the maintained increase in cytosolic GAPDH that was present at 3 to 9 h. Similar panels for experiments in which the cells were placed in MEM with 10^{29} M DES (bottom) after washing. Note that the DES prevents the progressive increase in GAPDH immunoreactivity in the nuclear subfraction. On all blots, identical amounts of total protein were loaded into each lane. *In the 12 h Cytosol. lane for the M/O panel, indicates that protein was not loaded onto that lane.

chondrial, and cytosolic fractions, respectively (see Fig. 4C for examples of the use of the three antibodies with protein subfractions taken from cells in M/S1 N). The blots indicated that GAPDH was largely concentrated in the cytosolic subfraction in control cells that were washed and then replaced into M/S1 N. GAPDH levels appeared to increase in the cytosolic subfraction after serum and NGF withdrawal and also progressively increased in the nuclear subfraction at each of the 3-, 6-, 9-, and 12-h time points. Treatment with 10^{29} M DES or CGP3466 largely prevented the increase in GAPDH immunoreaction for the nuclear fraction.

Recognizing that subcellular fractionation enriches the proportions of proteins localized in particular organelles but may not exclusively contain proteins from those organelles (see Fig. 4C), we also examined the subcellular distribution of GAPDH immunoreactivity using LCSM. The GAPDH immunocytochemistry combined with YOYO-1 staining for DNA showed that GAPDH was concentrated in the cytosol with only light punctate immunoreaction in the nuclei in control cells that were washed and then replaced in M/S1 N (see examples in Fig. 5, A1–A4). Serum and NGF withdrawal induced a dense increase in nuclear GAPDH immunoreaction, excluding the nucleolus (see examples in Fig. 5, B1–B4). The nuclear increase and subnuclear distribution were similar to those we demonstrated using a GAPDH-green fluorescent fusion protein in several other models of apoptosis (Shashidharan et al., 1999).

During the first 24 h after washing and replacement into medium with serum and NGF, about 2 to 3% of control cells showed baseline dense nuclear GAPDH immunoreactivity at all time points (Fig. 6C2), contrasting with those that were NGF and serum withdrawn, in which about 6% showed dense nuclear GAPDH immunoreactivity by 3 h, followed by a progressive increase to about 25% by 12 h. On average, the increase in nuclei with dense nuclear GAPDH immunoreaction preceded the increase in nuclei with chromatin condensation, as demonstrated by YOYO-1 staining by at least 3 h (compare Fig. 6, C1 and C2). Treatment with 10^{29} M DES or CGP3466 markedly reduced both the percentage of nuclei with chromatin condensation and those with dense GAPDH immunoreaction at all time points (Fig. 6, B1 and B2). Accordingly, Western blotting and LCSM immunocytochemistry indicated that both DES and CGP3466 reduce the increased levels of GAPDH and the nuclear accumulation of GAPDH that occurs early in apoptosis induced in PND-PC12 cells by serum and NGF withdrawal.

In an attempt to understand the basis for DES and CGP3466 prevention of increases in GAPDH levels and GAPDH nuclear accumulation, we first examined the effect of CGP3466 and DES on the glycolytic activity of GAPDH in vitro. The addition of 10^{29} M CGP3466 to GAPDH in solution by itself did not alter the extent or rate of NAD^1 conversion to NADH (Fig. 6A1). The Rossman fold region of GAPDH binds tRNA and AU-rich RNA, particularly AUUUA base sequences ((Nagy and Rigby, 1995; also see a computer model of RNA binding in the Rossman fold in Fig. 6 of Borden, 1998). We therefore added a synthetic RNA with repeated AUUUA sequences to the solution and found that the addition reduced the extent of NADH production by about 25% (Fig. 6A1). The addition of CGP3466 to the solution containing both GAPDH and the synthetic RNA resulted in almost complete recovery of the NADH production. Similar results were obtained with DES (not shown).

We then examined the conversion of NAD^1 to NADH in cell lysates after washing (Fig. 6A2). We chose a 6-h time point because GAPDH levels were markedly increased (Fig. 4A) but relatively few cells had entered the phase of nuclear degradation at that time (Fig. 5C1). Lysates from cells that had undergone serum and NGF withdrawal showed marked increases in both the extent and rate of NAD^1 to NADH conversion compared with control cells in M/S1 N. The addition of 10^{29} M DES to the withdrawn cells induced a partial reduction in the extent of NAD^1 to NADH conversion. Accordingly, these data suggest that the addition of DEP-like compounds can alter GAPDH glycolytic activity, possibly by altering the configuration of GAPDH or its interaction with AU-rich RNA.

Because binding of CGP3466 in the channel of tetrameric GAPDH might alter the interface between the substituent GAPDH monomers (Fig. 7A2), we used size exclusion chromatography to determine whether CGP3466 or DES affected the oligomeric form of the enzyme. The addition of 10^{29} M CGP3466 (or DES) to GAPDH in solution altered a major proportion of the protein from a size equivalence of 148 kDa to 74 kDa (Fig. 6B1, see size exclusion calibration scale below Fig. 6B3), consistent with a change from a tetrameric form to a dimeric form. Similarly, the addition of poly(U) RNA to GAPDH in solution shifted the peak to a size equivalence of more than 200 kDa, and the addition of CGP3466 (or DES) induced size equivalence changes indicative of the freeing of tetrameric GAPDH from the RNA and its conversion to a dimeric form (Fig. 6B2). GAPDH was placed in SDS to convert it to a monomer. The addition of CGP3466 or DES to the solution containing SDS induced a shift in the size equivalence of the major peak, suggesting a change in the configuration of the monomeric form, and converted a small proportion of the protein to a size equivalence consistent with a dimer (Fig. 6B3).

Discussion

The serum and NGF-withdrawn PND-PC12 cells showed increases in GAPDH levels and nuclear GAPDH accumulation that were similar to those reported for other apoptosis models (Sunaga et al., 1995; Ishitani et al., 1996, 1997, 1998; Saunders et al., 1997; Sawa et al., 1997; Shashidharan et al., 1999). Most importantly, CGP3466 and DES prevented both the increases in GAPDH and the nuclear accumulation. Transcriptional or translational inhibitors can reduce the increase in GAPDH levels in early apoptosis (Ishitani et al., 1997), suggesting that newly synthesized GAPDH contributes to the protein's role in apoptosis. The signaling pathways that lead to increased GAPDH levels in early apoptosis are not known. p53 overexpression induces apoptosis that is associated with downstream increases in expression of a large number of genes, including GAPDH (Polyak et al., 1997). Accordingly, a p53-dependent signaling pathway may contribute to GAPDH-associated apoptosis. Our recent studies using the expression of GAPDH/green fluorescent fusion protein have shown accumulation of the fusion protein in the nuclei of a variety of cell types in early apoptosis (Shashidharan et al., 1999). The accumulation of the fusion protein was similar to that shown in the serum and NGF-withdrawn PND-PC12 cells in the present study and pro-

vided evidence that at least part of the GAPDH that accumulates in the nucleus was previously resident in the cytoplasm and was not newly synthesized.

This study, similar to our previous studies (Tatton et al., 1994; Wadia et al., 1998), showed that apoptotic nuclear degradation begins in the PND-PC12 cells at about 6 h after serum and NGF withdrawal and is maximal at 12 to 18 h. Therefore, the increases in GAPDH levels and GAPDH nuclear accumulation are early events in this form of apoptosis and precedes the onset of nuclear degradation by 3 or more hours. Hence, the participation of GAPDH in the apoptotic cascade seems to be well upstream from the events that mediate apoptotic degradation.

DES is a relatively poor MAO-B inhibitor compared with DEP (Heinonen et al., 1997), and CGP3466 does not inhibit MAO-B (Kragten et al., 1998). Decreases in apoptosis with

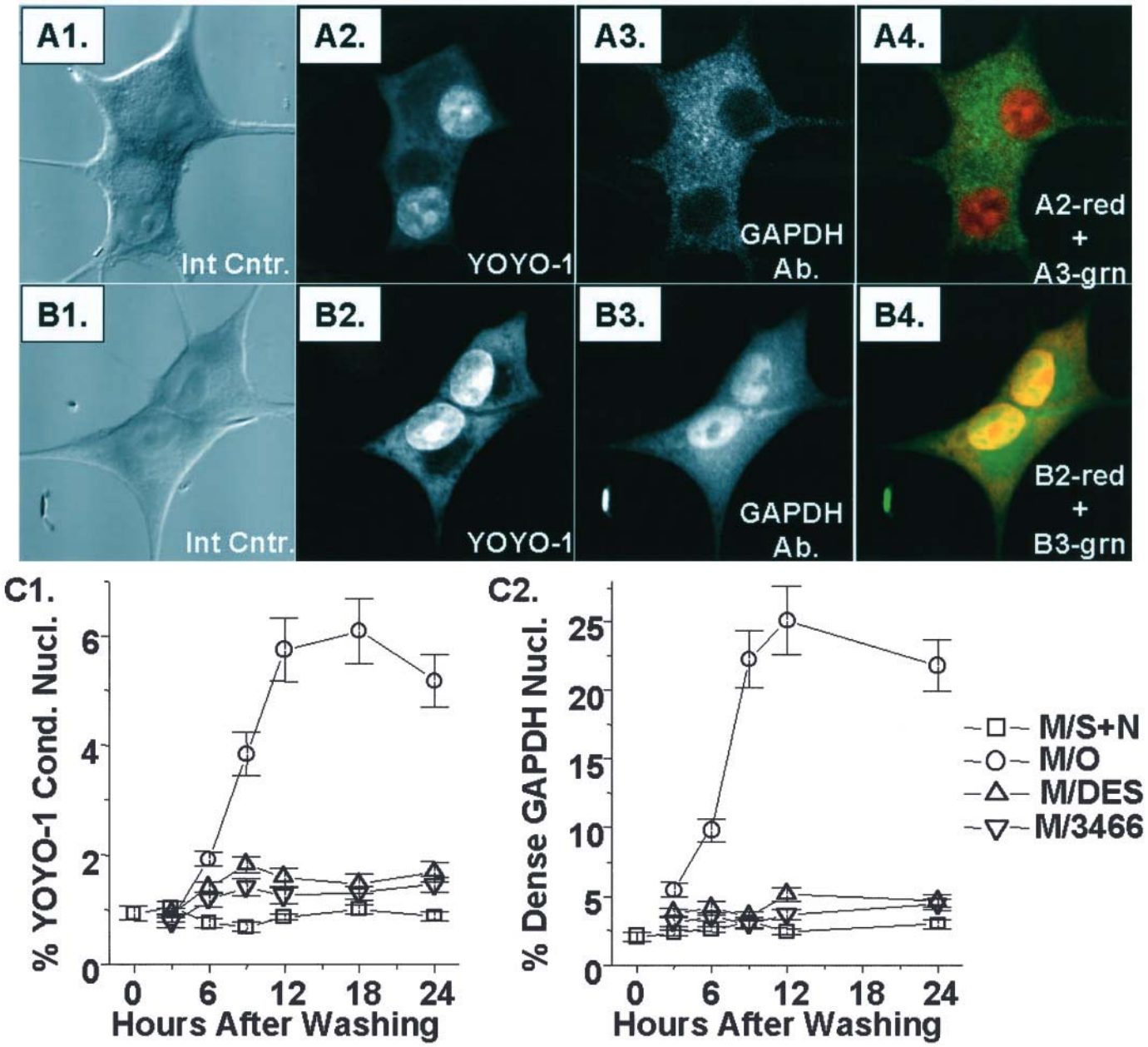

Fig. 5. GAPDH immunoreactivity in PND-PC12 cells after serum and NGF withdrawal visualized with LCSM. A1–A4, LCSM micrographs from identical image fields consist of an interference contrast micrograph, fluorescence micrograph for YOYO-1 DNA binding, immunoctrochemistry for GAPDH, and a combined image in which A2 (recolored red) and A3 (recolored green) were digitally added. The cells were washed and then replaced in MS1 N as a control (example at 6 h after washing). The maintained separation of the red and green color in A4 shows that GAPDH is largely extranuclear in location. B1–B4, an identical series of LCSM micrographs for cells that were washed and placed in MO to induce apoptosis by serum and NGF withdrawal showed dense GAPDH immunoreaction in the nucleus that spared the nucleolus (example at 6 h after washing). The orange-yellow color in B4 shows the colocalization of DNA YOYO-1 binding and GAPDH immunoreaction and illustrates typical dense nuclear GAPDH accumulation. C1 and C2, counts of cells with nuclei showing YOYO-1-stained chromatin condensation, and those with dense GAPDH nuclear immunoreaction, respectively, show that the percentages of nuclei with GAPDH nuclear accumulation was significantly increased by 3 h after washing, whereas the percentages with apoptotic chromatin condensation did not begin to increase until 6 h after washing and placement in MEM only. DES (plots labeled M/DES) and CGP3466 (plots labeled M/3466) at 10^{29} M markedly decreased the percentage of nuclei with chromatin condensation and those with dense GAPDH nuclear immunoreaction.

DEP or DES can be obtained at concentrations or dosages that do not inhibit MAO-A or MAO-B (Ansari et al., 1993; Tatton and Chalmers-Redman, 1996; Le et al., 1997). In this study, concentrations of DEP and DES ranging from 10^{25} to 10^{213} M showed similar capacities to increase survival, whereas CGP3466 induced greater levels of survival, particularly at concentrations of less than 10^{29} M. Cytochrome P-450 inhibitors block the capacity of DEP, but not DES, to reduce apoptosis in a variety of apoptosis models (W. G. Tatton and R. M. Chalmers-Redman, unpublished observations). Accordingly, the antiapoptotic capacity of DEP appears to depend on its metabolism to DES.

Based on our results with photoaffinity CGP3466 and the BL-labeled compounds, it is likely that CGP3466 and DES bind to GAPDH in the PND-PC12 cells in a similar manner to that shown for rat hippocampus (Kragten et al., 1998). Our antibody studies suggest that the binding may occur in or near to the channel of GAPDH tetramer. Size exclusion data indicate that a portion of GAPDH converts to a dimer in the presence of CGP3466 or DES. There are three possible dimers that could be produced (Fig. 7, D1–D3): 1) the channel could be bisected lengthwise, resulting in a loss of the channel but retaining the RNA binding site in the Rossman fold; 2) the channel is bisected across its width, resulting in a dimer with a channel but no RNA binding site; and 3) the channel is cut across its width so that two diagonally associated monomers form the dimer. At this time, we do not have data to predict which of these dimer forms predominate. DEP that has not been metabolized to DES may not bind to GAPDH. Studies using photoaffinity-labeled DEP in the presence of cytochrome P-450 inhibitors will be required to determine whether DEP itself can bind to GAPDH.

CGP3466 differs from DES in the replacement of the single phenol ring with three rings, the center of which includes an oxygen. In BL-CGP3466 and BL-DES, the BODIPY was attached to the ring portions of the compounds through a flexible link (Zimmermann et al., 1998). We showed that both BL compounds retain most of their capacity to reduce apoptosis in the serum and NGF-withdrawn PND PC12 cells. Furthermore, even with the attachment of the relatively bulky BODIPY moiety, BL-CGP3466 accumulated in the cells with a subcellular distribution similar to those found for GAPDH immunoreactivity. Our modeling suggests that the bulky BODIPY moiety should not interfere with binding in the channel. BL-CGP3466 entry to the subcellular sites could be blocked by preincubation with higher concentrations of

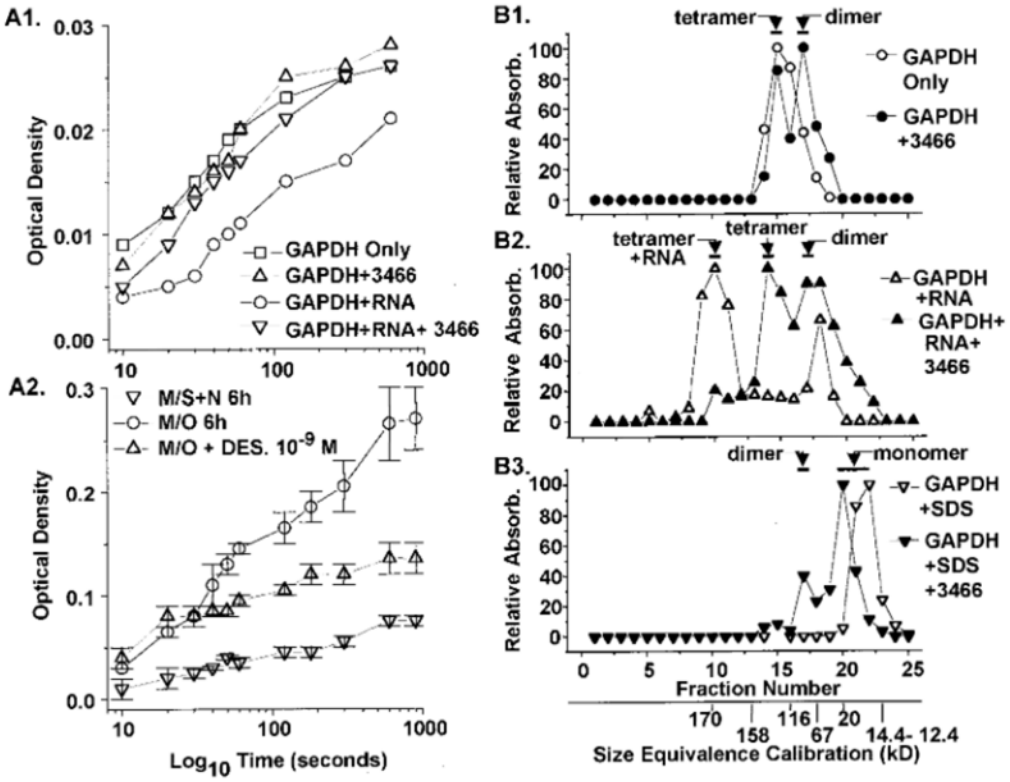

Fig. 6. Effects of CGP3466 on the glycolytic capacity of GAPDH in vitro and in vivo and evidence for the conversion of GAPDH to a dimer by CGP3466. A1, NADH production from NAD^1 over time was measured in an in vitro system. The addition of CGP3466 does not significantly alter enzymatic activity of GAPDH, whereas the addition of AUUUA synthetic RNA sequences had little effect on the rate but reduced extent of the glycolytic activity of GAPDH. The addition of 10^{29} M CGP3466 induced a recovery of glycolytic activity, suggesting that the compound altered the relationship between GAPDH and RNA. A2, measurement of NAD^1 to NADH conversion in lysates taken at 6 h after washing from control cells (M/S1 N 6 h), cells after NGF and serum withdrawal (M/O 6 h)m and cells after serum and NGF withdrawal treated with 10^{29} M DES (M/O1 DES 6 h). B1–B3, size exclusion chromatography for GAPDH in solution alone, with poly(U) RNA, or with detergent. B1. GAPDH alone in solution forms a tetramer with a size equivalence of 148 kDa in fraction 14. In the presence of 10^{29} M CGP3466, more than half of GAPDH appears as a dimer in fraction 17 with a size equivalence of 74 kDa. B2, GAPDH binds to poly(U) RNA. The peak at fraction 10, which indicates a size equivalence of more than 170 kDa, indicates an amalgam of RNA and GAPDH. Fraction 10 was also shown to include RNA by the finding of a peak at 260 nm on the spectrophotometer. In the presence of 10^{29} M CGP3466, the shifts in the equivalence values of the peaks indicate that GAPDH has separated from RNA and that there is a large increase in GAPDH dimer. B3, in the presence of 0.1% SDS, GAPDH alone is found in fraction 23 with a size equivalence consistent with a monomer. After the addition of 10^{29} M CGP3466, a small proportion of GAPDH shows a size equivalence consistent with a dimer, even in the presence of the detergent.

unlabeled CGP3466, which indicated the specificity of the BL compounds for CGP3466 binding sites. This is the first report of the use of a fluorescently labeled compound with LCSM to examine the subcellular localization and the binding specificity of a compound in living or fixed cells.

GAPDH largely exists as a tetramer with minor populations of dimers and monomers. Our data indicate that CGP3466 and DES increase the stability of GAPDH as a dimer. We therefore propose that agents that stabilize GAPDH as a dimer, rather than a tetramer, prevent the early apoptotic GAPDH increase and nuclear accumulation and thereby induces a decrease in apoptosis. If GAPDH dimer cannot accumulate in the nucleus, it would explain part of our results. It is more difficult to understand how the presence of GAPDH dimer would prevent GAPDH up-regulation. The increased expression may depend on nuclear accumulation of constitutive protein. Our findings indicating a tetrameric/dimeric conversion were obtained in vitro, and it is therefore possible that GAPDH dimerization does not occur in vivo in response to DES or CGP3466 binding. In vivo, the binding of the DEP-related compounds to GAPDH might result in a more subtle change in GAPDH structure. If, as we have hypothesized, the conversion of GAPDH to a dimer robs the protein of its capacity to participate in apoptosis, the DEP-related compounds will be the first compounds shown to reduce cell death by altering oligomerization.

In vitro, the DEP-like compound binding results in stabilization of the dimer, increases the catalysis of glycolytic activity by GAPDH, and decreases GAPDH affinity for RNA. These effects are likely interrelated. The glycolytic action and RNA binding of GAPDH occur in the same region of the protein. Conversion of GAPDH from a tetramer to a dimer is known to increase its glycolytic capacity (Minton and Wilf, 1981). Dimerization of GAPDH, together with a freeing of GAPDH from AUUUA RNA, could explain the facilitation of glycolysis by CGP3466 and DES in vitro.

This is the first study to show increased glycolytic activity in cells entering apoptosis. The increase may result from the increase in GAPDH levels associated with apoptosis in the PND-PC12 cells. It also could result, in part, from freeing of the Rossman fold region of the protein from AUUUA-rich RNA binding with consequent increased availability of the fold for NAD^1 to NADH conversion. The relative decrease in glycolysis induced by the DEP-like compounds likely reflects their capacity to reduce or prevent the increase in GAPDH levels that we found in early apoptosis.

The DEP-related compounds appear to reduce the apoptotic function of GAPDH while at the same time facilitating or maintaining the glycolytic function of protein at levels that exceed those in control cells but are reduced compared with those in apoptotic cells. GAPDH is a multifunction protein and participates in functions like tubulin polymerization, endocytosis, translational control of gene expression, nuclear tRNA export, DNA replication, and DNA repair (see Sirover,

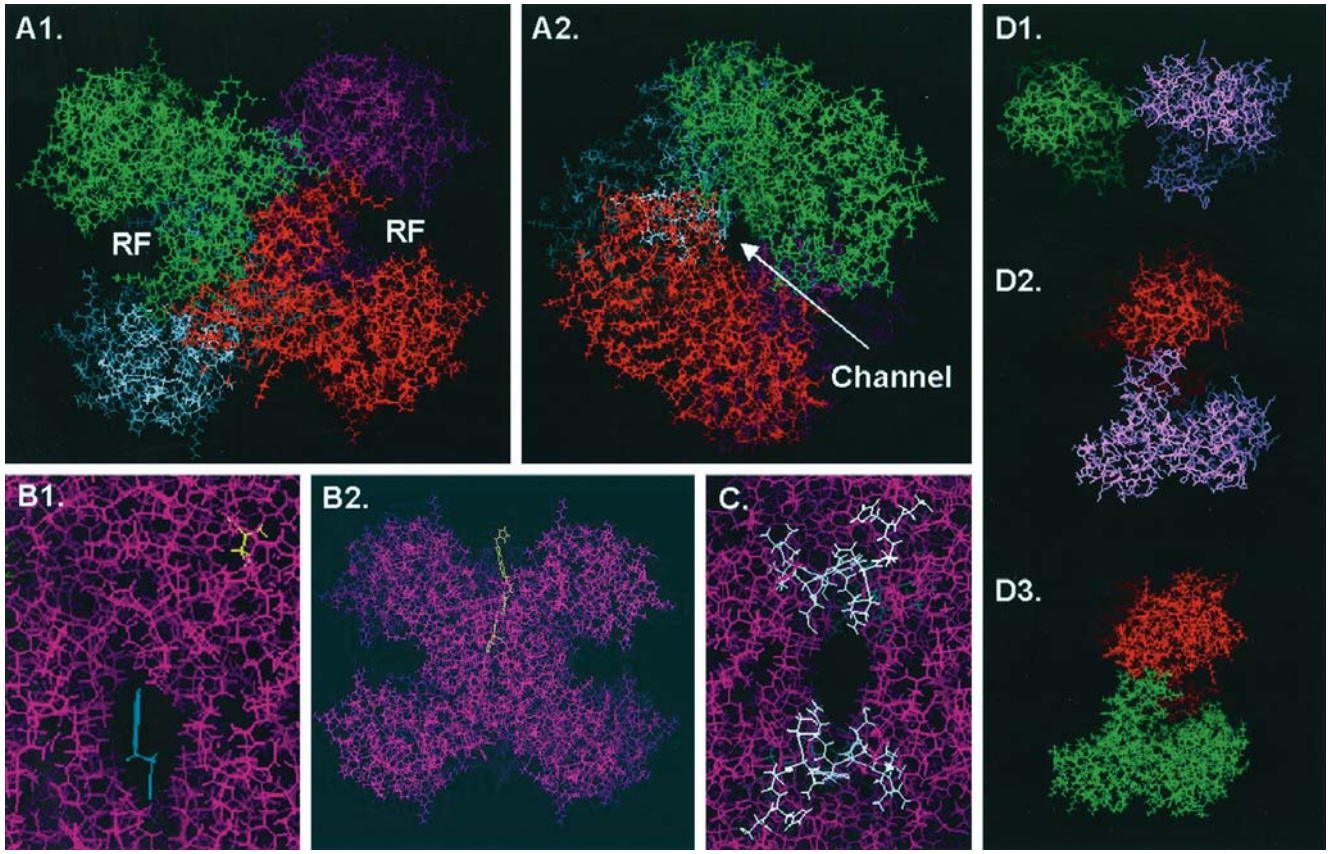

Fig. 7. Models of the rat GAPDH tetramer showing the putative DEP-like compound binding channel. A1, the four identical monomers which make up the GAPDH tetramer are shown in different colors. The NAD^1 binding site, the Rossmann fold, is indicated by RF. A2, a 90-degree rotation of the image in A1. The putative DEP-like compound binding channel is indicated where the four monomers join. B1, CGP3466 (blue) is shown in the channel. B2, a view of CGP3466-BODIPY (yellow) located in the channel. C, residues in white indicate the epitope site for the sheep polyclonal antibody, which reduced the cellular accumulation of BL-CGP3466. D1–D3, the three possible dimers of GAPDH that might be formed by the binding of DEP-like compounds. All images were produced in Insight (Biosym).

1997). It will be interesting to determine which of those functions are maintained and which are altered by the binding of DEP-related compounds.

In normal nuclei, GAPDH binds to promyelocytic leukemia (PML) protein in an RNA-dependent fashion (Carlile et al., 1998). PML localizes to PML nuclear bodies, which have been implicated in apoptosis, suppression of oncogenic transformation and growth suppression (Melnick and Licht, 1999). PML and the other protein components of PML nuclear bodies appear to function in regulation of both transcription and translation (Borden et al., 1998). Nuclear GAPDH could therefore contribute to apoptosis by modifying either transcription (Ronai, 1993) or translation (Sioud and Jespersen, 1996), perhaps mediated through an interaction with PML.

Finally, DEP-related compounds have been shown to reduce neuronal and non-neuronal death in a wide variety of models, many of which are independent of MAO-B inhibition (Tatton and Chalmers-Redman, 1996). The basis for clinical slowing of the progression of PD (Parkinson's Study Group, 1993; Olanow et al., 1995) and the preliminary indications of improvement in HD with DEP treatment (Patel et al., 1996) are unknown and have been variously suggested to result from slowed neuronal death (Olanow et al., 1995), improved dopaminergic transmission or increased dopamine levels (Schulzer et al., 1992), and the actions of the DEP metabolites (2)-amphetamine and (2)-methamphetamine (Karoum et al., 1982). If GAPDH contributes to a reduction in neuronal death in PD, the clinical benefits of DEP treatment may result, in part, from the action of DES on GAPDH rather than on MAO-B.

Acknowledgments

CGP3466, photoaffinity-labeled CGP3466, BL-CGP3466, and BL-DES were provided by Novartis (Basel, Switzerland). Dr. J. Casals contributed to the preparation of the manuscript.

References

Ansari KS, Yu PH, Kruck TP and Tatton WG. (1993) Rescue of axotomized immature rat facial motoneurons by R(2)-deprenyl: Stereospecificity and independence from monoamine oxidase inhibition. J Neurosci 13:4042–4053.
Borden KL (1998) Structure/function in neuroprotection and apoptosis. Ann Neurol 44:S65–S71.
Borden KL, Campbell Dwyer EJ, Carlile GW, Djavani M and Salvato MS (1998) Two ring finger proteins, the ocoprotein PMB and the arenavirus protein Z associate with the ribosomal P-proteins. J Virol 72:3819–3826.
Burke JR, Enghild JJ, Martin ME, Jou YS, Myers RM, Roses AD, Vance JM and Strittmatter WJ (1996) Huntington and DRPLA proteins selectively interact with the enzyme GAPDH. Nat Med 2:347–350.
Carlile GW, Tatton WG and Borden KLB (1998) Demonstration of a RNA-dependent nuclear interaction between the promelocytic leukaemia protein and glyceraldehyde-3-phosphate dehydrogenase. Biochem J 335:691–696.
Cotman CW (1998) Apoptosis decision cascades and neuronal degeneration in Alzheimer's disease. Neurobiol Aging 19:S29–S32.
Fahn S (1996) Controversies in the therapy of Parkinson's disease. Adv Neurol 69:477–486.
Heinonen EH, Anttila MI, Karnani HL, Nyman LM, Vuorinen JA, Pyykko KA and Lammintausta RA (1997) Desmethylselegiline, a metabolite of selegiline, is an irreversible inhibitor of monoamine oxidase type B in humans. J Clin Pharmacol 37:602–509.
Ishitani R, Sunaga K, Hirano A, Saunders P, Katsube N and Chuang DM (1996) Evidence that glyceraldehyde-3-phosphate dehydrogenase is involved in age-induced apoptosis in mature cerebellar neurons in culture. J Neurochem 66:928–935.
Ishitani R, Sunaga K, Tanaka M, Aishita H and Chuang DM (1997) Overexpression of glyceraldehyde-3-phosphate dehydrogenase is involved in low K^+-induced apoptosis but not necrosis of cultured cerebellar granule cells. Mol Pharmacol 51:542–550.
Ishitani R, Tanaka M, Sunaga K, Katsube N and Chuang DM (1998) Nuclear localization of overexpressed glyceraldehyde-3-phosphate dehydrogenase in cultured cerebellar neurons undergoing apoptosis. Mol Pharmacol 53:701–707.
Karoum F, Chuang LW, Eisler T, Calne DB, Liebowitz MR, Quitkin FM, Klein DF and Wyatt RJ (1982) Metabolism of (2) deprenyl to amphetamine and methamphetamine may be responsible for deprenyl's therapeutic benefit: A biochemical assessment. Neurology 32:503–509.
Kim H, Feil IK, Verlinde CL, Petra PH and Hol WG (1995) Crystal structure of glycosomal glyceraldehyde-3-phosphate dehydrogenase from Leishmania mexicana: Implications for structure-based drug design and a new position for the inorganic phosphate binding site. Biochemistry 34:14975–14986.
Kish SJ, Lopes-Cendes I, Guttman M, Furukawa Y, Pandolfo M, Rouleau GA, Ross BM, Nance M, Schut L, Ang L and DiStefano L (1998) Brain glyceraldehyde-3-phosphate dehydrogenase activity in human trinucleotide repeat disorders. Arch Neurol 55:1299–1304.
Kragten E, Lalande I, Zimmermann K, Roggo S, Schindler P, Muller D, van Oostrum J, Waldmeier P and Furst P (1998) Glyceraldehyde-3-phosphate dehydrogenase, the putative target of the antiapoptotic compounds CGP 3466 and R-(2)-deprenyl. J Biol Chem 273:5821–5828.
Le W, Jankovic J, Xie W, Kong R and Appel SH (1997) (2)-Deprenyl protection of 1-methyl-4 phenylpyridium ion (MPP1)-induced apoptosis independent of MAO-B inhibition. Neurosci Lett 224:197–200.
Magyar K, Szende B, Lengyel J, Tarczali J and Szatmary I (1998) The neuroprotective and neuronal rescue effects of (2)-deprenyl. J Neural Transm Suppl 52:109–123.
Maruyama W, Takahashi T and Naoi M (1998) (2)-Deprenyl protects human dopaminergic neuroblastoma SH-SY5Y cells from apoptosis induced by peroxynitrite and nitric oxide. J Neurochem 70:2510–2515.
Melnick A and Licht JD (1999) Deconstructing a disease: RARalpha, its fusion partners, and their roles in the pathogenesis of acute promyelocytic leukemia. Blood 93:3167–3215.
Minton AP and Wilf J (1981) Effect of macromolecular crowding upon the structure and function of an enzyme: Glyceraldehyde-3-phosphate dehydrogenase. Biochemistry 20:4821–4826.
Nagy E and Rigby WF (1995) Glyceraldehyde-3-phosphate dehydrogenase selectively binds AU-rich RNA in the NAD(1)-binding region (Rossmann fold). J Biol Chem 270:2755–2763.
Olanow CW, Hauser RA, Gauger L, Malapira T, Koller W, Hubble J, Bushenbark K, Lilienfeld D and Esterlitz J (1995) The effect of deprenyl and levodopa on the progression of Parkinson's disease. Ann Neurol 38:771–777.
Parkinson's Study Group (1993) Effects of tocopherol and deprenyl on the progression of disability in early Parkinson's disease. N Engl J Med 328:176–183.
Patel SV, Tariot PN and Asnis J (1996) L-Deprenyl augmentation of fluoxetine in a patient with Huntington's disease. Ann Clin Psychiatry 8:23–26.
Paterson IA, Barber AJ, Gelowitz DL and Voll C (1997) (2)Deprenyl reduces delayed neuronal death of hippocampal pyramidal cells. Neurosci Biobehav Rev 21:181–186.
Paterson IA, Zhang D, Warrington RC and Boulton AA (1998) R-Deprenyl and R-2-heptyl-N-methylpropargylamine prevent apoptosis in cerebellar granule neurons induced by cytosine arabinoside but not low extracellular potassium. J Neurochem 70:515–523.
Petersen A, Mani K and Brundin P (1999) Recent advances on the pathogenesis of Huntington's disease. Exp Neurol 157:1–18.
Polyak K, Xia Y, Zweier JL, Kinzler KW and Vogelstein B (1997) A model for p53-induced apoptosis [see comments]. Nature (Lond) 389:300–305.
Ronai Z (1993) Glycolytic enzymes as DNA binding proteins. Int J Biochem 25:1073–1076.
Saunders PA, Chalecka-Franaszek E and Chuang DM (1997) Subcellular distribution of glyceraldehyde-3-phosphate dehydrogenase in cerebellar granule cells undergoing cytosine arabinoside-induced apoptosis. J Neurochem 69:1820–1828.
Sawa A, Khan AA, Hester LD and Snyder SH (1997) Glyceraldehyde-3-phosphate dehydrogenase: Nuclear translocation participates in neuronal and nonneuronal cell death. Proc Nat Acad Sci USA 94:11669–11674.
Schulzer M, Mak E and Calne DB (1992) The antiparkinson efficacy of deprenyl derives from transient improvement that is likely to be symptomatic [see comments]. Ann Neurol 32:795–798.
Shashidharan P, Chalmers-Redman RM, Carlile GW, Rodic V, Gurvich N, Yuen T, Tatton WG and Sealfon SC (1999) Nuclear translocation of GAPDH-GFP fusion protein during apoptosis. Neuroreport 10:1149–1153.
Sioud M and Jespersen L (1996) Enhancement of hammerhead ribozyme catalysis by glyceraldehyde-3- phosphate dehydrogenase. J Mol Biol 257:775–789.
Sirover MA (1997) Role of the glycolytic protein, glyceraldehyde-3-phosphate dehydrogenase, in normal cell function and in cell pathology. J Cell Biochem 66:133–140.
Sunaga K, Takahashi H, Chuang DM and Ishitani R (1995) Glyceraldehyde-3-phosphate dehydrogenase is over-expressed during apoptotic death of neuronal cultures and is recognized by a monoclonal antibody against amyloid plaques from Alzheimer's brain. Neurosci Lett 200:133–136.
Tatton NA, Maclean-Fraser A, Tatton WG, Perl DP and Olanow CW (1998) A fluorescent double-labeling method to detect and confirm apoptotic nuclei in Parkinson's disease. Ann Neurol 44:S142–S148.
Tatton WG and Chalmers-Redman RM (1996) Modulation of gene expression rather than monoamine oxidase inhibition: (2)-Deprenyl-related compounds in controling neurodegeneration. Neurology 47:S171–S183.
Tatton WG, Ju WY, Holland DP, Tai C and Kwan M (1994) (2)-Deprenyl reduces PC12 cell apoptosis by inducing new protein synthesis. J Neurochem 63:1572–1575.
Wadia JS, Chalmers-Redman RME, Ju WJH, Carlile GW, Phillips JL, Fraser AD and Tatton WG (1998) Mitochondrial membrane potential and nuclear changes in apoptosis caused by serum and nerve growth factor withdrawal: Time course and modification by (2)-deprenyl. J Neurosci 18:932–947.
Zimmermann K, Roggo S, Kragten E, Furst P and Waldmeier P (1998) Synthesis of tools for target identification of the anti-apoptotic compound CGP 3466: Part I. Bioorg Med Chem Let 8:1195–1200.

Send reprint requests to: Dr. William G. Tatton, Department of Neurology, Annenberg 14-70, Mount Sinai Medical Center, One Gustave L. Levy Place, New York, NY 10029. E-mail: william_tatton@smtplink.mssm.edu

0022-3565/02/3012-753–764$7.00
THE JOURNAL OF PHARMACOLOGY AND EXPERIMENTAL THERAPEUTICS
JPET 301:753–764, 2002

Vol. 301, No. 2
4061/981641
Printed in U.S.A.

Propargylamines Induce Antiapoptotic New Protein Synthesis in Serum- and Nerve Growth Factor (NGF)-Withdrawn, NGF-Differentiated PC-12 Cells

W. G. TATTON, R. M. E. CHALMERS-REDMAN, W. J. H. JU, M. MAMMEN, G. W. CARLILE, A. W. PONG, and N. A. TATTON

Department of Neurology, Mount Sinai School of Medicine, New York, New York

Received April 19, 2001; accepted January 24, 2002 This article is available online at http://jpet.aspetjournals.org

ABSTRACT

(□)-Deprenyl and structurally related propargylamines increase neuronal survival independently of monoamine oxidase B (MAO-B) inhibition, in part by decreasing apoptosis. We found that deprenyl and two other propargylamines, one of which does not inhibit monoamine oxidase B, increased survival in trophically withdrawn 6-day nerve growth factor (NGF)- and 9-day NGF-differentiated PC-12 cells but not in NGF naive or 3-day NGF-differentiated PC-12 cells. Four days of prior NGF exposure were required for the propargylamine-mediated antiapoptosis. Studies using actinomycin D, cycloheximide, and camptothecin revealed that the maintenance of both transcription and translation, particularly between 2 and 6 h after trophic withdrawal, was required for propargylamine-mediated antiapoptosis. Metabolic labeling of newly synthesized proteins for two-dimensional protein gel autoradiography and scintillation counting showed that the propargylamines either increased or reduced the levels of new synthesis or induced de novo synthesis of a number of different proteins, most notably proteins in the mitochondrial and nuclear subfractions. Western blotting for whole cell or subcellular fraction lysates showed that the timing of new protein synthesis changes or subcellular redistribution of apoptosis-related proteins induced by the propargylamines were appropriate to antiapoptosis. The apoptosis-related proteins included superoxide dismutases (SOD1 and SOD2), glutathione peroxidase, c-JUN, and glyceraldehyde-3-phosphate dehydrogenase. Most notable were the prevention of apoptotic decreases in BCL-2 levels and increases in mitochondrial BAX levels. In general, (□)-deprenyl-related propargylamines appear to reduce apoptosis by altering the levels or subcellular localization of proteins that affect mitochondrial membrane permeability, scavenge oxidative radicals, or participate in specific apoptosis signaling pathways.

The propargylamine (□)-deprenyl (DEP) inhibits monoamine oxidase B (MAO-B). DEP was first shown to reduce the death of primate nigrostriatal dopaminergic neurons exposed to 1-methyl-4-phenyl-1,2,3,6-tetrahydropyridine (MPTP) (Cohen et al., 1984) and to slow the clinical progress of human Parkinson's disease (Parkinson, 1993). Both actions appeared to depend on MAO-B inhibition. Subsequently, DEP and deprenyl-related propargylamines (DRPs) were demonstrated to reduce neuronal loss independently of MAO-B inhibition in a variety of experimental models including cortical catecholaminergic neurons exposed to N-(-2-chloroethyl)-N-ethyl-2-bromobenzylamine, murine or primate substantia nigra dopaminergic neurons exposed to MPTP, rat facial motoneurons after axotomy, dopaminergic cells treated with the 1-methyl-4-phenylpyridinium ion (MPP□) or nitric oxide, and hippocampal neurons exposed to kainate (see Tatton et al., 2000 for details and references). The MAO-B-independent increases in neuronal survival by DRPs were shown to involve decreased apoptosis in a number of the above models (e.g., kainate-exposed hippocampal neurons, nitric oxide, or MPP□-treated dopaminergic cells). DRP antiapoptosis also has been found in other models including partially NGF-differentiated PC-12 cells after serum and NGF withdrawal, rat hippocampal neurons after ischemia/hypoxia, neuroblastoma cells treated with rotenone, rat cerebellar granule neurons exposed to cytosine arabinoside, serum-deprived human

This research was supported by a grant from the Lowenstein Foundation and U.S. Army Grant PSA280. Novartis Pharmaceuticals provided CGP 3466, and RetinaPharma International provided (□)-desmethyldeprenyl.

ABBREVIATIONS: DEP, (□)-deprenyl; □□$_M$, mitochondrial membrane potential; DES, (□)-desmethyldeprenyl; DRP, (□)-deprenyl-related propargylamine; GAPDH, glyceraldehyde-3-phosphate dehydrogenase; HBSS, Hanks' balanced salt solution; JNK, c-Jun N-terminal kinase; MAO-B, monoamine oxidase B; MAP-2, microtubule-associated protein 2; NGF, nerve growth factor; MEM, minimum essential medium; mfMEM, methionine-free MEM; M/O, MEM only; MPTP, 1-methyl-4-phenyl-1,2,3,6-tetrahydropyridine; M/S, MEM with serum only; M/S□N, MEM with serum and NGF; MPP□, 1-methyl-4-phenylpyridinium ion; PBS, phosphate-buffered saline; acetyl-DEVD aldehyde, Ac-Asp-Glu-Val-Asp-CH; SOD1, anti-CuZn superoxide dismutase; SOD2, Mn superoxide dismutase; zVAD-fmk, N-benzyloxycarbonyl-Val-Ala-Asp-fluoromethylketone; 2D, two-dimensional; MOPS, 4-morpholinepropanesulfonic acid.

melanoma cells, rat retinal neurons after hypoxia, ischemia, or serum withdrawal, and rat hippocampal neurons, cerebellar neurons, or neuroblastoma cells exposed to okadaic acid (see Tatton et al., 2000 for details and references). Notably, DRPs do not reduce all forms of apoptosis as has been shown in NGF-naive PC-12 cells (Vaglini et al., 1996), thymocytes treated with dexamethasone (Fang et al., 1995), and cerebellar granule neurons exposed to low-media K□ levels (Paterson et al., 1998).

The mechanisms of DRP antiapoptosis are not known. DRPs bind to glyceraldehyde-3-phosphate dehydrogenase (GAPDH) (Kragten et al., 1998; Carlile et al., 2000) and prevents the GAPDH up-regulation essential to some forms of neuronal apoptosis (see Tatton et al., 2000 for a review). Whether or how DRP binding to GAPDH results in decreased apoptosis is not known. DRP antiapoptosis can require new protein synthesis (Tatton et al., 1994). In keeping with a protein synthesis-dependent mechanism, DEP has been shown to alter the levels, message expression, or activity of a variety of different proteins, each in a different cell type (see Tatton et al., 2000 for references and details). Although some of the protein alterations may contribute to antiapoptosis, the extent of DRP-induced antiapoptotic protein synthesis is not known nor whether any protein synthesis changes are appropriately timed to interrupt apoptosis signaling. DRPs can prevent mitochondrial membrane potential ($\Delta\Psi_M$) dissipation in some forms of apoptosis in which $\Delta\Psi_M$ dissipation results from increases in mitochondrial membrane permeability (Paterson et al., 1998; Wadia et al., 1998; Zhang et al., 1999). In some forms of apoptosis, increases in mitochondrial membrane permeability allow the release of mitochondrial factors that signal for apoptotic degradation (Jacotot et al., 1999). Accordingly, DRPs may alter the synthesis of proteins that influence mitochondrial membrane permeability.

We therefore examined the effects of three DRPs, DEP and desmethyldeprenyl (DES), both of which inhibit MAO-B, and 10-(N-methyl-N-propargyl-amino)methyldibenz[b,f]oxepine (CGP 3466), which does not inhibit MAO-B (see Waldmeier et al., 2000 for a review of CGP 3466) in trophically withdrawn PC-12 cells that were previously exposed to NGF for varying periods. We found that the DRPs reduced apoptosis in PC-12 cells exposed to NGF for 4 days or more but not in NGF-naive PC-12 cells. The decreased apoptosis required new protein synthesis and involved alterations in the expression of a number of proteins. Proteins in the mitochondrial and nuclear fractions were most markedly involved, including proteins known to scavenge oxidative radicals and those that can alter mitochondrial membrane permeability. The time course of the changes in expression was appropriate to antiapoptosis.

Materials and Methods

Cell Culture, Treatment, and Counting. PC-12 cells (American Type Culture Collection, Manassas, VA) were propagated in minimum essential medium (MEM) containing 10% horse serum, 5% fetal bovine serum, 2 mM L-glutamine, 50 units/ml penicillin, and 50 □g/ml streptomycin (M/S, MEM with serum), all purchased from Invitrogen (Carlsbad, CA). The cells were grown on 24-well plates (8×10^4 cells/well) for counting of intact nuclei as an estimate of survival, poly-L-lysine-treated coverslips (1×10^4 cells/coverslip) for imaging with laser confocal scanning microscopy, or 100-mm dishes (1×10^6 cells/plate) for protein chemistry. The cells were differentiated for up to 9 days in M/S supplemented with 100 ng/ml 7S NGF (Upstate Biotechnology, Lake Placid, NY). MEM with serum and NGF is abbreviated as M/S□N (see Tatton et al., 1994; Wadia et al., 1998; and Carlile et al., 2000 for further details of culture and treatment). Following incubation for 1 to 9 days in M/S□N, cells underwent three successive washes in Hanks' balanced salt solution (HBSS; Invitrogen) to remove NGF and serum-borne trophic agents and then were replaced into M/S□N for controls or into MEM only (M/O) to induce apoptosis by serum and NGF withdrawal. Varying concentrations of DEP (Sigma-Aldrich, St. Louis, MO), DES (Toronto Chemical, Toronto, ON, Canada), CGP 3466 (Novartis AG, Basel, Switzerland), actinomycin D, camptothecin, or cycloheximide (all from Sigma-Aldrich) were added to the M/S□N or M/O cultures at varying times to oppose apoptosis or to inhibit new protein synthesis. The NGF-naive undifferentiated PC-12 cells were maintained in M/S on plates, wells, or coverslips for 6 days prior to washing to induce apoptosis by serum withdrawal. Washed cells were replaced into M/S or M/O with or without identical additives to those above.

Both cell survival and the percentages of cells with evidence of apoptotic nuclear degradation were assessed for all treatments. To estimate survival, the cells were seeded at a density of 8×10^4 cells/well in 24-well plates. Cells were harvested 24 h after treatment and lysed. Intact nuclei were counted using a hemocytometer (see Tatton et al., 1994; Wadia et al., 1998; and Carlile et al., 2000 for details of treatment and counting methods). Percentages of cells with apoptotic nuclei were determined for cells grown on poly-L-lysine-treated coverslips (density, 1×10^4/coverslip). At varying times after treatment, the cells were stained with the DNA binding dye YOYO-1 (Molecular Probes, Eugene, OR) to reveal chromatin condensation as a marker of apoptotic nuclear degradation (Tatton et al., 1994; Wadia et al., 1998; Carlile et al., 2000). Cells on coverslips were washed three times in PBS followed by 100% methanol incubation at □20°C for 30 s. The methanol was then replaced with YOYO-1 (1.5 □M in PBS) for thirty min at room temperature. After three PBS washes, the cells on coverslips were mounted in Aquamount Gurr (EM Industries, Cincinnati, OH) for laser confocal scanning microscopy imaging. The total number of YOYO-1-stained nuclei with chromatin condensation was counted on twenty-five 40□ fields for each coverslip. Each field was chosen by pairs of randomly generated x-y coordinates. The proportion of nuclei with chromatin condensation was expressed as a percentage of the total number of cells in each field. The values were pooled for three coverslips for each treatment and time point.

Caspase Inhibition of Cells. Two caspase inhibitors, N-benzyloxycarbonyl-Val-Ala-Asp-fluomethylketone (zVAD-fmk; Sigma/RBI, Natick, MA) and Ac-Asp-Glu-Val-Asp-CH (acetyl-DEVD aldehyde; Sigma/RBI) were used with PC-12 cells that were supported with serum and NGF and those that were serum- and NGF-withdrawn. Both inhibitors were applied in MEM with the addition of 0.25% dimethyl sulfoxide. zVAD-fmk has K_i's that show it to be a general caspase inhibitor whereas acetyl-DEVD aldehyde has a K_i for caspase-3 that indicates a strong predilection for that caspase (Garcia-Calvo et al., 1998).

DNA Electrophoresis. Cells grown in medium-sized flasks and trophically withdrawn as above were examined for internucleosomal DNA digestion characteristic of apoptosis. At 6 to 18 h after washing, 2×10^6 cells were rinsed with isotonic PBS, and DNA was extracted and prepared according to the methods of Batistatou and Greene (1993). The samples were incubated with 50 mg/ml DNase free Rnase (Roche Applied Science, Indianapolis, IN) at 37°C for 30 min. The recovered soluble DNA was electrophoresed on a 1.2% agarose gel and blotted onto Gene Screen Plus membrane (PerkinElmer Life Sciences, Boston, MA). Blots were probed with total genomic DNA digested with Sau 3A (Roche Applied Science). ^{33}P-labeled probe was prepared by the random priming reaction, and hybridization and washings were performed according to the manufacturer's protocol.

Metabolic Labeling of Cells for Two-Dimensional Gel Electrophoresis of Total Cell Protein. After a methionine-free MEM

(mfMEM; Sigma-Aldrich) wash, the PC-12 cells were pulse-labeled for 1.5 h with trans-[^{35}S]methionine (75 Ci/ml; Amersham Biosciences, Piscataway, NJ) in the mfMEM at 37°C to label newly synthesized proteins and to estimate overall de novo protein synthesis. Cells undergoing treatment with DRPs were incubated in mfMEM with 10^{-9} M concentrations of each DRP. mfMEM was removed from the dishes and replaced with M/S N, M/O, or MEM with one of the DRPs for up to 4.5 h. At 6 h after the initial washing, all media were removed, and the labeled PC-12 cells were lysed (lysis buffer: 9.5 M urea, 2% 3-[(3-cholamidopropyl)dimethylammonio]-propanesulfonate, 1.6% Servalyt, pH 5 to 7, 0.4% Servalyt, pH 2 to 11, and 5% -mercaptoethanol; all from Sigma-Aldrich) directly on tissue culture dishes, scraped, and mechanically homogenized. To remove unincorporated radiolabel, the lysates were precipitated in 1 ml of 7% trichloroacetic acid with deoxycholate (Sigma-Aldrich) (100 g/ml) and centrifuged for 30 min at 15,000g. The resulting pellets were resuspended in 1 ml of 5% trichloroacetic acid, recentrifuged, and the supernatants discarded. The pellets were finally solubilized in 50 ml of the lysis buffer.

The lysate proteins were initially separated by isoelectric focusing on 0.20 15 cm cylindrical gels [4% acrylamide, 9.5 M urea, 2% 3-[(3-cholamidopropyl)dimethylammonio]propanesulfonate, 3.2% carrier ampholytes 5–7, and 0.75% carrier ampholytes 3–10]. The proteins were then further separated according to molecular mass (second dimension) in the presence of 0.1% SDS on linear 5 to 15% gradients of acrylamide using a discontinuous buffer system. Gels were fixed in 10% acetic acid and 30% methanol and gently soaked with EN^{3}HANCE solution (Amersham Biosciences) for 1 h followed by incubation in 10% v/v glycerol in PBS for another hour and then vacuum-dried onto 3-MM Whatman filter paper (Whatman, Clifton, NJ). Exposure of the gel to preflashed Hyperfilm MP (Amersham Biosciences) required 7 days for optimal resolution.

Scintillation Counting and Two-Dimensional Gel Electrophoresis of Subcellular Protein Fractions. PC-12 cells were grown and treated as described above, after washing in HBSS, and cells were metabolically labeled as above with trans-[^{35}S]methionine label in mfMEM for 1.5 h in M/S N, M/O, or MEM with DRPs as above. At 6 h after the HBSS washing step, cells were harvested and homogenized in MOPS/sucrose/EDTA buffer (pH 7.2) with the addition of phenylmethylsulfonyl fluoride, dithiothreitol, and leupeptin (Sigma-Aldrich) to inhibit protease activity prior to homogenization. The suspension of PC-12 cells in PBS was then centrifuged four times at 200g for 10 min at 4°C, the final wash being in nuclear buffer containing 10 mM 1,4-piperazinediethanesulfonic acid, pH 7.4, 10 mM KCl, 2 mM $MgCl_2$, 1 mM dithiothreitol, 10 M cytochalasin B, and 1 mM phenylmethylsulfonyl fluoride (all from Sigma-Aldrich). The cells were allowed to swell for 20 min and homogenized by 30 strokes of a Dounce glass homogenizer. The resulting pellet was layered over 30% sucrose and centrifuged at 800g for 10 min to isolate the nuclear fraction. The final nuclear pellet was suspended in a small volume of nuclear buffer containing 250 mM sucrose and frozen until further analysis was performed. The supernatants above the nuclear pellet were differentially centrifuged to isolate the mitochondrial fraction by a 4°C centrifugation at 14,000g for 10 min. The resulting mitochondrial pellet was resuspended in mitochondrial containing 250 mM mannitol with 0.1% (w/v) bovine serum albumin, pH 7.2, 0.5 mM EGTA, and 5 mM HEPES supplemented with 1 g/ml leupeptin, 1 g/ml pepstatin A, 50 g/ml antipain, and 10 g/ml chymostatin (all from Sigma-Aldrich) and recentrifuged. The pellet was then suspended in a small volume of mitochondrial buffer and stored until further processing. The supernatant resulting from the mitochondrial isolation containing enriched peroxisomes and soluble cytoplasmic proteins was then centrifuged at 100,000g for 1 h to pellet peroxisomal and cytoplasmic proteins. Finally, the above mitochondrial samples were then applied to metrizamide gradients (Sigma-Aldrich) to further separate the mitochondrial proteins from those of the plasma membrane and the Golgi. Protein concentrations were determined for individual subcellular fractions using a BCA protein assay kit (Pierce Chemical, Rockford, IL), and identical amounts of subcellular proteins were analyzed by scintillation counting or by preparative gels. To demonstrate the enrichment of the subfractions, equal amounts of proteins from each fraction were Western blotted and probed with antibodies for nucleolin, 14-3-3-, and cytochrome oxidase (see Carlile et al., 2000 for details and examples of our use of these methods).

Similarly prepared samples of the protein fractions were then used for scintillation counting of relative trans-[^{35}S]methionine label incorporation. For scintillation counts, each sample was applied to one glass fiber filter (Ahlstrom Filtration, Mt. Holly Springs, PA) and allowed to adsorb. Each filter was then washed with 0.05 M Tris buffer (pH 7.2). Filters were analyzed using a Beckman scintillation counter (Beckman Coulter, Inc., Fullerton, CA) using the windows open option. Counts of the individual fractions were compared with those for total protein.

For the analysis of individual protein subcellular fractions, 20 g of each fraction were loaded onto isoelectric focusing gels (pI, 3–10 range) and then taken through linear gradient gels in the second dimension (5–15% denaturing gradient gels). The different subcellular fractions from the different treatment groups were transferred to polyvinylidene difluoride sequencing membranes overnight by semidry transfer and then exposed to preflashed film for a period of 7 to 9 days. Individual new proteins from the different subcellular fractions and different treatment groups were then imaged and examined using MetaMorph software (Universal Imaging Corp., Downingtown, PA).

Western Blots for Protein Levels. Alterations in the expression of specific proteins were examined using Western blots of protein lysates that were extracted at various times 3, 6, 9, 12, 18, and 24 h after washing in HBSS and incubation in either M/S N, M/O, or MEM with DRP added. PC-12 cell proteins were extracted as total soluble lysates or lysates for the nuclear, mitochondrial, and cytosolic fractions (detailed methods and confirmation of fractionation purity are presented in Carlile et al., 2000). Briefly, the cells were treated as above, scraped from Petri dishes in cold PBS, and harvested by centrifugation at 300g for 5 min at 4°C. The pellets were washed twice in cold PBS and resuspended in buffer containing 25 mM Hepes-KOH, pH 7.5, 10 mM KCl, 1.5 mM $MgCl_2$, 1 mM sodium EDTA, 1 mM sodium EGTA, 1 mM dithiothreitol, and 5 g/ml leupeptin, 5 g/ml chymostatin, 5 g/ml pepstatin A, 5 g/ml aprotinin, plus 1 mM benzamidine and 250 mM sucrose (all from Sigma-Aldrich). The cells were homogenized by 12 to 15 strokes of a glass Dounce homogenizer and centrifuged at 800g for 10 min at 4°C to pellet the nuclear fraction. The supernatants were again centrifuged at 10,000g for 15 min at 4°C. These pellets contained the mitochondrially enriched fraction, and the supernatant included the cytoplasmic fraction. Both nuclearly and mitochondrially enriched fractions were resuspended in 50 l of the above buffer and frozen at 30°C. Prior to use, the samples were protein assayed by the BCA protein assay method. The protein fraction lysates (30–40 g) were electrophoresed on either 10 or 12% SDS-polyacrylamide gels and then transferred to nitrocellulose blotting membranes (Bio-Rad, Hercules CA). Membranes were agitated at room temperature for 2 h with primary antibodies [dilutions being 1:500 for anti-BCL-2 (Santa Cruz Biotechnology, Inc., Santa Cruz, CA), 1:2000 for anti-BAX (BD Biosciences, San Jose, CA), 1:800 for anti-c-FOS (Geneka Biotechnology Inc., Montreal, QC, Canada), 1 g/ml anti-c-JUN (Stressgen Biotechnologies Corp., Collegeville, PA), 1:5,000 anti-CuZn superoxide dismutase (SOD1)/Mn superoxide dismutase (SOD2) (BioDesign International, Abingdon, UK), 1 g/ml tubulin (Molecular Probes), 1:2000 neurofilament light protein (Sternberger Monoclonals Inc., Lutherville, PA), 1:1000 anti-GAPDH (Chemicon International, Temecula, CA), 1:1000 anti-MAP-2 (Sigma-Aldrich), 1:1200 anti-tyrosine hydroxylase (Zymed Laboratories, South San Francisco, CA), and 1:100 g/ml anti-glutathione peroxidase (MBL International, Watertown, MA)] in 3% blocking solution (Amersham Biosciences).

Following washing in Tris-buffered saline (pH 7.4), membranes were incubated for 1 to 2 h in the appropriate alkaline phosphatase- or horseradish peroxidase-labeled secondary antibody (Amersham Biosciences). Reactions were visualized using either 3,3-diaminobenzidine/0.2% H_2O_2 or nitrotetrazolium blue/5-bromo-4-chloro-3-indolyl-phosphate (all from Sigma-Aldrich) as substrates. All detected bands were then digitized using a charge-coupled device camera and imaged and analyzed using MetaMorph software.

Statistical Evaluation. To statistically evaluate the data, the individual measurements of data from different treatment groups were first analyzed using Statistica software (StatSoft, Tulsa, OK) to carry out two-tailed independent sample t testing. Levene's testing for homogeneity of variances showed that most pairs of samples were not homogeneous and χ^2 evaluation of the distributions showed that most did not fit a normal distribution (see Siegel, 1956). Accordingly, analysis with parametric methods such as the t test may not provide valid results. The data were rank ordered and first tested with the Kruskal-Wallis analysis of variance by ranks (Siegel, 1956) using Statistica. Post hoc analysis was carried out using Mann-Whitney U testing. Both methods do not require homogeneity of variances, that the underlying distributions for the data be known, or that the values are linearly related (Siegel, 1956). Kruskal-Wallis analysis of variance values are presented in the text, and Mann-Whitney U values are only presented where they differ from the Kruskal-Wallis. Asterisks in figures indicate $p < 0.05$.

Results

Dependence of PC-12 Survival after Protein Synthesis Inhibition on Duration of Previous NGF Exposure. Previous studies have shown differing effects of protein synthesis inhibitors on PC-12 cell survival. Those studies seemed to suggest that the duration of previous NGF exposure could determine how the inhibitors affect PC-12 cell survival. Protein synthesis inhibitors have decreased survival of serum-supported, NGF-naive PC-12 cells (i.e., cells maintained in medium with serum) (Torocsik and Szeberenyi, 2000) whereas they did not alter the decreased survival induced by serum withdrawal in the NGF-naive cells (Rukenstein et al., 1991). In marked contrast, protein synthesis inhibitors prevented much of the decreased survival caused by serum and NGF withdrawal in PC-12 cells that had been previously exposed to NGF for 12 days (Mesner et al., 1995). Alternatively, protein synthesis inhibitors did not alter the reduced survival caused by serum and NGF withdrawal in PC-12 cells previously exposed to serum and NGF for 6 days (Tatton et al., 1994).

We examined cell survival after serum withdrawal in NGF-naive PC-12 cells and after serum and NGF withdrawal in PC-12 cells previously maintained in serum and NGF for 3, 6, or 9 days (Fig. 1). In all figures, M/S or M/S+N indicates serum or serum and NGF-supported cells, respectively, whereas M/O indicates serum- or serum- and NGF-withdrawn cells. In the different experimental groups, mean cell losses at 24 h after the withdrawal ranged from 56.3 to 60.5%, with the losses being greater for the serum-withdrawn than the serum- and NGF-withdrawn cells. We used a range of concentrations of actinomycin D (0.06–30 μg/ml), camptothecin (0.02–200 μg/ml), and cycloheximide (0.01–100 μg/ml) to determine the effects of protein synthesis inhibition on cell survival. Figure 1, A1 through A3, shows that actinomycin D concentrations of 1 μg/ml or greater, camptothecin concentrations of 2 μg/ml or greater, or cycloheximide concentrations of 1 μg/ml or greater decreased NGF-naive PC-12 cell survival whether the cells were serum-supported or serum-withdrawn. The decreases in survival are similar to those reported for NGF-naive PC-12 cells treated with the protein synthesis inhibitor anisomycin (Torocsik and Szeberenyi, 2000).

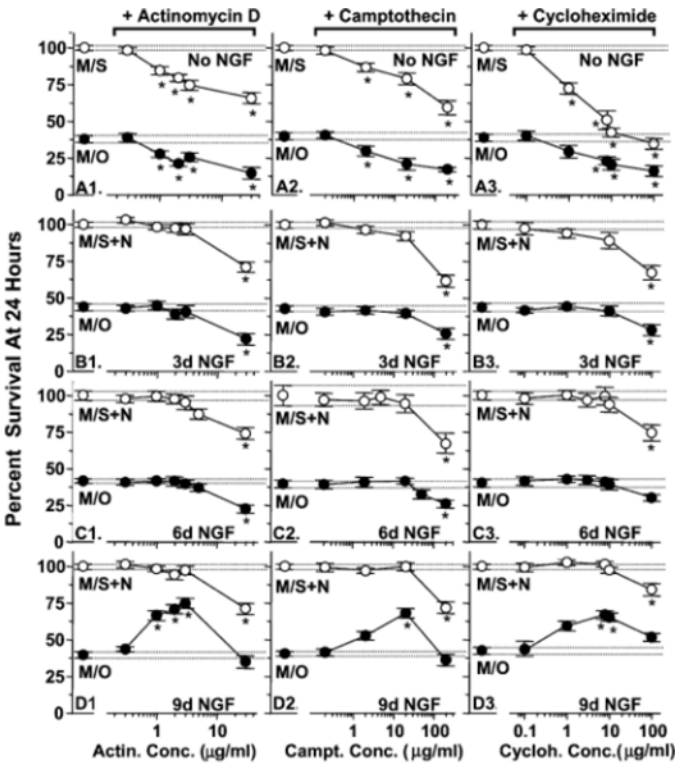

Fig. 1. Effect of protein synthesis inhibitors on PC-12 survival depends on previous NGF exposure. Varying concentrations of actinomycin D (A1, B1, C1, and D1), camptothecin (A2, B2, C2, and D2), and cycloheximide (A3, B3, C3, and D3) were applied to NGF-naive PC-12 cells (A1-A3) or PC-12 cells previously exposed to NGF for 3 (B1-B3), 6 (C1-C3), or 9 days (D1-D3) to determine whether the duration of previous NGF exposure altered the effect of protein synthesis inhibition on cell survival. Cells were either trophically supported by serum or serum and NGF (open circles) or trophically withdrawn (filled circles). Values are means ± S.E.M. in all figures. Means are for 8 to 16 measurements in this and other plots of survival. Distance between dotted lines show the extent of control S.E.M. values for trophically supported (labeled M/S or M/S+N) or trophically withdrawn (M/O) survival without protein inhibitor treatment. *, values significantly differ from controls ($p < 0.05$ relative to M/S, M/S + N, or M/O); E, washed and returned to M/S; F, washed and placed in M/O, serum- or serum- and NGF-withdrawn.

In contrast, PC-12 cells exposed to serum and NGF for 9 days showed increased survival after serum and NGF withdrawal when treated with actinomycin D concentrations of 1 to 3 μg/ml, camptothecin concentrations of 20 μg/ml, or cycloheximide concentrations of 8 to 10 μg/ml (Fig. 1, D1–D3). Those concentrations did not alter the survival of 9-day NGF-differentiated PC-12 cells that were serum- and NGF-supported, whereas higher concentrations of the inhibitors (i.e., 30 μg/ml actinomycin D, 200 μg/ml camptothecin, and 100 μg/ml cycloheximide) reduced the survival of the serum- and NGF-supported, 9-day NGF-differentiated cells. PC-12 cells exposed to serum and NGF for 3 (Fig. 1, B1–B3) or 6 days (Fig. 1, C1 and C2) did not show any inhibitor-induced alterations in the reduced survival caused by serum and NGF withdrawal except for decreases induced by the high inhibitor concentrations that decreased survival in the 9-day NGF-differentiated cells.

Our studies were aimed at examining the dependence of DRP antiapoptosis on new protein synthesis in PC-12 cells that were maximally NGF-differentiated. Based on the data in Fig. 1, we chose to examine PC-12 cells that had been exposed to serum and NGF for 6 days. Although the use of PC-12 cells after 9 days of serum and NGF exposure would provide a greater degree of NGF differentiation, any changes in survival induced by protein synthesis inhibitors after DRP treatment would have to be subtracted or added to the increases in survival that the inhibitors induced after serum and NGF withdrawal.

DRPs Induce Concentration-Dependent Survival Increases in PC-12 Cells Exposed to NGF for 6 Days But Not Those Exposed to NGF for Less Than 4 Days. About 4 days of NGF exposure were required before DRPs increased the survival of serum- and NGF-withdrawn cells. First, we found that DRPs increased the survival of 6-day NGF-differentiated PC-12 cells after serum and NGF withdrawal but did not increase the survival of serum-withdrawn, NGF-naive cells (Fig. 2, A1–A3). DEP (Fig. 2A1) and DES (Fig. 2A2) induced significant increases in survival ($p < 0.05$ for MEM with DRP addition compared with M/O) over a concentration range of 10^{-5} to 10^{-11} M, with the greatest increase at 10^{-9} M. CGP 3466 induced a similar survival-concentration relationship (Fig. 3A3) but also significantly increased survival at 10^{-13} M ($p < 0.05$ for MEM with CGP 3466 addition compared with M/O). As shown in the same plots, the DRPs did not alter the survival of NGF-naive PC-12 cells that were maintained in MEM with serum for 6 days prior to undergoing serum withdrawal. DRPs induced similar increases in survival in the 9-day NGF-differentiated cells to those found for the 6-day NGF-differentiated cells (data not shown).

Second, we examined the relationship between the duration of NGF exposure to the capacity of the DRPs to increase survival after serum and NGF withdrawal. The 10^{-9} M concentration of each DRP was tested on PC-12 cells previously exposed to NGF for periods varying between 1 and 9 days (Fig. 2, B1–B3). Significant increases in survival relative to that for cells maintained in medium with serum without NGF ($p < 0.05$) for the same periods become evident at the fourth to fifth day of exposure to NGF and continued to day 9. Accordingly, the capacity of the DRPs to increase survival after NGF and serum withdrawal requires at least 4 days of previous exposure to NGF. The plots in Fig. 2, B1 through B3, are normalized to the mean survival for cells that underwent serum or serum and NGF withdrawal and therefore represent the percentage of increase in survival induced by the DRPs, whereas those in Fig. 2, A1 through A3, present the percentage of survival relative to that for serum- or serum- and NGF-supported cells. We altered the ordinate scale in Fig. 2, B1 through B3, to percentage of increase in survival, since serum-withdrawn cells showed a lower level of survival than serum- and NGF-withdrawn cells as shown in Fig. 1 and Fig. 2, A1 through A3. By normalizing the survival to mean values after serum or serum and NGF withdrawal, we were able to determine the timing of DRP-induced increases in survival.

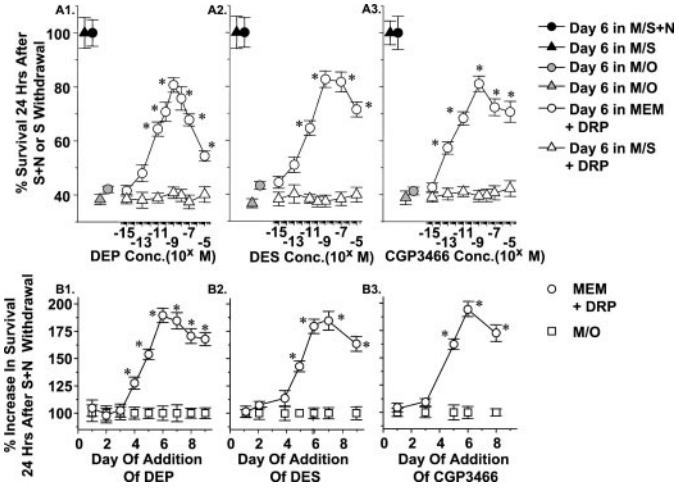

Fig. 2. Concentration relations for DRP increases in survival and duration of NGF exposure necessary for DRP-induced increases in survival after serum and NGF withdrawal. A1, A2, and A3 show that DEP, DES, and CGP 3466 concentrations of 10^{-5} to 10^{-11} M increase the survival of 6-day NGF-differentiated PC-12 cells after serum and NGF withdrawal but similar concentrations do not increase the survival of NGF-naive cells after serum withdrawal. B1, B2, and B3 show that approximately 4 days of prior NGF exposure is necessary for the three propargylamines to increase the survival of PC-12 cells after serum and NGF withdrawal. *, significant increases ($p < 0.05$) in survival relative to those for M/O.

Decreased Survival after Serum and NGF Withdrawal in the 6-Day NGF-Differentiated PC-12 Cells Involves Apoptosis. We previously showed that partially NGF-differentiated PC-12 cells undergo apoptotic degradation after serum and NGF withdrawal using 1) DNA gel electrophoresis to demonstrate nuclear DNA cleavage, 2) in situ DNA end labeling with Apop Tag (Sigma-Aldrich) or Bodipy dUTP (Serologicals Corp., Norcross, GA) for nuclear DNA cleavage, 3) DNA staining with Hoechst 33258 (Molecular Probes, Eugene, OR) or YOYO-1 for nuclear chromatin condensation, and 4) immunocytochemistry for antibodies against nuclear histones to demonstrate nuclear protein reorganization (Tatton et al., 1994; Wadia et al., 1998; Carlile et al., 2000).

The apoptotic nuclear degradation after serum and NGF withdrawal is accompanied by shrinkage of NGF-induced neuron-like processes. The laser scanning confocal, interference contrast micrographs in Fig. 3, A1 and B1, serve to compare the process development in PC-12 cells exposed to serum for 6 days plus 12 h versus those exposed to serum and NGF for the same period. The NGF-naive PC-12 cells were typically smaller and did not show the neuron-like process development found for the 6-day NGF-differentiated cells. Serum and NGF withdrawal induced partial process retraction and blunting of processes in the 6-day NGF-differentiated cells as illustrated in Fig. 3D1 for cells at 12 h after serum and NGF withdrawal. The interference contrast micrographs for the serum- and NGF-withdrawn cell also showed membrane blebbing typical of apoptosis.

Figure 3, A2 and B2 show typical YOYO-1 nucleic acid staining in nuclei of serum or serum- and NGF-supported cells, respectively, at 6 days plus 12 h. Figure 3, C2 and D2 show typical nuclei undergoing chromatin condensation at 12 h after serum or serum and NGF withdrawal, respectively. Typically, nuclei undergoing chromatin condensation were highly condensed with smooth edges that are found as a single intensely fluorescent body or as multiple intensely fluorescent bodies surrounded by condensed cytoplasm. Apoptotic nuclear shrinkage was evident on both the interference contrast and YOYO-1 fluorescence images. A relatively

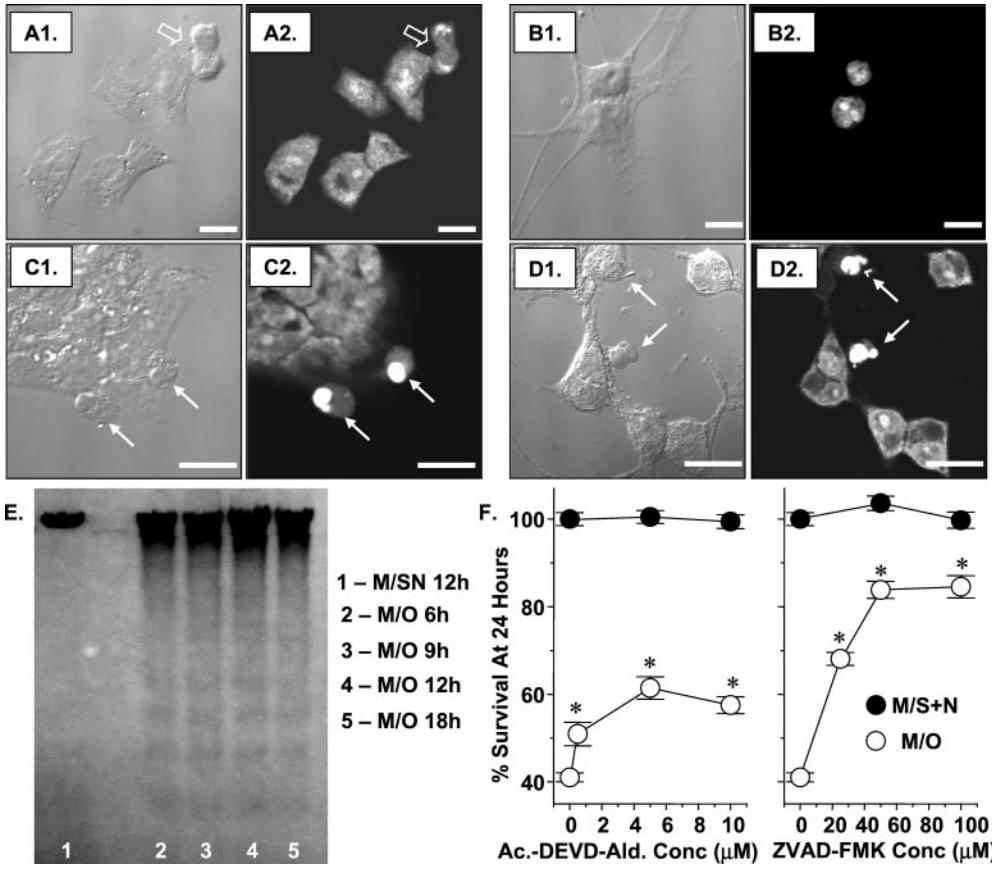

Fig. 3. Apoptotic markers in NGF-naive and 6-day NGF-differentiated PC-12 cells. A1 through D2, each horizontal pair of laser confocal scanning micrographs is for an identical image field. The left-hand member presents an interference contrast image and the right-hand image presents YOYO-1 fluorescence. A1, A2, B1, and B2 are for NGF-naive PC-12 cells maintained in M/S for 6 days and 6-day NGF-differentiated PC-12 cells, respectively, that were washed repeatedly and replaced into M/S or M/S□N to maintain trophic support. C1, C2, D1, and D2 are for NGF-naive PC-12 cells maintained in M/S for 6 days and 6-day NGF-differentiated PC-12 cells, respectively, that were trophically withdrawn by repeated washing and placement into M/O. The interference contrast images for 6-day NGF-differentiated PC-12 cells show apoptotic membrane blebbing and process withdrawal (compare B1 and D1). The filled arrows indicate nuclei with chromatin condensation whereas the open arrow indicates a nucleus undergoing mitosis for comparison. E, DNA electrophoresis gels showing laddering typical of internucleosomal DNA digestion at 6 to 18 h after serum and NGF withdrawal in 6-day NGF-differentiated PC-12 cells. F, acetyl-DEVD aldehyde, a caspase inhibitor with a predilection for caspase-3, and zVAD-fmk, a general caspase inhibitor, induce about 45 and 65% reductions, respectively, in the decreased survival induced by serum and NGF withdrawal in 6-day NGF-differentiated PC-12 cells. □, significant increases in survival (p □ 0.05) compared with cells not treated with a caspase inhibitor (0 □M concentration).

high proportion of NGF-naive cells was undergoing division as evidenced by YOYO-1 staining of mitotic spindles. A YOYO-1-stained naive PC-12 cell undergoing mitosis is shown in Fig. 3A2 for comparison with those undergoing nuclear chromatin condensation.

"Ladder" patterns could be discerned on DNA gel electrophoresis for the 6-day NGF-differentiated PC-12 cells after serum and NGF withdrawal. The ladders were best defined at 6 to 18 h after serum and NGF withdrawal as illustrated in Fig. 3E. Finally, treatment with either a caspase-3 inhibitor (acetyl-DEVD aldehyde) or a general caspase inhibitor (zVAD-fmk) induced concentration-dependent reductions in the decreased survival caused by serum and NGF withdrawal in the 6-day NGF-differentiated PC-12 cells (Fig. 3F). ZVAD increased the survival to a maximum of 82% whereas acetyl-DEVD aldehyde increased survival to a maximum of 61%. The caspase inhibitors did not alter survival of the 6-day NGF-differentiated cells when they were serum- and NGF-supported. These findings indicate that the apoptosis signaling induced by the serum and NGF withdrawal in the 6-day NGF- differentiated PC-12 cells was caspase-dependent, apparently to the greatest extent for caspases other than caspase-3.

The percentage of YOYO-1-stained nuclei showing chromatin condensation in the 6-day NGF-differentiated PC-12 cells first increased above baseline at 6 h after serum and NGF withdrawal, reaching a maximum of 12 to 13% approximately 12 h after the withdrawal of serum and NGF (Fig. 4, A1–A3). Treatment with 10^{-9} M DEP (Fig. 4A1), DES (Fig. 4A2), or CGP 3466 (Fig. 4A3) decreased the percentages of nuclei with chromatin condensation to less than 4% at all time points. Since nuclei with chromatin condensation exist for a limited period of time during apoptotic degradation, the numbers of condensed YOYO-1-stained nuclei at a given time point reflects only those cells in the degradative phase at the time of fixation and do not provide an estimate of the overall cell loss resulting from apoptosis.

We therefore also performed counts of intact nuclei taken from PC-12 cells that were grown in wells and exposed to identical conditions as those stained with YOYO-1 on coverglasses. The counts provide a cumulative estimate of cell loss prior to a given time point and were expressed as the per-

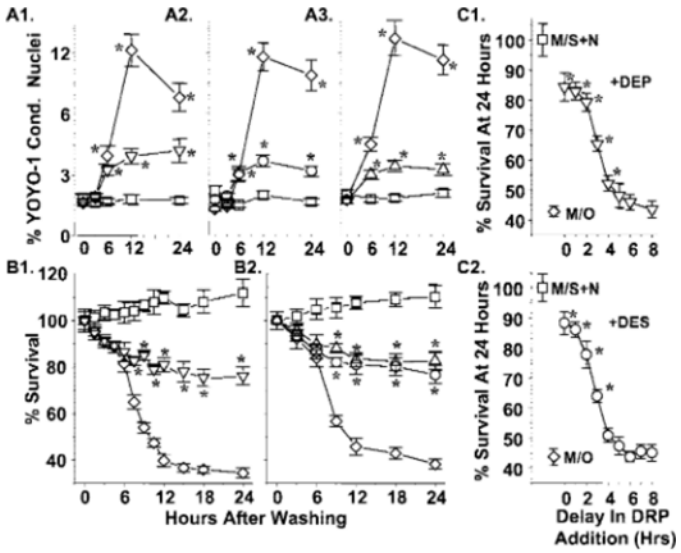

Fig. 4. DRP alterations in the time courses of appearance of nuclear chromatin condensation and decreased survival initiated in NGF-differentiated PC-12 cells by serum and NGF withdrawal. A1, A2, and A3 show the time course of the appearance of nuclei with chromatin condensation shown by YOYO-1 staining in 6-day NGF-differentiated PC-12 cells and the time course of reductions in nuclei with chromatin condensation induced by 10^{-9} M DEP, DES, or CGP 3466, respectively. B1 and B2 show the time course of decreased 6-day NGF-differentiated PC-12 cell survival initiated by serum and NGF withdrawal and the time course of the increased survival induced by 10^{-9} M DEP, DES, or CGP 3466 after serum and NGF withdrawal. C1 and C2 show that delays in the administration of 10^{-9} M DEP or DES administration, respectively, of less than 2 h did not alter the increase in survival induced by the DRPs whereas delays in administration of 3 to 5 h progressively reduced the capacity of the DRPs to increase survival of the 6-day NGF-differentiated PC-12 cells. □, significant increases in survival ($p < 0.05$) compared with M/O; □, M/S − N; □, M/O; ƒ, DEP 10^{-9} M; E, DES 10^{-9} M; ,, CGP 3466 10^{-9} M.

centage of surviving cells compared with that found for the 0-h time point. Survival was reduced to about 40% of the number of serum- and NGF-supported cells by 24 h after the withdrawal of serum and NGF (Fig. 4, B1 and B2). The reductions in survival appeared to occur in two phases: a first phase involving losses of 16 to 18% of the cells occurring over the first 4.5 to 6 h after serum and NGF withdrawal, and a second phase involving the further loss of about 45% of the cells between 6 h and 24 h after serum and NGF withdrawal. The approximate 9% decrease in survival that was evident at 3 h was not accompanied by an increase in the percentage of nuclei with chromatin condensation at the same time point (compare Fig. 4, A1–A3 with Fig. 4, B1 and B2). The absence of an increase in cells with evidence of nuclear chromatin condensation at times of less than 6 h suggest that the cell loss during the first phase was not apoptotic. Accordingly, the data in Fig. 3E and Fig. 4, B1 and B2 suggest that the general caspase inhibitor rescued most, if not all, of the apoptotic cells.

The DRPs increased cell survival and slowed the rate of cell loss over phase 2 but not during phase 1 (Fig. 4, B1 and B2). The findings suggest that the mechanisms underlying cell loss during the first 6 h after serum and NGF withdrawal were not altered by the DRPs whereas those operating after 6 h were responsive to DRP treatment. Data like that in Fig. 4B indicate that the DRPs decrease apoptosis in phase 2 by 79 to 94%.

We progressively delayed the addition of the DRPs relative to the time of serum and NGF withdrawal in the 6-day NGF-differentiated cells (Fig. 4, C1 and C2). DRP addition could be delayed for 2 to 3 h before the capacity of the DRPs to increase survival was diminished ($p < 0.05$ compared with survival for adding DRPs at time 0). After delays of 4 or 5 h or more, the DRPs did not provide any increase in survival ($p < .05$ compared with survival for M/O). Accordingly, the maximum effect of DRPs on apoptosis caused by serum and NGF withdrawal occurs during the first 2 h after their addition followed by a gradual decrease in the antiapoptosis over hours 2 to 5. Figure 4, A1–A3 and our previous work (Wadia et al., 1998) indicate that nuclear apoptotic degradation begins at about 6 h after serum and NGF withdrawal and is maximal at 12 h. Hence, the delay experiments suggest that the DRPs act relatively early in the apoptosis signaling process.

Dependence of DRP Antiapoptosis on New Protein Synthesis. Metabolic labeling using [^{35}S]methionine incorporation was determined for the three protein synthesis inhibitors at maximum concentrations (see Fig. 1, C1–C3) that did not reduce survival (3 □g/ml actinomycin D, 10 □g/ml cycloheximide, and 20 □g/ml camptothecin). Scintillation counting showed that new protein synthesis was decreased by 92% or more for each of those concentrations (bar graphs in Fig. 5, A1–A3) when the maximum concentrations of the protein synthesis inhibitors that did not decrease survival were applied. Those concentrations of the protein synthesis inhibitors were applied to the 6-day NGF-differentiated PC-12 cells following serum and NGF withdrawal. Similar to

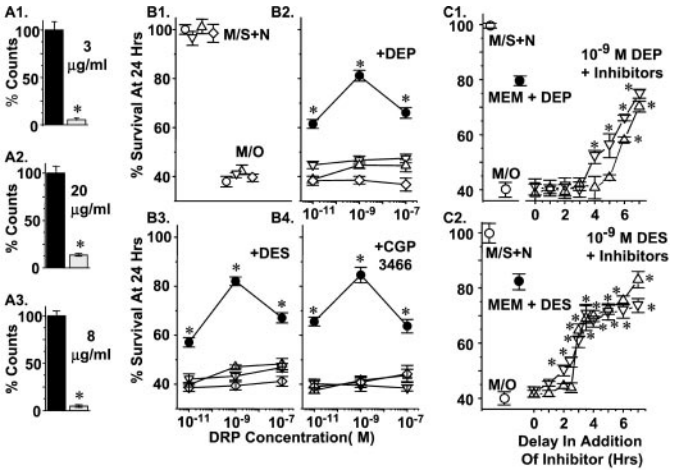

Fig. 5. Transcriptional or translational inhibition prevents DRP antiapoptosis in NGF-differentiated PC-12 cells after serum and NGF withdrawal. A1, A2, and A3 show that 3 □g/ml of actinomycin D, 20 □g/ml of camptothecin, or 8 □g/ml of cycloheximide, respectively, which do not reduce the survival of 6-day NGF-differentiated PC-12 cells, reduce new protein synthesis by 94% or more (black bars, serum- □ NGF-supported, gray bars, serum- □ NGF-withdrawn). Employment of the three protein synthesis inhibitor at those concentrations did not alter the survival of serum- and NGF-supported or serum- and NGF-withdrawn cells (B1) but prevented the three DRPs administered at 10^{-7}, 10^{-9}, and 10^{-11} M (B2, B3, and B4) from increasing survival after serum and NGF withdrawal. Progressive delays in the administration of 3 □g/ml actinomycin D (C1) or 8 □g/ml of cycloheximide (C2) showed that the protein synthesis inhibitors completely blocked the capacity of 10^{-9} M DEP from increasing survival for delays of up to 5 h and 10^{-9} M DES for delays of up to 3 h. Longer delays in the administration of the two inhibitors allowed for progressive increases in survival. □, significant increases in survival ($p < 0.05$) compared with M/O; E, no inhibitor or DRP addition; ƒ, DRP □ actinomycin D addition; ,, DRP □ cycloheximide addition; F, DRP addition; □, DRP □ camptothecin addition.

Fig. 1, Fig. 5B1 shows that those concentrations of the protein synthesis inhibitors did not affect the survival of the 6-day NGF- differentiated PC-12 cells when they were serum- and NGF-supported or after serum- and NGF-withdrawn ($p > 0.05$).

Treatment with each protein synthesis inhibitor blocked or markedly reduced the increased survival afforded by the DRPs at concentrations of 10^{-7} to 10^{-11} M (Fig. 5, B2–B4, $p < 0.05$). Accordingly, new protein synthesis is necessary for the antiapoptosis provided by the three DRPs. Experiments in which the addition of the protein synthesis inhibitors were delayed relative to the withdrawal of serum and NGF and the addition of 10^{-9} M DRP showed that DRP antiapoptosis progressively decreased for inhibitor addition delays beyond 3 to 7 h (Fig. 5, C1 and C2). The delay curves for DEP (Fig. 5C1) were shifted to about 2-h longer times compared with those for DES (Fig. 5C2). Delay curves similar to those for DES were found for CGP 3466 (data not shown).

DRPs Alter the New Synthesis of a Number of Proteins during Apoptosis. We examined metabolically labeled 2D protein gels for whole cell lysates at 6 h after washing. Six hours represents the end of the first phase of decreased survival, which corresponded to the onset of increased apoptotic nuclear degradation revealed by chromatin condensation and the time at which delays in the addition of protein synthesis inhibitors allowed for maximal increases in survival to be induced by the DRPs (Fig. 5, B1 and B2). Autoradiograms like those in Fig. 6 represent the incorporation of [^{35}S]methionine into proteins and hence, provided an estimate of the synthesis of new proteins during the first 6 h after washing. The partially NGF-differentiated PC-12 cells maintained in serum and NGF after washing were found to incorporate the ^{35}S label into a relatively large number of proteins as indicated by the distribution and number of punctate autoradiographic densities (Fig. 6A1). In contrast, relatively fewer densities were detected in samples taken from cells that were NGF- and serum-withdrawn (Fig. 6A2). As well as the overall decrease in densities, a number of densities were evident in serum- and NGF-withdrawn cells that did not appear to be present in the serum- and NGF-supported cells (compare Fig. 6, A1 and A2). The autoradiograms also appeared to show that DRP treatment at 10^{-9} M increased the number of densities in the serum- and NGF-withdrawn cells (compare Fig. 6A2 to Fig. 6A3). The autoradiograms were repeated for three experiments, each of which offered similar changes in the numbers and distributions of densities for labeled proteins. The DRP-induced increase in densities appeared to result from the recovery of some densities lost with serum and NGF withdrawal together with the appearance of other densities that were not evident in either serum- and NGF-supported or serum- and NGF-withdrawn cells.

Scintillation counting for ^{35}S in the whole cell lysates appeared to support the autoradiographic results. New protein

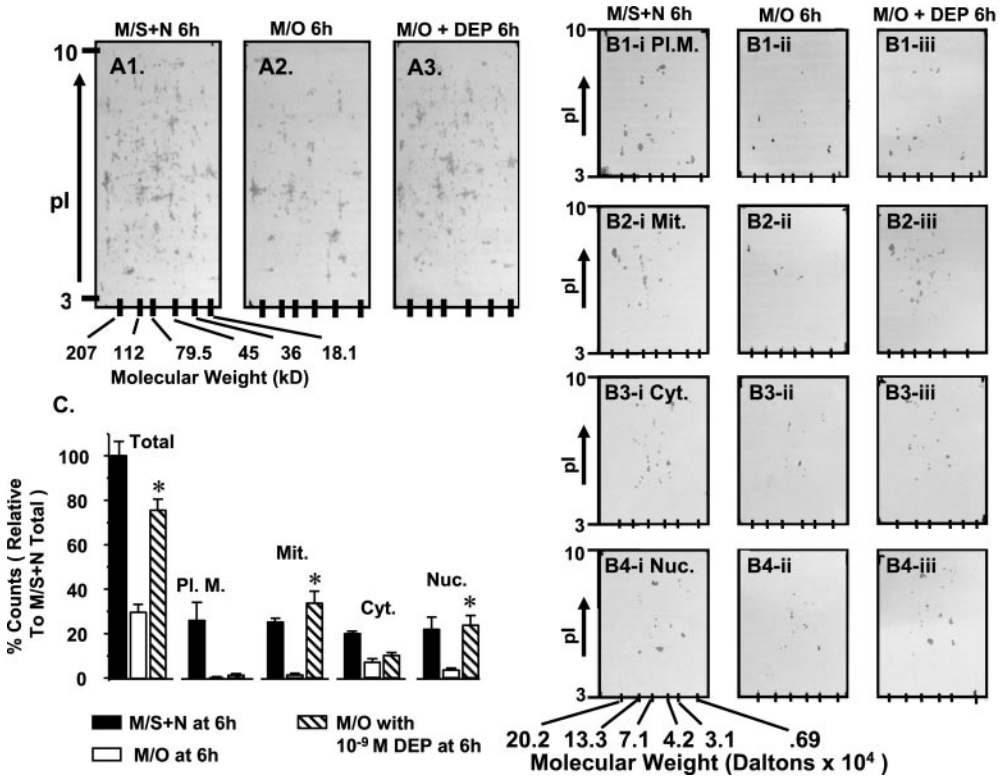

Fig. 6. DEP induces widespread changes in new protein synthesis, notably in nuclear and mitochondrial proteins, in 6-day NGF-differentiated PC-12 cells entering apoptosis after serum and NGF withdrawal. Typical autoradiograms for 2D protein gels for metabolically labeled total protein at 6 h after washing and replacement in medium with serum and NGF (A1), washing and placement in medium without serum or NGF (A2), and washing and placement in medium without serum or NGF with 10^{-9} M DEP (A3). B1-i to B1-iii, B2-i to B2-iii, B3-i to B3-iii, and B4-i to B4-iii present 2D autoradiograms for the plasma membrane, mitochondrial, cytosolic, and nuclear protein subfractions, respectively, at 6 h after washing and replacement in serum and NGF (i panels), washing and placement in MEM only (ii panels), and washing and placement in MEM with 10^{-9} M DEP (iii panels). C presents scintillation counts for metabolically labeled proteins corresponding to those for total protein and each of the subcellular fractions. Pl. M., Mit., Cyt., and Nuc. indicate plasma membrane, mitochondrial, cytosolic, and nuclear subfractions, respectively. *, significant increases in counts ($p < 0.05$) compared with those for M/O.

synthesis for the serum- and NGF-withdrawn cells at 6 h (M/O in Fig. 6C) was reduced to 29.8 □ 3.4% of that for cells that were washed and replaced in medium with serum and NGF (M/S□N at 6 h, p □.001 for M/O compared with M/S□N), whereas treatment of the serum- and NGF-withdrawn cells with $10^{□9}$ M DEP resulted in a recovery to 75.8 □ 4.7% of that for cells that were washed and maintained in medium with serum and NGF (p □.001 compared with M/O).

Evidence that the DRPs differentially affected new protein synthesis in different subcellular protein fractions was found with both 2D autoradiograms and scintillation counting (Fig. 6, B1–B4 and C). Two-dimensional gel autoradiograms for the plasma membrane (Fig. 6, B1-i to B1-iii) and mitochondrial (Fig. 6, B2-i to B2-iii), cytosolic (Fig. 6, B3-i to B3-iii), and nuclear fractions (Fig. 6, B4-i to B4-iii) revealed overall decreases in autoradiographic densities for serum- and NGF-withdrawn cells at 6 h. The DRPs induced clear changes in densities on the 2D gel autoradiograms for the mitochondrial (Fig. 6B2-iii) and nuclear fractions (Fig. 6B4-iii). For example, treatment with $10^{□9}$ M DEP induced recovery of some densities in all subfractions, most notably in the mitochondrial subfraction. Like those for the total protein pool, the autoradiograms for the subfractions indicated that the DRPs induced the recovery of some densities lost with serum and NGF withdrawal but also induced the disappearance of some densities evident in either serum- and NGF-supported or serum- and NGF-withdrawn cells. The autoradiograms also suggested that the DRPs induced the synthesis of some novel proteins that were not newly synthesized in either serum- and NGF-supported or serum- and NGF-withdrawn cells or that the DRPs induced the subcellular movement of newly synthesized proteins from one subcellular fraction to another. The appearance of novel densities appeared most evident in the mitochondrial fraction (compare Fig. 6B2-iii to Fig. 6B2-i and Fig. 6B2-ii).

Figure 6C also shows the scintillation counts for the subfractions. New protein synthesis in the plasma membrane fraction was reduced from 25.9 □ 8.1% of total new protein in serum- and NGF-supported cells to less than 0.4 □ 0.2 in serum- and NGF-withdrawn cells (p □. 001 for M/O compared with M/S□N). DEP, or the other DRPs, did not significantly increase the labeled protein in the plasma membrane fraction (1.2 □ 0.8, p □.05 for M/O compared with MEM with DEP). The reduction in new protein synthesis after serum and NGF withdrawal was less marked in the cytoplasmic fraction (19.7 □ 0.4% of total labeled protein for M/S□N and 7.0 □ 1.5% for M/O, p □.01 for M/S□N compared with M/O). DEP did not significantly increase the counts for the cytoplasmic fraction (10.1 □ 1.4%, p □.05 for M/O compared with MEM with DEP). Serum and NGF withdrawal markedly reduced new protein synthesis in the mitochondrial fraction (25.1 □ 1.7% of total labeled protein for M/S□N and 1.2 □ 0.7% for M/O, p □.01 for M/S□N compared with M/O) and in the nuclear fraction (21.5 □ 1.6% of total labeled protein for M/S□N and 3.5 □ 1.6% for M/O, p □.01 for M/S□N compared with M/O). DEP treatment induced levels of new protein synthesis for the mitochondrial and nuclear fractions in the serum- and NGF-withdrawn cells that were not significantly reduced from those for serum- and NGF-supported cells (33.6 □ 5.7% for the mitochondrial fraction and 23.6 □ 4.2% for the nuclear fraction, p □.05 for M/O with DEP compared with M/S□N). Accordingly, DEP treatment returned the levels of newly synthesized protein in the mitochondrial and nuclear fractions to the levels found in serum- and NGF-supported cells.

Proteins Affected by DRPs. Western blots for multiple time points were performed to identify some of the proteins of which synthesis was altered by DRP treatment. Examples of typical Western blots are presented in Fig. 7, whereas optical density measurements taken from Western blot bands are presented in Fig. 8. Figure 7, A1, A2, B1, and B2 show typical changes in BCL-2 immunoreaction induced by DES or DEP at 1, 3, 6, and 9 h or 3, 6, 12, and 24 h, respectively, following serum and NGF withdrawal. Levels of BCL-2 immunoreaction were reduced by 3 h following serum and NGF withdrawal, with a further decline in protein levels over subsequent hours (Fig. 7, A2 and B1 and Fig. 8A). DEP (Fig. 7B2), DES (Fig. 7A2), and CGP 3466 (not shown) at $10^{□9}$ M maintained BCL-2 immunoreaction at levels similar to those found in serum- and NGF-supported cells (Fig. 8A). Notably, the DRPs did not alter levels of BCL-2 immunoreaction in cells that were maintained in M/S□N after washing and therefore were not entering apoptosis (see right-hand four bands in Fig. 7A1 for an example).

Proteins like SOD1 (Fig. 8C), SOD2 (Fig. 8D), glutathione peroxidase (Fig. 8E), and tyrosine hydroxylase (Fig. 8H) showed progressive decreases after serum and NGF withdrawal that were similar to those found for BCL-2. They were maintained at serum- and NGF-supported levels or were increased above those levels by DRP treatment.

Several proteins including c-FOS (Fig. 8F), c-JUN (Fig. 7, C1-1, C1-2, C2-1, C2-2, and Fig. 8G), and GAPDH (Fig. 8I; also see Carlile et al., 2000) showed increased immunoreac-

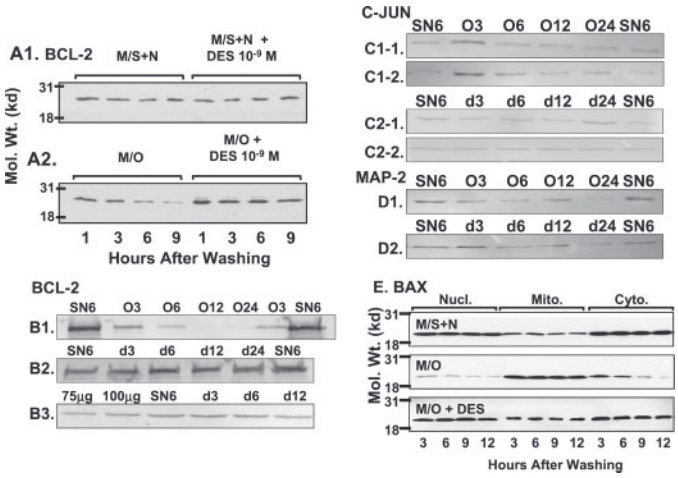

Fig. 7. Western blots for the immunodensity of selected proteins after serum and NGF withdrawal with and without DRP treatment. BCL-2 immunodensity at 1, 3, 6, and 9 h after washing and replacement in medium with serum and NGF support (A1) or placement into medium without serum and NGF (A2). Immunodensity for BCL-2 (B1-B3), c-JUN (C1-1, C1-2, C2-1 and C2-2), and MAP-2 (D1 and D2). SN6, 6 h after washing and replacement in medium with serum and NGF support; O3, O6, O12, and O24, 3, 6, 12, and 24 h, respectively, after washing and placement into medium without serum and NGF; and d3, d6, d12, and d24, 3, 6, 12, and 24 h, respectively, after washing and placement into medium without serum and NGF with added $10^{□9}$ M DEP. E, BAX immunodensity for nuclear, mitochondrial, and cytosolic subfractions at 3, 6, 9, and 12 h after washing and replacement in medium with serum and NGF support (top panel), after washing and placement into medium without serum and NGF (middle panel), and after washing and placement into medium without serum and NGF with added $10^{□9}$ M DES (bottom panel).

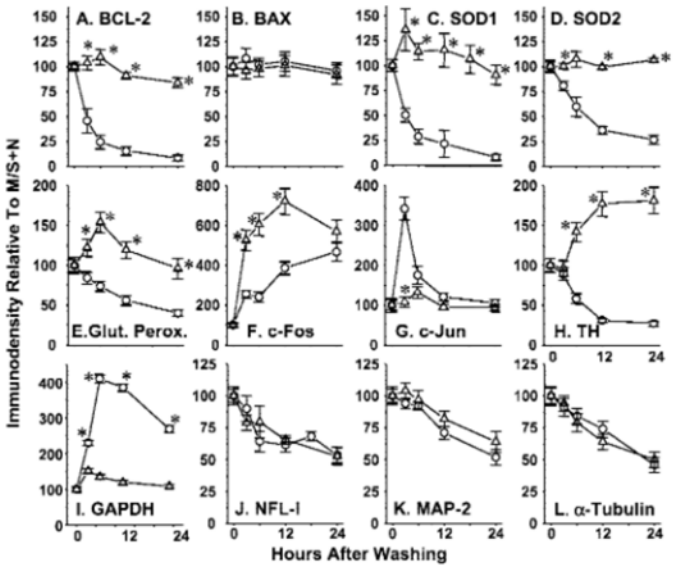

Fig. 8. Plots of average Western blot immunodensity above background for selected proteins at 0, 3, 6, 12, and 24 h after serum and NGF withdrawal. Each point represents the average ± S.E.M. optical density for immunodensity bands from three experiments and is normalized against the average optical density for bands from serum and NGF-supported, 6-day NGF-differentiated PC-12 cells at 6 h after washing. The values for serum- and NGF-supported, 6-day NGF-differentiated PC-12 cells are plotted at time 0. Other points represent the time after washing for serum- and NGF-withdrawn cells. Each plot is labeled for the respective primary antibody. A 9-h time point was substituted for the 12-h time point for GAPDH. E, serum ± NGF withdrawal; , , serum ± NGF withdrawal ± 10^{-9} M DEP. Glut. Perox., glutathione peroxidase; TH, tyrosine hydroxylase; NFL, neurofilament light protein.

tion after serum and NGF withdrawal that were decreased by DRP treatment. c-JUN underwent a rapid transient increase that was only detected at the 3-h time point. Two examples of Western blots for c-JUN are presented in Fig. 7, C1 and C2 to demonstrate the reproducibility of the transient c-JUN increase and its disappearance with DRP treatment.

Four proteins that we examined did not show any differences in immunoreaction for the whole cell lysates with DRP treatment: BAX (Fig. 8B), neurofilament light protein (Fig. 8J), MAP-2 (Fig. 7, D1 and D2 and Fig. 8K), and -tubulin (Fig. 8L). Although BAX levels for the whole cell lysates did not decrease after serum and NGF withdrawal, we found differences in BAX immunoreaction in nuclear, mitochondrial, and cytosolic fractions after serum and NGF withdrawal and following DRP treatment. In cells that were washed and then maintained in medium with serum and NGF, BAX immunoreaction was more strongly evident in the nuclear and cytosolic fractions than in the mitochondrial fraction (Fig. 7E, upper panel labeled M/S±N). BAX immunoreaction progressively decreased in the cytosolic and nuclear fractions but was increased in the mitochondrial fraction by 3 h after serum and NGF withdrawal (Fig. 7E, middle panel labeled M/O). DRP treatment prevented or reduced the decreased immunoreaction in the nuclear and cytosolic fractions and also appeared to reduce the increased BAX immunoreaction in the mitochondrial fraction after serum and NGF withdrawal (Fig. 7E, lower panel labeled M/O ± DES).

Discussion

NGF induces multiple changes in PC-12 cells including: 1) differentiation into an action potential-generating, neurite-bearing, sympathetic neuron-like phenotype; 2) a reduction in proliferation; and 3) an increase in survival (Greene and Tischler, 1982). Similar to previous reports, we found that DEP does not decrease apoptosis caused by serum withdrawal from NGF-naive PC-12 cells (Vaglini et al., 1996). We found that 4 days of prior NGF exposure is necessary before DRPs can reduce PC-12 cell apoptosis initiated by serum and NGF withdrawal.

DEP was first shown to prevent decreases in dopaminergic indices of nigrostriatal neuronal survival caused by MPTP exposure in primates (Cohen et al., 1984), which was interpreted to show that DEP protected the neurons by blocking MPTP conversion to MPP± by MAO-B. A number of clinical trials showed that DEP can slow the clinical progression of Parkinson's disease (see Parkinson, 1993 as an example), but it is uncertain whether the slowing represents reduced neuronal death or alterations in dopamine metabolism. It is certain that DEP and other DRPs reduce neuronal death induced in vivo and in vitro by a wide variety of insults in a number of different neuronal models. Those insults have included 6-hydroxydopamine, MPP±, MPTP, nitric oxide or peroxynitrite, N-(-2-chloroethyl)-N-ethyl-2-bromobenzylamine, glutathione depletion, peripheral nerve crush or axotomy, optic nerve crush, hypoxia and/or ischemia, cytosine arabinoside, excitotoxins, trophic insufficiency, thiamine deficiency, okadaic acid, and aging. The neurons or neuron-like cells have included mesencephalic or nigral dopaminergic neurons, hippocampal neurons, dentate neurons, cerebellar granule and Purkinje neurons, cerebral cortical neurons, thalamic neurons, retinal ganglion neurons, spinal and facial motoneurons, neuroblastoma cells, and partially differentiated PC-12 cells (reviewed in Tatton et al., 2000). Studies involving a range of models have shown that DRPs can increase neuronal survival without MAO-B inhibition and by reducing apoptosis (Tatton et al., 2000). Since PC-12 cells do not express MAO-B (Youdim et al., 1986) and CGP 3466 does not inhibit MAO-B (Kragten et al., 1998; Waldmeier et al., 2000), DRP antiapoptosis in the serum- and NGF-withdrawn, 6-day NGF-differentiated PC-12 cells is also MAO-B-independent.

As before, we examined multiple indices to determine whether the increases in cell survival result from antiapoptosis. Time course studies of survival versus the percentage of cells with nuclear chromatin condensation showed that about 16% of the cells die during the first 6 h after serum and NGF withdrawal by a process that is unlikely to be apoptotic. The remaining cell loss, occurring after 6 h, meets multiple criteria for apoptosis and is responsive to DRP treatment. zVAD-fmk, a general caspase inhibitor, prevented almost 100% of the apoptosis whereas acetyl-DEVD aldehyde, a caspase-3 inhibitor, prevented less than 50%. This is in keeping with previous studies of NGF-differentiated PC-12 cells, which have shown that general caspase or caspase-2 inhibitors almost completely prevent apoptosis initiated by NGF or serum and NGF withdrawal whereas caspase-3 inhibition only partially prevents the apoptosis (Haviv et al., 1997, 1998; Stefanis et al., 1998).

We found that new protein synthesis is necessary for reductions in apoptosis induced by the three DRPs. In various models, protein synthesis inhibitors can slow or reduce apoptosis, induce apoptosis, or may not affect the extent or timing of apoptosis (Eastman, 1993). Hence, the use of protein synthesis inhibitors to examine antiapoptotic agents can be complicated if the apoptosis itself requires new protein

synthesis or if a protein synthesis inhibitor induces apoptosis. Apoptosis initiated by serum withdrawal from NGF-naive PC-12 cells (Rukenstein et al., 1991; Mesner et al., 1995) or serum and NGF withdrawal from partially NGF-differentiated PC-12 cells (Tatton et al., 1994) are not new protein synthesis-dependent. Alternatively, apoptosis initiated in fully differentiated PC-12 cells by NGF withdrawal requires new protein synthesis (Mesner et al., 1995). Some protein synthesis inhibitors induce apoptosis over one concentration range and reduce apoptosis over another (Torocsik and Szeberenyi, 2000). Our findings suggest that the duration of previous exposure to NGF determines how protein synthesis inhibitors influence apoptosis signaling initiated by serum and NGF withdrawal in PC-12 cells.

Our experiments in which protein synthesis inhibitor addition was delayed relative to serum and NGF withdrawal and DRP addition suggested that critical antiapoptotic alterations in transcription/translation induced by DES begin prior to 3 h after DES addition whereas those for DEP continue to 5 h. DES is a principal metabolite of DEP (Baker et al., 1999), and studies using cytochrome P450 inhibitors suggest that DEP antiapoptosis requires DEP metabolism to DES (Tatton and Chalmers-Redman, 1996). The relative prolongation of the protein synthesis inhibitor blockade of DEP antiapoptosis may reflect a period necessary for DEP metabolism to DES. The experiments in which DRP addition was delayed relative to the onset of serum and NGF withdrawal indicate that the apoptosis signaling events that are critical to DRP antiapoptosis occur between 2 and 5 h after serum and NGF withdrawal, which is within the same time domain for critical DRP-induced new protein synthesis suggested by the protein synthesis inhibitor delay experiments.

Metabolic labeling suggested that DRPs induced changes in the new synthesis of a number of proteins, with the most marked changes involving the mitochondrial and nuclear protein subfractions. Previous work used differential display-polymerase chain reaction to identify four genes, c-jun, heat-shock protein 70, phosphoglycerate kinase, and calpactin I heavy chain, of which expression was increased in retinal ganglion neurons initiated into apoptosis by serum deprivation or hypoxia (Xu et al., 1999). In that study, 10^{-9} M DEP reversed the increases in c-jun and heat-shock protein 70 gene expression but not that for the other genes. Like with the retinal study, we have found that DRPs alter the synthesis of some proteins but not others and found a transient increase in c-JUN. As well as for c-JUN, we found alterations for a number of proteins that previously were shown to play a role in PC-12 cell apoptosis, including BCL-2, BAX, SOD1, SOD2, c-FOS, glutathione peroxidase, and GAPDH.

Importantly, we found that the timing of alterations in the levels or subcellular distribution of those proteins induced by DRPs were appropriate to antiapoptosis. In this and previous studies (Wadia et al., 1998; Carlile et al., 2000), we found that apoptotic nuclear degradation first became evident at about 6 h after serum and NGF withdrawal. Western blots showed that the levels of antiapoptotic proteins decreased and those of pro-apoptotic proteins increased by 3 h after serum and NGF withdrawal. DRP treatment caused those early alterations to return toward control levels in association with a decrease in the percentage of cells with apoptotic nuclear degradation. The timing for changes in the levels of apoptotic and antiapoptotic proteins appear in accord with that found by the protein synthesis inhibition and DRP addition delay experiments.

Increases in the phosphorylation and levels of c-JUN are induced by NGF withdrawal from sympathetic neurons or NGF-differentiated PC-12 cells and involves the up-regulation of c-Jun N-terminal kinase (JNK) and/or p38 mitogen-activated protein kinase (Xia et al., 1995; Maroney et al., 1999). Pharmacological inhibition of JNK blocks apoptosis in NGF-differentiated PC-12 cells induced by NGF withdrawal but not apoptosis induced in NGF-naive PC-12 cells induced by serum withdrawal (Maroney et al., 1999). NGF withdrawal in 6-day NGF-differentiated PC-12 cells induced an increase in the levels of an endogenous mitogen-activated protein kinase kinase kinase, apoptosis signal-regulating kinase 1 (Kanamoto et al., 2000). Apoptosis signal-regulating kinase 1 up-regulation was necessary for c-JUN up-regulation and apoptosis initiated by NGF withdrawal in the cells (Hatai et al., 2000; Kanamoto et al., 2000). The timing of the c-JUN up-regulation was consistent with the transient c-JUN increase that we found 3 h after serum and NGF withdrawal.

The prevention of decreases in BCL-2 and the decreased mitochondrial BAX localization induced by the DRPs may contribute to the maintenance of $\Delta\Psi_M$ found with DRP treatment of neurons or neuron-like cells entering apoptosis (Paterson et al., 1998; Wadia et al., 1998). BCL-2 prevents decreases in $\Delta\Psi_M$ caused by agents that increase mitochondrial membrane permeability and induce apoptosis in PC-12 cells (Dispersyn et al., 1999). Mitochondrial BAX accumulation, similar to our finding in the NGF-differentiated PC-12 cells, has been shown for a number of forms of apoptosis including NGF withdrawal from sympathetic neurons (Putcha et al., 2000). Mitochondrial BAX accumulation increases mitochondrial membrane permeability and decreases $\Delta\Psi_M$ (Narita et al., 1998). Prevention of increased mitochondrial membrane permeability can be a key step in blocking apoptotic degradation (Jacotot et al., 1999).

DRPs have been shown to bind to GAPDH in association with reductions in apoptosis (Kragten et al., 1998; Carlile et al., 2000). Up-regulation of GAPDH together with the dense nuclear accumulation of GAPDH immunoreactivity is characteristic of apoptosis that can be blocked by GAPDH antisense oligonucleotides (reviewed in Tatton et al., 2000). The tumor suppressor protein, p53, has been shown to up-regulate GAPDH in neuronal apoptosis (Chen et al., 1999). p53 activation is downstream to JNK activation but upstream to BAX (Aloyz et al., 1998; Mielke and Herdegen, 2000) in a variety of apoptosis models, which may suggest that DRP binding to GAPDH could uncouple a JNK-p53-GAPDH apoptosis signaling pathway.

References

Aloyz RS, Bamji SX, Pozniak CD, Toma JG, Atwal J, Kaplan DR, and Miller FD (1998) p53 is essential for developmental neuron death as regulated by the TrkA and p75 neurotrophin receptors. J Cell Biol 143:1691–1703.

Baker GB, Urichuk LJ, McKenna KF, and Kennedy SH (1999) Metabolism of monoamine oxidase inhibitors. Cell Mol Neurobiol 19:411–426.

Batistatou A and Greene LA (1993) Aurintricarboxylic acid rescues PC12 cells and sympathetic neurons from cell death caused by nerve growth factor deprivation: correlation with suppression of endonuclease activity. J Cell Biol 115:461–471.

Carlile GW, Chalmers-Redman RM, Tatton NA, Pong A, Borden KE, and Tatton WG (2000) Reduced apoptosis after nerve growth factor and serum withdrawal: conversion of tetrameric glyceraldehyde-3-phosphate dehydrogenase to a dimer. Mol Pharmacol 57:2–12.

Chen RW, Saunders PA, Wei H, Li Z, Seth P, and Chuang DM (1999) Involvement of glyceraldehyde-3-phosphate dehydrogenase (GAPDH) and p53 in neuronal apoptosis: evidence that GAPDH is upregulated by p53. J Neurosci 19:9654–9662.

Cohen G, Pasik P, Cohen B, Leist A, Mytilineau C, and Yahr MD (1984) Pargyline and deprenyl prevent the neurotoxicity of 1-methyl-4-phenyl-1,2,3,6-tetrahydropyridine (MPTP) in monkeys. Eur J Pharmacol 106:209–210.
Dispersyn G, Nuydens R, Connors R, Borgers M, and Geerts H (1999) Bcl-2 protects against FCCP-induced apoptosis and mitochondrial membrane potential depolarization in PC12 cells. Biochim Biophys Acta 1428:357–371.
Eastman A (1993) Apoptosis: a product of programmed and unprogrammed cell death. Toxicol Appl Pharmacol 121:160–164.
Fang J, Zuo DM, and Yu PH (1995) Lack of protective effect of R(□)-deprenyl on programmed cell death of mouse thymocytes induced by dexamethasone. Life Sci 57:15–22.
Garcia-Calvo M, Peterson EP, Leiting B, Ruel R, Nicholson DW, and Thornberry NA (1998) Inhibition of human caspases by peptide-based and macromolecular inhibitors. J Biol Chem 273:32608–32613.
Greene L and Tischler A (1982) PC12 Pheochromocytoma cultures in neurological research. Adv Cell Neurobiol 3:373–414.
Hatai T, Matsuzzawa A, Onoshita S, Mochida Y, Kurodai T, Sakamaki K, Kuida K, Yonehara S, Ichijo H, and Takeda K (2000) Execution of apoptosis signal-regulating kinase 1 (ASK1)-induced apoptosis by the mitochondria-dependent caspase activation. J Biol Chem 275:26576–26581.
Haviv R, Lindenboim L, Li H, Yuan J, and Stein R (1997) Need for caspases in apoptosis of trophic factor-deprived PC12 cells. J Neurosci Res 50:69–80.
Haviv R, Lindenboim L, Yuan J, and Stein R (1998) Need for caspase-2 in apoptosis of growth-factor-deprived PC12 cells. J Neurosci Res 52:491–497.
Jacotot E, Costantini P, Laboureau E, Zamzami N, Susin SA, and Kroemer G (1999) Mitochondrial membrane permeabilization during the apoptotic process. Ann NY Acad Sci 887:18–30.
Kanamoto T, Mota M, Takeda K, Rubin LL, Miyazono K, Ichijo H, and Bazenet CE (2000) Role of apoptosis signal-regulating kinase in regulation of the c-Jun N-terminal kinase pathway and apoptosis in sympathetic neurons. Mol Cell Biol 20:196–204.
Kragten E, Lalande I, Zimmermann K, Roggo S, Schindler P, Muller D, van Oostrum J, Waldmeier P, and Furst P (1998) Glyceraldehyde-3-phosphate dehydrogenase, the putative target of the antiapoptotic compounds CGP 3466 and R-(□)-deprenyl. J Biol Chem 273:5821–5828.
Maroney AC, Finn JP, Bozyczko-Coyne D, O'Kane TM, Neff NT, Tolkovsky AM, Park DS, Yan CY, Troy CM, and Greene LA (1999) CEP-1347 (KT7515), an inhibitor of JNK activation, rescues sympathetic neurons and neuronally differentiated PC12 cells from death evoked by three distinct insults. J Neurochem 73:1901–1912.
Mesner PW, Epting CL, Hegarty JL, and Green SH (1995) A timetable of events during programmed cell death induced by trophic factor withdrawal from neuronal PC12 cells. J Neurosci 15:7357–7366.
Mielke K and Herdegen T (2000) JNK and p38 stress kinases–degenerative effectors of signal-transduction-cascades in the nervous system. Prog Neurobiol (NY) 61: 45–60.
Narita M, Shimizu S. Ito T, Chittenden T, Lutz RJ, Matsuda H, and Tsujimoto, Y (1998) Bax interacts with the permeability transition pore to induce permeability transition and cytochrome c release in isolated mitochondria. Proc Natl Acad Sci USA 95:14681–14686.
Parkinson SG (1993) Effects of tocopherol and deprenyl on the progression of disability in early Parkinson's disease. N Engl J Med 328:176–183.
Paterson IA, Zhang D, Warrington RC, and Boulton AA (1998) R-deprenyl and R-2-heptyl-N-methylpropargylamine prevent apoptosis in cerebellar granule neurons induced by cytosine arabinoside but not low extracellular potassium. J Neurochem 70:515–523.
Putcha GV, Deshmukh M, and Johnson EM Jr (2000) Inhibition of apoptotic signaling cascades causes loss of trophic factor dependence during neuronal maturation. J Cell Biol 149:1011–1018.
Rukenstein A, Rydel RE, and Greene LA (1991) Multiple agents rescue PC12 cells from serum-free cell death by translation- and transcription-independent mechanisms. J Neurosci 11:2552–2563.
Siegel S (1956) Non-Parametric Statistics for the Behavioral Sciences. McGraw-Hill, New York.
Stefanis L, Troy CM, Haiqing Q, Shelanski ML, and Greene LA (1998) Caspase-2 (nedd-2) processing and death of trophic factor-deprived PC12 cells and sympathetic neurons occur independently of caspase-3 (CPP32)-like activity. J Neurosci 18:9204–9215.
Tatton WG and Chalmers-Redman RME (1996) Modulation of gene expression rather than monoamine oxidase inhibition: (□)-deprenyl-related compounds in controlling neurodegeneration. Neurology 47:S171–S183.
Tatton WG, Ju WY, Holland DP, Tai C, and Kwan M (1994) (□)-Deprenyl reduces PC12 cell apoptosis by inducing new protein synthesis. J Neurochem 63:1572–1575.
Tatton WG, Tatton NA, Elstner M, and Chalmers-Redman RME (2000) Glyceraldehyde-3-phosphate dehydrogenase in neurodegeneration and apoptosis signaling J Neural Trans S60:61–84.
Torocsik B and Szeberenyi J (2000) Anisomycin affects both pro- and antiapoptotic mechanisms in PC12 cells. Biochem Biophys Res Commun 278:550–556.
Vaglini F, Pardini C, Cavalletti M, Maggio R, and Corsini GU (1996) L-deprenyl fails to protect mesencephalic dopamine neurons and PC12 cells from the neurotoxic effect of 1-methyl-4-phenylpyridinium ion. Brain Res 741:68–74.
Wadia JS, Chalmers-Redman RME, Ju WJH, Carlile GW, Phillips JL, Fraser AD, and Tatton WG (1998) Mitochondrial membrane potential and nuclear changes in apoptosis caused by serum and nerve growth factor withdrawal: time course and modification by (□)-deprenyl. J Neurosci 18:932–947.
Waldmeier PC, Boulton AA, Cools AR, Kato AC, and Tatton WG (2000) Neurorescuing effects of the GAPDH ligand CGP 3466B. J Neural Transm Suppl 60:197–214.
Xia Z, Dickens M, Raingeaud J, Davis RJ, and Greenberg ME (1995) Opposing effects of ERK and JNK-p38 MAP kinases on apoptosis. Science (Wash DC) 270:1326–1331.
Xu L, Ma J, Seigel GM, and Ma JX (1999) L-deprenyl, blocking apoptosis and regulating gene expression in cultured retinal neurons. Biochem Pharmacol 58: 1183–1190.
Youdim MB, Heldman E, Pollard HB, Fleming P, and McHugh E (1986) Contrasting monoamine oxidase activity and tyramine induced catecholamine release in PC12 and chromaffin cells. Neuroscience 19:1311–1318.
Zhang D, Berry MD, Paterson IA, and Boulton AA (1999) Loss of mitochondrial membrane potential is dependent on the apoptotic program activated: prevention by R-2HMP. J Neurosci Res 58:284–292.

Address correspondence to: Dr. William G. Tatton, Mount Sinai School of Medicine, Department of Neurology, One Gustave L. Levy Place, Annenberg 1494, Box 1137, New York, NY 10029-6574. E-mail: william.tatton@mssm.edu